A11102 678980

NBS PUBLICATIONS

NBSIR 87-3588

RADC/NBS International Workshop Moisture Measurement and Control for Microelectronics (IV)

Proceedings of the RADC/NBS Workshop
held at the National Bureau of Standards
Gaithersburg, MD

November 12-14, 1986

Didier Kane, Benjamin A. Moore, and E. Jane Walters, Editors

U.S. DEPARTMENT OF COMMERCE
National Bureau of Standards
National Engineering Laboratory
Center for Electronics and Electrical Engineering
Semiconductor Electronics Division
Gaithersburg, MD 20899

June 1987

This activity was sponsored by:

Rome Air Development Center/RBRE
[illegible]iss AFB, NY 13441-5700

[illegible]onal Bureau of Standards

QC
100
U56
#87-3588
1987
c.2

Research Information Center
National Bureau of Standards
Gaithersburg, Maryland 20899

NBSC
QC100
.U56
no. 87-3588
1987
c.2

NBSIR 87-3588

RADC/NBS INTERNATIONAL WORKSHOP MOISTURE MEASUREMENT AND CONTROL FOR MICROELECTRONICS (IV)

Proceedings of the RADC/NBS Workshop
held at the National Bureau of Standards
Gaithersburg, MD

November 12-14, 1986

Didier Kane, Benjamin A. Moore, and E. Jane Walters, Editors

U.S. DEPARTMENT OF COMMERCE
National Bureau of Standards
National Engineering Laboratory
Center for Electronics and Electrical Engineering
Semiconductor Electronics Division
Gaithersburg, MD 20899

June 1987

This activity was sponsored by:
Rome Air Development Center/RBRE
Griffiss AFB, NY 13441-5700
and
National Bureau of Standards

U.S. DEPARTMENT OF COMMERCE, Malcolm Baldrige, *Secretary*
NATIONAL BUREAU OF STANDARDS, Ernest Ambler, *Director*

Table of Contents

Page

Workshop Officers vi

Foreword vii

Introduction 1

Opening Talk by S. Hasegawa (NBS) 2

Session I, Chairman, A. DerMarderosian (Raytheon)

1.1: Helium Leak Detector for Small Components
L. E. Bergquist and S. R. Schertz
(Martin Marietta Denver Aerospace) 6

1.2: Permissible Leak Rates and Moisture Ingress
A. DerMarderosian (Raytheon) 15

1.3: The Negative Ion Detection (NID) Vapor Detection Technique: A Breakthrough in Gross Leak Detection
B. Evan (WEB Technology) 47

1.4: Reusable Moisture Standard Development for Package Gas Analysis
R. F. Haack (California Institute of Technology/Jet Propulsion Laboratory) . 62

Session II, Chairman, R. K. Lowry (Harris Semiconductor)

2.1: Moisture Process Control and Mass Spectrometer Correlations
R.K. Lowry (Harris Semiconductor) 73

2.2: Laboratory Correlation and Survey Experiment: A Status Report
B. A. Moore and D. Kane (RADC) 96

2.3: Accuracy and Reproducibility of the Mass Spectrometer/Carousel Method for Moisture Analysis
L.J. Rigby (STC Technology Ltd., UK)
Presented by J. Pernicka (Pernicka Corp.) 104

Page

Session III, Chairman, S. D. Senturia (MIT)

3.1: New Failure Mechanisms in Temperature and Humidity Stress
D.Y. Guan, T.F. Gukelberger, E.C. Cahoon,
T.W. Joseph, and J.M. Snowdon (IBM) 124

3.2: Studies of Moisture in Polyimide: A Summary
S.D. Senturia (MIT) 128

3.3: Moisture Control in Hermetic Leadless Chip Carriers with Silver-Epoxy Die-Attach Adhesive
D.R. Carley and R.W. Nearhoff (RCA) 138

3.4: Polymeric Materials for Moisture Protection of Medical Implants
P. R. Troyk (IIT) 161

Session IV, Chairman, J. Mucha (AT&T)

4.1: Pin Selection Criteria for AC Conduction Technique
N.K. Annamalai and E.C. Blackburn (RADC) and
S.M.R. Islam (Clarkson University) 173

4.2: Evaluation of a Parasitic Charge-Spreading Transistor as a Moisture Sensor
K. Hultén and Ö. Hallberg (RIFA AB, Sweden) 189

4.3: Moisture Measurement by AC-Biased Surface Conductivity Sensors
D. Kane and B.A. Moore (RADC) 198

4.4: Tunable Diode Laser Systems for Moisture Measurement in Integrated Circuit Packages
D. Wall, J. Sproul, and A. Mantz (Spectra Physics) 214

4.5: Using Panametrics Mini-Mod Moisture Sensors for Moisture Measurements Inside Sealed Microelectronic Packages
D. Pinsky (Raytheon Co.) 254

4.6: Aluminum Oxide Sensor: A Tutorial Update
V. Fong (Panametrics) 276

Page

Session V, Chairman, P. Schuessler (IBM)

5.1: Reliable Plastic ICs for Automotive Electronics
R.J. Straub (Delco Electronics) 277
5.2: A Test Program to Assess Reliability of Plastic Packages and Gel Coatings for Military Environments
E.C. Blackburn and D. Kane (RADC) 290
5.3: Moisture Monitor for Plastic Packaged Integrated Circuits
H.L. Blaz (Harris Semiconductor)
Presented by R.K. Lowry (Harris Semiconductor) 298
5.4: High Reliability Molded Plastic Packaging Through a Systematic Approach
L. Liang (Fairchild Semiconductors) 307
5.5: High Lead Count/High Reliability Plastic Packaging: Issues and Approaches
G. Pitts (MCC) 319

Workshop Participants

6.1: List of Speakers 326
6.2: List of Attendees 329

WORKSHOP OFFICERS

GENERAL CHAIRMAN: Benjamin A. Moore
Rome Air Development Center
RADC/RBRE
Griffiss AFB NY 13441-5700
(315) 330-4055

VICE GENERAL CHAIRMAN: Stanley Ruthberg
National Bureau of Standards
Semiconductor Electronics Division
Bldg. 225 - Rm A331
Gaithersburg, MD 20899
(301) 975-2082

TECHNICAL PROGRAM CHAIRMAN: Didier Kane(*)
Rome Air Development Center
RADC/RBRE
Griffiss AFB NY 13441-5700
(315) 330-4055

(*) present address: AT&T Bell Laboratories
Rm 3B-126
555 Union Blvd
Allentown, PA 18103
(215) 439-6639

TECHNICAL PROGRAM COMMITTEE

George B. Cvijanovitch
AMP Inc.
Winston-Salem, NC

J. Gordon Davy
Westinghouse
Columbia, MD

Aaron DerMarderosian
Raytheon Co.
Sudbury, MA

Didier Kane
RADC
Griffiss AFB, NY

Robert K. Lowry
Harris Corp.
Melbourne, FL

Benjamin A. Moore
RADC
Griffiss AFB, NY

John A. Mucha
AT&T Bell Labs
Murray Hill, NJ

Stanley Ruthberg
NBS
Gaithersburg, MD

Phillipp Schuessler
IBM Corp.
Owego, NY

Steven D. Senturia
MIT
Cambridge, MA

FOREWORD

These proceedings are dedicated to the memory of Stanley Ruthberg, Vice General Chairman of this 1986 Moisture Workshop, who did most of the groundwork for the organization of the conference before becoming one of the many victims of cancer.

Stan had co-chaired this RADC/NBS workshop several times in the past and always worked hard to make it the meeting that anybody concerned with moisture in electronics should attend. Despite numerous tasks at the National Bureau of Standards, and outstanding contributions to the field of hermeticity, Stan always managed to devote the time necessary to make this conference a success.

His untimely death, shortly after the workshop, is deeply felt by all who knew him, his colleagues, and friends. We extend our heartfelt sympathy to his family. May his spirit of intellectual curiosity guided by scientific principles exist in all those who follow him.

INTRODUCTION

A fourth workshop on Moisture Measurement and Control for Microelectronics was held at the Gaithersburg, Maryland facility of the National Bureau of Standards on November 12-14, 1986. It was co-sponsored by Rome Air Development Center (RADC) and the National Bureau of Standards (NBS).

The three previous workshops have been mostly dedicated to the enhancement of measurement technologies needed by the microelectronics industry to ensure a higher reliability of manufactured parts. This year strong emphasis was also put on materials and on packaging. The reason for broadening the workshop in these directions was to help the industry in identifying moisture-related problems, and in understanding and preventing them at the design level rather than measuring only their extent.

The 22 selected presentations were centered around 5 sessions (Hermeticity and Standards, Residual Gas Analysis, Materials Related Issues, Other Moisture Measurement Methods, and Plastic Packaging), all of which were very well attended. A newly introduced Informal Workshops Session allowed the participants to discuss topics of their choice with others sharing the same concerns.

This 1986 workshop has been made possible by:

- Benjamin A. Moore of RADC and Stanley Ruthberg of NBS, who took care of the general organization,
- Didier Kane of RADC who took care of the Technical Program and the publicity,
- The ten members of the Technical Program committee who selected and reviewed the papers presented,
- Barbara Lipford and Kathleen Kilmer of NBS who coordinated local arrangements,
- E. Jane Walters and Josephine Gonzalez of NBS who assisted in the preparation of these proceedings,
- Sandra B. Kelley of NBS who was responsible for fiscal matters,
- Barbara Lipford of NBS who took care of the registration, and
- Barbara Lipford and Sandra B. Kelley of NBS who assisted in operational details.

DISCLAIMERS

The views and conclusions expressed are those of the authors and do not necessarily represent the official policies of the U.S. Department of Defense, U.S. Department of Commerce, or the United States Government.

Certain commercial equipment, instruments, or materials are identified in papers published in this report in order to adequately specify the experimental procedure. In no case does such identification imply recommendation or endorsement by the National Bureau of Standards, nor does it imply that the material or equipment identified is necessarily the best available for the purpose.

Papers in this volume have not been edited by the National Bureau of Standards. Authors are solely responsible for the content and quality of their submissions.

Definitions of Humidity Terms

Saburo Hasegawa
Chemical Process Metrology Division
National Bureau of Standards
Gaithersburg, MD 20899

(301) 975-2620 or FTS 879-2620

Abstract: The units of humidity, assuming ideal gas behavior, are defined. The assumption of ideal gas behavior for the mixture of carrier gas and water vapor should not contribute uncertainties greater than 0.5% when making humidity measurements for hermetic semiconductor devices.

Key Words: absolute humidity; dew point; mixing ratio; relative humidity; specific humidity; volume ratio

1. INTRODUCTION

The subject of hygrometry is concerned with the determination or measurement of the water vapor content in a given free volume, occasionally as a separate entity, but more usually as a component of a mixture of gases. Humidity measurement involves, to a large extent, the basic laws of gaseous behavior. In many applications, it is sufficient to assume that the mixture of water vapor with a variety of gases obey the perfect gas laws. In actuality, the mixture deviates from ideal behavior, although at low densities the departures from ideality tend to a minimum. This assumption of ideal gas behavior for the mixture of water vapor and carrier gas found in hermetic semiconductor devices should not contribute uncertainties in excess of approximately 0.5%.

2. DEFINITIONS

As stated above, humidity measurement is the measurement of the water vapor content in a free volume. When vacuum and/or heat is applied to a material, free and bound water is released from the material. The total water content is often referred to as the sum of the released water vapor from the material and the water vapor of the free volume. The amount of water released from a particular material is dependent on such variables as the vacuum and temperature applied to the material and the duration of the test. In general, there is no one-to-one correlation between the measurements of

total water and water vapor in the free volume. However, for a specific artifact it may be possible to develop a detailed testing recipe to correlate the measurement of total water content to humidity.

Occasionally, it may be desired to convert from a reported humidity unit to one which is more descriptive of the environmental condition for a particular application [1]. This should pose no problem if the temperature and pressure of the free volume are reported with the humidity unit. Then the conversion to other units can be made easily by using the perfect gas laws.

a) Absolute humidity, vapor concentration or vapor density, d_v - the ratio of the mass of water vapor m_v to the total volume of the moist gas V:

$$d_v = \frac{m_v}{V} = \frac{e}{T} \frac{M_v}{R}$$

where e is the partial pressure of the water vapor in the moist gas, T is the absolute temperature, M_v is the molecular weight of water, and R is the universal gas constant.

b) Dew point, t_d - the temperature at which ambient water vapor begins to condense on a flat surface. The saturation vapor pressure of water at the dew-point temperature $e_s(t_d)$ is equal to the partial pressure of the water vapor in the moist gas.

$$e_s(t_d) = e$$

The equilibrium humidity in a small volume package can be significantly altered by an in-situ dew-point measurement. The amount of water vapor required for the detection of the condensation point can reduce the amount of water vapor in the small volume and cause an underestimation of the humidity.

c) Mixing ratio, humidity ratio, mass ratio, r - the ratio of the mass of water vapor m_v to the mass of dry gas m_g present in the moist gas:

$$r = \frac{m_v}{m_g} = \frac{e}{P-e} \frac{M_v}{M_g}$$

where P is the total pressure and M_g is the molecular weight of the carrier gas.

d) Relative humidity, U - the ratio of the partial pressure of the water vapor in the moist gas e to the saturation vapor pressure e_s at the temperature of the gas:

$$U = \frac{e}{e_s} \times 100, \%$$

e) Specific humidity, q - the ratio of the mass of water vapor m_v to the total mass $(m_v + m_g)$ of the moist gas:

$$q = \frac{m_v}{m_v + m_g} = \frac{r}{1+r}$$

f) Volume ratio expressed as parts per million, ppm-V - the ratio of the volume of the water vapor V_v to the total volume:

$$\frac{V_v}{V} \times 10^6 = \frac{e}{P} \times 10^6, \text{ ppm-V}$$

With the use of the above definitions for the units of humidity and by referencing the measured unit to the temperature and pressure of the package and reporting the temperature and pressure, the in-situ humidity can be easily converted to other units with the use of a saturation vapor pressure table for water. Additional information on hygrometry definitions is given in references [2,3].

3. VAPOR PRESSURE FORMULATIONS

There are a number of formulations for the saturation vapor pressure for water and ice. The following are a few examples of suitable formulations for use in most application of hygrometry.

Formulations for saturation vapor pressure over plane surface of water:

Goff-Gratch [4]. The saturation vapor pressure tables for temperatures -50 to 100° C are also published in the Smithsonian Meteorological Tables, 6th revised edition, Smithsonian Institution Press, Washington, DC.

Wexler [5]. The saturation vapor pressure tables for temperatures -50 to 100° C are also published in the ASTM D4230, "Standard Method for Measuring Humidity with Cooled-Surface Condensation (Dew-Point) Hygrometer," American Society for Testing and Materials, Philadelphia, PA 19103.

Wexler and Hyland [6]. Covers the temperature range 273.15 to 473.15 K.

Haar, Gallapher and Kell [7]. NBS/NRC Steam Tables covering the temperature range 260 to 2500 K.

Formulations for saturation vapor pressure over plane surface of ice:

Goff-Gratch [4]. The saturation vapor pressure tables for temperatures 0 to -100° C are also published in the Smithsonian

Meteorological Tables, 6th revised ed., Smithsonian Institution Press, Washington, DC.

Wexler [8]. The saturation vapor pressure tables for temperatures 0 to -100° C are also published in the ASTM D4230, "Standard Method for Measuring Humidity with Cooled-Surface Condensation (Dew-Point) Hygrometer," American Society for Testing and Materials, Philadelphia, PA 19103.

Wexler and Hyland [6]. Covers the temperature range 173.15 to 273.15 K.

4. DISCUSSION

A set of definitions for humidity units, assuming ideal gas behavior for the mixture of water vapor and carrier gas, has been presented. If the pressure and temperature are reported with humidity, the conversions from one humidity unit to another may be made.

REFERENCES

1. Davy, J. G., Thermodynamic and Kinetic Considerations of Moisture Sorption Phenomena, Proc. of the NBS/RADC Workshop on Moisture Measurement Technology for Hermetic Semiconductor Devices, II, Gaithersburg, MD, Nov. 5-7, 1980, pp. 184-200.

2. Harrison, L. P., Fundamental Concepts and Definitions, Humidity and Moisture, A. Wexler (ed.), Vol. 3, Reinhold Publishing Corp., NY, 1965, pp. 3-69.

3. D4023, Standard Definitions of Terms Relating to Humidity Measurement, American Society of Testing and Materials, Philadelphia, PA 19103.

4. Goff, J. A., Saturation Pressure of Water on the New Kelvin Scale, Humidity and Moisture, A. Wexler (ed.), Vol. 3, Reinhold Publishing Corp., NY, 1965, pp. 289-292.

5. Wexler, A., Vapor Pressure Formulation for Water in the Range 0 to 100° C, A Revision, J. Res. Nat. Bur. Stand. (U.S.), 80A, No. 3, 505 (1976).

6. Wexler, A. and Hyland, R. W., Formulation for the Thermodynamic Properties of the Saturated Phases of H_2O From 173.15 to 473.15 K, ASHRAE Trans., 89, Part 2A, 550-519 (1983).

7. Haar, L., Gallagher, J. S., and Kell, G. S., NBS/NRS Steam Tables, Hemisphere Publishing Corp., Washington, DC, 1983.

8. Wexler, A., Vapor Pressure Formulation for Ice, J. Res. Nat. Bur. Stand. (U.S.), 81A, 5(1977).

1.1 HELIUM LEAK DETECTOR FOR SMALL COMPONENTS

Lyle E. Bergquist and Stephen R. Shertz

Martin Marietta Denver Aerospace
Department 0560
Post Office Box 179
Denver, Colorado 80201

ABSTRACT

A helium leak detector has been developed that detects both gross and fine leaks in small components. Leaks in a 0.15 cc component are measurable with a hole as large as 0.5 mm in diameter to as small as 10^{-12} atm cc/s of helium at 22°C. The unique component in the leak detector system is a modified cryopump that is used both as a roughing pump and entrainment pump for gases other than helium. Helium, if entrapped, is at a very low level. With the great range of system sensitivity, bombing of parts can be eliminated in most cases. Use of 1% helium in the fill gas when the part is sealed will be an adequate fine leak test if tested within a few minutes after being sealed. Gross leaks can be detected by using the helium in the atmosphere. This system reduces test time and unit costs.

INTRODUCTION

The reliability of small electronic components depends to a great extent upon how well the component is sealed from reactive gases and water vapor. The test for determining the hermetic seal is important. The method described in this paper is a concept where both gross and fine leaks are measured in one test. This concept uses a modified cryopump where the gases from in the test manifold are cryopumped and the helium that escapes from the component remains in a gaseous state. If the leak is a gross leak, the amount of helium is indicated; if the leak is a small leak, the rate of helium coming from the part is measured. After the measurement is completed, the helium is evacuated from the system by either a turbomolecular pump or a diffusion pump.

BACKGROUND

Presently, there are several methods for determining the leak rates in small components. First, the component is placed in a pressurized container and then backfilled with a gas. The gas is usually helium or krypton. After a specified time and pressure the component is removed and then tested. With helium, the component may be fine leak tested with a helium-type mass spectrometer or gross-leak tested by submerging the compound in a heated fluid and

observing the bubbles that emerge as helium escapes from the component. In krypton, a radioactive isotope is present and tests are made to determine if any radioactive emissions can be detected.

There are two other approaches used for gross-leak tests: (1) measure the weight change; and (2) measure the hydrocarbon vapor release after pressurizing with a gas.

The bubble test is reported to find only a portion of nonsealed components. Radioactive krypton is reported to damage memory storage components. Hydrocarbons entering a device can contaminate and reduce the efficiency in certain hybrid components and this test presently is useful only for gross-leak testing. The major advantages of the method described in this paper are that both gross and fine leaks can be measured with the same instrument and during the same test cycle. The unit test costs are reduced as well as the handling costs. Leaks in a 0.15 cc component can be determined for a hole as large as 0.5 mm in diameter to as small as 10^{-12} atm cc/s of helium at 22°C. A recommended operational procedure is to use 1% helium in the gas when sealing the component. This will allow leak rate measurements in the 10^{-8} atm cc/s for many components for a period of a year. Helium pressure bombing of the components may be necessary to measure leak rates in the 10^{-4} to 10^{-6} atm cc/s at 20°C unless the component is tested immediately after being sealed. Gross leaks can be detected by using the helium that enters the component along with the atmospheric air.

APPROACH

In this system, a modified cryopump is used as a roughing pump as well as a high vacuum pump. A turbomolecular pump is used to exhaust the helium once it is measured. A quadrupole gas analyzer is currently being used as a detector, but a simpler magnetic, sector-type mass spectrometer can also be used.

Figure 1 is a schematic of the leak detector. The operational sequence is as follows:

1) The system is evacuated and the cryopump cooled.
2) V_1 and V_3 are closed and V_2 is opened: the purge gas fills the test volume.
3) V_1 is opened: the test components are removed and new ones are inserted in the test volume.
4) V_1 and V_2 are closed and also V_4: the chamber is sealed and the detector is protected.
5) V_3 is opened: the purge gas is cryopumped. The helium that escapes from the components under test remains in a gaseous state. All the helium that escapes from the components under test is contained.
6) V_5 is closed.
7) V_4 is opened: the amount of helium in the system is measured or the rate of rise of helium is determined. From this the size of the leak can be calculated.
8) V_5 is opened: the helium is exhausted.
9) V_3 is closed and the cycle is repeated.

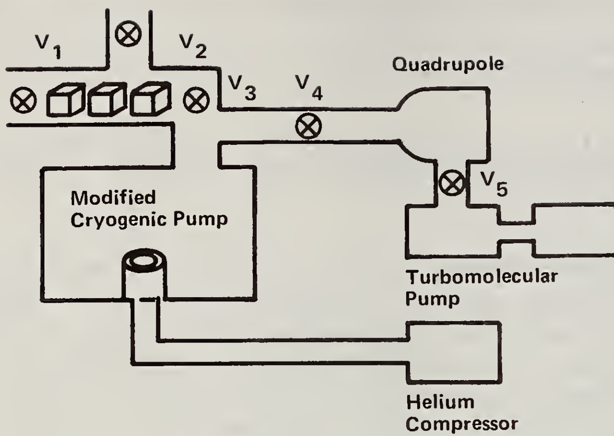

Figure 1 Schematic of Leak Detector System

The time for a cycle depends upon the size of the manifold in which the component or components are placed for test. If the volume is 5 cc, the time can be a few seconds. If the volume is 80 cc, a cycle can be completed in about 30 seconds. If the volume is 250 cc, the time is longer, about 2 minutes. With 250 atm cc of gas the cryopump warms up slightly and must recover its heat loss. With 5 atm cc of gas the time depends upon the sticking coefficient of the gas on the cryopump and then the actual measurement of the helium. With this system at least 400 atm liters of nitrogen (manifold gas) can be entrapped in the cryopump before the cryopump needs to be regenerated.

A significant factor in this system is that the sensitivity of the system is enhanced because the pumping speed is almost zero for helium.

The equation is:

$$\text{Sensitivity of System} = \frac{\text{Sensitivity of Detector}}{\text{Pumping Speed of Trace Gas}}$$

If the pumping speed for helium is zero, the theoretical sensitivity for the system is infinite and the helium will accumulate. This sensitivity may be limited because a small amount of helium may be pumped by the cryopump. This amount has not been determined, but is less than an equivalent leak rate of 2×10^{-12} atm cc/s. Also, a small amount of helium may be in the gas that fills the manifold. In this vacuum system, it is necessary to have low helium desorption rates. This is accomplished by eliminating all organic seals as well as glass feedthroughs. Metallic gaskets and ceramic feedthroughs are used throughout the vacuum system.

This system measures either the amount of helium or the rate in which the helium is released from the component. If the leak is gross, all the helium will have escaped from the package during the evacuation and the amount will be detected. This will be measured as a flat line. If the leak is small, the rate in which it escapes will be measured.

Figure 2 is a graph of some leak rate possibilities. Components having large leaks in small packages will be exhausted in one second or less since no helium pumping is occurring during the time. The turbopump is valved out of the system. The output from the detector in amperes will indicate a constant level. With smaller leaks the output will indicate a rate of rise versus time by using a calibrated leak and recording this rate of rise.

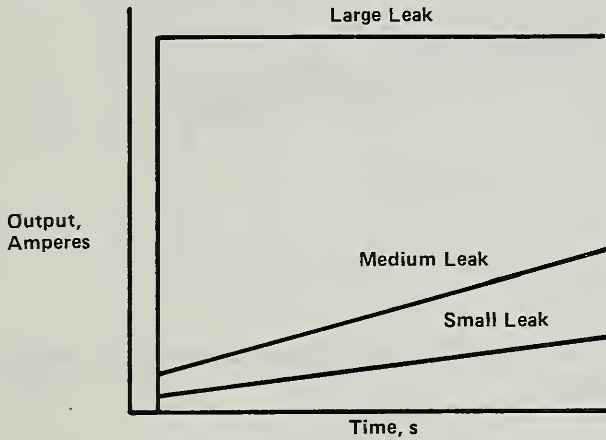

Figure 2 Helium Leakage Measurement

The measurement of low-level helium levels requires a mass analyzer that can resolve HD with a mass-to-charge rate of 3 to helium with a mass-to-charger rate of 4. Figure 3 is a graph of these two masses. The resolution is adequate so no interference comes from mass 3 while monitoring the helium peak.

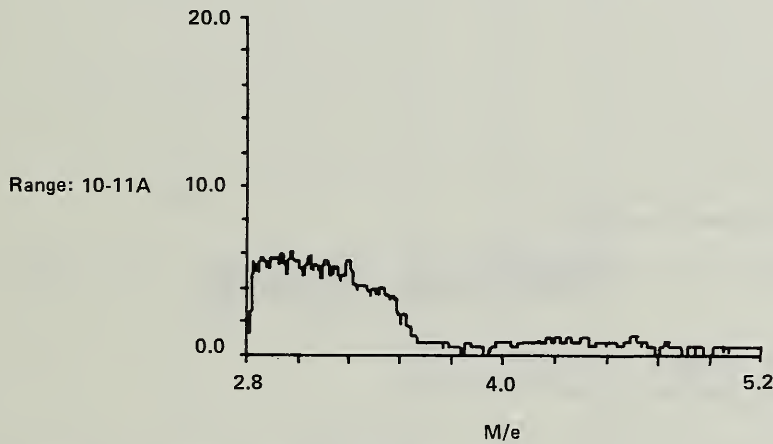

Figure 3 Resolution between M/e 3 and M/e 4

Figure 4 is a typical rate of rise from a calibrated helium leak with a leak rate of 7.6×10^{-10} atm cc/s at 20°C. Using this measurement, it can be compared with other rates of rise to determine the leak rate of other components under test.

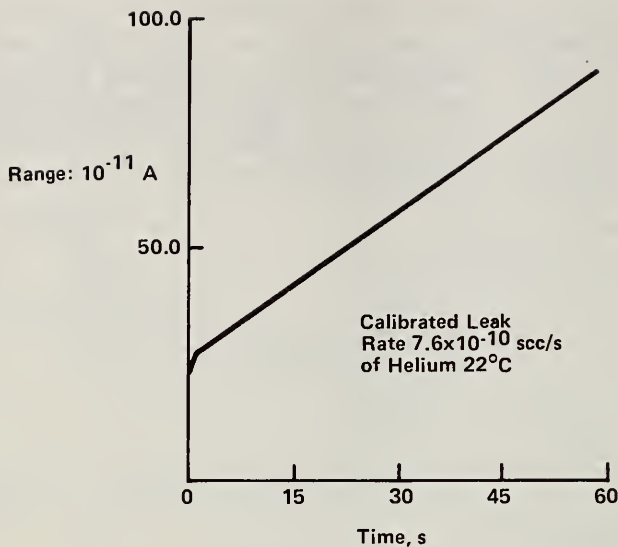

Figure 4 Calibration of System Valve to Turbo-Molecular Pump Closed

Figure 4 shows the result when a 0.10 cc volume with a conductance of 1.5 cc/s is measured. Only helium in atmospheric air was used for this measurement. The line is straight, which indicates that all the helium escaped the 0.10 cc volume when the backfill gas in the manifold was cryopumped.

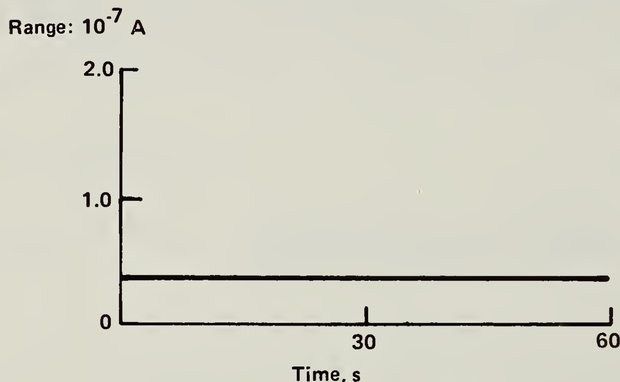

Figure 5 Calibration of System Using 0.1-cc Volume with Conductance of ≈ 1.5 cc/s Helium in Air

Figure 6 shows the helium background caused by having a glass-enclosed ion gauge in the system. This particular gauge had a helium leak equivalent to $1.6x10^{-12}$ atm cc/s of helium at 22°C. Ion gauges of this type have helium leakages from $2x10^{-11}$ to about $1x10^{-12}$ atm cc/s of helium. This device is used to see if helium is being cryopumped in the system.

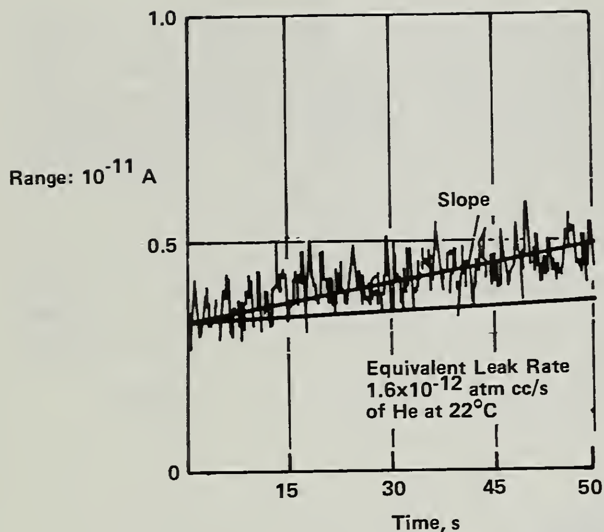

Figure 6 Helium Entering System from Glass Ion Gauge

Figure 7 shows a graph of the helium in the system when the ion gauge is valved out of the system. The rate of rise is 6×10^{-13} atm cc/s of helium at 22°C.

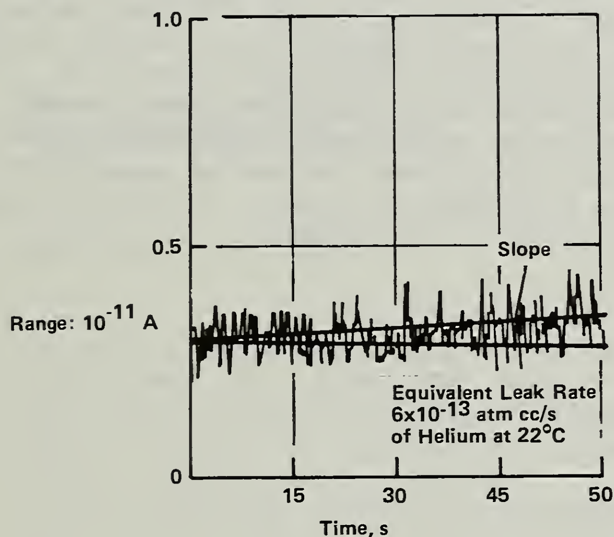

Figure 7 Helium Background in System

Figure 7 is an example of testing TO5 transistor packages with a different size hole in each package. These holes were 0.2, 0.3, and 0.4 mm in diameter. In a package with 0.8 mm, the air escaped while inserting it into the manifold. In these tests only atmospheric air and the helium in the air was used.

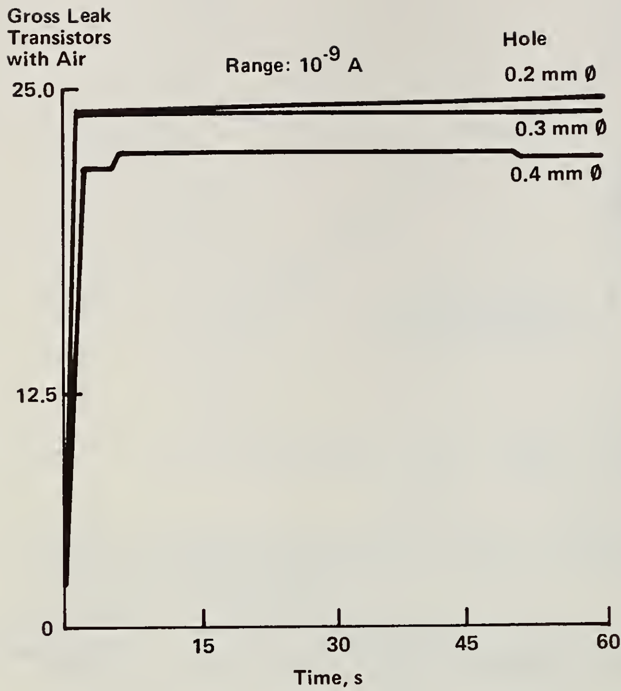

Figure 8 Gross Leaks in TO5 Transistor Package Using Helium in Air

Figure 9 shows the findings when a hybrid package was tested. The dimensions of this package were 2x2x1/4 in. and were backfilled with 10% helium, with the remainder being nitrogen. The free space in the hybrid was about 3 cc. The volume of the manifold was nearly 300 cc and a little helium from the air entered. If the leak was gross, the measured output would have been several decades higher. A stabilizer plate was placed over the sealed plate with epoxy and some air bubbles could have come from the epoxy. Air bubbles were detected in a previous test using the bubble test method.

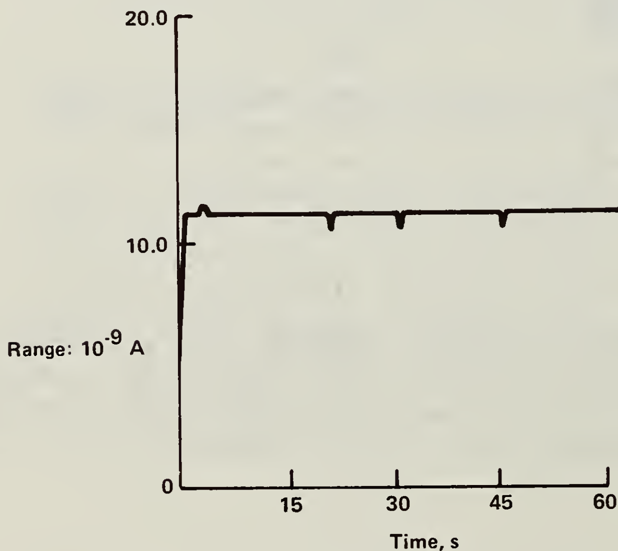

Figure 9 Test for Gross Leaks in Package 2x2x1/4 in.

Figure 10 shows fine leak testing the same hybrid by evacuating the helium from the previous measurement and detecting the rate of rise of helium coming from the hybrid package. This rate was less than 10^{-10} atm cc/s of helium at 22°C. The requirement for this component was less than 10^{-8} atm cc/s for helium.

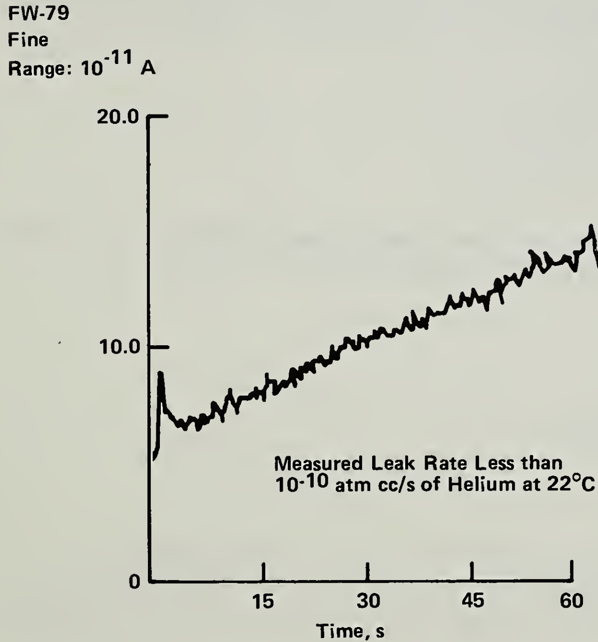

Figure 10 Fine Leak Test in Package Sealed with 10% Helium Package 2x2x1/4 in.

ANALYSIS OF FINDINGS

The system has a sensitivity range to easily measure leak rates filled with 1% helium that have actual leak rates of 1×10^{-8} atm cc/s at 20°C. Gross leaks with holes as large as 0.4 mm in diameter can be detected in 0.15 cc components. This can be determined by detecting the helium that entered the component from the atmospheric air. If 0.1 cc component remains in atmospheric air for more than 2 hours, bombing with helium will be necessary to measure leak rates in the 10^{-5} - 10^{-6} atm cc/s region.

Bubbles were observed in the hybrid package during the gross leak checking process using the bubble test method. However, it was proven that these bubbles came from the epoxy and not from the sealed hybrid. The hybrid was later tested by opening it and had 10% helium with the nitrogen. This was a costly hybrid design and saved the manufacturer from scraping the unit.

CONCLUSIONS

A helium leak detector has been designed that can test for both gross and fine leaks. Either the helium that has escaped from the component is measured or the rate in which it escapes is measured. With this detector system most components can be tested if the component is filled with 1% helium during the sealing process and immediately tested. Otherwise, bombing with helium is necessary. This saves several operations during the leak checking process.

REFERENCE

Bergquist, L. E.: "A Helium Leak Detector for Small Components," in 23rd Annual Proceedings Reliability Physics, 1985, pp 65-67.

1.2 PERMISSIBLE LEAK RATES AND MOISTURE INGRESS

Aaron DerMarderosian
Raytheon Company
Equipment Division
Sudbury, MA 01776

ABSTRACT

A guideline is presented which addresses the maximum leak rate acceptable for hermetically sealed devices as a function of internal package volume and moisture content.

The guideline is based on work detailing the rate at which water vapor penetrates packages with known leak rates and calculations on the quantity of water needed to form an ionically conductive film on the internal surfaces of the package. The results indicate in general that present standards are far too lenient.

Introduction

A review of the literature dealing with packaged semiconductors reveals that a large percentage of the failures are associated with one type of corrosion mechanism or another.[1-8] Moisture has, and continues to play a large part in this mode of failure. The sources of moisture in these packages have been delineated in various papers [9-11] and may be categorized as follows: 1) entrapped water due to poor bake out procedures 2) generated internally by decomposition, material outgassing or devitrification of sealing glasses 3) permeation thru polymer seals and 4) penetration of cracks and/or faulty seals. It is this latter area which is probably the least well understood and has, in part, been due to the lack of published information on this subject matter. Some work in this area has been published by Davy [12, 13] and Stroehle [14] highlighting the inadequacies of present leak testing practices and specifications. The work by Davy was essentially limited to a theoretical treatment while the work of Stroehle combined a theoretical discussion with the experimental failure rate of a specific part type in high humidity to its leak rate as measured on a helium leak detector. The purpose of this work is to add to this data base and provide for some rationale in the specification of maximum allowable leak rates for hermetically sealed devices. The study focuses, experimentally, on the rate of moisture penetration into cavities (at zero total pressure difference as one might expect at normal ambient conditions) as a function of leak rate measured during standard test conditions of 15 psi pressure differential. The results of these experiments are then compared to a theoretical analysis using established gas flow equations typically used in vacuum technology.

Experimental Studies

Gross Leak Range (10^{-1} to 10^{-5} atm cc/sec)

The test samples used in this portion of the study were fabricated using a standard TO-5 transistor can fitted with a 1 mm glass capillary tube and a miniature surface conductivity type moisture sensor.

The capillary tubes were intially exposed to a flame at one end until melting occurred. This heating subsequently reduced the I.D. of the tip of the tubing, thereby providing for a method of producing leakers over the range of interest (see Figure 1). Tubes fashioned in this manner were then calibrated by using the rate of pressure rise method, a technique which determines the air leak rate at standard conditions of 15 psi differential. Briefly, the procedure is as follows; tubes are connected to a container of a known volume at a known pressure (usually 1 torr). Air is then allowed to leak through the capillary and into the container. The time required to raise the pressure to 2 torr (or 10 torr depending on the leak range) is measured and used to calculate the air leak rate for the capillary using the gas law equation ($PV = MRT$). This equation is used to determine the quantity of gas which leaks into the container, and when divided by the time in seconds required to raise this pressure to the set amount (2 torr or 10 torr), yields the air leak rate in atm cc/sec (see Figure 2).

This method is cumbersome and time consuming, however, and an alternate quicker method was employed to calibrate the remainder

of the capillaries. The technique is as follows; the calibrated end of the tube was submerged in FC-77 liquid while the other end was connected to a source of nitrogen gas. The gas pressure was slowly raised until bubbling was initiated at the leaky end. A graph was then constructed which depicts the differential pressure required to initiate bubbling as a function of air leak rate (see Figure 3).

Each of the capillary tubes which were calibrated with this faster method were then sealed to the cover of a TO-5 can containing a calibrated moisture sensor (see Figures 4 & 5).

The moisture sensors were calibrated prior to sealing by exposing them to various saturated salt solutions of known relative humidities at room temperature and monitoring the change in surface leakage at each of these conditions (see Figure 6).

Test Procedure and Results. The completed test samples were placed, leaker side down, thru a test plate pre-drilled to accept the TO-5 package cover. The parts were then wax sealed at the edges and then exposed to a relative humidity (saturated salt solution) of 80% at room temperature (~22°C average). The rate of moisture penetration was monitored as a function of time with each of the surface conductivity sensors. Prior to the test the parts were stored for ~ 1 month in an ambient environment of 15% RH @ 22°C, thereby establishing an initial water vapor pressure of ~3.4 torr within the package.

The parts remained in the 80% R.H. ambient until equilibrium was reached for the smallest leakers. The time constant for each of the devices was then obtained from this data and ranged from

$\sim$ 0.6 hours (10^{-1} atm cc/sec, air) to $\sim$ 700 hours (10^{-5} atm cc/sec, air). From these time constants the "water vapor" leak rate in cc/sec* was calculated using the following:

[1] $Q = \frac{V}{T}$ Where: Q = water vapor leak rate in cc/sec.
V = volume of package in cubic centimeters (TO-5 = .17 cc)
T = time constant (time required to reach 63% of equilibrium pressure) in seconds.

The values of these time constants and the water vapor leak rate data are plotted in Figures 7 and 8.

Fine Leak Range (10^{-6} to 10^{-8} atm cc/sec)

The test samples used for this portion of the study were fabricated from 14 lead, 1/4 X 1/4 inch ceramic flat packages. The samples contained surface conductivity moisture sensors of lower sensitivity than those used in the gross leak study (only 2 parallel strips) and were calibrated in a manner similar to the method used in the TO-5 study. The leakers were generated by thermally shocking the devices from +200°C air to -196°C (liquid nitrogen). The shapes of the leaks created by this method were found to be cracks in the seal area in and around the leads. The leak testing of the devices was performed by using method 1014 of MIL-STD-883 B (flexible method A_2 - Helium). The leak rates were established through the use of computer generated curves which

---

* A cc of water vapor is defined here as that quantity of moisture contained in one cubic centimeter of air at atmospheric pressure and 22.2°C when the partial pressure of water vapor is 16.1 torr ($\sim$ 80% R.H. @ 22.2°C).

plot the indicated leak rate (R) as a function of air leak rate (L) and take into account the volume of the part and the various bombing parameters[15] (e.g. pressure, pressurizing time, etc.). All parts were tested on the leak detector at least twice at known intervals to help establish the leak rate more accurately e.g. typically an indicated or measured leak rate has two points on the curve, one of which corresponds to the lower end of the spectrum while the other point corresponds to the higher end (see Figure 9). To determine which of the two possible leak rates it is, another measurement is necessary at some period of time later (typically 1-2 hours). If the second reading remains the same as the first, then the leak rate is determined from the fine leak end, conversely if it is significantly less, then the leak rate is determined from the higher leak end.

Approximately 25 pieces were measured to have an air leak rate in the 10^{-6} atm cc/sec range; another 16 in the 10^{-7} atm cc/sec range; 10 in the 10^{-8} atm cc/sec range and 1 in the 10^{-9} atm cc/sec range.

<u>Test Procedure and Results</u>. The completed samples were placed into a dessicator jar which contained a saturated salt solution identical to that used in the gross leak study (80% RH @ 22°C). The devices were periodically removed from the chamber and monitored for moisture content by measuring the change in surface leakage on the moisture sensors. Prior to this test, the devices were subjected to an ambient of P_2O_5 for a period of three weeks. It is conservatively estimated that the parts reached an internal dew point

of $-15^{o}C$ (water partial pressure of ~ 1.4 torr) under these conditions.

The parts remained in the 80% RH ambient until equilibrium was reached for the smallest leakers (as noted by the sensors) the time constant for each of these devices was then obtained from this data and ranged from a low of ~ 10 hours (10^{-6} range) to a high of ~ 280 hours (10^{-9} range). The water vapor leak rates were calculated as before (equation 1) using an internal volume of 0.008 cc for these devices. The values of these time constants and leak rate data are plotted in Figures 10 and 11.

The performance of these devices were markedly different from the performance of the capillary leakers used in the gross leak tests. The main difference was the wide variation in equilibration times noted between parts with the same air leak rate. In some cases, varying by nearly an order of magnitude! This type of performance possibly suggests that the leak rate may be affected by pressure differentials either during test and/or during the helium "bombing" environment of 75 psig.

Another likely possibility may have been capillary condensation within the crack which may have altered the penetration rate significantly. This effect was substantiated somewhat by post humidity leak test measurements. Approximately 35% of the devices had indicated that they had been plugged sometime during the test while another 15% indicated a change in leak rate. A subsequent bake @ $150^{o}C$ for 24 hours returned many of the parts to their original values yet nearly 4% remained plugged while another 25% never returned to their former leak rates.

A greater understanding of the behavior of these irregular leak paths is necessary before much more can be concluded from this data. It is clear, from the short time constants measured, that water vapor can penetrate so called fine leakers and, if these parts are typical, it becomes obvious that present specifications (MIL-STD-883B) for maximum allowable leak rates are too lenient for high reliability devices.

Theoretical Studies

Gross Leak Range (10^{-1} to 10^{-5} atm cc/sec)

A review of the fundamental gas flow equations[16] delineates three definable areas of flow regime; namely viscous, transitional and molecular each of which is described below.

Viscous Flow

Viscous flow occurs when the mean free path of the gas is smaller than the cross-section dimension of the physical leak. Poiseuille's Law for viscous flow through a cylindrical tube is shown.

$$Q = \frac{\pi r^4}{8\,nl} \times 10^{-3} \quad P_a \quad (P_1 - P_2) \qquad [2]$$

or

$$Q = \frac{\pi r^4}{16\,nl} \times 10^{-3} \quad P_1^2 - P_2^2 \qquad [3]$$

where:

Q = flow rate in micron liters/sec

r = radius of tube in centimeters

n = viscosity of gas in poise

l = length of tube in centimeters

P_a = average pressure $\frac{P_1 + P_2}{2}$ in microns

P_1 = upstream pressure in microns

P_2 = downstream pressure in microns

Transition Flow

Transition flow occurs when the mean free path of the gas is approximately equal to the cross-section dimension of the leak and it occurs under conditions intermediate between viscous flow and molecular flow. Again for a long tube, the flow may be expressed as shown below. As can be seen, the expression is more complex than that for the other types of flow. Note that the portion outside the brackets is identical to the expression for molecular flow.

$$Q = \frac{30.48 \quad r^3}{l} \sqrt{\frac{T}{M}} \quad (P_1 - P_2) \left[\frac{0.1472r}{La} + \frac{1 + 2.507 \quad r/La}{1 + 3.095 \quad r/La} \right] \qquad [4]$$

where:

Q = flow rate in micron liters/sec

r = radius of the tube in cm

l = length of the tube in cm

M = molecular weight of gas in amu

P_1 = upstream pressure in microns

P_2 = downstream pressure in im microns

T = temperature in $^{\circ}K$

L_a = mean free path in cm at the average pressure

$$\frac{P_1 + P_2}{2}$$

Molecular Flow

Molecular flow occurs when the mean free path of the gas is greater than the longest cross-section dimension of the physical leak. Knudsen's Law for molecular flow neglecting the end effect is shown.

where:

$$Q = \frac{30.48 r^3}{l} \sqrt{\frac{T}{M}} \left(P_1 - P_2\right) \qquad [5]$$

Q = flow rate in micron liters/sec

r = radius of tube in centimeters

l = length of tube in centimeters

M = Molecular weight of gas in amu

P_1 = upstream pressure in microns

P_2 = downstream pressure in microns

T = absolute temperature in ^oK

Each regime has its own equation describing the effects of the geometric considerations of the leak path along with various gas parameters. An examination of these equations and methods used to determine flow characteristics (Figure 12), suggests that leakers in the gross leak range (10^{-1} to 10^{-5} atm cc/sec) fall into the viscous and transitional flow regime under standard test conditions (15 PSIA on one side of the leak and 0 PSIA on the other side of the leak). Using these assumptions and a leak length path of 0.6 mm, calculations of the air leak rate as a function of hole diameter at standard conditions were performed and are shown graphically in Figure 13. Knowing this "effective"

diameter of the capillary leaker enables one to then calculate the water vapor leak rate as a function of the hole diameter under any of the gaseous flow regimes using the equations given. Since, in the case of our experiment with the capillary leakers, there was no difference in total pressure between the inside and outside of the device during humidity exposure, we chose the molecular flow equation to calculate the rate of moisture penetration and plotted the results in Figure 14. In addition to this, the results of calculations for water vapor penetration using the Combined Flow Equation of Davy[12] were plotted with it. The two equations differ considerably at the larger diameters (~2 orders of magnitude) yet join together and agree closely at the smaller diameters and are essentially the same thereafter. There is no intent here to suggest which equation is more correct, rather they are offered as a point of discussion to help place the problem within certain boundaries.

Calculations of water vapor leak rates at a partial pressure difference of 12.7 torr, as a function of air leak rates (15 psi pressure differential) were then performed using the molecular flow equation. These results along with the results of experimental data are shown graphically in Figure 15. Again, the results of calculations taken from the Combined Flow Equation are presented with it for the sake of comparison. It can be seen from this graph that the experimental data tends to agree more closely with the molecular flow equation at the higher leak rates while either one of the equations adequately describes the moisture penetration rate at the lower values of air leak rates.

Finally, calculations were performed @ 80% R.H. (molecular flow eq.) which indicate the rise in dew point of the TO-5 package vs time as a function of air leak rate. The results are shown in Figure 16.

<u>Fine Leak Range (10^{-6} to 10^{-8} atm cc/sec</u>

The theoretical considerations in this portion of the study were simplified somewhat because of the general agreement among various investigators[12,18] in that the predominant flow mechanism in the fine leak end of the spectrum is molecular. This agrument is further strengthened by analysis of the geometry of leaks (essentially thin cracks) and their approximate dimensions (on the order of 10^{-5} cm or less in thickness and up to ~ 1/2 a cm in length). A detailed analysis of this subject is given by Davy[13] and is recommended for those wishing to pursue this matter further.

In performing the calculations for the fine leak spectrum the following assumptions were made: the flow was molecular and the gas passed through a single capillary hole of "equivalent effective" diameter (0.9 mm long). The results of calculations of hole diameter as a function of std. air leak rate are shown in Figure 17. Knowing this "effective" diameter we then calculated the water vapor leak rate as a function of hole diameter. The results of these calculations are shown in Figure 18 and are combined with the experimental data, generated earlier, in Figure 19. Examination of the latter graph indicates a significant difference in the 10^{-7} to 10^{-8} atm cc/sec range between the experimental and theoretical

data while reasonable agreement exists in the 10^{-6} range. It is not known at this time why such a variance exists between the data. Several areas are suspected and will be addressed in follow-on experiments.

Finally, a series of calculations were performed which determined the water vapor penetration time constant for several typical package types as a function of standard air leak rate. The results are shown in Figure 20 and highlight again the leniency of leak rate specifications and the need for more definative limits for high reliability applications.

Discussion

Many fundamental questions relating to the rate of moisture penetration into packages with known air leak rates have been answered during this study. Although some questions remain, the author feels that sufficient data was obtained to establish analytical methods that address this issue. It is interesting to note that the test results of this program support the basic premise of Davy[13] and Stroehle[14], that moisture rapidly penetrates devices with leak rates as low as 1×10^{-8} atm cc/sec.

Gross Leak Range (10^{-1} to 10^{-5} cc/sec)

The results of this portion of the study were encouranging to say the least, considering the close correlation obtained between the experimental and theoretical data. Regardless of this agreement, however, it was perfectly clear that the water vapor penetrated these small diameter holes very rapidly, thereby resolving long standing questions relating to this issue. Another frequently raised question is that of capillary plugging due to condensation

in small diameter holes. The glass tubes used in this study were very informative with regard to this matter. Approximately 20% of the devices were plugged with water almost immediately after exposure to the high humidity atmosphere. Optical inspection of the larger leakers ($\sim 10^{-2}$ cc/sec range) revealed that liquid water was trapped in the narrow passageway. Subsequent heating in a flame, however, quickly removed the moisture and exposed small quantities of contaminants believed to be responsible for the initial absorption of moisture. When these tubes were returned to the high humidity conditions they allowed water vapor to pass through at a normal rate. It is felt that the rapid heating and high temperature obtained with the flame altered the behavior of the contaminants thereby allowing the moisture to pass through. Since all of the plugged devices could be "cleaned" by flame heating, it was concluded that the condensation was not related to true adsorption on the walls of the capillary.

Fine Leak Range (10^{-6} to 10^{-8} atm cc/sec)

The deviation noted between the experimental and theoretical data obtained in this part of the study was somewhat discouraging at the outset. Considering the complexity of the leak path geometry, however, and the method of determining their leak rates this could be expected. The author feels that a follow on study addressing these issues in greater detail, will answer most of the questions raised during this experiment. It is important to note and stress, however, that water vapor did penetrate those parts with leak rates as low as 1×10^{-8} cc/sec in a relatively short period of time.

As mentioned earlier in the test results, many of the fine leakers indicated that they had plugged during exposure to the high humidity atmosphere, and that most of them returned to their original leak rates after heating. Since visual observation of the leak paths was not possible (cracks widths in the order of 10^{-5} cm) little could be learned about the details of the plugging and if contamination was a factor. The fact that some parts (~4%) were plugged "permanently" and that others (~ 25% did not return to their original leak rate suggests that true capillary condensation may have occurred and/or the leak pathway had been altered. The unrepeatable behavior of these parts suggests that the cause of problems encountered with leak test correlation studies may be related to ambient humidity levels or handling seen at the testing facilities or during transport.

Leak Rate Specification*

In view of the results of the moisture ingress study, a set of guidelines were developed which can be useful for those involved in component specification and procurement. The guidelines were developed by first examining the present military standard (MIL-STD-883B) which specifies maximum allowable leak rate and maximum allowable package ambient moisture content. Assuming that a package is dry when sealed, a series of calculations were made utilizing the moisture ingress equations developed in our earlier work. The following equation defines the moisture ingress time constant of any size package as a function of its standard air leak

---

*The reader is encouraged to examine the work by others who have addressed this same issue.[12,13,19,20]

rate and is given as:

$$T = \frac{.011V}{Q_A}$$

where T = Time constant in hours for H_2O vapor ingress (63%)

V = Internal volume of device in cubic cent.

Q_A = Air leak rate in std. cc/sec

This equation was used to calculate the time required to exceed a moisture level of both 5000 ppm_V (present limit for Method 1018, MIL-STD-883B) and 500 ppm_V (proposed future standard 1988-1990) for packages with internal volumes ranging from .009 to 5cc. The information was then compared to the maximum allowable leak rates as specified in method 1014 of MIL-STD-883B fine leak test helium and krypton 85. Figures 21 through 23 show the results of these calculations and dramatically highlight the inadequacy of the fine leak test specifications for the greatest majority of today's packages. These inadequacies are shown in three major areas: 1) The helium "fixed" method (Test Condition A_1) is inconsistant with the "flexible" method (Test Condition A_2) i.e., reject limits vary by a factor of 2 to 1. 2) The helium method is far more lenient than the krypton method (Test Condition B) i.e., reject limits are as much as 40 times more stringent, especially for larger volume packages and 3) None of these test conditions are adequate with respect to moisture ingress rates; especially for the lower volume packages (~ 1 cc). Although

the specification leaves much to be desired, it at least attempted to address the issue at that time ($\sim$1968 - 1977). Prior to the issuance of this specification, leak testing procedures were much more arbitrary and even more poorly executed.

In an attempt to update this specification and to provide the reader with a rationale for specifying a leak rate for high reliability semiconductor devices, a model was developed using the following assumptions:

1. The critical minimum water layer thickness which can support ionic transport is three (3) monolayers or 1.2×10^{-7} cm (1.2×10^{-7} gms/sq. cm).
2. The leak rate of the device does not change with time or temperature.
3. The package internal surfaces have a roughness factor of unity.
4. There is no absorption into the package materials (i.e., such as plastics or dessicants) nor any chemical reactions which would reduce the moisture level.
5. All of the moisture which leaks into the package is available for condensation and that it does not freeze.
6. The water condenses uniformly on all internal surfaces.
7. The package is equal in length and width and the thickness is one fifth of the length.
8. No serious consideration was given to non-uniform condensation. This is a rather lenient position taken on the part of the author and will be addressed at a future date.

Using the assumptions of item 7, a table was generated detailing the package dimensions, internal surface area, internal volume, and the ratio of the area to volume (see Figure 24). From this data and the three (3) monolayer threshold (Item 1) another table was generated which establishes the maximum allowable moisture content for packages with internal volumes ranging from 10^{-3} to 10^{2} cubic centimeters. These values of maximum moisture level range from 13,000 ppm_V for the smallest package to 280 ppm_V for the largest package! This might be surprising since some may intuitively feel that the numbers should be reversed. Examination of the role of the ratio of internal surface area to internal volume and the absolute moisture content, however, will quickly subdue these "feelings" (see Figures 25 and 26). Briefly, the high ratio of the surface area to volume in the smaller packages allows for more surface proportionately for moisture to condense on, hence, allowing for a more tolerant moisture content and vice versa for the large volume package with its small ratio of surface area to volume.

Examination of Figure 26 reveals the rather curious or possibly ironic piece of information concerning the present moisture limit of method 1018 in MIL-STD-883B. At the intersection of the dotted horizontal line at 5000 ppm_V and the three (3) monolayer sloped line, it can be seen that most D.I.P. and flat packages with volumes that range from 0.01 to 0.05cc have a limit of moisture content that is within ~20% of the current limit!

Finally, a series of calculations were made which involved the determination of the moisture ingress time (at a 13,000 ppm_V external

ambient)as a function of air leak rate using the three (3) monolayer limit discussed earlier. The information was obtained graphically by using Figure 27, the moisture ingress time displayed in an exponential curve as a function of time constant and the external ambient moisture level in ppm_V. These calculations appear in Figure 28. It should be noted that the .001cc volume has three (3) monolayer package moisture value of 13,000 ppm_V (Figure 25) and that five (5) time constants (T) were used to obtain the values for this package to reach this level. This departure from the straight line relationship is graphically illustrated in Figure 29. Further examination of Figure 29 again underscores the inadequacy of present leak rate specifications for "hermetic" devices with an expected life of $\geq$ 10 years. In addition, it is apparent that for packages with an internal volume of less than $\sim$ one (1) cm^3, the air leak rate should not exceed 1×10^{-8} atm cc/sec near the one (1) cm^3 range and 1×10^{-9} atm cc/sec near the 0.03 cm^3 range! Considering what the industry in general has been testing to, this is not welcome news. There is, however, some encouraging data from those who have examined overall leak rate distributions in devices. It has been noted that most devices which do not exhibit leakage greater than 1×10^{-8} atm cc of air/sec,tend not to leak at all. This is primarily due to the nature of defects in this size range, i.e., they are simply extremely difficult to produce intentionally or otherwise. This is no cause for complacency, however, since there

are other issues, such as crack propragation, package strength, etc., which could override these factors. This set of rather complicated factors suggests that packages and their resultant state of hermeticity should be carefully designed to assure initial and long term integrity. In the final analysis, the burden for this task lies with the packaging industry and those of us involved in reliability issues should exert the pressure necessary to accomplish it.

One important issue yet to be resolved is the correlation between moisture levels in the package and time to device failure. Although beyond the scope of this paper, the author feels that this question may be answered best by performing operational tests on open devices during exposure to humidity conditions. Various acceleration factors may be obtained from this data and be used to predict life times of devices with known leak rates at any given ambient humidity. Once established, this data could then be used along with other factors to help guide those involved in procurement specifications which address these types of reliability issues.

Conclusions

Based on the results of this study, several conslusions may be drawn. Some of the more important ones are as listed below:

1. Water vapor rapidly penetrates typical integrated circuit packages with leak rates as low as 1×10^{-8} atm cc/sec.

2. The rate of penetration of water vapor into packages which leak may be approximated by assuming molecular flow.

3. The maximum allowable leak rates specified in MIL-STD-883B (Method 1014) are too lenient in general and are especially so when considering the maximum proposed moisture level specification of Method 1018 (500 ppm).
4. The "fixed" methods of fine leak testing in MIL-STD-883B should be eliminated, allowing only for the flexible method.
5. The maximum allowable leak rate for all packages should be less than 1×10^{-8} STD cc of air/sec.

References

1. "Principles of Corrosion" S. Kolesar; 12th Annual Proceedings, Reliability Physics 1974 pages 155-167.

2. "Metallization Corrosion in Silicon Devices by Moisture Induced Electrolysis" H. Koelmans; 12th Annual Proceedings, Reliability Physics 1974 pages 168-171.

3. "The Effects of Phosphorous - Doped Passivation Glass on the Corrosion of Aluminum", W. Paulson and L.W. Kirk; 12th Annual Proceedings, Reliability Physics 1974 pages 172-179.

4. "Temperature Humidity Acceleration of Metal - Electrolysis Failures in Semiconductor Devices", D.S. Peck and C.H. Zierdt, Jr. Bell Telephone Laboratories Report.

5. "Failure Analysis Techniques Applied in Resolving Hybrid Microcircuit Reliability Problems", G.H. Ebel 15th Annual Proceedings, Reliability Physics 1977.

6. "Migrated-Gold Resistive Shorts in Microcircuits", A. Shumka and R. Piety, 13th Annual Proceedings, Reliability Physics 1975.

7. "Further Studies on the Reliability of Thin-Film Nickel-Chromium Resistors", W. Paulson 11th Annual Proceedings, Reliability Physics 1973.

8. "Reliability Technology for Cardiac Pacemakers" NBS Special Publication 400-28, Editor H.A. Schafft, 1976.

9. "Moisture, Myths and Microcircuits", R. Thomas, Proceedings 26th Electronic Component Conference, 1976 page 272.

10. "Nichrome Resistor Investigation", A. DerMarderosian, Raytheon Internal Report, IS:72:6 dated 26 January 1972.

11. "Non-Hermeticity of Polymeric Lid Sealants", R. K. Traeger, IIEE Transactions on Parts, Hybrids and Packaging VOL PHP-13 No. 2 June 1977.

12. "Model Calculations for Maximum Allowable Leak Rates of Hermetic Devices", J.G. Davy, J. Vac, Sci. Tech. Vol 12 No. 1 Jan/Feb 1975.

13. "Calculations for Leak Rates of Hermetic Packages", J.G. Davy, IIEE Transactions of Parts, Hybrids and Packaging, Vol PHP-11 No. 3 September 1975.

14. "On the Penetration of Gases and Water Vapor Into Packages With Cavities and a Maximum Allowable Leak Rates" D. Stroehle, Reliability Physics Symposium Proceedings 1977.

15. MIL-STD-883B, Helium Test Leak Rate Equation Method 1014.

16. C.E.C. Leak Detection Manual (#992249-0011) Pages 2-2, 2-3.

17. MIL-STD-883B, Method 1014.

18. "Back Pressurizing Technique of Leak Testing", D.A. Howl and C.A. Mann, Vacuum, 15, 347 (1965).

19. "Guidelines for Sealing and Leak Testing of Hermetic Packages", J. Gordon Davy, Editor Westinghouse Defense and Electronics Center Baltimore, MD. Internal Report.

20. "The Objectives and Limitations of the Hermeticity Tests Performed on Semiconductor Encapsulations". R.P. Merritt, British Telecom, Internal Memorandum No. R20/014/83.

CALIBRATED GROSS LEAKER CONSTRUCTED FROM 1 MM CAPILLARY

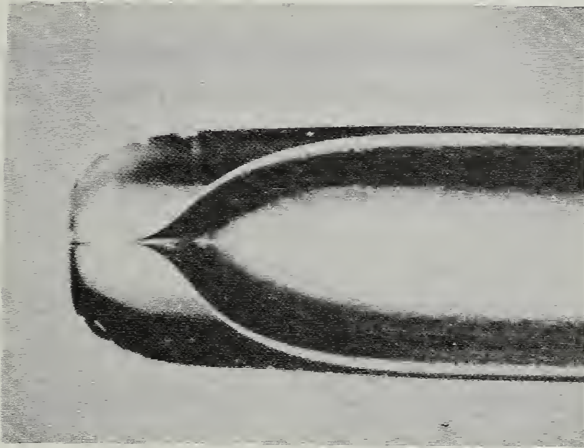

Figure 1

COMPLETED ASSEMBLY OF CALIBRATED GROSS LEAKER AND TO-5 CAN

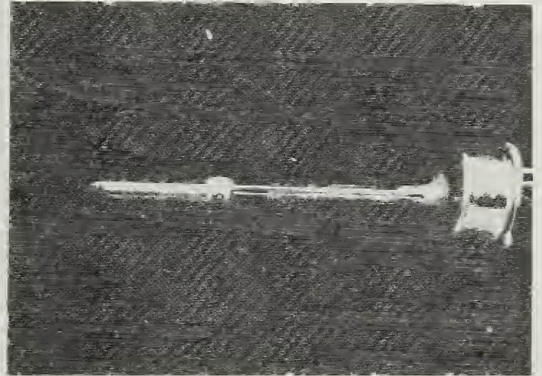

Figure 4

CALIBRATION OF CAPILLARY LEAKERS (RATE OF PRESSURE RISE METHOD)

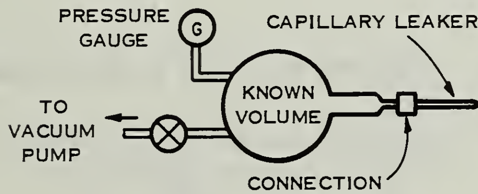

Figure 2

SURFACE CONDUCTIVITY MOISTURE SENSOR

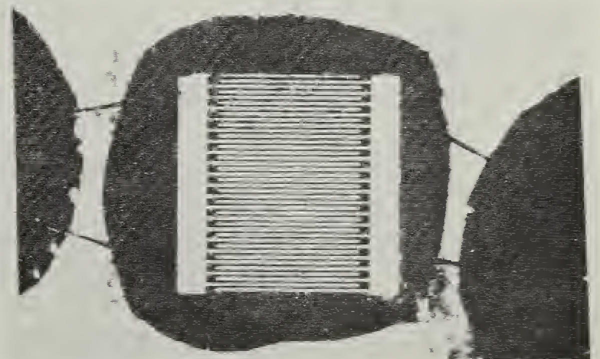

Figure 5

DIFFERENTIAL PRESSURE REQUIRED TO INITIATE BUBBLING VS AIR LEAK RATE OF CAPILLARY (FC-77 LIQUID)

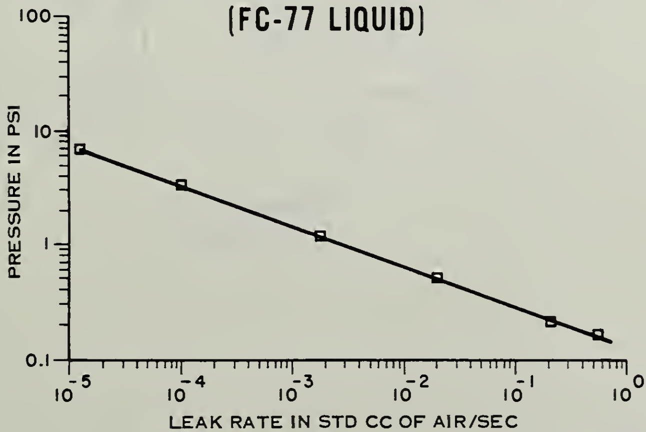

Figure 3

HYGROMITE CALIBRATION RELATIVE HUMIDITY VS SURFACE LEAKAGE CURRENT

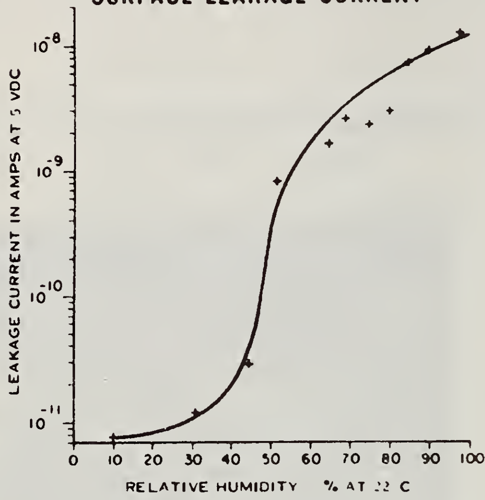

Figure 6

AIR LEAK RATE VS WATER VAPOR LEAK RATE FOR CAPILLARY TUBES

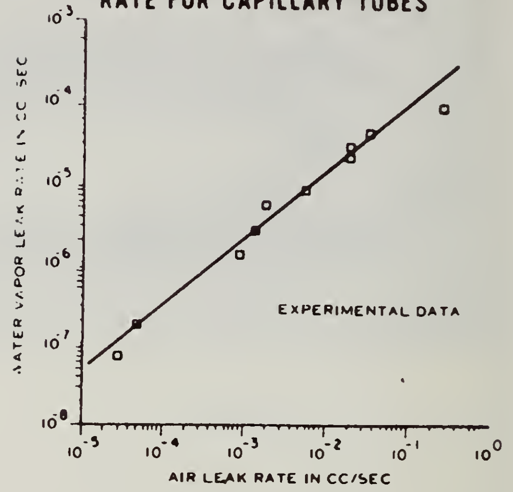

Figure 8

TIME CONSTANT FOR WATER VAPOR PENETRATION VS AIR LEAK RATE FOR TO-5 CAN

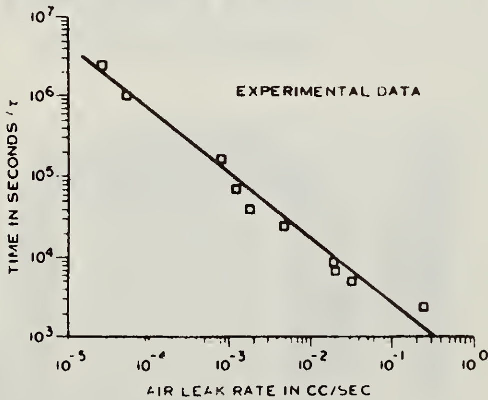

Figure 7

MEASURED LEAK RATE VS AIR LEAK RATE

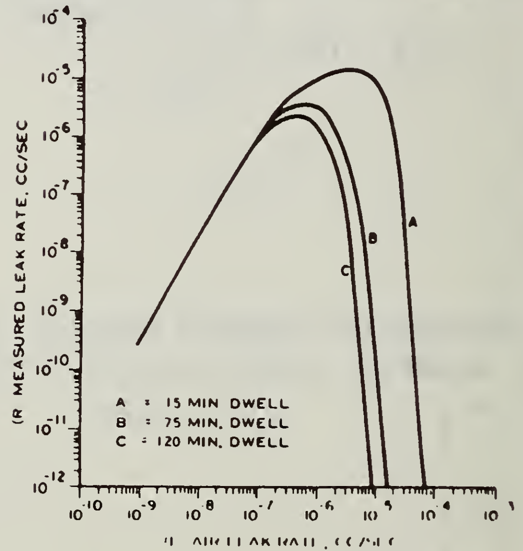

Figure 9

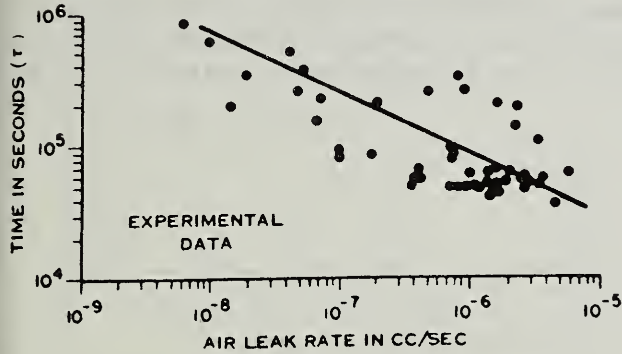

Figure 10

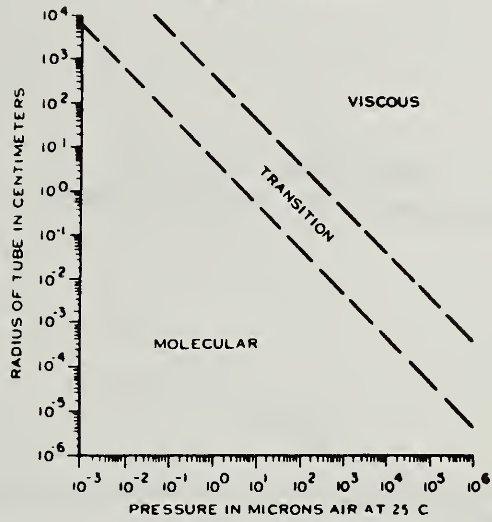

Figure 12

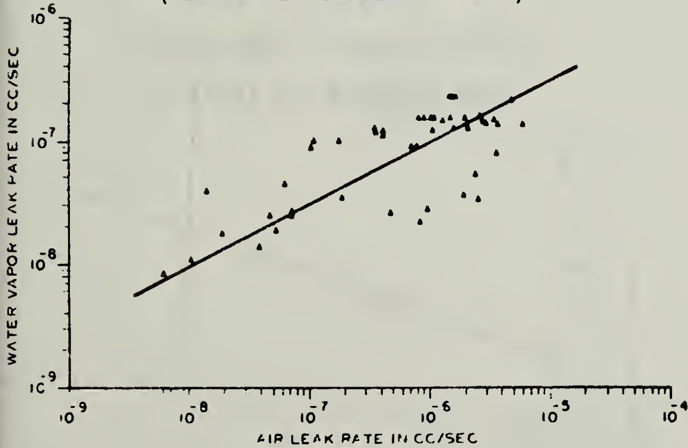

Figure 11

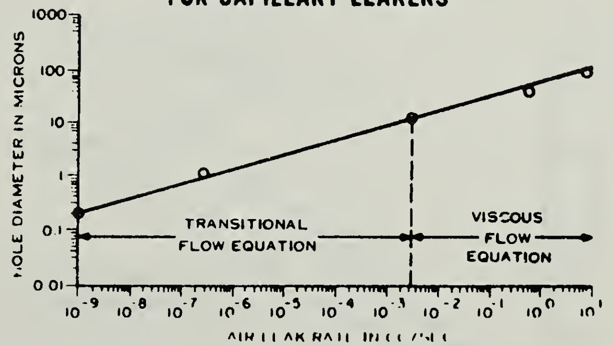

Figure 13

WATER VAPOR LEAK RATE VS
HOLE DIAMETER FOR CAPILLARY LEAKERS

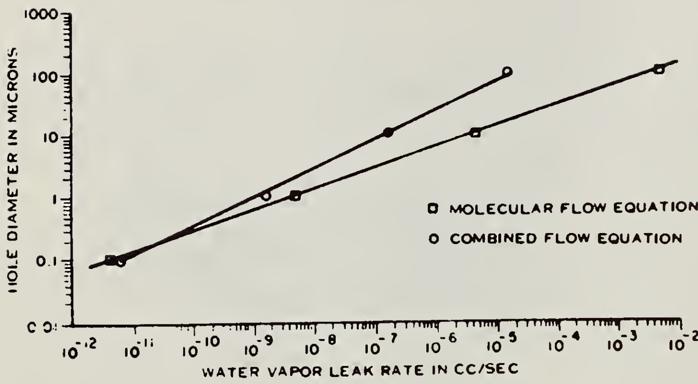

Figure 14

CHANGE IN DEWPOINT VS TIME AS A FUNCTION OF STD. AIR LEAK RATE IN AMBIENT ENVIRONMENT OF 80% R.H. AT 22.2°C (TO-5 PACKAGE WITH A VOLUME OF 0.17 CC)

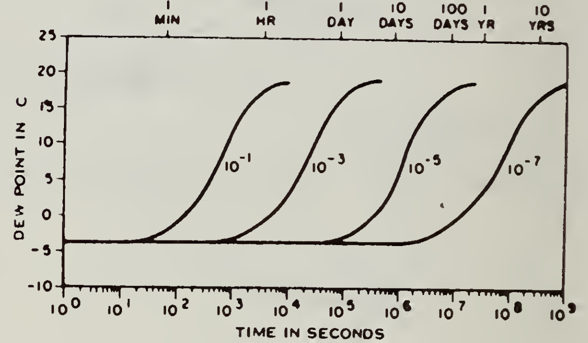

Figure 16

AIR LEAK RATE VS WATER VAPOR LEAK RATE

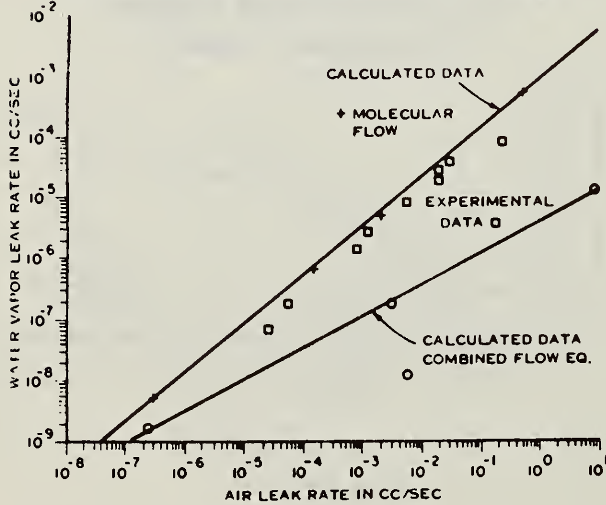

Figure 15

AIR LEAK RATE VS "EQUIVALENT"
HOLE DIAMETER FOR FLATPAK

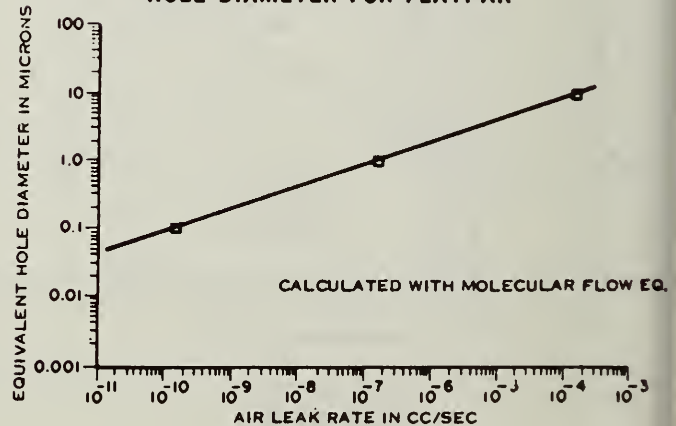

Figure 17

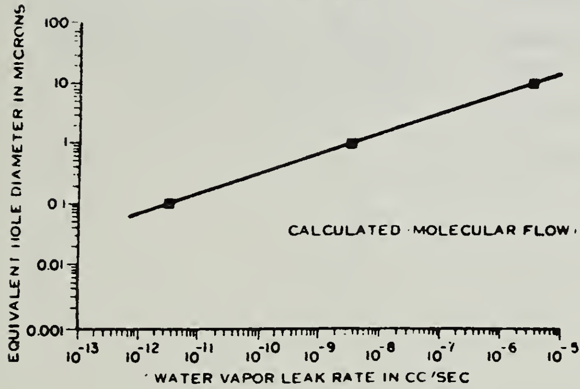

Figure 18

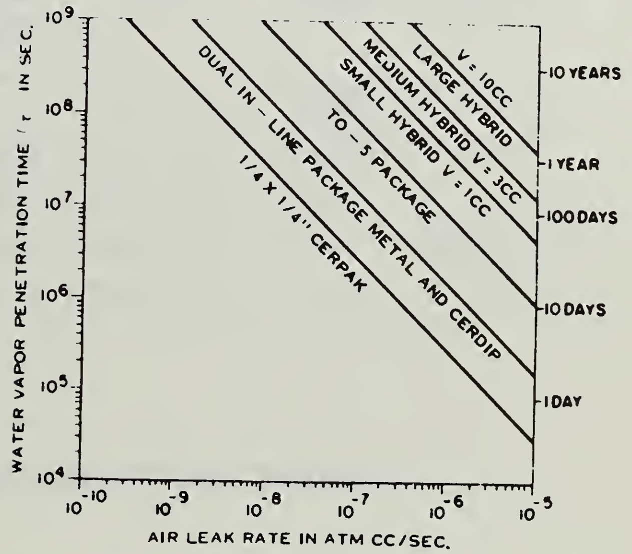

Figure 20

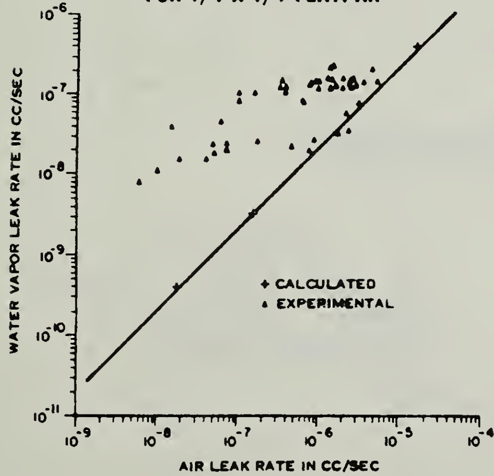

Figure 19

MOISTURE PENETRATION TIMES

VOLUME	METHOD	MAX. ALLOW. L.R. (L)	TIME TO EXCEED (1018) AVG. AMB. – 10,000 PPM	
			5000 PPM	500 PPM
< 0.4 CC R = (5 × 10^{-8} CC/SEC)	FIXED He (.01 CC)	4.5 × 10^{-8} CC/SEC	71 DAYS	5 DAYS
< 0.4 CC R = (5 × 10^{-8} CC/SEC)	FIXED He (.39 CC)	2.8 × 10^{-7} CC/SEC	1.2 YEARS	32 DAYS
≥ 0.4 CC R = (2 × 10^{-7} CC/SEC)	FIXED He (.4 CC)	6 × 10^{-7} CC/SEC	214 DAYS	15 DAYS
≥ 0.4 CC R = (2 × 10^{-7} CC/SEC)	FIXED He (5 CC)	2 × 10^{-8} CC/SEC	2.2 YEARS	57 DAYS

Figure 21

MIL-STD-883B; "FIXED" METHOD, HELIUM FINE LEAK TEST. (A_1)

MOISTURE PENETRATION TIMES

VOLUME	METHOD	MAX. ALLOW. L.R. (L)	TIME TO EXCEED (1018) AVG. AMB. = 10,000 PPM	
			5000 PPM	500 PPM
< 0.01 CC	FLEXIBLE (He) (.009 CC)	5 × 10^{-8} CC/SEC	58 DAYS	4.1 DAYS
.01-.4 CC	FLEXIBLE (He) (.01 CC)	1 × 10^{-7} CC/SEC	32 DAYS	2.3 DAYS
	(.4 CC)	1 × 10^{-7} CC/SEC	3.5 YEARS	92 DAYS
> 0.4 CC	.41 CC	1 × 10^{-8} CC/SEC	132 DAYS	9.4 DAYS
	5 CC	1 × 10^{-8} CC/SEC	4.4 YEARS	114 DAYS

Figure 22

MIL-STD-883B: "FLEXIBLE" METHOD, HELIUM FINE LEAK TEST. (A_2)

MOISTURE PENETRATION TIMES

VOLUME	METHOD	MAX. ALLOW. L.R. (L)	TIME TO EXCEED (1018) AVG. AMB. 10,000 PPM	
			5000 PPM	500 PPM
< 0.01 CC	FIXED (Kr^{85}) (.009 CC)	1 × 10^{-8} CC/SEC	.79 YEARS	21 DAYS
≥ 0.01	FIXED (Kr^{85}) (0.01 CC)	5 × 10^{-8} CC/SEC	64 DAYS	4.6 DAYS
	(0.4 CC)	5 × 10^{-8} CC/SEC	7.0 YEARS	.5 YEAR
	(5 CC)	5 × 10^{-8} CC/SEC	88 YEARS	6.3 YEARS

Figure 23

MIL-STD-883B; "FIXED" METHOD, KRYPTON 85 FINE LEAK TEST (B)

COMPARISON OF THE MAXIMUM ALLOWABLE LEAK RATES ACCORDING TO MIL-STD-883B, METHOD 1014, FINE LEAK TESTS (CONDITION A_1, A_2 and B) AND THE TIME TO EXCEED PRESENT (5000 ppm_v) AND FUTURE (500 ppm_v) MAXIMUM ALLOWABLE INTERNAL PACKAGE MOISTURE LEVELS (METHOD 1018).

EFFECTS OF PACKAGE VOLUME

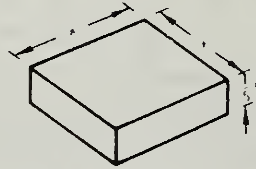

MODEL FOR CALCULATIONS

X	INTERNAL AREA	INTERNAL VOLUME	RATIO $\frac{AREA}{VOL.}$
CM	CM^2	CM^3	
.17	.08	.001	80
.37	.38	.01	38
.79	1.7	.1	17
1.7	8.2	1	8.2
3.7	38	10	3.8
7.9	175	100	1.75

Figure 24

MAXIMUM ALLOWABLE PACKAGE MOISTURE CONTENT

VOLUME	MOISTURE CONTENT	MOISTURE CONTENT	APPARENT SURFACE AREA	WATER THICKNESS	NUMBER OF MONOLAYERS
CM^3	PPM_v	GRAMS	CM^2	CM	—
.001	13,000	$9.6 \cdot 10^{9}$	.08	$1.2 \cdot 10^{7}$	3
.01	6,200	$4.6 \cdot 10^{8}$	.38	$1.2 \cdot 10^{7}$	3
0.1	2,700	2×10^{7}	1.7	$1.2 \cdot 10^{7}$	3
1.0	1,300	9.8×10^{7}	8.2	$1.2 \cdot 10^{7}$	3
10	600	4.6×10^{6}	38	$1.2 \cdot 10^{7}$	3
100	280	2.1×10^{5}	175	$1.2 \cdot 10^{7}$	3

Figure 25

MAXIMUM ALLOWABLE MOISTURE CONTENT AS A FUNCTION OF INTERNAL PACKAGE VOLUME

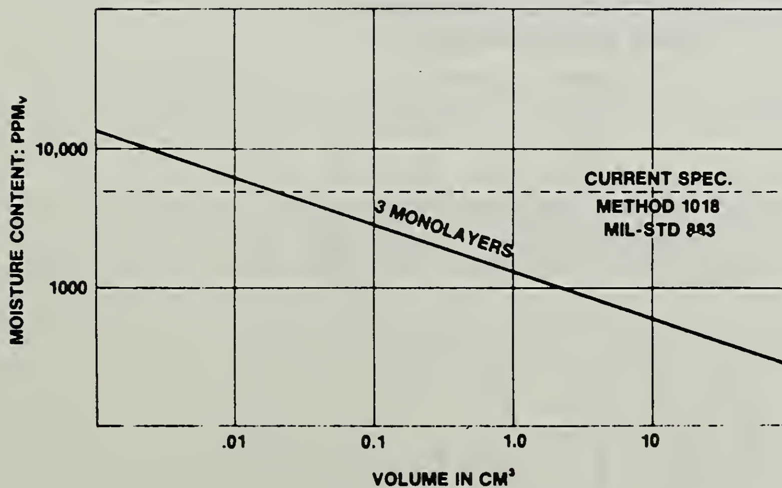

Figure 26

MOISTURE INGRESS TIME

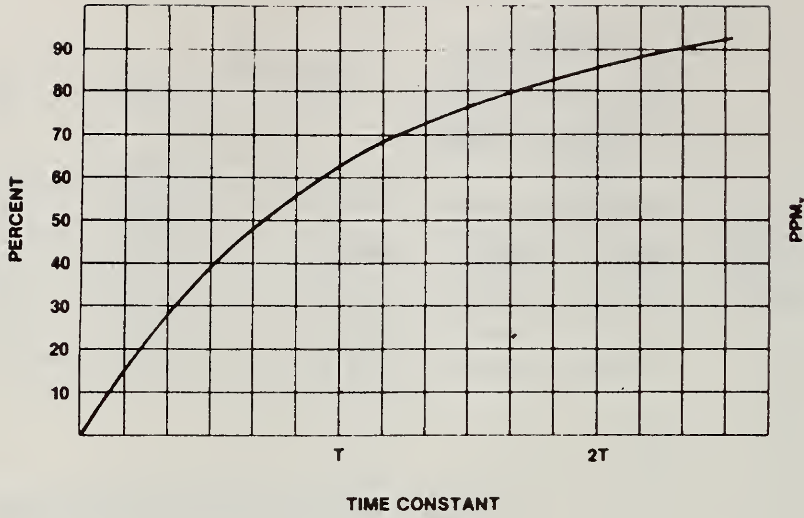

Figure 27

TIME TO REACH ONE(1) T AND 3 MONOLAYERS OF H_2O

VOLUME C.C.	L.R. ATM CC/SEC	T HOURS	TIME TO REACH 3 MONOLAYERS HOURS (AVG AMB 13K PPM$_v$)
.001	1×10^{6}	11	55
.001	1×10^{7}	110	550
.001	1×10^{8}	1,100	5,500
.01	1×10^{6}	110	66
.01	1×10^{7}	1,100	660
.01	10^{8}	11,000	6,600
.1	10^{6}	1,100	257
.1	10^{7}	11,000	2,570
.1	10^{8}	110,000	25,700
1	10^{6}	11,000	1,283
1	10^{7}	110,000	12,830
1	10^{8}	1,100,000	128,300
10	10^{6}	110,000	5,500
10	10^{7}	1,100,000	55,000
10	10^{8}	11,000,000	550,000
100	10^{6}	1,100,000	27,500
100	10^{7}	11,000,000	275,000
100	10^{8}	110,000,000	2,750,000

Figure 28

TIME TO REACH 3 MONOLAYERS OF H_2O AS A FUNCTION OF PACKAGE INTERNAL VOLUME AND AIR LEAK RATE.

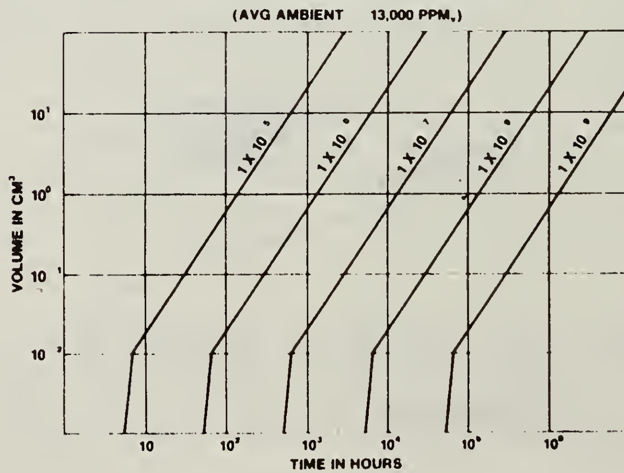

Figure 29

1.3 THE NID® VAPOR DETECTION TECHNIQUE; A BREAKTHROUGH IN GROSS LEAK TESTING

by: Bill Evans, WEB Technology, Inc, Dallas, Texas

Leak detection in integrated circuits is a very important high reliability test which is unfortunately often underemphasized. Moisture penetration and the subsequent device corrosion is a major cause of field package failures, some of which have recently been highly publicized. The sources of moisture in these packages have been described in several papers and can basically be categorized into the following four groups:

1) Entrapment due to poor bake out procedures and/or sealing environment.
2) Generated internally by decomposition, material outgassing or devitrification of sealing glasses
3) Permeation thru polymer seals
4) Penetration thru cracks and/or faulty seals

It is catagory #4 that this paper will deal with:

Although all packages will leak at some rate, a device can be described as hermetic provided the leak rate is small enough to assure the internal atmosphere can be maintained at an acceptable humidity level for the desired service life of the specimen. Due to the relatively small internal volumes present within most IC's, the allowable leak rate constraints are very stringent. It is generally considered necessary by Mil Standard requirements to reject any device with a leak rate greater than 1 X 10-8 atm cc/sec. Some would argue that this is not stringent enough since it has been proven that water vapor readily penetrates typical IC packages with leak rates in this range. However, it is not feasible to detect leak rates smaller than this value in a production environment by current methods due to surface porosity, ambient background levels, and equipment utilization. Luckily, considerable evidence indicates that virtually all leaks occur at glass-to-metal seals, ceramic-to-metal seals, etc. and are 5 X 10-7 atm cc/sec or larger. Also, for devices with larger internal cavity volumes, slightly larger leak rates are allowable because more moisture is required to reach a concentration level that causes corrosion.

To facilitate testing over the entire range from 1 X 10-1 to 1 X 10-8 atm cc/sec, it is almost always necessary to split the hermiticity test into at least two catagories; fine leaks and gross

leaks. (Sometimes a third category, visual rejects, is also included). This is due in part to the characteristics of leaks and which type of flow will occur into the package. This flow will depend on the relative magnitude of the minimum dimension of the leak path and the mean free path of the gas molecule. If the rate at which the gas flows through the leak is governed by wall-to-molecule collisions, the flow is considered to be molecular. This occurs when the mean free path is much greater than the leak path "diameter". In this flow regime, the flow rate is proportional to the difference between the partial pressures at either end of the leak and is inversely proportional to the square root of the molecular weight of the gas passing through the leak path. If the rate at which the gas flows through the leak is governed by molecule-to-molecule collisions the flow is considered to be viscous. This occurs when the mean free path is much smaller than the leak path "diameter". In this flow regime, the flow rate is dependent on the viscosity of the gas and the difference in the pressures at either end of the leak. Between these two limits there is a gradual change from molecular to viscous flow. This region is considered the transitional flow regime.

Leakers in the gross leak range (usually considered to be 10-1 to 10-5 atm cc/sec.) typically fall into the viscous and/or transitional flow regime, while leakers in the fine leak range (10-6 to 10-8 atm cc/sec) are almost completely of the molecular flow type. See Figure 1 below.

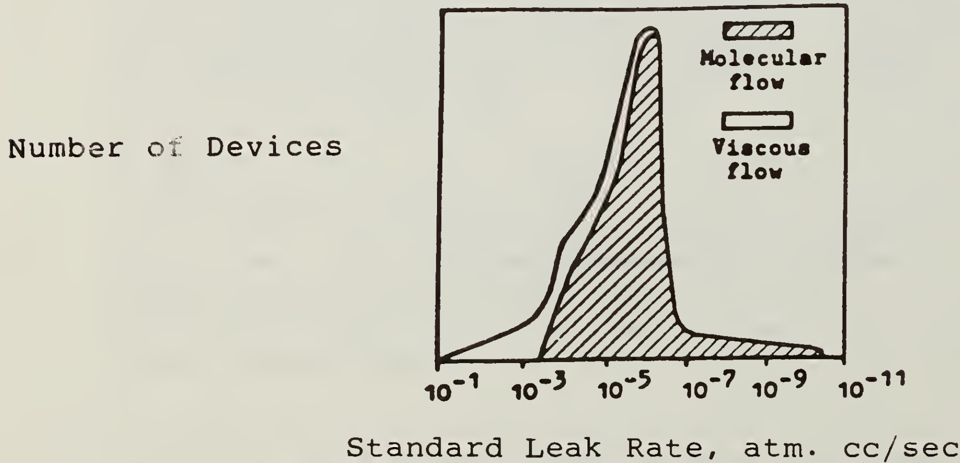

FIGURE 1

Distribution of leak rates and the flow regimes for a large number and variety of packages. (From reference 1)

The most commonly used methods for detecting the smallest leak rates utilize either a helium mass spectrometer or the Kr85 radioisotope technique. These methods incorporate preconditioning the package with a tracer gas. Due to the molecular flow characteristics for a fine leak, only gases have a molecular size and design small enough to penetrate these microscopic leak paths. If a large enough path is present, during preconditioning this tracer gas will be forced into the cavity. A reject can then be detected by using either a helium mass spectrometer or by detecting the gamma radiation being emitted by a reject with a scintillation crystal and associated circuitry, depending on the gas used.

In order to prevent rejections of good product caused by surface adsorption of the tracer gas, it is necessary to have a "dwell" time to rid the surface of any residual gas. The loss of tracer gas from the package cavity through the leak path during the dwell time restricts the largest leak which can be detected. For a .1cc cavity device and a dwell time of 1 hour (permitted by Mil Std. 883), the upper detectable limit is about 1 X 10-4 for the helium test and 3 X 10-4 atm cc/sec. for the radioisotope method. Because of this, there is a tremendous need for an accurate test method for detecting leak rates larger than these values and also showing excellent crossover into the smaller leaks for picking up the rejects which do not conform to the molecular flow assumption.

There are currently many detection techniques used for detecting these larger leak rates, known as the gross leak range. However, only a very few are approved by military test standards. These tests include the fluorocarbon bubble test, weight gain analysis, dye penetrant inspection, and recently the fluorocarbon vapor detection technique (a.k.a. NID® Method). Each of these methods involves a preconditioning of the device(s) prior to actual testing. This preconditioning in each case deals with attempting to force a liquid through any available leak path. The presence of this liquid is then later detected and the device is rejected.

The dye penetrant inspection became popular in the 1960's and was first used on glass diodes and other devices with glass envelopes. In effect, a dye is pressurized into the devices and a 100% inspection is performed. The leakers are identified by looking for the presence of dye inside the package. As you may suspect, this method is very limited for production use and has its largest application when used with non-glass devices as a destructive failure analysis tool.

The weight gain test also became accepted during this period. The idea behind this method is that when an empty device is preconditioned with a liquid, and a leak path is available, it will fill with the liquid and gain weight. By taking initial and final weight measurements on each part, you can determine which devices leak by the weight increase. This method, when correctly applied using the proper weight scales, preconditioning sequence, viscosity fluid, and rejection level, is probably the most accurate method for detecting gross leakers in most semiconductor packages. However, due to the operator intensive nature of the test and the fact that it is considerably slower than other methods, it is much more expensive to perform and is thus not very popular in high volume applications.

Undeniably, the most widely used method currently for high reliability Military Standard gross leak testing of semiconductors is the two fluid bubble test. This test method developed from what is now commonly referred to as the "Old C1" bubble test. This original test consisted of submerging the packaged semiconductor in a bath of fluid which was typically maintained at a temperature of 125 degrees C. This increase in temperature caused the air inside the cavity to expand and thus a bubble would occur as the air escaped, if a leak path was available. It was soon determined that this method did not consistently detect the leakers in the 10-4 to 10-5 atm cc/sec range. Because of this lack of crossover with the fine leak tests, it was realized that a better test was a necessity. This led to the development of the "two fluid" test which utilizes two separate fluids with significantly different boiling points. The package is first preconditioned with an inert liquid having a relatively low boiling point to force some of this liquid into the internal cavity through any available leak path. This preconditioning consists of first subjecting the package to a vacuum environment in an attempt to completely evacuate the cavity of the device. The vacuum chamber is then backfilled with the low boiling point liquid, without breaking the vacuum, and pressure is applied to the chamber to drive the liquid through any large enough leak path. This pressure is later released and the devices remain submerged in the liquid bath until just prior to the actual test. The package is then removed and allowed to dry for a short period of time before being immersed in the second liquid which is held at a temperature that far exceeds the boiling point of the preconditioning liquid. After immersion, the package temperature

is raised which causes vaporization of any preconditioning liquid in the internal cavity, resulting in a substantial rise in the internal pressure which is vented through the leak path. This venting creates bubbles with significantly greater frequency and duration than the single fluid bubble test. This test in a "lab" environment, when only testing 1 to 3 parts at a time, can be shown to be accurate and repeatable down to the 1Ø-5 range and can detect a substantial number of devices with leaks as small as 1Ø-6 atm cc/sec.

However, there are some distinct draw backs to this technique when placed in a high production, high stress environment. Foremost is the dependence on an operator, doing a highly subjective task, under what are less than ideal circumstances. These bubbles have to be detected by the operator who may have to contend with particles floating in the liquid, spurious bubbles created by contamination and porous surfaces, bubbles caused by the release of trapped air during submersion of the tray on which the devices rest, and eye fatigue. Other factors which can easily result in poor detectability of leakers lie in the number of packages which are typically loaded into the bubble tester at a time, and the way in which they are loaded. For example, some suppliers are currently testing up to 175 DIPs at a time, stacked side by side on the tray. Since the largest majority of leaks occur between the leads on the side of DIP packages (this is the shortest distance between the cavity and the outside environment), if the packages are placed side by side and a stream of bubbles are coming up between them, it is very difficult to determine which package is leaking. Also, because the reject package is generally not removed until after the tray is taken out of the liquid, even if it was obvious which package was leaking in the bath, there is a high probability of error in the operator loosing his/her place and rejecting the wrong part. It is because of this abuse that the government agencies reportedly will be applying pressure to decrease the number of packages which can be tested at once with the bubble method; the number most often mentioned is 1Ø devices/test maximum.

Other, often overlooked, factors concern the repetitive non-stimulating nature of this test and the effect on the human operator. These human effects are generally broken down into three basic catagories, all of which are interdependent. These catagories are the job characteristics, the operator characteristics, and the signal characteristics.

The job task is inherently boring which has many negative implications. It gives an employee no sense of satisfaction because they do not receive feedback about their work, or see how it contributes significantly to the world. The task demands nothing of the operator and quickly becomes habitual which allows the person to direct attention elsewhere. One method of overcoming this boredom is to intentionally increase the rate of rejection (actually elevating the "false alarm" or "overkill" rate at the company's expense) in order to demonstrate to themselves and others that their job does serve a useful function. The most unsatisfied employee would likely be one who puts in a full day's work only to segregate out a minimal number of leakers. At the end of the month, the work volume typically increases and the task becomes more stressful. This could actually improve performance in that the work is no longer seen as boring. However, at this time, the job will also take on the characteristics of a dual task because the operator is required to monitor the tank and load and unload trays in rapid succession. Because the trays require active physical involvement (movement of arms to do the loading and unloading), this portion of the job will receive the majority of an operator's attention. This activity serves as a needed source of excitement, which has been called response induced stimulation. Again the less bored worker is one who may be producing at a high rate (processing many ICs) and they would therefore typically be directing attention to loading and unloading trays instead of observing the tank.

Performance feedback on this task can be related to quality and quantity of work by an employee. Generally the most notable type of feedback to the bubble test relates to the number of units processed, while the quality feedback may generally be nonexistant or delayed over a long period of time which weakens its impact. The sooner the feedback, the more readily it is attended to. One form of quality feedback, which is generally at the operators disposal, can result in what is referred to as probability matching. This is a task related problem encountered in which the operator knows the number of targets per hour that should on the average be detected and accordingly reports such findings regardless of the number of actual targets. This may increase or decrease both the overkill rate and the escapement rate merely because an operator knows that he or she should find only "two leakers per hour"; and that is what they consistently will do. As time passes, the expectation of detecting a leaker will increase because an operator is anticipating a leaker to be

more probable. When a questionable IC is detected after a long period of finding no leakers, an operator will be more likely to throw it out (regardless of its real status) just to satisfy the quota. The detection threshold then rises because the operator does not expect another leaker for "half an hour".

On a more abstract level, humans are naturally programmed to do poorly on the task. From an evolutionary perspective, it is more "adaptive" to expend energy in challenging or stressful situations and conserve energy in monotonous or boring situations. This conservation of energy idea is most clearly seen in development of habits in order to avoid useless energy expenditures on simple everyday tasks. In essence, people are "hard wired" to habitualize the boring task of detecting leakers so that when a stressful situation arises they will have the energy to attend to it. Escapement of bad product is associated with neglect or the misdirection of attention that commonly comes with this boredom.

As it appears in Quality Assurance:

> If not enough signals from the outside world are received, the reticular formation ceases to send the awakening pulses to the meninges, which then turn off the brain. The person dozes off and eventually falls asleep. This is an ingenious procedure to give the brain a pause to relax and recuperate when it is not needed.
>
> (1982 June, pp. 37)

With this, we could say that the fault is not with the dozing operator but instead with the job design. A normal person should be expected to either sleep or have wandering thoughts to other more stimulating stimuli. From this, we can predict that initially escapement rates would be low and increase with time as the individual gets bored. Likewise, the overkill rate is high initially and decreases with time. Studies have shown this to be true and defined it in terms of "thresholds of sensitivity". At the beginning of a vigilance task, the individual is set and poised to find the leaker. They are expecting it to occur. They would rather be safe than sorry and reject a greater number of items, thereby proving to self and boss their value. Their threshold of rejection is very low, and they will throw out many good semiconductrs because of their excessive attentiveness to

the task. Put another way, they are too attentive to the task. With time however, attention wanes and escapement becomes the greater problem. This is the insurmountable problem for the bubble test. It provides no variation of stimulation for an individual's five senses. The only support for the test is that there is some arm movement which keeps the worker somewhat attentive to the task. But even then, escapement may be elevated because this activity is the more stimulating portion of the job. As mentioned before, this is especially true when time pressures become critical at the end of the month.

The paradox of vigilance performance in this situation is that the task demands attention but has a low stimulous payoff. If there was more of an interaction between the operator and the task, performance would increase. As previously mentioned, operators can artifically raise the rejection rate (creating false alarms), thereby making the job more interesting. This "false alarm" strategy has been used in the military for radar operators who have to detect green acoustically-silent "blips" on a CRT screen. Phantom "blips" are identical to actual signals but there is no actual object to correspond to its presentation. It serves only to arouse the operator while also giving performance feedback to upper level personnel who sent the phantom signal. Incentives have been shown to have little impact on the quality of detection rates; money, and threats have yielded little improvement. Only changes in stimulation levels (via frequent work-breaks, supervisor observation, and random ambient auditory stimulation) have been shown to improve performance; but these are costly and interfere with other employees.

One basic operational characteristic finding relates to personality dimensions of introversion and extroversion. The findings are generally that extroverts do better on vigilance tasks because they direct their attention outwards to the task at hand. Introverts do worse because they are prone to attend more to their own personal thoughts at the expense of heightened environmental sensitivity. This finding must be qualified by the fact that the extroverts are also going to have a greater need to interact and talk with others which would cause a performance decrement. To summarize, there is no ideal personality type to run a bubble tester for prolonged periods of time. Persons in general will do their best in the morning, at about 11:00 A.M., which is when most people are at the peek of their ciradian rhythm. Performance in the afternoon is markedly worse than performance in the morning. Also, the fewer the number of breaks the worse the performance will be.

From a signal characteristics point of view, the overkill and escapement rate are clearly related to the perceptibility of a leaker relative to the other good ICs. This is what is commonly referred to as figure ground perception. With the bubble test, there is not much of a figure ground distinction; that is, "targets" are not readily identifiable because a large number of bubbles are occuring each time the tray is set in the fluid. Secondly, the color of the bubbles is not conspicuous relative to the color of the rest of the tank, which further reduces the discriminatibility of a target. Also, the signal is highly variable (as defined by the many criteria of defining a leaker) which adds to the confusion of determining whether a device is a reject or not.

Each of the findings presented above may be said to have at least some impact on the vigilance task relating to detecting leakers. Taken as a whole, it is clear that there may be multiple causes for the poor performance records found on this task. The factors are time and stimulous related, which make the job exceedingly difficult to adapt to human weaknesses. This problem is best handled by letting a machine detect the rejects.

Other negative aspects of the bubble test in production involve problems associated with material flow through the process steps. Because the bubble test is inherently a batch test and involves operator intervention, there has been little to no success in automating this technique. Also because of this batch loading, many manufacturers insist upon doing 100% testing prior to lead trim operations to help avoid bent lead problems. This results in only a sample test after trim which is undesirable since the trimming operation is known to be a significant cause of both fine and gross leaks, especially for cer-dip devices.

THE NID GROSS LEAK DETECTION TECHNIQUE OVERCOMES VIRTUALLY ALL OF THE PROBLEMS ASSOCIATED WITH THE BUBBLE TEST AND IS WELL SUITED FOR THE HIGH VOLUME PRODUCTION ENVIRONMENT. THIS METHOD:

1) Removes operator dependence and subjectivity.
2) Is automatable and thus allows gross leak testing to be performed end-of-line (where it should be) without causing bent leads
3) Is very accurate in detecting leaks in the gross leak range.
4) Has very good crossover with both fine leak tests currently in use.
5) Has certain operating cost improvements.

This method utilizes a vapor detection technique. The packages are preconditioned in a manner similar to the 2 fluid bubble test; however vacuum and pressure times are reduced due to the improved sensitivity of the technique. After removal from the preconditioning fluid, the package to be tested is placed, either manually or automatically, into a test cell heated well above the boiling point of the preconditioning liquid in such a manner as to achieve good thermal contact. This causes the package temperature to elevate and thus an internal vaporization of the liquid occurs. Much like the bubble test, these vapors build up an internal pressure and an outgassing through the leak path will occur. The air around the device is passed through a proprietary detector and is sensed for the presence of these vapors. This detector is designed for maximum accuracy with a minimum of service related problems. It features a very low zero drift, is repeatable over long periods of time, is not flow sensitive, and the gas sample is isolated from the actual detector thus avoiding contamination. Another very important design criteria is that, in the event an equipment failure does occur, virtually anything that happens will result in the detector going "off scale" insuring a failsafe condition.

The sensitivity of the test is a function of the dilution volume, the integrating time, and the lower detectable limit of the analyzer relative to any leak rate. This dilution volume is the volume of air contained in the test cell and all connecting tubing between this test cell and the detector when the unit is integrating the gas concentration (this is commonly referred to as the measure or test mode). The leak rate, or outgassing, of a device is a function of the fluorocarbon boiling point, the temperature (and corresponding vapor pressure) inside the cavity, the geometry of the leak path(s), and the preconditioning conditions.

It can be shown mathamatically that a 10-5 atm cc/sec leaker would leak at the rate of 10 ppm into a 1cc volume at standard conditions. As the temperature is increased, this flow will increase as the square of the resulting pressure increase, assuming the leak rate is in the viscous flow range. Since the lower detectable limit of the NID approaches 10 ppb with a 1cc volume dilution, the sensitivity is sufficient to detect leakers well below the 10-5 atm cc/sec level thus assuring good fine leak crossover. Also, since the device is outgassing into a vapor

environment, the NID method should be more sensitive than the bubble test because the internal pressure of the device does not have to overcome any detector liquid's static pressure to achieve outgassing.

To go from a laboratory detection technique to an automatic high volume production test, with the ability to accurately test one part at a time, required determining measuring time parameters, acceptable dilution volumes, preconditioning times, etc. This was done and reported in SME report #IQ84-679 presented at the Qualtest 3 conference in October of 1984. Based on the test data on the NID, the production parameters of a 3 1/2 second measure cycle after preheat in 125 degree C heated test cell and a reject level of 200 were shown to be adequate to crossover with the fine leak test. To increase this overlap, features were added to the computer controlled automatic NID. These include a P.A.L. (pre alarm level) reject and also a software extrapolation mode reject. These features essentially detect the presence of escaping vapors. If the vapor concentration does not achieve the reject level, but is high enough or would become high enough given additional testing time to warrant further investigation, the software can be directed to either reject the device or put it in a special output tube. Based on correlation studies at numerous locations and parallel screens, the system as designed has demonstrated that a bad part will be detected by either the NID or by the fine leak test(s). Besides the measurement parameters, the design had to also accommodate actual production conditions. For example, the fluorocarbon background at various manufacturing facilities has been found to vary considerably. If the NID sensitivity were increased above current levels, it would make the instrument more sensitive to these background levels and could result in good parts being rejected due to fluctuations in the fluorocarbon concentration of the atmosphere surrounding the test cell. This concentration can increase substantially as a result of nearby venting of preconditioning tanks, spillage of fluorocarbon, or several other common production occurances.

In as much as the sensitivity data was based on perfect conditions (i.e., a single, straight, round hole), one can not do an exact one to one correlation. Hence, adequate overlap must be demonstrated in production testing. In several tests involving groups of fine leak rejects, the NID method was found to detect up to 70% of the samples. The explanation for this excellent crossover is due to the NID system relying on opposite parameters

than the fine leak tests. Specifically if a part is a large leaker in the viscous flow range, the fluorocarbon outgassing will occur at a significant rate to be easily detected by the NID, whereas the helium or krypton gas would have escaped prior to measurement. If, on the other hand, a fine leaker in the molecular flow range is tested, the opposite will be true; the helium or krypton will remain to be detected and the hole size will be too small to either allow liquid fluorocarbon in and/or adequate fluorocarbon outgassing to achieve a NID failure (200 count threshold). Further analysis of samples which did outgas readings greater than zero but less than 200 have been repeatably shown to be either fine or false leakers. These parts will typically have a zero or minimal weight gain, may show a short burst of bubbles in the bubble test and fail fine leak. It appears from x-rays that many times the parts have a ceramic or seal porosity problem and may or may not actually have a leak path to the cavity; if there is a leak path it is of the fine leak variety.

This method has shown excellent correlation with the weight gain, dye penetrant, and bubble test procedures in one on one correlations under laboratory conditions. In similar tests with the 2 fluid bubble test in a production environment, the NID method has proven to greatly reduce overkill and escapements (as predicted by the preceding paragraphs dealing with the human effects and job design of the bubble test). See Tables 1 & 2. These tables dramatically point out the need for a nonsubjective gross leak hermiticity test technique. These samples were all supplied by major I.C. manufacturers as either random samples from the gross leak reject "bin" or a random sample of "good" outgoing product. It should also be noted that these are typical results, not worst case.

On top of the quality improvements realized when testing with the NID, several operating cost improvements are obtained. The most apparent of these savings is the reduction in the fluorocarbon usage over the bubble test. With the NID, there is no need for the high temperature fluorocarbon liquid bath. This liquid costs in the neighborhood of $ 400 per gallon and must constantly be replenished due to "drag out" and evaporation. Condensing coils on top of the bubble tank can help minimize the evaporation out the top of the tank, however most losses occur from the evaporation of the liquid from the surfaces of the devices and loading tray once removed from the tank. This saving is generally estimated at 1 to 5 cents/part for standard DIPs and is dependant on the surface area of the package. Another cost saving which is realized deals with the reduction in any bent or scratched leads

TABLE #1

OVERKILL CORRELATION TESTS

TEST #	DEVICE TYPE	NUMBER PARTS TESTED (1)	NUMBER GOOD	NUMBER FINE	NUMBER GROSS	% OVERKILL (2)
1	DIP	425	400	10	15	94.1 %
2	DIP	100	45	0	55	45.0
3	DIP	50	4	3	43	8.0
4	DIP	100	35	0	65	35.0
5	DIP	108	81	0	27	75.0
6	DIP	100	96	0	4	96.0
7	DIP	54	5	0	49	9.3
8	LCC	102	14	0	88	13.7
9	DIP	4000	1602	N/A	2398	40.0
10	DIP	228	196	4	28	86.0
11	Flatpack	77	25	0	52	32.5

TABLE #2

ESCAPEMENT CORRELATION TESTS

TEST #	DEVICE TYPE	NUMBER PARTS TESTED (3)	NUMBER GOOD	NUMBER FINE	NUMBER GROSS	% BAD PRODUCT OUTGOING (4)
1	DIP	598	584	0	14	2.3 %
2	DIP	1000	998	0	2	.2
3	DIP	600	592	0	8	1.3

(1) Parts failed bubble test
(2) Number good divided by total number parts tested
(3) Parts passed bubble test
(4) Number gross divided by total number parts tested

resulting from the batch preconditioning and testing of devices in the bubble test. These savings are difficult to put a price tag on unless you have a very good grasp of your rework costs or until you have been faced with a return by a major customer. With the current quality thrust in the industry, a return of product for a reason such as this is not only embarrassing and very costly from a monetary point of view, but more importantly, affects the reputation of your company.

Sometimes, a non apparent cost savings results from the ability with the NID to do gross leak testing end-of-line where it belongs and to eliminate most or all non-necessary sample testing steps. This test technique, because it is automatable, can greatly improve and streamline the product test flows of assembled packages.

In summary, this new technique is based on the utilization of an existing, proven technology. Its introduction has finally made this reliability test step more accurate, less costly, and automatable. Because of these advantages over the current most popular methods, measures can now be taken which will greatly improve the outgoing hermiticity quality level of Military Standard tested product, namely taking steps to do away with the bubble test for most high reliability applications.

REFERENCES

Robert Merrett, Test Methods and Their Limitations, 1984 International Reliability Physics Symposium Hermeticity Tutorial, 1-2.2 through 1-2.35, April 1984.

Aaron DerMarderosian, Permissable Leak Rates & Moisutre Ingress, 1984 International Reliability Physics Symposium Hermeticity Tutorial, 1-3.3 through 1-3.14, April 1984.

Ralph McCullough , Introduction/History, 1984 International Reliability Physics Symposium Hermeticity Tutorial, 1-1.1 through 1-1.3, April 1984.

W.E. Briggs & S.G. Burnett, Helium Mass Spectrometer Leak Testing Of Pressure - "Bombed" Sealed Enclosures, Varian Vacuum Division, 8, October 1, 1968.

S.B. Banks, R.E. McCullough & E.G. Roberts, Investigation of Microcircuit Seal Testing, Air Force Systems Command, Rome Air Development Center, Tech Rep RADC-TR-75-89, April 1975.

Chuck Wilkinson, Leak Testing Microelectronic Devices In Accordance With MIL STD 883, Microelectronic Manufacturing & Testing, 16-17, May 1985.

Richard Cole, Human Error and Vigilance in Relation to the Bubble Test, July 1986.

Edward Etess, Development of the NID system for performing gross leak testing in compliance with Military Standard 883, Qual-test 3 conference, tech report 1Q84-679, October 1984.

1.4 Reusable Moisture Standard Development for Package Gas Analysis*

Ray F. Haack
Jet Propulsion Laboratory
California Institute of Technology
MS 125-112
4800 Oak Grove Drive
Pasadena, CA 91109
(818) 354-6568

ABSTRACT

Initial design and testing of a device for application as a moisture standard for IC package gas analysis by mass spectrometry was reported at the RADC/NBS Moisture Workshop III. This device can be assembled at the analysis site and analyzed concurrently with IC packages. After analysis, the device can be disassembled and the sealing disc replaced; thus the package can be reused. Several packages have been sealed at ambient temperature in an atmosphere of either air or nitrogen with a known moisture content. A constant humidifer and optical dew-point hygrometer connected to a glove box provided the sealing environment. Following helium leak test certification, the packages were analyzed for moisture content by participating laboratories using mass spectrometric techniques. The study involved the use of packages consisting of vacuum melt stainless steel cavity material, a 16-mil gold-flashed aluminum sealing disc, and a threaded brass cap for applying the proper torque and pressure on the sealing disc. The effects of using air and nitrogen as the sealant gas will be presented and their correlation discussed.

INTRODUCTION

Further improvements in moisture standard packages are needed for attaining a high level of credibility in the electronic package gas analysis via the mass spectrometer (MIL STD 883B, method 1018.2). As specifications decrease the maximum allowable moisture level, the role of the standard becomes even more important. In an effort to meet this need, the concept of a reusable moisture standard package was investigated. The initial package design and test results were reported at the previous workshop[1].

The review and evaluation of the standard package design resulted in a package consisting of: 1) 304 vacuum melt stainless steel body with a cavity volume of ~0.05 cc, 2) gold-flashed 16 mil aluminum sealing disc and, 3) threaded brass cap. Correspondingly, these specific materials were selected to provide: 1) uniform cavity surface, 2) seal surface capability and moisture inertness and, 3) torque ease and reusability (anti-galling of threaded surfaces with brass and stainless steel).

---

*This paper represents one phase of research performed by the Jet Propulsion Laboratory, California Institute of Technology, sponsored by the National Aeronautics and Space Administration, Contract NAS7-918.

EXPERIMENTAL

The sealing surface of the stainless steel body was polished (1 micron alumina powder on felt); then cleaned ultrasonically. The three parts of the package unit were cleaned, rinsed with methyl alcohol, and air dried at 110°C for 16 hours. The dry parts were transferred to a dessicator for cooling and then to the glove box for assembly and sealing in an atmosphere of nitrogen or air at room temperature (25 ± 1°C) as outlined in Figure 1. The humidifier[2] and hygrometer provided moisture control of the environment during the sealing operation. The package components and glove box were equilibrated for one hour near the desired dew-point before beginning assembly. An additional one hour was required to assemble and torque (100 in-lbs) the packages in each series. Components of the package were handled with forceps. Continous monitoring of the sealing chamber exit gas showed a dew-point variation of ±0.3°C during the operation.

Sealed packages were subjected to hermeticity testing (15 psig for 12-16 hours). A helium leak rate of $> 1 \times 10^{-8}$ atm·cm^3/s was initially used as the criteria for rejecting units. Gas analysis for helium indicated that a leak rate of $< 0.2 \times 10^{-8}$ atm·cm^3/s provided better assurance that the standard was hermetic. Laboratories were requested to air or vacuum bake the samples at 100°C for a period of 12-16 hours prior to the puncture and gas analysis. However, the packages were not analyzed in an identical manner. Laboratory A used a batch system with a 12-16 hour vacuum bakeout at 100°C, Laboratory B used the rapid cycle method at 100°C, and Laboratory C used the rapid cycle method at 100°C preceeded with an air oven bakeout at 100°C for 12-16 hours.

RESULTS AND DISCUSSION

It must be emphasized that the primary task objective was to seal units at a given time and to establish if consistent results for these packages could be obtained. Fabrication and process control factors such as materials uniformity and treatment, hermeticity, and the sealing environment were maintained constant. The quality of the packages submitted for analysis should be assessed by the following:

1. relative burst pressure at puncture,
2. presence of argon when air was the sealant gas or, lack of argon when nitrogen was the sealant gas,
3. minor constituent gas anomolies,
4. percent moisture (volume/volume)*.

This study consisted of three series of experiments using the same reusable packages. Sealing discs were replaced after each use. The packages were sealed in an air atmosphere (~6000 ppm moisture) for series 1 and 2. For series 3, the packages were sealed in a nitrogen atmosphere (~6000 ppm moisture).

*Note: The percent moisture should represent that of the sealant gas as monitored by the dew-point hygrometer <u>and</u> the adsorbed surface moisture from the package cavity and seal disc.

Results for the three series of packages as analyzed by three different laboratories are shown in Table I. Graphical representation of relative burst pressure, percent argon, and percent moisture appears in Figures 2, 3, and 4 (the package designation corresponds to the order sequence in Table I).

The interval between seal date and analysis date varied as follows: Series 1, 20-60 days; Series 2, 29-48 days; Series 3, 13-14 days.

Series 1. For seven of the nine packages, the water content ranged from 0.49 to 1.08 with an average of 0.75%. Two other packages were outliers with 0.17% (S/N 52) and 3.99% (S/N 51). The argon percentages (Table I, Figures 2, 3, 4) are relatively consistent for the packages sealed in an air atmosphere and analyzed by a particular laboratory. The trace amounts of carbon dioxide (~0.1%) should be expected since the sealant gas was breathing air. Carbon dioxide is customarily a part of the gas analysis for electronic packages. In that case, its abundance is important to the understanding of chemical and/or physical changes which may have occured within the package.

The burst pressures may be subject to the method of analysis (either batch system or rapid cycle puncture device), the package cavity size, sealing conditions, and quality of the hermetic seal. The batch system probably produces the more accurate burst pressure since it represents a static state whereas in the rapid-cycle system the pressure depends dynamically upon the size of the puncture hole produced. Batch system measurements (capacitance manometer, readout of ±0.001 Torr) and corresponding package cavity volumes are shown in Figure 5. The close grouping of packages of a given size should be expected when they are hermetically sealed under similar conditions of temperature and barometric pressure.

Series 2. For eight of the eleven packages, the water content ranged from 0.40 to 1.07 with an average of 0.66%. Two other packages (S/N's 51 and 55) showed a trace of helium and therefore cannot be considered hermetic. Serial Number 43 (5.79% water content) was an outlier. The percentage of argon found in the packages (S/N's 42, 46, 52) was high (the nominal value for argon in air is 0.93%). Since these packages were analyzed by the same laboratory, the determined argon sensitivity factor for the mass spectrometer at that time could be in error.

Two factors were different for Series 1 and 2. The measured helium leak rates for the packages in Series 1 were $< 0.2 \times 10^{-8}$ atm·cm^3/s; whereas the rate for Series 2 packages was $\sim 1 \times 10^{-8}$ atm·cm^3/s. The second factor was a replacement of gloves for the glove box before beginning the Series 2 experiment. Although there does not appear to be correlation with these factors and this data, earlier work showed that traces of helium were detected in the packages having a helium leak rate in excess of 1×10^{-8} atm·cm^3/s.

Series 3. At this point, these packages are not considered as a valid moisture standard test. For this series, only S/N 49 can be considered acceptable. The other packages must be rejected because of measurable quantities of helium, argon, and oxygen. Several irregularities are apparent for the nitrogen-filled packages. Detectable amounts of hydrogen were found (seven out of 10); coincidentally these packages contained seal discs gold-flashed by a different vendor (Figure 7). The presence of oxygen could be due to either the sealant gas quality and/or a leak in the seal. It is not likely that the sealant gas

contained oxygen since the analyses do not show a correlation with the sealing sequence (all packages were filled in sequence within a one hour uninterrupted time interval). The results for package S/N 48 (presence of air consitituents) probably indicate an invalid sample; also it was a leaker in both Series 1 and 2.

The moisture content distribution exhibited by the samples submitted for analysis is shown in Figure 6. As discussed in the previous section (Series 1, 2, 3), some of the samples cannot be considered as valid standard package tests. Thermal cycling effects may have accounted for the random distribution of results obtained by Laboratory C. The laboratories which performed the analyses did not use the same type of sample introduction system although all analyses were performed at 100°C (method requirement). A random selection of samples for each laboratory was made so as to minimize any effect from the sequence of package fill and sealing. If the laboratory used the rapid cycle method, it was requested that the sample be oven heated at 100°C for 12-16 hours. This may not have been a wise decision considering that the package was thermally cycled twice. With the batch system, each package is thermally cycled only once. One would expect the total moisture to be in excess of 0.6% since it includes moisture in the sealant gas <u>and</u> the surface-adsorbed moisture. The later could conceivably add as much as 50% although the preparation and handling of the parts precludes it being more (seal hermeticity excepting).

Significant correlation exists between package hermiticity and the vendors providing "gold flashing" of the sealing discs. Gas analysis of packages sealed with discs from Vendor B (Table 1) showed the presence of helium, oxygen and argon and a potential chemical problem (the presence of hydrogen). The limited sample base precludes any postulation as to the source of hydrogen. The differences in hermiticity cannot be accounted for on the basis of the sealing atmosphere. Scanning electron micrographs revealed dramatic differences for the type of gold-flashed seal discs used (S/N 49 and S/N 56). Extensive penetration of the gold flash into the aluminum was shown by SEM using the backscattered detection mode, 100X (Figure 7b). The normal detection mode, 100X, (Figure 7d) also indicates potential leakage paths which would allow a loss of hermeticity. The depth of the gold flashing on the discs from each vendor was also compared (Figure 7e, 7f). The gold thickness for S/N 49 (Vendor A) was 2-3 microns, and that for S/N 56 was 4-5 microns. It should be noted that further conclusions must include the fact that the other components of the packages (particularly the seal edge) were not necessarily identical.

CONCLUSION

One important role for a moisture standard package is to calibrate the sensitivity of the mass spectrometer, particularly in the 2,000 to 5,000 ppm range which includes the maximum level allowed by MIL STD 883B, Method 1018.2. The use of this standard would prevent packages with very high moisture content from escaping detection. The air-filled package has merit since it can be easily assembled using ambient air. From the analytical chemistry view point, the nitrogen-filled package can be more definitive, i.e., the hermetic integrity can be readily determined from the presence of helium, argon, or oxygen. Also, the nitrogen-filled package has a practical merit in that the major percentage of semiconductor packages are currently sealed in a nitrogen

atmosphere. This package design is readily adapted for various cavity volumes; its ease of assembly makes it possible to prepare standards with various levels of moisture.

ACKNOWLEDGEMENT

The package hermeticity testing was performed by Kenneth C. Evans; SEM analysis by Ronald T. Ruiz. The author also wishes to acknowledge the review assistance from Dr. Alex Shumka (Electronic Parts Failure Analysis Group) and from Sheryl Bergstrom (Analytical Chemistry Group).

REFERENCES

1. Haack, Ray F., "A Moisture Standard for IC Package Gas Analysis," RADC/NBS Workshop Moisture Measurement and Control for Semiconductor Devices, III, NBSIR 84-2852, May, 1984.

2. Weaver, E.R., Hughes, E.E., and Diniak, A.W., "Determination of Water Vapor from the Change in Electrical Resistance of a Hydroscopic Film," Journal of Research of the National Bureau of Standards, Vol. 60, No.5, May 1958, pp. 489-508.

LIST OF TITLES AND ORDER

Figure 1. Package Sealing in Controlled Environment

Table I. Package Gas Analysis

Figure 2. Laboratory A Gas Analysis

Figure 3. Laboratory B Gas Analysis

Figure 4. Laboratory C Gas Analysis

Figure 5. Measured Burst Pressures

Figure 6. Moisture Content Distribution for Respective Laboratories

Figure 7. SEM - Gold-flashed Sealing Discs

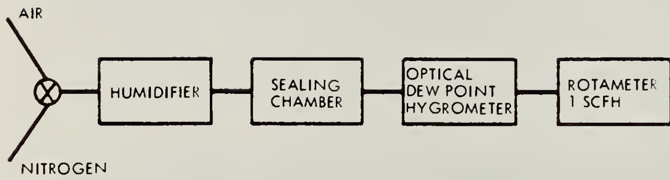

Figure 1. Package Sealing in Controlled Environment

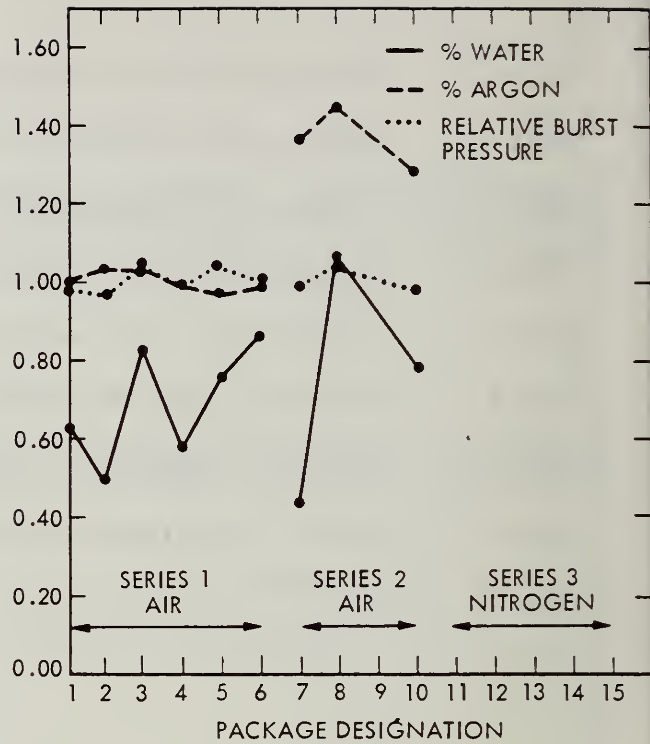

Figure 2. Laboratory A Gas Analysis

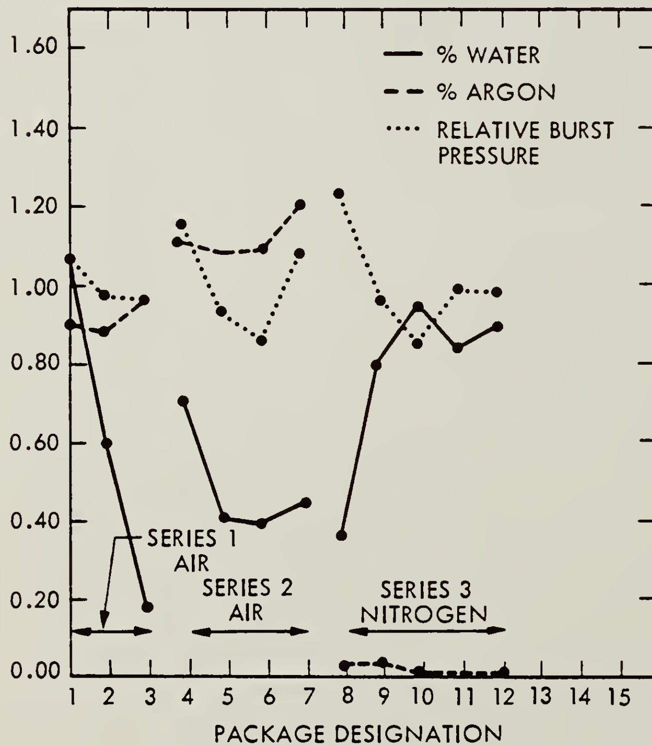

Figure 3. Laboratory B Gas Analysis

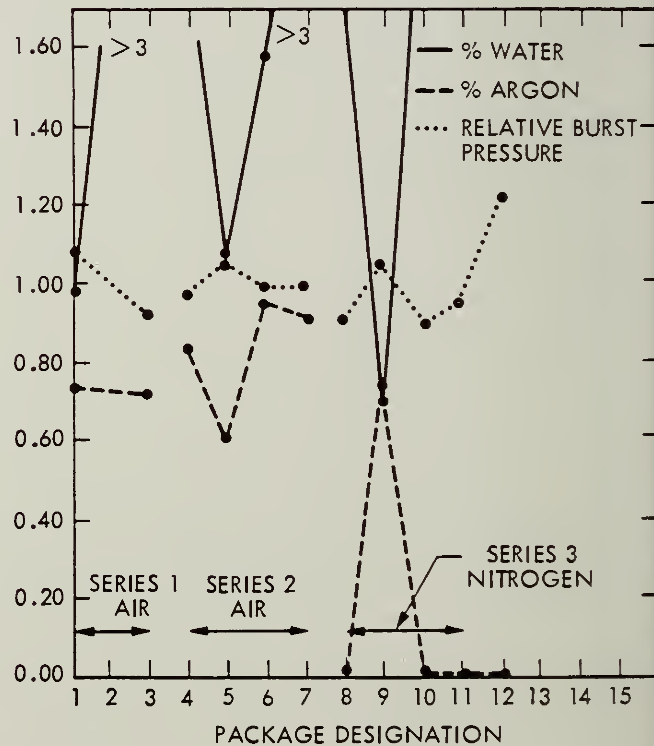

Figure 4. Laboratory C Gas Analysis

TABLE I. Package Gas Analysis

S/N	Relative Burst Pressure[1]	COMPONENTS (% volume/volume)						
		He	Ar	H_2O	N_2	O_2	CO_2	H_2
Series 1								
42	0.98	NA[2]	1.00	0.62	85.9	12.4	0.12	NA
45	0.96	NA	1.03	0.49	84.5	13.9	0.12	NA
46	1.04	NA	1.03	0.83	84.9	13.1	0.15	NA
47	0.98	NA	0.99	0.57	80.1	18.2	0.13	NA
54	1.04	NA	0.97	0.76	79.8	18.5	0.15	NA
55	1.01	NA	0.99	0.87	82.8	15.2	0.16	NA
43	1.08	ND[3]	0.90	1.08	77.3	20.5	0.16	ND
49	0.97[4]	ND	0.88	0.59	78.5	19.8	0.18	ND
52	0.95[4]	ND	0.96	0.17	77.6	21.2	0.08	ND
44	1.08	0.013	0.74	0.98	79.0	18.8	0.04	0.00
48	0.00	NA						
51	0.92	0.00	0.72	3.99	77.7	17.3	0.02	0.00
Series 2								
42	0.99	NA	1.36	0.43	83.2	15.0	ND	NA
46	1.04	NA	1.46	1.07	83.2	14.3	<0.3	NA
48	0.00	NA						
52	0.98	NA	1.29	0.78	81.5	16.4	<0.3	NA
44	1.15	ND	1.11	0.71	76.0	22.2	0.02	ND
45	0.93	ND	1.08	0.40	77.0	21.4	0.09	0.01
49	0.86	ND	1.09	0.39	76.8	21.7	0.06	0.03
54	1.07	ND	1.20	0.44	76.1	22.2	0.05	<0.01
43	0.98	<0.01	0.83	5.79	75.3	17.6	0.02	0.00
47	1.05	<0.01	0.61	1.07	81.0	17.2	<0.01	0.00
51	0.99	0.01	0.95	1.57	78.3	18.7	0.01	0.00
55	0.98	0.01	0.92	3.85	77.0	17.7	0.02	0.00
Series 3								
44*	1.22	2.89	0.03	0.36	95.7	0.99	0.01	0.04
45	0.98	ND	0.03	0.80	98.4	0.75	0.01	ND
49	0.85	ND	ND	0.95	99.0	ND	<0.01	ND
52*	0.98	0.68	ND	0.83	98.2	0.32	<0.01	0.01
56*	0.98	1.42	ND	0.89	97.3	0.37	<0.01	0.04
43*	0.91	1.22	0.01	4.48	85.8	5.35	<0.01	3.15
48*	1.05	<0.01	0.75	0.70	79.8	18.7	0.01	0.00
51	0.90	0.01	0.00	3.77	96.2	<0.01	0.00	0.01
54*	0.95	<0.01	0.00	63	35.0	0.19	0.00	1.76
57[5]	1.20	0.09	<0.01	2.64	94.3	0.38	0.00	2.55

[1] Calculated with average of each analysis group as reference.
[2] Not Available.
[3] None Detected.
[4] Seal disc decreased in thickness at time of analysis.
[5] Machined cavity depth of 0.145"; other packages 0.110 ± 0.005"
* Gold flashing by Vendor B.

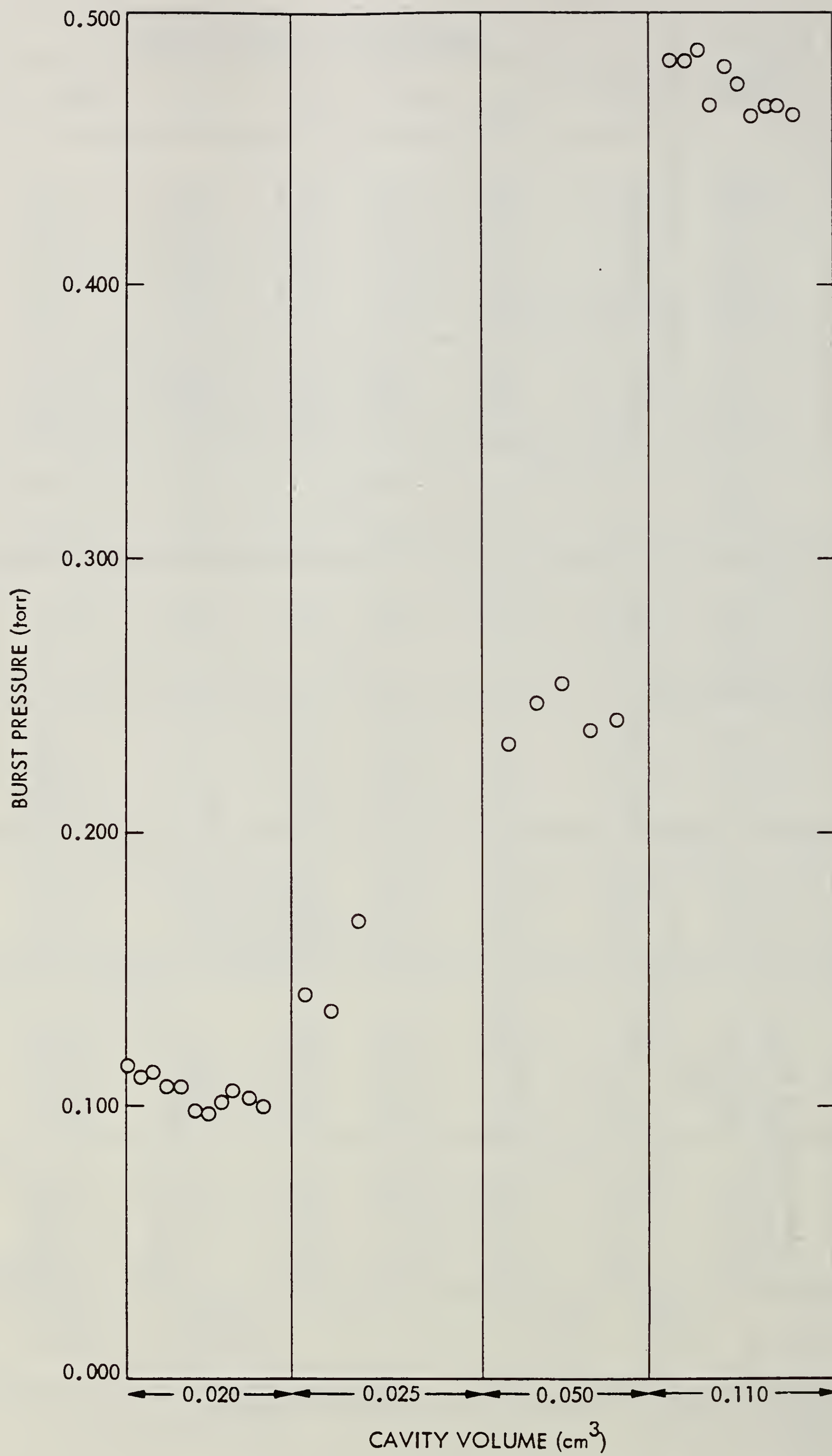

Figure 5. Measured Burst Pressures

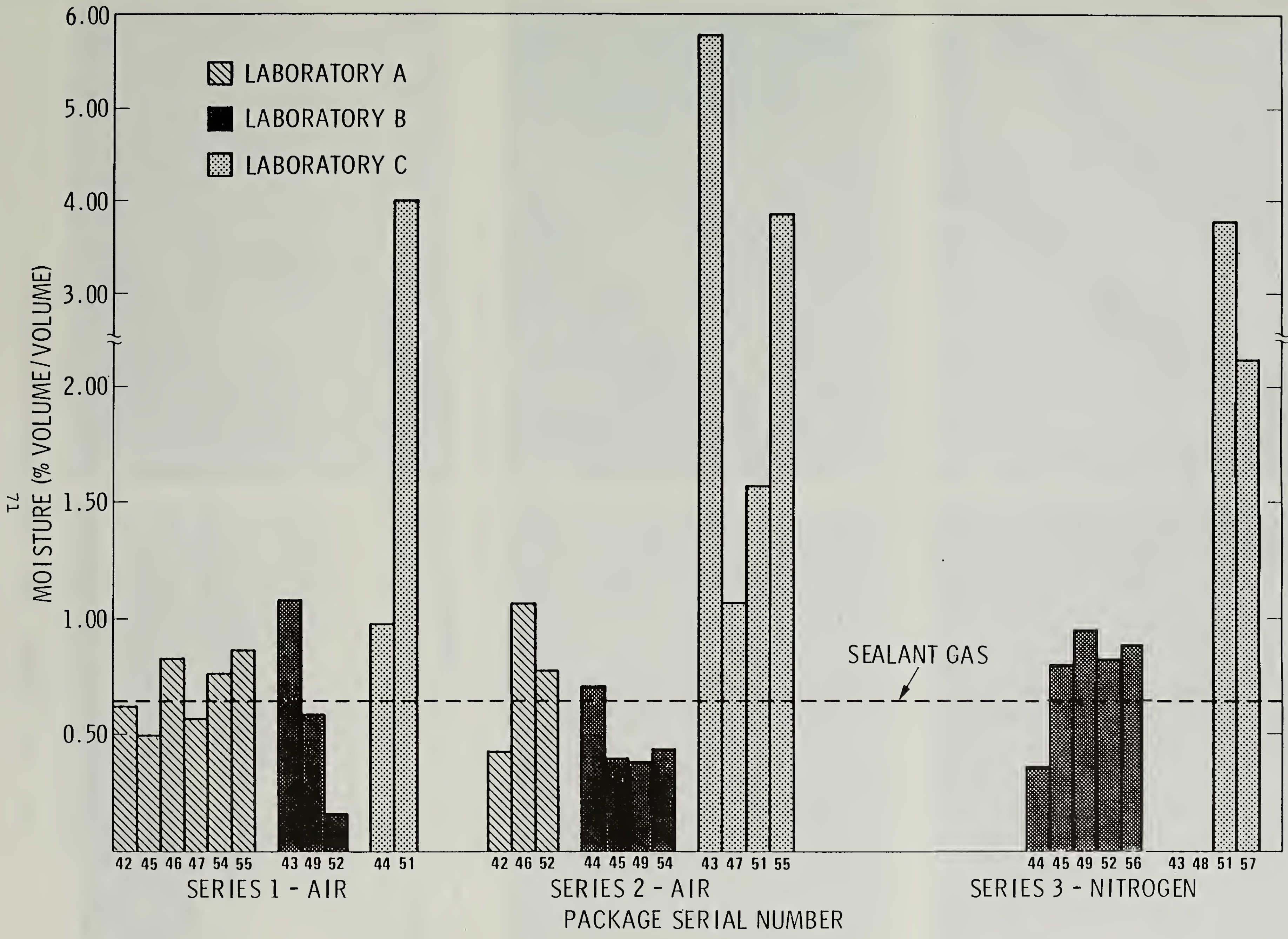

Figure 6. Moisture Content Distribution for Respective Laboratories

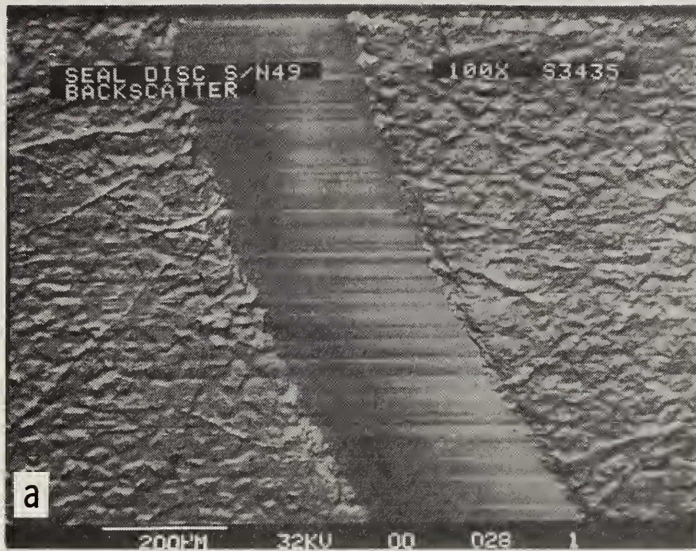

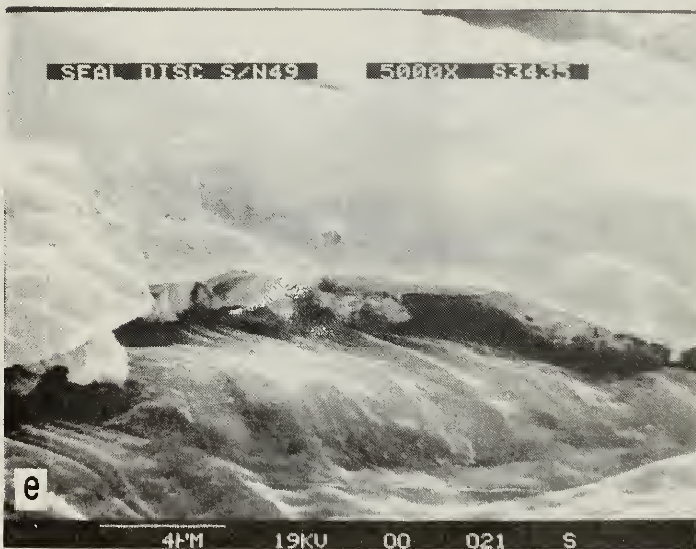

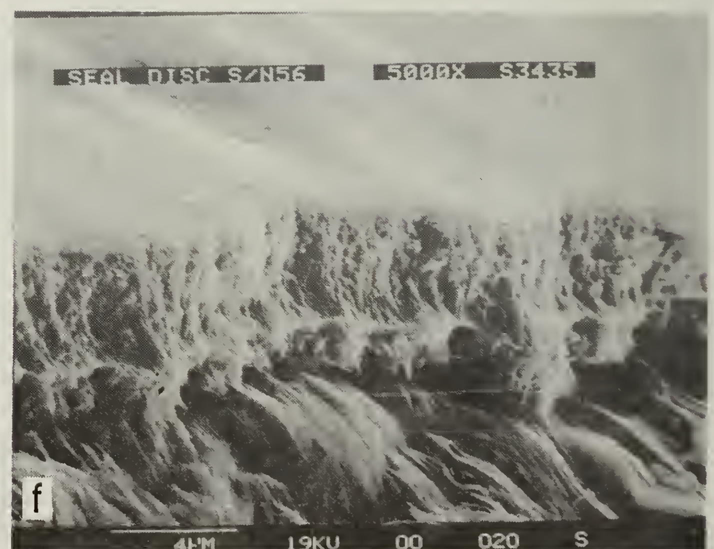

Figure 7. SEM - Gold-flashed Sealing Discs

2.1 MOISTURE PROCESS CONTROL AND MASS SPECTROMETER CORRELATIONS

R.K. LOWRY
Harris Semiconductor Analytical Services Department
P.O. Box 883, M/S 62-07
Melbourne, Fla. 32901
305/724-7566

I. Introduction

Technologies for controlling internal water vapor content of hermetically sealed IC packages have matured greatly over the past decade.[1-3] In fact, for semiconductor packages which do not contain organic materials, achieving low internal moisture at seal is primarily a matter of conscientious and consistent process execution.

The MIL-SPEC internal water vapor limit has evolved as a generic specification for the IC industry. Users of IC products have come to expect that hermetically sealed packages, whether "hi-rel" for aerospace/military applications or "commercial" for less stringent uses, will contain less than 5000ppmv of moisture sealed in the cavity.

For this reason extensive moisture control precautions are common practice in most manufacturers' assembly sealing operations. This paper discusses a body of data from an overseas assembly facility for commercial IC products being sealed into TO-99 header-style packages.

II. TO Package Assembly Engineering

A. Package Construction

The TO-99 package consists of a gold plated metal substrate with hard glass feed throughs for the pins and a nickel cap. The cap is welded onto the header near room

temperature in a controlled N_2 atmosphere to form the package seal. The internal volume of the sealed cavity is typically 0.05cc. This is a batch operation in which 200-2000 packages are sealed in a group in the welder chamber, and then removed to allow another large group of piece parts to be placed in the chamber for sealing.

Engineering studies over the years at the overseas assembly location where this process is run revealed a number of precautions necessary for controlling internal water vapor content of TO-99 cans.

B. Moisture Control in TO Packages

With the advent of the TO package years ago, it was thought that the principal requirement for product dryness was keeping moisture low in the sealing chamber. Welders have always contained sensors for monitoring "drybox" moisture. But experience has shown that low welder moisture levels are a necessary but far from sufficient condition to assure package dryness.

The piece part materials themselves are the principal source of moisture in TO cans. The seal glass and the metal parts contain both chemisorbed surface water and bulk water which can off-gas after seal to contaminate the package cavity. An examination of the condition of the sealing glass at 30X will reveal its potential for moisture volatilazation. The parts can exhibit blowholes and/or meniscus cracking of the glass, providing escape paths for internally trapped water to the cavity.

Vacuum baking is imperative to dependably desiccate the package piece parts. Both headers and caps are loaded into a vacuum chamber directly adjacent to the sealing chamber. They are vacuum baked well below 100 mtorr pressure. Pumpdown time to working pressure is in addition to the low pressure residence time. When the vacuum bake is concluded, the parts are transferred to the sealing chamber with minimal exposure to room ambient. The chamber contains appropriate moisture sensors and its ambient is ultra-dry N_2 at atmospheric pressure.

III. Mass Spectrometry and SPC for Moisture Control

Process optimizations described above were reached as a result of extensive engineering studies. All the moisture measurements for the studies were made by mass spectrometry. As an outgrowth of the studies, a plan evolved for the ongoing assurance of moisture control in the TO sealing process. The plan is based on the principles of statistical process control (SPC). The SPC approach verifies the quality of a process based on sampling for attributes, in this case package moisture content. It helps maintain a consistent mean for the process with a continual monitor of the process' natural variability. An SPC approach to moisture control in Cerdips has previously been reported.[4]

In the SPC plan, two assembled cans are randomly pulled from each sealing lot. These are logged along with all

pertinent information regarding the sealing of that lot. All samples of each day's production are accumulated and forwarded to the analytical laboratory. The laboratory analyzes one sealing lot per day each of eutectically mounted product (two specimens) and epoxy mounted product (two specimens) by mass spectrometry. The mean moisture level and variability are monitored by SPC charts maintained separately on the eutectic and epoxy mount processes. Any reading above the Upper Control Limit (UCL) for the process being monitored causes samples of the lots sealed just before and just after the out-of-control lot to be immediately pulled and analyzed.

In this way, out-of-control conditions are quickly identified and time-bracketed while an assignable cause for the out-of-control condition is found. This also provides a means of isolating any product lots which may exceed engineering tolerances on internal water vapor.

Process control data governing the TO sealing as well as other hermetic package sealing processes have been measured for a number of years in the Harris analytical services mass spectrometer. This is a Pernicka Corporation rapid cycle instrument with three volume calibration valve providing calibration bursts of 0.01, 0.1 and 0.8cc. This instrument was certified by DESC in 1985 for measurements pertinent to the 5000ppmv MIL SPEC limit after a series of calibration and round robin analysis experiments. The SPC data discussed here span the time before, during, and after all the certification activities.

IV. Process Baseline Statistical Data

A. Eutectic Process

Fig 1 is the histogram for 362 data points which characterize the eutectic sealing process for a one year time period approximating CY 1985. The data is normally distributed.

Figs 2A and 2B are the control charts governing the process. The process mean is 1527ppmv, with a three sigma Upper Control Limit of 2623ppmv (as calculated from the R value).

B. Epoxy Die Attach Process

Though carried out in the same process equipment, the epoxy process is charted and controlled entirely separately from the eutectic process because the presence of epoxy in the sealed headers adds a new technical dimension to controlling the moisture attribute.

Fig 3 is the histogram for 173 data points which characterize the epoxy sealing process for the same time period as the above eutectic data. The data is approximately normally distributed, with a bit of tail-off in the high end of the range.

Figs 4A and 4B are the xR charts for the epoxy process. The process operated at a mean of 2267ppmv with a UCL of 4541ppmv.

C. State-of-the-Process

Table IA summarizes the state of the header sealing process for both eutectic and epoxy processes, during approximately CY 1985.

TABLE IA*

	PROCESS MEAN	UPPER CONTROL LIMIT
Eutectic	1527ppmv	2623ppmv
Epoxy	2267ppmv	4541ppmv

*Individual mass spectrometer readings are significant only to the nearest 100ppmv. All values in this paper are the result of statistical treatment of sets of data, and thus carry more figures than are significant to help comparisons of means and control limits.

These numbers describe the fundamental capability of the process through CY 1985. The process appears to be operating at its optimum using approaches described in the previous sections. No samples of eutectic exceeded 5000ppmv while three of the epoxies exceeded 5000ppmv. Both processes had means and UCL's below the MIL-SPEC moisture limit. In every case, where a lot sample exceeded the UCL, the lots before and after it were analyzed and found to be in control. And in most cases, lots measured as out of control were found to have an assignable cause for the excess moisture, e.g. non-hermeticity of the analyzed sample, process log entries indicating inadequate bake cycles, etc.

D. Concern for the Process

With the attributes of Table IA, the header sealing operation was considered to be providing product from a controlled process. But concern began to build that if/when the MIL-SPEC engineering limit for moisture were lowered from 5000ppmv to 3000ppmv or 2000ppmv the majority of the parts containing epoxy as well as a non-trivial number of the eutectic parts would not meet the specification, even though they were coming from a process operating within statistical control.

While pondering this concern, but before any actions could be formulated to address the matter, the mass spectrometer became inoperable. It went out of service for more than 2 months.

Production continued, however, and provisions of the SPC plan called for maintaining all elements of the plan by obtaining mass spectrometer data from a certified commercial laboratory. Consequently sampling and mass spec analysis continued uninterrupted, and data began to flow in from the commercial lab.

V. Statistical Definition of the Process By a Different Mass Spectrometer

As the data came in, a different picture of the process started to emerge. Though the sample size is much smaller than the above data set, the data led to a much different perception of moisture level in the process.

A. Eutectic Process

Fig 5 is a histogram of the 38 samples of the eutectic process measured at the commercial laboratory. While there are insufficient samples to judge whether the data is normally distributed, the histogram still gives a good picture of how this mass spectrometer measures moisture in the process.

Figs 6A and 6B are the xR charts for these data points. Thirty eight points are sufficient for valid control charts with process attributes calculated as described previously.

The process' mean moisture content is now defined as 504ppmv, with a UCL of 1602ppmv!

When analyzed in this mass spectrometer, the process attributes are very different. So different, in fact, that even if the MIL-SPEC moisture limit were reduced to 2000ppmv, all eutectic product delivered from within the process control limit would easily meet that specification. We thus get a very different impression of the process from this second analytical instrument.

B. Epoxy Process

Figs 7A and 7B are the xR charts for the epoxy process. Sixteen data points are not sufficient for valid control charts, so the process mean of 774ppmv and the UCL of 2967ppmv must be considered trial values. Nevertheless, it appears that a significant downward shift in the process attribute has occurred just as in the eutectic process.

C. The "Revised" State-of-the-Process

Table IB summarizes the newly-defined process attributes. The values to the left of the heavy line are the process attributes determined in the Harris mass spectrometer and are repeated from Table IA.

TABLE IB

	Harris Mass Spec Repeated from Table IA		Commercial Lab	
	Process Mean	UCL	Process Mean	UCL
Eutectic	1527	2623	504	1602
Epoxy	2267	4541	774	2967

It is essential to remember that samples analyzed at the commercial lab are from the same uninterrupted manufacturing process, operating essentially in control. The only apparent assignable cause for the shift in means and UCLs is the change in analytical equipment.

During the time that the SPC data-gathering plan was being fulfilled by data from the commercial laboratory, the mass spectrometer in the Harris laboratory underwent extensive refurbishment.

This included:

- Installation of a computer for instrument control and data acquisition.
- Change-out of all valve tips, seats, and gaskets.
- Re-build of all pumps.
- Re-build of controller boards.
- Re-build of all seals and flanges.
- Cleaning of all seals and flanges.
- Installation of new stainless lines and complete assurance of leak-free instrument operation.

All of the hardware upgrading resulted in a like-new analytical system. It returned to service more than 2 months after breakdown. With the mass spectrometer up, the SPC analysis plan reverted back to the Harris equipment before full consideration could be given to the import of the differences in analytical equipment evident in Table IB.

VI. Another Statistical Definition of the Process

As data accumulated from the ongoing operation of the re-built Harris instrument, yet a third picture of the moisture attribute emerged.

A. Eutectic Process

Fig 8 is a histogram of the 56 samples of the eutectic process measured from the return to service of the Harris machine to the writing of this text. While there are insufficient samples to judge whether the data is normally distributed, the histogram gives a good picture of how the re-built mass spectrometer sees the moisture distribution in the process. It is especially interesting to overlay Fig 8 with Fig 5, to compare the distributions defined by the commercial laboratory instrument and the re-built Harris instrument.

Figs 9A and 9B are the xR charts of the process as measured by the re-built Harris instrument. The process' mean moisture content is now defined as 865ppmv, with UCL of 3087ppmv.

B. Epoxy Process

Figs 10A and 10B are the xR charts for the epoxy process. The 44 data points constitute a statistically valid chart, indicating a new mean for the epoxy process of 1478ppmv with a UCL of 4067ppmv.

C. The "Re-revised" State-of-the Process

Table IC summarizes the newly-redefined process attributes. Values to the left of the heavy line are repeated

from Tables IA and IB for ease of comparison.

TABLE IC

	Harris Mass Spec Repeated from Table IA		Commercial Lab Repeated from IB		Harris Re-built Mass Spec	
	Process Mean	UCL	Process Mean	UCL	Process Mean	UCL
Eutectic	1527	2623	504	1602	864	3087
Epoxy	2267	4541	774	2967	1478	4067

VII. Comparison of Means for the Analytical Equipment

The "inter-ocular exam" of Table IC and Fig 11 certainly suggests that the moisture attribute of this sealing process depends upon which analytical system is being used to characterize it.

To compare whether or not these various means are equivalent statistical tests of the data were carried out. A t-statistic[5] was computed for each pair of means to be compared by

$$t = \frac{\bar{Y}_1 - \bar{Y}_2}{\sqrt{\frac{s_1^2}{n_1} + \frac{s_1^2}{n_2}}}$$

Where $\bar{Y}$ = mean for a given set of data

s = the variance for that set of data

n = the number of points in the data set.

This formula comprehends large differences in s and n between data sets, and also is not especially sensitive to whether or not the data are normally distributed. Summary statistics for the data sets are in Table II.

Table II

Summary Statistics

		Data Set	n	Mean	Variance
Eutectic Process	Historical Harris Values	I	362	1527	275975
	Commerical Lab	II	38	504	442971
	Re-built Harris Instument	III	56	865	949221
Epoxy Process	Historical Harris Values	IV	173	2267	1022717
	Commercial Lab	V	16	774	486478
	Re-built Harris Instrument	VI	44	1478	1643908

Table III records the results of the comparison of means.

Table III

Equality of Means

	Comparing Data Set	Computed t-Statistic	Critical Value of t	Means Equivalent?
Eutectic Process	I with II	9.18	1.96	no
	II with III	2.13	1.96	no
	I with III	4.97	1.96	no
Epoxy Process	IV with V	7.83	2.12	no
	V with VI	2.70	2.12	no
	IV with VI	3.79	1.96	no

The critical values of t are for $\alpha = .05$ and are for degrees of freedom dictated by the least value of n for the two data sets being compared. The value of 1.96 is common for all degrees of freedom >29. In all cases, the computed t-statistic exceeds the critical value of t. In all these cases, it can be stated with 95% confidence that no two compared data sets are the same. The only apparent assignable cause for this is the change in analytical equipment.

It can be seen from Fig. 11 that not only do the process means shift with changes in equipment but so do the UCL's. The shifting UCL's indicate a change in the variability of the moisture attribute. And it is interesting to note that when the re-built instrument resumed operation, the process mean

for eutectic was substantially lower than originally, but its associated UCL was higher.

The total variability of any attribute is the sum of its natural variability plus the variability inherent in the equipment used to measure the attribute. In the data summarized in Fig 11 there is apparently an increase in the variability of the sealing process or of the measurement or of both.

Given the lack of "standard" packages, we do not have a good definition of measurement variability. The minimum amount of measurement variability is defined by the reproducibility of the moisture values read on bursts of humidified N_2 whose moisture content has been determined by a calibrated dewpoint hygrometer. For 0.10cc bursts of N_2 humidified to 5000 ppmv moisture, the variances for replicate bursts observed in the Harris instrument were 18068 and 19233 before and after re-build, respectively. These variances are much smaller than all those for the various process measurements in Table II (all are >275,000).

From this it is assumed that much of the observed variability is process variability. It must also be assumed that measurements after the re-building of the instrument indicate a lower process mean, but that the process variability for that particular measurement window is greater. This is observable for both the eutectic and epoxy process.

VIII. Summary and Conclusions

It is clear that analytical mass spectrometers applied to the nontrival problem of measuring water vapor in small

enclosures must be absolutely optimized with respect to hardware. Optimized vacuum practices and equipment maintenance, with assurance of no virtual vacuum leaks, account for the apparent reduction in process mean obtained by re-building the equipment.

But even after instrument improvements, the eutectic process UCL is 3087ppmv, higher than that attained in the old system. This could be a consequence of a higher natural tolerance for the segment of the process represented by the 56 samples, even though the mean is lower.

Even though the re-built instrument is now operating to the very best of its mechanical ability, a discrepancy remains between it and the commercial laboratory instrument. This discrepancy:

(1) is statistically significant.

(2) is specification-conformance significant. That is, if the process is qualified at the commercial laboratory it would produce parts capable of meeting an engineering maximum tolerance reduced from 5000ppmv to 2000ppmv, but the same process qualified by the manufacturer's own analytical equipment would not conform to an engineering maximum tolerance reduced from 5000ppmv to only 3000ppmv.

There is a need, in future efforts to build "standard" packages for mass spectrometric calibrations, to consider both the accuracy and precision of water vapor determinations. This is because the notion of process control, which is so

critical for both cost-effective as well as inherently-reliable processing, must comprehend knowing both the value of the process mean (accuracy) as well as the variability (precision) with which measurements are made, so that true <u>process variability</u> can be known. "Standards' must be prepared with this in mind, and participating laboratories must be willing to measure enough replicate samples to establish precision. It is not sufficient to assume that calibration bursts identify all measurement variability, because that procedure does not duplicate the physics of moisture release from the component materials of sealed packages into the mass spectrometer.

Acknowledgments: The invaluable efforts of Steve Slasor and Dr. Jack Linn with mass spectometer operation are gratefully acknowledged along with the work of Caroline Connor in typing the manuscript.

References

1. White, M.L., Striny, K.M., and Sammons, R.E., "Attaining Low Moisture Levels in Hermetic Packages," in Proceeedings of the 20th Annual Reliability Physics Symposium, March 30-April 1, 1982, San Diego, CA, pp. 253-259.
2. Proceedings of the RADC/NBS Workshop, Moisture Measurement and Control for Semiconductor Devices, III, May, 1984, Sessions IV-VII, pp. 180-313.
3. Loo, M.C., "Influence of Seal Glass on the Hermeticity of Cerdip Packages," Solid State Technology, 29(8), August, 1986, pp. 163-165.
4. Elo, R.B., and Massoletti, A.M., "Control Chart Analysis of Moisture in CERDIPS," in Proceedings of the RADC/NBS Workshop, Moisture Measurement and Control for Semiconductor Devices, III, May, 1984, pp. 24-39.
5. Parr, W.C., "Economical and Informative Experimentation for Process Improvement and Development," Harris Semiconductor technical memorandum, 1985, pp. 1.77.

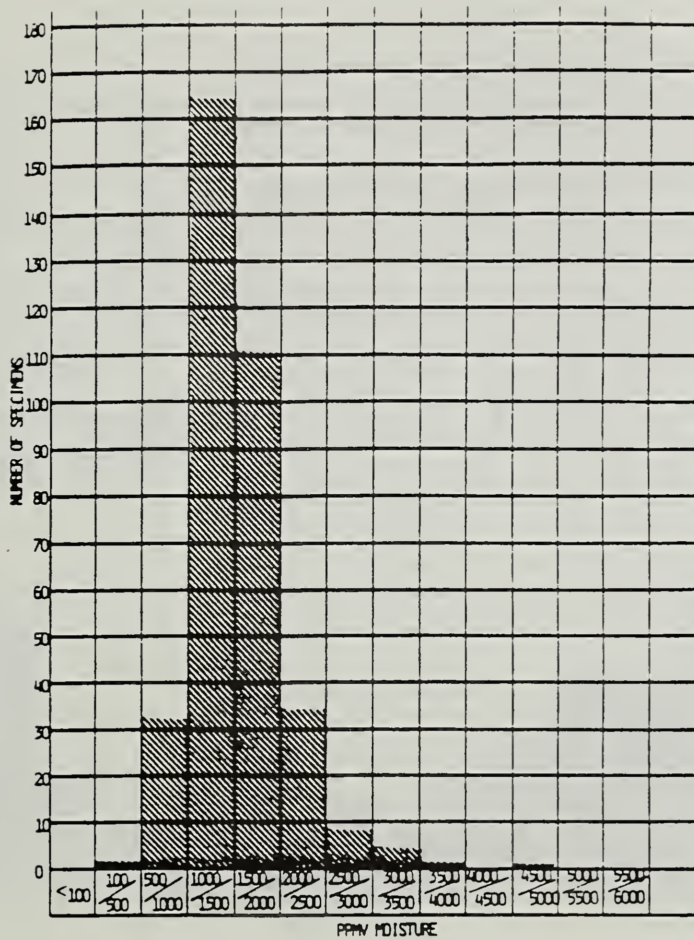

Figure 1.

Histogram, Eutectic Seal Process, 1985

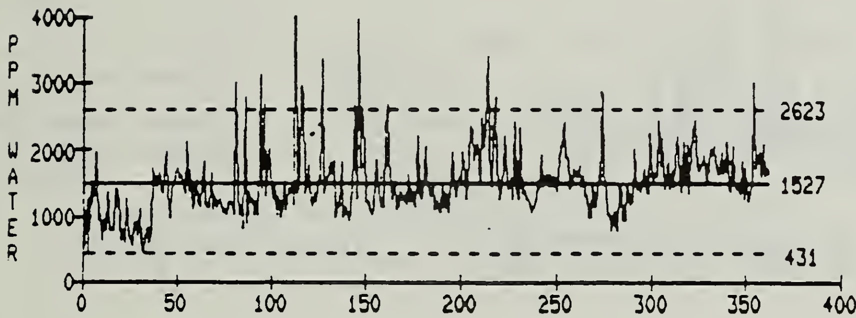

Figure 2A.

x Chart, Eutectic Seal Process, 1985

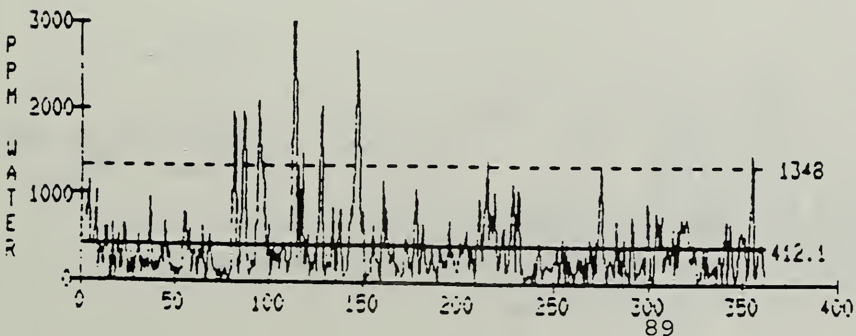

Figure 2B.

R Chart, Eutectic Seal Process, 1985

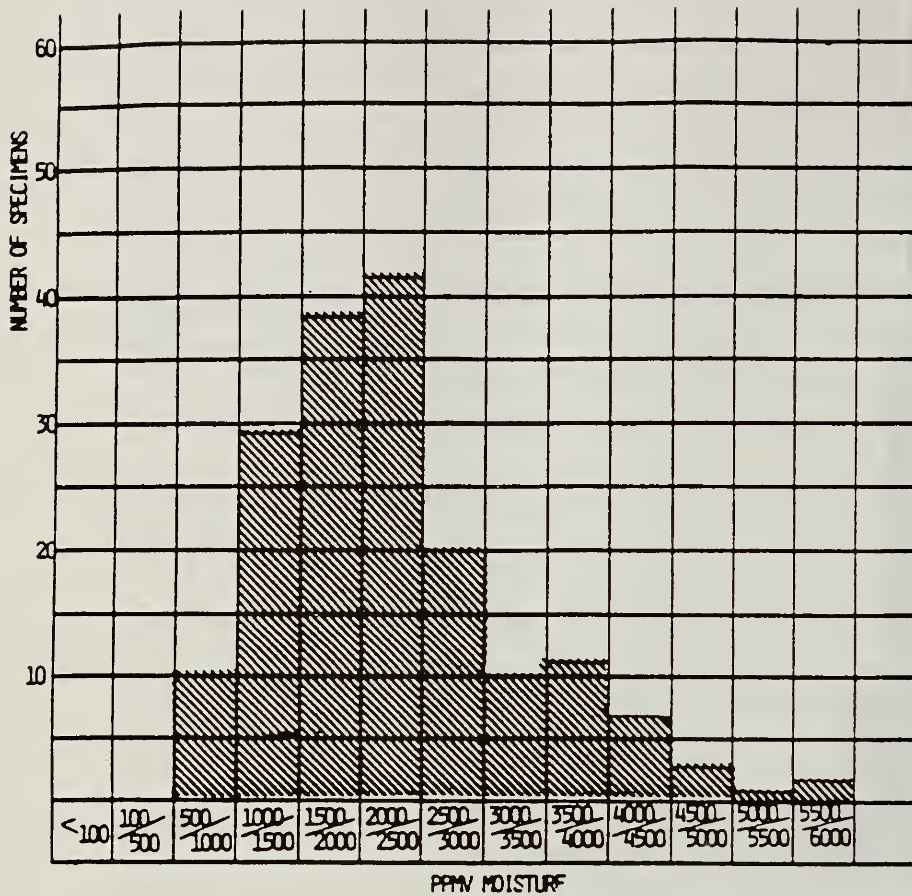

Figure 3.

Histogram, Epoxy Seal Process, 1985

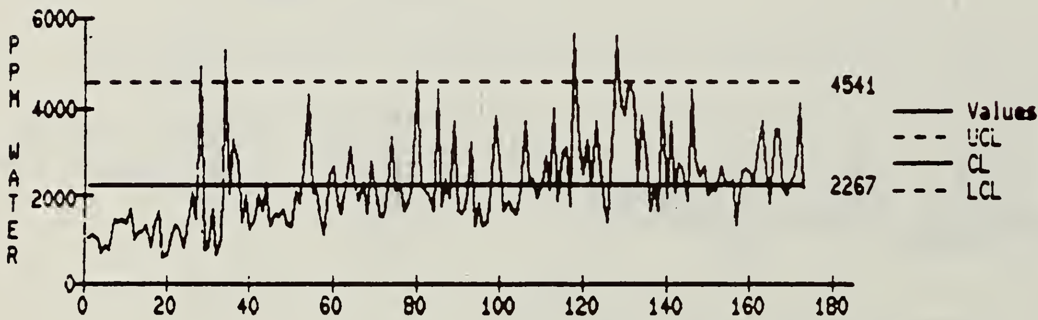

Figure 4A.

x Chart, Epoxy Seal Process, 1985.

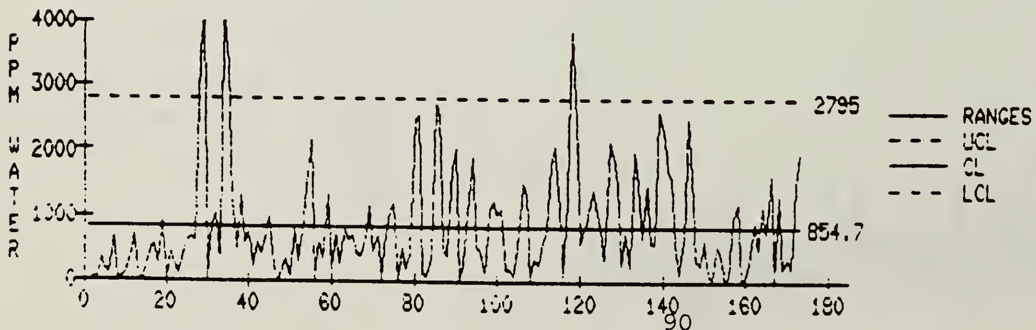

Figure 4B.

R Chart, Epoxy Seal Process, 1985

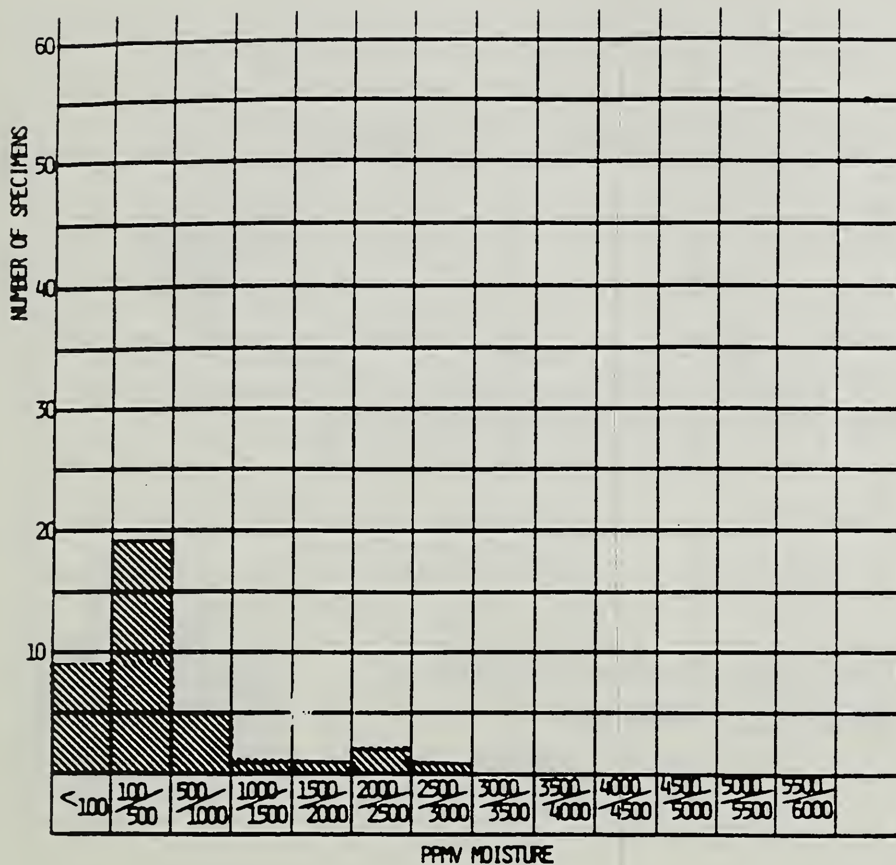

Figure 5.

Histogram, Eutectic Seal Process, measured by commercial laboratory.

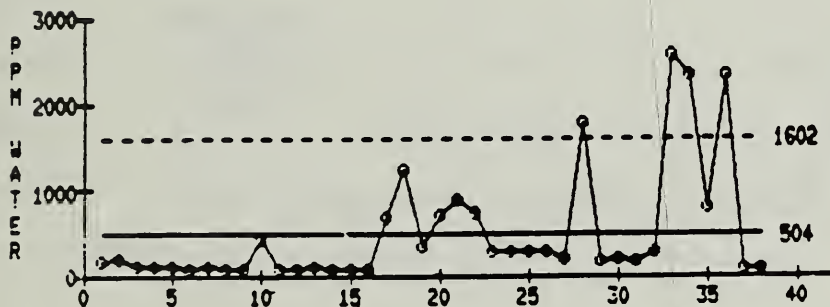

Figure 6A

x Chart, Eutectic seal Process, measured by commercial laboratory.

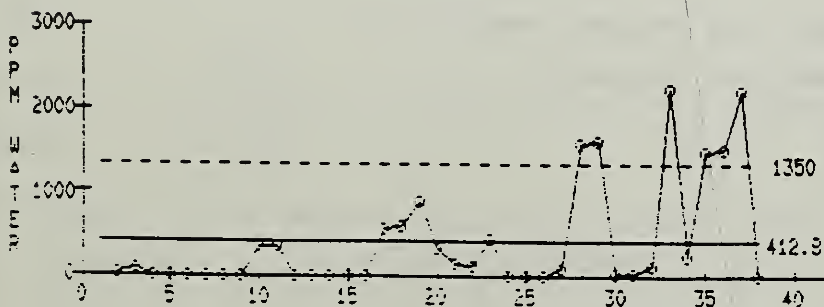

Figure 6B

R Chart, Eutectic Seal Process, measured by commercial laboratory.

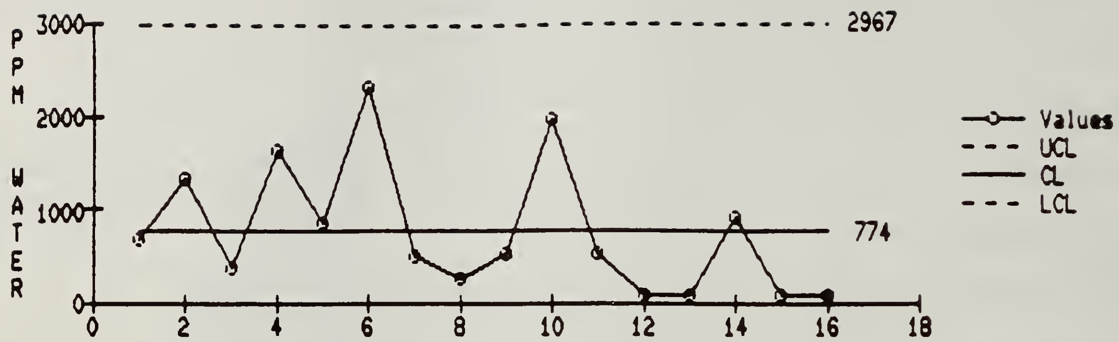

Figure 7A.

x Chart, Epoxy Seal Process, measured by commercial laboratory.

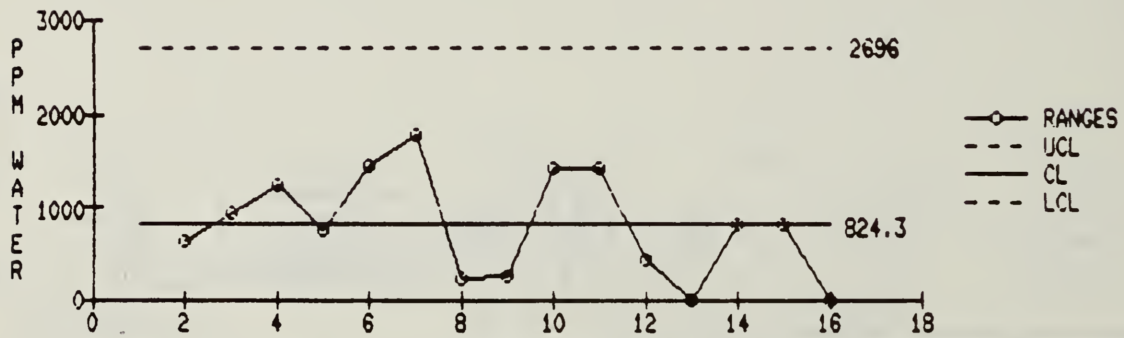

Figure 7B.

R Chart, Epoxy Seal Process, Measured by commercial laboratory.

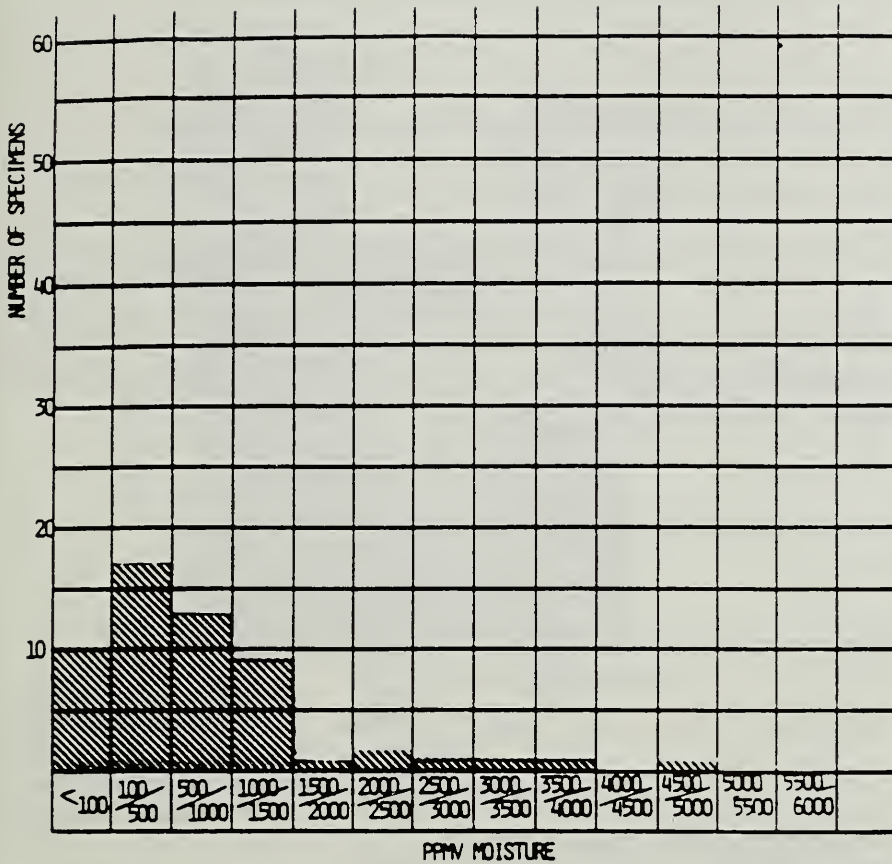

Figure 8.

Histogram, Eutectic Seal Process, measured in original mass spectrometer after major instrument renovation.

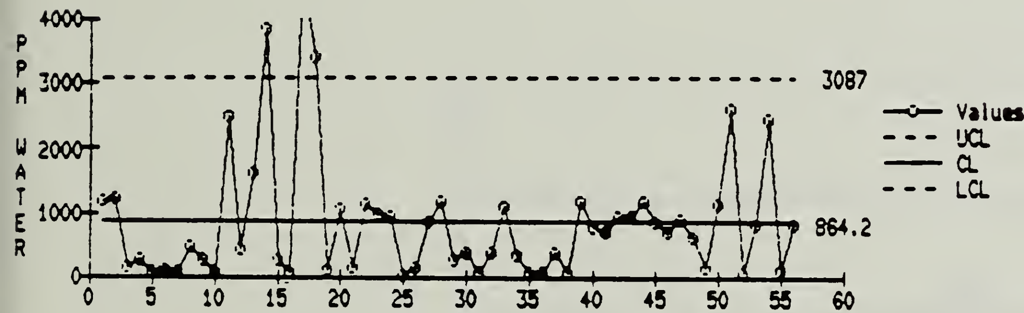

Figure 9A.

x Chart, Eutectic Seal Process, measured in original mass spectrometer after major instrument renovation.

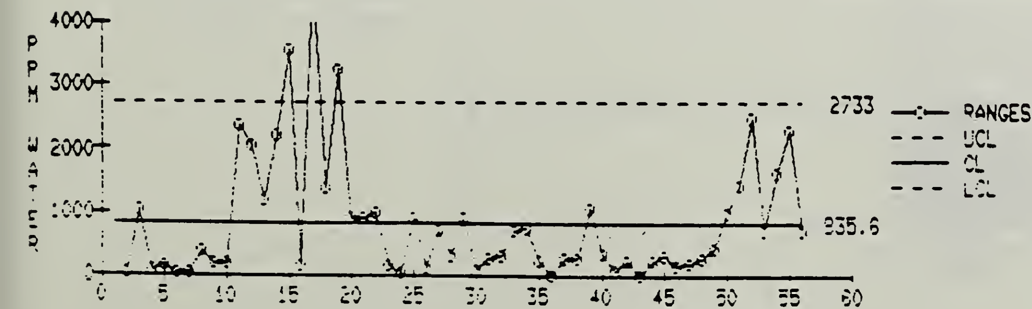

Figure 9B.

R Chart, Eutectic Seal Process, measured in original mass spectrometer after major instrument renovation.

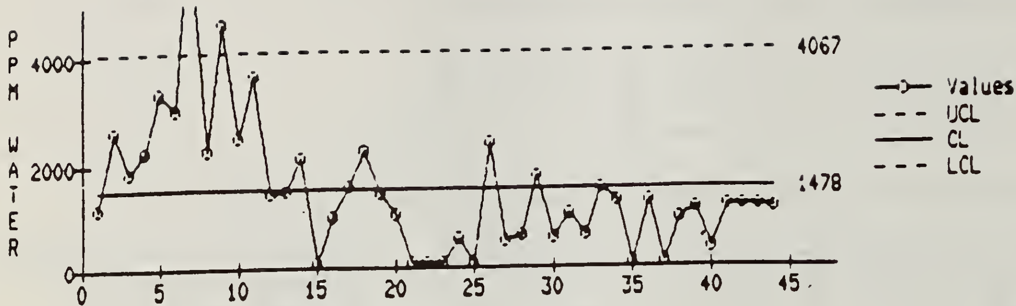

Figure 10A.

x Chart, Epoxy Seal Process, measured in original mass spectrometer after major instrument renovation.

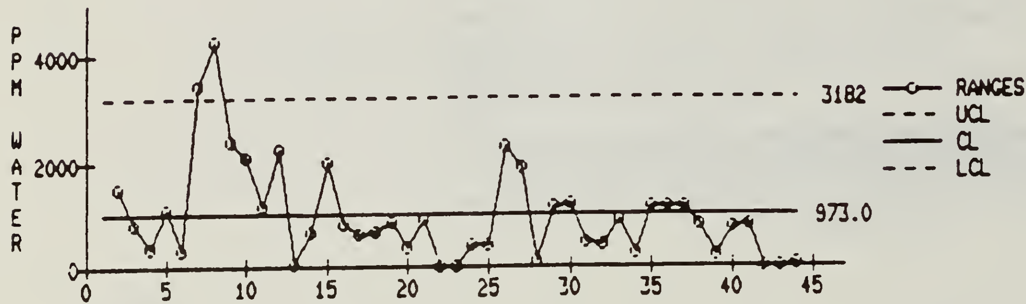

Figure 10B.

R Chart, Epoxy Seal Process, measured in original mass spectrometer after major instrument renovation.

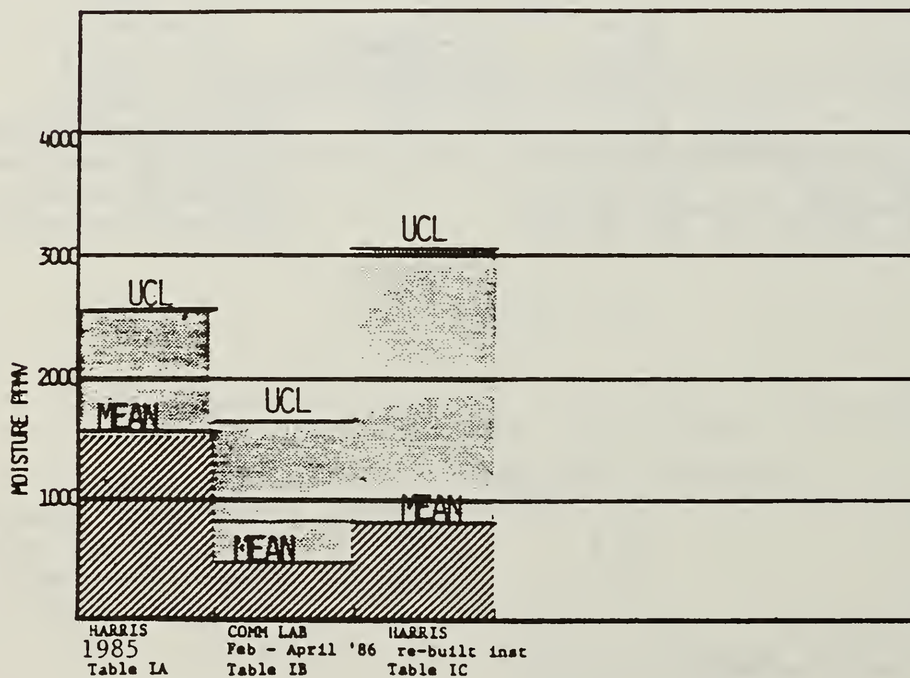

Figure 11A.

Chronological Plot of Means and UCL's for Eutectic Process.

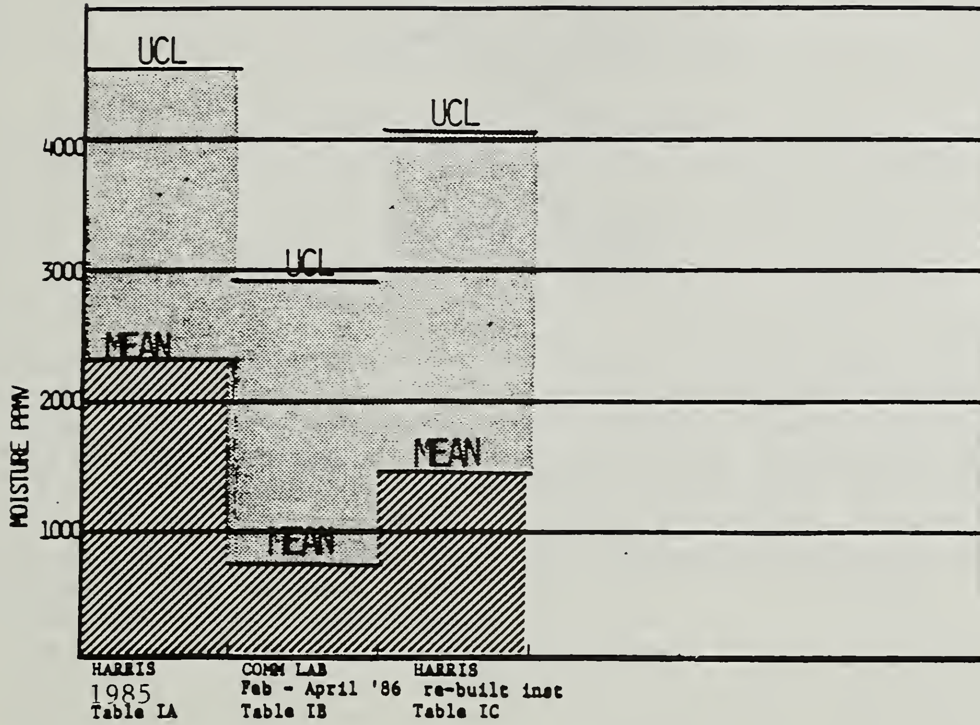

Figure 11B

Chronological Plot of Means and UCL's for Epoxy Process.

2.2 Laboratory Correlation and Survey Experiment: A Status Report

Benjamin A. Moore
Rome Air Development Center
RBRE
Griffiss AFB NY 13441-5700

Didier Kane
Clarkson University
Potsdam NY 13676

Abstract: The presence of moisture within a microelectronic package can have a detrimental effect upon the reliability of the enclosed device. In order to screen these reliability hazards from military systems, a test method, 1018 (Internal Water Vapor Content) was developed and made part of MIL-STD-883, Test Methods and Procedures for Microelectronics. The most prevalent method of measuring moisture is mass spectrometric quantitative analysis (Procedure 1 of Method 1018). However, in order to assure accurate and reproducible mass spectrometric moisture measurements from commercial analytical facilities, several laboratory correlation experiments have been performed. This paper briefly details past correlation results and then presents the status of the current analytical laboratory comparison. Preliminary results indicate correlation for most samples, at approximately 2500 ppm_v among all laboratories reporting. However, unresolved problems and incomplete data prevent final conclusions from being made.

Key Words: Moisture; mass spectrometry; correlation; Method 1018; calibration; standards.

1. INTRODUCTION

The purpose of this work was to determine (1) whether analytical correlation at 5000 ppm_v moisture has been maintained by both commercial and in-house (semiconductor manufacturers) analytical facilities and (2) if correlation could be established in the 2000-3000 ppm_v range. This would justify proposed changes to the upper acceptable limit for moisture in Method 1018 and Methods 5005 (Qualification and Quality Conformance Procedures) and 5008 (Test Procedures for Hybrid and Multichip Microcircuits) of MIL-STD-883.[1]

The Product Evaluation Branch (RBRE) of the Rome Air Development Center (RADC) is the responsible Government agency for the technical aspects of Method 1018 and, as such, deals with such issues as the determination of laboratory correlation to assure accurate and precise analyses and the implementation of changes to Method 1018 to reflect current military requirements. It is also responsible for the development of nondestructive, low cost alternative moisture test methods, resolution of conflict analyses from Government certified laboratories on military qualification samples, the investigation of gas matrix effects (i.e., the presence of hydrogen and/or oxygen)

on analytical accuracy, the certification of the technical competence of analytical facilities to accurately and precisely measure moisture, the expansion of certification volume range to include VHSIC, VLSI, and hybrid devices, and the evaluation of the effects of organic material on moisture analysis techniques.

Field experience and failure information derived from the Government-Industry Data Exchange Program (GIDEP) Alert system suggests several changes should be made to Method 1018. These include (1) assurance of no cold spots (moisture condensing surfaces) in analytical systems by requiring all gas transfer passages be baked at a minimum of 100 ^{o}C, (2) pre-analysis bake of all parts for 12 hours prior to hot insertion into analysis system (not required for batch systems with inherent 12 hour pre-analysis bake) to assure consistent device preconditioning and (3) lowering the upper acceptable moisture limit to 2000-3000 ppm_v. Moisture aided failures have been observed at approximately 2500 ppm_v.[2] In order to improve the test method itself, several changes will be requested. These include formalizing the concept of correlation samples (in lieu of the now required bienniel examination by the Government dewpoint hygrometer), reporting of all gases detected within the accuracy limits of each analytical laboratory, and inclusion of a requirement for documented procedures to detect and, if necessary, compensate for gas matrix effects. These proposed changes were important factors in the design of the current correlation experiment.

2. PROCEDURE

2.1 Prior Experience

Two prior correlation experiments have been conducted. The first, conducted in late 1979, served as the basis for implementation of Method 1018.[3] As shown in Table I, RADC and the commercial analytical facilities demonstrated excellent agreement with standard deviations of less than 10% of the mean values. In order to assure continuing analytical correlation, to answer questions raised by unofficial and ill-conceived laboratory comparisons, to investigate correlation at moisture concentrations other than 5000ppm_v, and to evaluate different packaging technologies for correlation sample production, a second experiment was conducted in late 1981.[4] Table II summarizes the results of this recertification program. Analyses of Lot RA, which were samples remaining from the original 1979 correlation experiment, resulted in an overall mean differing only 82 ppm_v from the originally determined value. Lots RC (X=9358), RE (X=6483), and HA (X=1863) correlated close to their target values. Lot HA samples were ceramic dual-in-line packages (CERDIPs) supplied by Harris Corporation, several of which contained an interdigitated sensor that recorded a moisture mean value of 1562 ppm_v. Lot RD (X=2628) samples contained approximately 2½ times the target moisture value but analytical results generally exhibited good correlation. Results of this experiment demonstrated both the feasibility of producing a suitable moisture standard in the 2000-3000 ppm_v range and the possibility of extending laboratory correlation from a single point to a range of values. Subsequent observations made on remaining Lot HA samples have shown a gradual upward drift in moisture content (which can be thermally accelerated) to approximately 2500-3000 ppm_v.[4]

2.2 Experimental Plan

In order to (1) satisfy the biennial reexamination requirement dictated by Method 1018; (2) determine the degree of retention of laboratory correlation after the five year period since the last formal comparison; (3) provide data to support proposed changes to Method 1018; and (4) determine the state-of-the-art in mass spectrometric moisture measurement, a comprehensive experiment was designed and initiated in early 1986. All participating laboratories were required to be calibrated over the range of 1000-10000 ppm_v moisture for the sample volume range to which each laboratory had been certified. All testing, unless otherwise specified, was to be done in accordance with Method 1018.2 of MIL-STD-883C. Five samples were included in each sample group with a requirement that, if after testing three samples the data spread was greater than 20%, the remaining two samples would also be analyzed.

The experiment was divided into three phases. Each laboratory was to complete the initial phase, report results, and wait for instructions to proceed to subsequent phases of the experiment. The primary experiment consisted of two groups of TO-5 (B, B1) metal cans, two groups of TO-18 (A, A1) metal cans, and one group of CERDIP (H) samples. Groups A and B1 were designed and packaged to contain approximately 5000 ppm_v, while groups A1 and B were targeted for 2500 ppm_v. These devices were procured by the Government from the Raytheon Corporation. Group H was the remaining samples of Lot HA of the 1981 correlation experiment, and, as previously mentioned, contained 2500-3000 ppm_v moisture. This mix of samples featured three different cavity volumes and two different sealing technologies. Phase II devices included a variety of TO type metal cans of different volumes and moisture concentrations. These devices were supplied by National Semiconductor. A Latin square type experiment was designed with each laboratory to do some elements in the test matrix. A similar test plan, with additional devices from National, was used in the Phase III experiment. The Phase III portion of the correlation experiment, required of commercial laboratories only, was designed to evaluate the effect on analytical correlation of a preanalysis bake-out at various temperatures for various lengths of time. As seen in Table III, Phase I of the experiment is not yet complete. Therefore, technical data that is presented in this paper is preliminary and subject to change upon inclusion of data from laboratories whose testing is incomplete and any additional testing that may be required. The purpose of this paper is only to present a status report on the laboratory correlation and survey experiment. Official data will be presented to the appropriate Joint Electron Device Engineering Council (JEDEC) subcommittee(s).

Note that the Intel Corporation voluntarily requested removal from Method 1018 suitability shortly after samples were sent to each laboratory.

2.3 Results

An overall summary of available Phase I results is presented in Table V. Laboratory letter designations for this experiment are consistent within this experiment but differ from those used for the earlier correlation experiments (79 and 81). The results from Lots B, B1, and H are very encouraging and will be discussed in greater detail later in this paper. Results from Lots A and A1 (the smallest volume samples in this phase of the experiment) are puzzing. Within each laboratory, analytical results are consistent but there is no correlation among laboratories. A preliminary investigation of this problem centered on comparison of the analytical techniques

used by each laboratory. This comparison of measurement techniques is seen in Table V. The results from those laboratories with non-instantaneous moisture determinations are closer to the correlation sample target values. Data from Phase II of the correlation experiment should help resolve this problem. Additional low volume sample testing is being planned.

The results from Lot B are presented in Table VI. A graphical representation of this data is seen in Figure 1 with a comparison of the overall laboratory mean ± 20%. Each individual laboratory mean moisture value is seen in Figure 2. All laboratories correlate within ±20% of the overall mean of 2562 ppm_v. Results for Lot B1 are similarly detailed in Table VI and Figures 3 and 4 with correlation within ± 20% of the overall mean of 5462 ppm_v (lab E is actually -20.5% below the mean value). Lot H results are presented in Table VIII and Figures 5 and 6. Again, correlation within ±20% of the overall mean of 2517 ppm_v is demonstrated. A comparison of the range of all individual determinations within ±20% of the overall mean is made in Table IX. Data is presented as follows: minimum value, maximum value, number of samples outside ±20% range, ± symbol representing direction of deviation. Each < represents values less than 20%, while each > is for values greater than 20%.

3. OBSERVATIONS

Several disconcerting problems, in addition to the non-correlation of Lots A and A1, arose during the correlation experiment. One laboratory did not read the instructions before proceeding with Phase I. Since the laboratory did not calibrate for moisture from 1000-10000 ppm_v as required, all analyses had to be repeated. Two laboratories tested on systems that were operating improperly. In one case, the data acquisition system had a known intermittent fault. The other system was not allowed to attain equilibrium conditions after an extended repair cycle. In both cases all analyses had to be repeated. Some laboratories questioned the importance of these samples and delayed analyzing them. System downtime with long repair cycles hampered several laboratories. Lack of in-house technical and maintenance support, along with less than timely responses from analytical equipment manufacturers, severely hindered non-commercial laboratories, including RADC, from completing the experiments.

The Government has initiated several actions to reduce the severity of these problems. Correlation samples are being used to audit analytical laboratory performance and are required for maintenance of laboratory suitability to perform moisture analysis on parts for qualification for military applications. The Defense Electronic Suppy Center (DESC), the Government agency that grants laboratory suitability to perform Method 1018 analyses, will suspend the suitability of any laboratory not performing correlation analyses in a timely manner. In order to solve correlation problems, small volume samples from alternate sources are under consideration and investigations into alternate calibration equipment and procedures are proceeding.

Several other approaches to determining and maintaining laboratory correlation are being considered. These include (1) blind surveys through a contractor with random sampling of all laboratories, (2) direct purchase of analyses with subsequent "naming of names" when reporting data, and (3) direct or indirect supply of samples to be included with each analysis lot. The last approach could serve as the basis for in-laboratory statistical quality control measures and could possibly be accomplished by

encouraging the development of independent source of samples (indirect supply).

Communications between the Government and all analytical facilities need to be improved. More frequent visits, primarily technical in nature, to each laboratory are being contemplated. Plans for more complex audits of each facility are now being discussed by RADC and DESC.

4. CONCLUSIONS

Since Phase I of the correlation experiment is incomplete, only tentative conclusions can be made based upon available data. Maintenance of correlation at 5000 ppm_v moisture has been demonstrated by analytical results of Lot B1. In addition, correlation of moisture measurements at 2500 ppm_v has been established by analytical results of Lots B and H. However, uncertainty remains as to the volume range of correlation among laboratories due to the poor results of analyses of Lots A and A1. Additional analyses of low volume ($\sim$0.01-0.02cc) samples will be required to resolve this problem. Finally, more Government-laboratory interaction and dialogue is required to assure continued correlatable moisture measurements of microelectronic package ambients.

REFERENCES

1. B. A. Moore, "Correlation of Analytical Facilities," 21st Annual Proceedings of the International Reliability Physcis Symposium, Phoenix AZ, April 1983.

2. GIDEP Alert HA-A-83-01.

3. B. A. Moore, "Method 1018.2 Certification Results," Moisture Measurement and Control Workshop, National Bureau of Standards, Gaithersburg MD, November 1980.

4. B. A. Moore, "Method 1018 Moisture Measurement: The Evaluation of Analytical Correlation," Journal of Environmental Sciences, January/Febrauery 1987.

TABLE I

METHOD 1018 MOISTURE ANALYSIS CERTIFICATION
IO-18 STANDARD SAMPLE RESULTS

LABORATORY	TRIALS	DATES	MEAN ppmv	STD DEV ppmv
RADC	13	4	5280	436
C	8	2	5160	403
D	7	1	4767	156
B	5	1	5398	443
A	4	1	5335	282

MEAN VALUE, ppmv: 5188

TABLE II

METHOD 1018.2 RECERTIFICATION PROGRAM RESULTS
MOISTURE IN PPMV

LAB	RA	RB	RC	RD	RE	HA
RADC	5327	4535	10060	2663	6040	1570
C	5670	5730	9900	2800	7800	1920
D	5631	3317	8301	1981	5417	2062
A	4453	8690	9170	3067	6676	1901
MEAN	5270	5568	9358	2628	6483	1863
X-20%	4216	4454	7486	2102	5187	1491
X+20%	6324	6602	11229	3153	7780	2236
TARGET VALUE	5200	3000	10000	1000	6000	1562

TABLE III

METHOD 1018 CORRELATION EXPERIMENT STATUS

LAB	PHASE I	PHASE II	PHASE III
RADC	IN PROCESS	NOT STARTED	NOT STARTED
ATT	COMPLETE	NOT STARTED	————
GAS	COMPLETE	NOT STARTED	NOT STARTED
HARRIS	COMPLETE	NOT STARTED	————
INTEL	*	*	*
ITAS	COMPLETE	NOT STARTED	NOT STARTED
NORTHROP	IN PROCESS	NOT STARTED	————
ORS	COMPLETE	NOT STARTED	NOT STARTED
PC	IN PROCESS	NOT STARTED	NOT STARTED

* DROPPED METHOD 1018 SUITABILITY

TABLE IV

LABORATORY CORRELATION AND SURVEY EXPERIMENT RESULTS: PHASE I
MOISTURE IN PPMV

LAB	A	A1	B	B1	H
B	4458	3282	2342	5875	2923
C	6200	5300	3025	5633	2067
D	10149	5519	2529	5331	2653
E	2867	2240	2338	4345	2272
G	9000	6500	2567	5825	2733
MEAN	----	----	2562	5462	2517
X-20%	----	----	2050	4370	2014
X+20%	----	----	3074	6554	3020

TABLE V

COMPARISON OF MEASUREMENT TECHNIQUES: LOTS A & A1
MOISTURE IN PPMV

LAB	A MEAN	A1 MEAN	SAMPLE	BAKE	INSTANTANEOUS
B	4458	3282	SINGLE	N	N: QUASI-EQUILIBRIUM
C	6200	5300	BATCH	Y	Y: RATE OF RISE
D	10149	5519	SINGLE	N	Y: MAXIMUM
E	2867*	2240	SINGLE	N	N: LIMITED INTEGRATION
G	9000	6500	BATCH	Y	Y: MAXIMUM

* TWO VALUES @5000, TWO VALUES @500

TABLE IX

RANGE OF MOISTURE DETERMINATIONS COMPARED TO +/-20% OF MEAN VALUES
MOISTURE IN PPMV

LAB	B (2050-3074)	B1 (4370-6554)	H (2014-3020)
B	1990-2750-1<	5420-6580-1>	2770-3040-1>
C	2600-3400-2>	5300-5800-0	1800-2200-1<
D	2462-2593-0.	5189-5430-0	2574-2784-0
E	1780-2930-1<	3970-4950-2<	1860-2600-1<
G	2500-2700-0	5700-5900-0	2500-3000-0

TABLE VI

PHASE I LABORATORY CORRELATION AND SURVEY EXPERIMENT RESULTS: LOT B
MOISTURE IN PPMV

LAB	MEAN	STD DEV
B	2342	334
C	3025	330
D	2529	66
E	2338	470
G	2567	115
X	2562	392

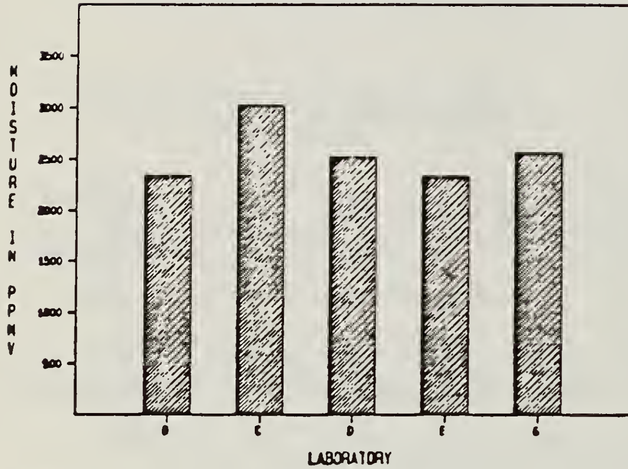

FIGURE 1

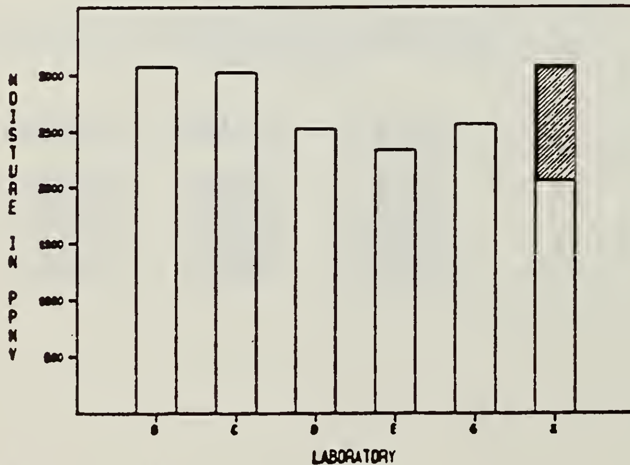

FIGURE 2

TABLE VII

PHASE I LABORATORY CORRELATION AND SURVEY EXPERIMENT RESULTS: LOT B1
MOISTURE IN PPMV

LAB	MEAN	STD DEV
B	5875	496
C	5633	289
D	5331	126
E	4345	441
G	5825	96
X	5462	723

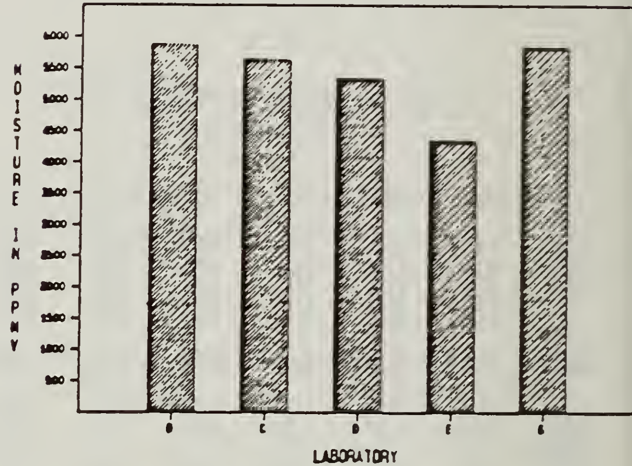

FIGURE 3

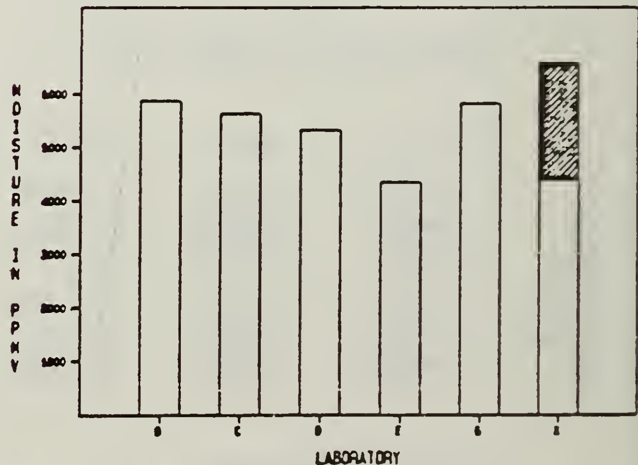

FIGURE 4

TABLE VIII

PHASE I LABORATIRY CORRELATION AND SURVEY EXPERIMENT RESULTS: LOT H
MOISTURE IN PPMV

LAB	MEAN	STD DEV
B	2933	139
C	2067	231
D	2663	109
E	2272	320
G	2733	252
X	2517	378

LOT H AVERAGE MOISTURE DETERMINATIONS

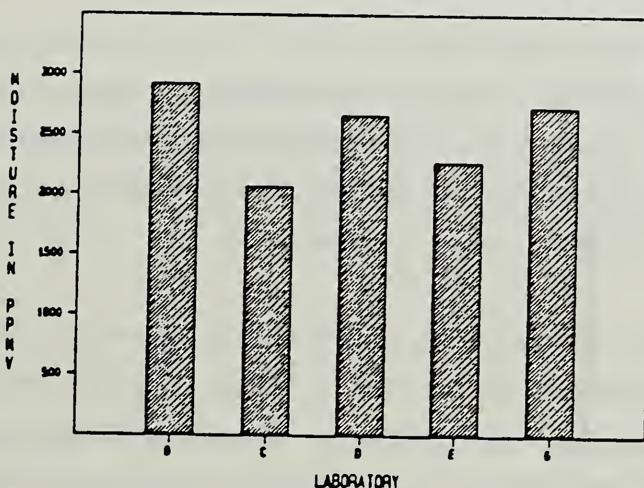

FIGURE 5

LOT H ACCEPTABLE MOISTURE LIMITS (+/- 20%)

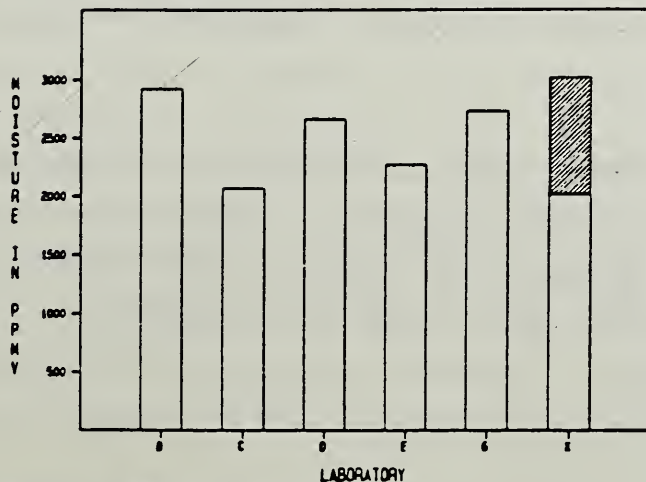

FIGURE 6

2.3 ACCURACY AND REPRODUCIBILITY OF THE MASS SPECTROMETER/CAROUSEL METHOD FOR MOISTURE ANALYSIS

Leslie J. Rigby,
STC Technology Limited
London Road, Harlow, Essex, CM17 9NA, UK

A computer controlled mass spectrometer system with a carousel sample chamber has been carefully evaluated using prefilled TO5 packages containing 1850 and 4300 ppmV of water vapour in nitrogen. The filling gases and the mass spectrometer calibration gases were all monitored with a cooled mirror hygrometer with calibration traceable to the NBS standard.

Over 36 samples of each type were analysed with excellent consistency over a period of 6 months. The ion integration method was used with a cut off point after 3 minutes. Samples and standards were alternatively measured and for both the typical standard deviations were 4 and 15% at the high and low moisture levels respectively.

The mass spectrometer sensitivity to water was found to increase with both moisture and oxygen content in the sample. These and other factors could contribute to measurement errors. Standard samples which contain similar contents of both water and oxygen in the sample are required for accurate measurement. Accuracy over a range of moisture levels requires extensive standardisation procedures, but invariance in both the internal hardware used and the sampling and measurement procedures yielded calibration data which were essentially consistent over the six month period.

These and other measurements have revealed the advantages and disadvantages of the carousel procedure. A modification to the carousel method will be described in which the benefits are retained but the disadvantages are reduced and in some cases eliminated.

1. INTRODUCTION

The EEC Community Bureau of Reference (BCR) has organised an interlaboratory comparison exercise within the EEC for moisture measurement in encapsulated packages. This report refers to the STC contribution to the exercise which was to prefill packages at two moisture levels, to test the filling procedure by mass spectrometric analysis of specimen packages, and to participate in the exercise by measurement of a selected sample of the final batches of packages. 120 packages were required at each moisture level which was set between 1000 and 2000 ppm at the low moisture level and between 4000 at 6000 ppm at the high moisture level. Close control was required to ensure that each batch had a minimum spread in moisture content. The final batches were produced in one run after an overnight equilibration of the moisture level.

A recording mirror dew point hygrometer (Michell 4000)[1] was provided by BCR to monitor the filling gas humidity and to check the calibration of the mass spectrometer during the analysis of the final batches.

2. ENCAPSULATION

A schematic diagram of the encapsulation equipment is shown in Fig. 1. This is the equipment normally used to dry fill high reliability packages but it has been modified to allow a controlled degree of moisture to be introduced into the filling gas. Dry nitrogen (moisture content 10 ppm) was split into two streams which were controlled by rotameter flow gauges. The moisture content in the wet stream was derived from deionised water in quartz with $\pm$ 0.2^{o}C temperature control. A high current weld sealed each nickel can to the corresponding gold plated kovar base. A few devices were rejected by visual inspection of the welded rim after assembly. The assembly enclosure requires a throughput of 12 litres of gas per minute and a sampling tube was introduced close to the encapsulation head to draw off 0.5 litres/min. to satisfy the requirements of the Michell hygrometer. Tables 1 - 5 list the measured water contents and will be discussed in more detail in Section 5.

For the low level samples (1000-2000 ppm) an initial batch of 12 packages were sealed in nitrogen with a dew point of between -16.80 and -16.90^{o}C. This corresponds to a moisture level of about 1400 ppm but the mass spectrometer analysis produced an average moisture content of less than 600 ppm (Table 1). The discrepancy was traced to the cooling rate setting on the hygrometer. The value recommended in the instruction manual was found to be too low and subsequent measurements were made to verify that the dew point reading did not increase as the cooling rate was increased. In the repeat experiment, a dew point of between -15.46 and -18.02 resulted in an average mass spectrometer reading of 1400 ppm (Table 2). The final batch of 120 devices had a dew point range of from -16.14 to -16.58 (1750-1690 ppm) and a measured content of 1850 ppm (Table 3).

The high level condition (4000-6000 ppm) required only 1 trial run (Table 4). A dew point of between 1.77 and 2.06^{o}C gave an average measured content of 10,000 ppm in the first six packages. Lower dew points of from -0.98 to -3.84 produced a measured package content of 8000 ppm. The humidity was reduced to an overnight dew point of -5°C and for the final batch of 120 packages, a dew point range of -4.5 to -5.1^{o}C (4400-4300 ppm) resulted in an average content of 4300 ppm for the measured packages (Table 5).

3. PROCESSING AND DISTRIBUTION

All of the 240 packages from the final encapsulation were soaked in 3 atmospheres pressure of helium at ambient temperature for 72 hours prior to distribution. 12 equally spaced samples were then removed from each group of 10 within a batch of 120 for immediate analysis with the STL mass spectrometer system. A second set of samples were similarly taken for a repeat analysis 4 weeks later. The remaining samples were randomly chosen, one per decade, so that the other participating laboratories would receive an unordered distribution from the samples available.

4. GAS ANALYSIS

The procedure used has been described previously[2] and remained consistent throughout. Twelve cans were loaded the previous afternoon and the whole system baked at 100°C in a background pressure reducing to between 20 to 30 nanotorr by a turbomolecular pump. The mass spectrometer background was less than 5 nanotorr.

A Protimeter[3] recording mirror dew point hygrometer was used to monitor the water content in the standard gas. A computer algorithm was used to read the output from this hygrometer and calculate the % water content. Comparison with the certified Michell Hygrometer revealed that the Protimeter dewpoints were within 0.1°C for mirror cooling of up to 15°C below the ambient temperature.

Prior to each analysis, 0.1 ml of room air was admitted to water saturate the surfaces of the sample chamber which was then evacuated for a further 5 minutes. Room air was also used to determine the mass spectrometer sensitivity to water vapour. A 0.5 l/min flow was generated with a small compression pump. This air stream was warmed by passing through the 100°C heated chamber in a 7 mm I.D. stainless steel pipe 60 cm long and onto the two calibration volumes of 0.1 and 0.01 ml. A short exit line passed initially through the Michell hygrometer and then to a Protimeter recording mirror hygrometer which was routinely used to calibrate the mass spectrometer system.

For all the data reported here, samples and standards were expanded into a chamber volume of 140 ml and transferred via a vernier needle valve with the same preset conductance to the mass spectrometer. 19 cyclic readings of all the relevant ion currents were completed in 3.3 minutes. During this time, over 99% of each original gas sample had passed through the mass spectrometer ion source. The room air standard gas was initially analysed until a consistent sensitivity to water was obtained and then remeasured after each sample to check for any variation in instrument sensitivity.

Room air was used to measure water vapour sensitivity as it was readily available and the water content was consistent showing only a slow increase over a 5 hour period. More importantly, typical dew points were above 5°C and allowed the Protimeter unit to be used without modification (Lower dew points would require additional cooling of the mirror and the negative dew point readings would not be understood by the digital microprocessor). However, the range of moisture levels can be covered by using air volumes of 0.1 and 0.01 atm. ml. (Section 5, para 1). This is valid because under the conditions of molecular flow used to transfer the sample gas to the mass spectrometer ion source, the partial pressure and the ionisation cross section of water should be unaffected by the predominant gas pressure. This statement was subsequently partially verified (Section 5, para 6).

5. RESULTS

Table 8 shows specimen results of the computer acquired data for standards and samples. The 0.1 ml air standard was used with the high level samples and the 0.01 ml standard with the low level samples. The peak ion current and the area indicate that the quantity of water in the 0.1 ml standard (Table 8) is approximately twice that in the high level sample (Table 11) whereas the reverse is the case for the 0.01 ml standard and the low level sample . The decay curves for these smaller quantities of water are much shallower and indicate the greater difficulty in measuring smaller water concentrations. Under these circumstances, area measurement is preferred to maximum peak height for water content measurement.

Standards and samples were alternately measured during each run. Tables 1 to 7 give the essential data for water content. The water content in all the standards has been calculated from the Protimeter hygrometer.

The average values from Tables 1 to 7 (corresponding to runs 1 to 7) may be summarised as follows:

	Sensitivity from Air Standard	% deviation	Sample % Water content	% deviation
1. Low Level Test 1	0.25	6.7	0.053	16
2. Low Level Test 2	0.29	6.8	0.18	11
3. Low Level 1	0.25	6.3	0.19	14
6. Low Level 2	0.21	7.7	0.18	13
4. High Level Test 1	0.38	2.9	1.0	8.5
			0.80	3.0
5. High Level 1	0.36	4.9	0.43	3.5
7. High Level 2	0.32	3.0	0.41	5.7

The sensitivity values are all relative to nitrogen (mass 28) and are all significantly less than 1. This may in part result from a lower ionisation cross section for the water molecule but mainly follows from water loss by surface adsorption. Table 8 indicates the much slower transfer of water to the mass spectrometer during the measurement time and a lower sensitivity for water is therefore not unexpected. Both measurement and filling consistency are good at the low level (1800 ppm) and significantly better at the higher level (4200 ppm).

Water calibration with moist nitrogen was carried out at a later date over a 5 day period (7-11/1/85) with a General Purpose Humidifier. Dry nitrogen is saturated with water at an elevated pressure (p_1). The water content at ambient pressure (p_o) may then be calculated from the saturation vapour pressure (p_s) and the pressure drop:

$$\%H_2O = 100\ p_s \cdot p_o / p_1 \cdot p_o = 100\ p_s / p_i$$

The actual moisture levels obtained were measured with the Michell hygrometer which was used to calibrate the mass spectrometer. As with the previous work, room air was used to presaturate the walls of the vacuum system prior to sample admittance. The relative sensitivities to water from air and nitrogen standards were as follows for % water in volumes of 0.1 atm. ml.:

$\%H_2O$	In air	In nitrogen			
0.1	0.21, 0.21, 0.25, 0.29		0.15	0.11	
0.2		0.13	0.30	0.14	0.19
0.4		0.20			0.21
0.6		0.20	0.28		0.23
0.8	0.38, 0.36, 0.32			0.28	0.25
1.0					0.27

The air calibrations were all on different days as indicated in the text and were nominally at two fixed points. The 0.1% level in air was in fact 1% in 0.01 atm. ml.

The above comparison indicates that a reduction in sensitivity of about 50% occurs when nitrogen is used instead of air. Oxygen is a very reactive gas at metal surfaces[4] and active gases have been shown to replace more labile molecules[5] Chemisorption of oxygen at surface sites could result in the release of preadsorbed water molecules and assist water transfer to the mass spectrometer. The deliberate act of conditioning the walls of the sample chamber with moist air would inevitably promote this effect.

Sample consistency in gas content, argon and carbon dioxide for Runs 4-7 were as follows with the % deviation in brackets:

	4-High level	5-Low level	6-High level	7-Low level
Content/m.bar.l	0.218 (2.1)	0.196 (1.3)	0.213 (1.4)	0.216 (2.8)
% Argon	0.017 (2.8)	0.016 (7.9)	0.017 (6.4)	0.014 (3.6)
% CO_2	0.029 (15)	0.035 (13)	0.032 (37)	0.033 (8.8)

These data give a good indication of the precision of measurement for the permanent gases. The higher CO_2 variability may result from variations in local heating during can welding.

All the calculations referred to above are based on an area integration of all the ion current/time data points generated by 19 repetitive cycles. The sensitivity of the mass spectrometer to water, hydrogen, helium, oxygen, argon and carbon monoxide relative to nitrogen, which was determined from area measurements, has also been used to calculate sample

concentrations from the ion current peak heights. In all cases, these are the initial ion current values and for argon and carbon dioxide the peak height calculation is in good agreement with the peak area determination. This indicates that the mass spectrometer sensitivity is the same for both calculations. For water, peak height calculations based on the peak area sensitivity result in a significantly lower % water. This is not surprising since even partial water retention within the sample chamber will broaden the water transfer curve and reduce the mass 18 peak maximum. The implied lower water sensitivity for peak height calculations indicates that the peak area method is to be preferred.

6. CONCLUSIONS

The ability to fill TO5 packages with moist nitrogen at the 2000 and 5000 ppm levels has been demonstrated. The agreement between the water content in the filling gas (1750-1690 and 4400-4200 ppm) agrees remarkably well with the average measured content in the samples tested (1850 and 4300 ppm). This may be partly fortuitous, but there was no discernable drift in water content throughout the procedure (120 capping operations at about 3 minute intervals).

The package contents were not measurably altered over a 5 week interval between testing. The precision of measurement was found to be within 6-8% at the low level and 3-5% at the high level. The difference between the % deviations in Tables 3, 5, 6 and 7 give the precision of filling as 5-7% and 3% at low and high levels respectively.

The analytical procedure outlined above is designed to measure total water content (i.e. adsorbed + gaseous) in small sealed volumes. Prebaking at $100^{\circ}C$ for intervals of 4 to 72 hours has not noticeably affected similar previous measurements although at higher temperatures ($\sim 300^{\circ}C$) water can be initially desorbed from the bulk of electrolytically gold plated layers and eventually reduced by dissociation at catalytically active metal surfaces. The more relevant criticisms of the measurement procedure are as follows:

1. Large potentially adsorptive surface areas in the sample chamber reduce the transfer rate of water to the detector. This places a limit on the quantity of water detectable to about 500 ppm in a 0.1 m.bar litre gas sample.

2. Sampling of the standard gas introduced an unknown quantity of water which had been adsorbed on the wall of the calibration volume. This quantity can be minimised by increasing the temperature of the calibration volume and utilising more hydrophobic surfaces. The present system is a viable working compromise but it does suggest that the larger water content in the standard will result in a measured value in the sample gas which is marginally lower than real value.

3. The effect of oxygen on the water sensitivity and the dependence of that sensitivity on water content should be taken into consideration. More extensive measurements over a longer time scale have indicated that providing the system is hermetic and has been processed in a routine manner, the precision of measurement does not change.

7 MODIFICATIONS IN PROGRESS

Several modifications are being made in order to minimise the problems already discussed.

Calibration procedures for moisture content are now utilised in which the partial pressures of water and oxygen in the standard gas are similar to those which were found for the samples. A Michell 3000 hygrometer has been installed to provide accurate dewpoint readings from +20 to $-30^{\circ}C$.

An improved sample chamber is also being constructed (Fig. 2). A much larger stainless steel system with a carousel located and supported on ball bearings allows packages to be accomodated in 3" diameter sample holders which are then sequentially presented to the analysis chamber for puncture and gas transfer. Steel bellows and Viton O-rings provide the necessary vacuum seals. This unit will maintain the integrity of the internal loading method with the following advantages over the old system:

a) Larger packages can be accommodated.

b) Interference effects from multiple packages within the same analysis chamber will be avoided.

c) The analysis chamber will have a lower volume and a much lower and consistent surface area.

d) Standard gases will be admitted from a heated calibration volume.

REFERENCES

1. Michell Instruments Ltd, Nuffield Road, Cambridge CB4 1SS, UK
2. NBSIR 84-2852, RADC/NBS Moisture Workshop, 1983, p 69.
3. Protimeter Ltd, Fieldhouse Lane, Marlow, Bucks SL7 1LX, UK.
4. J.A. Becker et al. J Appl Phys 32 ,p411 (1961)
5. L.J. Rigby, Can J. Phys 43, p1020 (1965)

ACKNOWLEDGEMENTS

The samples were prepared by J. McNicol and the analyses were carried out by M. Kumar. The author thanks the EEC Community Bureau of Reference for financial assistance and STL Ltd for permission to publish this paper.

Table 1 TO5 Low Level Test 1

File No	Sample	Protimeter Dew Pt/°C	Filling Dew point/°C	Gas volume /mbar.litre	Water sensitivity	% Water content
2	AIR	12.0		0.0101	0.235	
3	AIR	12.4		0.0101	0.224	
4	30696		-16.90	0.177		0.053
5	DRY NITROGEN			0.101		
6	AIR	12.4		0.0101	0.240	
7	30698		-16.89	0.179		0.060
8	AIR	12.6		0.0101	0.239	
9	30700		-16.85	0.171		0.040
10	AIR	12.8		0.0101	0.260	
11	30702		-16.84	0.131		0.048
12	AIR	13.0		0.0101	0.285	
13	30704		-16.84	0.174		0.046
14	AIR	14.0		0.0101	0.260	
15	30705		-16.82	0.176		0.051
16	AIR	13.8		0.0101	0.262	
17	30706		-16.83	0.174		0.048
18	AIR	14.0		0.0101	0.269	
19	30708		-16.84	0.174		0.062
20	AIR	14.1		0.0101	0.254	
21	30710		-16.80	0.155		0.069
22	AIR	13.6		0.0101	0.266	
			Average		0.254	0.053
			Std. deviation		0.017	0.0086
			% deviation		6.7	16

Data analysed 31st October, 1984
Atmosphere pressure 1012 mbar

Table 2 TO5 Low Level Test 1

File No	Sample	Protimeter Dew Pt/°C	Filling Dew point/°C	Gas volume /mbar.litre	Water sensitivity	% Water content
2	AIR	12.2		0.0101	0.229[x]	
3	30716		-18.02	0.181		0.140
4	AIR	12.5		0.0101	0.286	
5	30717		-17.60	0.177		0.163
6	AIR	13.0		0.0101	0.327	
7	30718		-17.40	0.175		0.192
8	AIR	13.2		0.0101	0.276	
9	30720		-17.20	0.134		0.181
10	AIR	13.5		0.0101	0.311	
11	30721		-16.17	0.174		0.208
12	AIR	13.8		0.0101	0.316	
13	30722		-15.46	0.177		0.195
14	AIR	13.9		0.0101	0.309	
15	30724		-16.86	0.178		0.182
16	AIR	13.9		0.0101	0.288	
17	30725		-16.90	0.180		0.179
18	AIR	13.9		0.0101	0.272	
19	30726		-16.94	0.174		0.207
20	AIR	14.0		0.0101	0.275	
21	30728		-16.72	0.177		0.175
22	AIR	14.0		0.0101	0.264	
23	30729		-16.88	0.176		0.203
24	AIR	14.1		0.101	0.309	
25	30730		-17.55	0.180		0.173
			Average		0.294	0.183
			Std. deviation		0.020	0.019
			% deviation		6.8	10.7

[x] Omitted from average

Data analysed 2nd November, 1984
Atmosphere pressure 1012 mbar

Table 3 TO5 Low Level 1

File No	Sample	Protimeter Dew Pt/°C	Deviation /°C	Gas volume/ mbar.litre	Water sensitivity	% Water content
1	AIR	9.1	0.3	0.101	0.260	
2	Background	9.3	0.4			
3	AIR	9.5	0.6	0.0101		
4	NITROGEN	9.5	0.6	0.100		
5	AIR	9.6	0.7	0.0101	0.264	
6	AIR	9.7	0.7	0.0101	0.239	
7	30582	9.7	0.6	0.194		0.211
8	AIR	9.7	0.5	0.0101	0.234	
9	30594	9.8	0.5	0.196		0.137
10	AIR	9.9	0.5	0.0101	0.239	
11	30606	9.9	0.5	0.172		0.151
12	30617	10.0	0.6	0.171		0.181
13	AIR	10.1	1.2	0.0101	0.237	
14	30631	9.3	0.3	0.165		0.237
15	30644	9.8	0.4	0.165		0.182
16	AIR	10.2	0.6	0.0101	0.255	
17	30656	10.2	0.8	0.184		0.172
18	30668	10.5	0.8	0.182		0.189
19	AIR	10.5	0.7	0.0101	0.236	
20	30680	10.4	0.6	0.167		0.185
21	30692	10.4	0.6	0.167		0.174
22	AIR	10.4	0.6	0.0101	0.284	
23	30738	10.3	0.5	0.176		0.205
24	30751	10.4	0.6	0.174		0.197
25	AIR	10.4	0.7	0.0101	0.264	
			Average		0.251	0.185
			Std. deviation		0.016	0.025
			% deviation		6.3	13.5

Water content during filling = 0.176% (Michell dew point -16.2)

Data analysed 13th November, 1984
Atmosphere pressure 1008 mbar

Table 4 T05 High Level (Test)

File No	Sample	Protimeter Dew Pt/°C	Filling Dew point/°C	Gas volume/ mbar.litre	Water sensitivity	% Water content	
3	AIR	9.2		0.100	0.306^{x}		
4	30773		1.79	0.218		0.85	
5	AIR	9.6		0.100	0.364		
6	30774		0.77	0.219		0.94	
7	AIR	9.9		0.100	0.362		
8	30775		1.88	0.210		0.96	
9	AIR	10.2		0.100	0.367		
10	30776		2.06	0.210		0.11	
11	AIR	10.4		0.100	0.383		
12	30777		1.86	0.233		1.02	
13	AIR	10.8		0.100	0.367		
14	30778		1.78	0.213		0.12	
15	AIR	11.0		0.100	0.379		
16	30783		-1.65	0.210			0.81
17	AIR	11.4		0.100	0.379		
18	30784		-3.84	0.219			0.77
19	AIR	11.3		0.100	0.384		
20	30782		-1.42	0.222			0.78
21	AIR	11.5		0.000	0.361		
22	30781		1.98	0.214			0.78
23	30780		-1.40	0.213			0.78
24	30779		-0.98	0.213			0.84
25	AIR	12.1		0.100	0.393		
			Average		0.375	1.00	0.80
			Std. deviation		0.011	0.085	0.024
			% deviation		2.9	8.5	3.0

Cans were filled in numbered sequence at 10 min. intervals but with 40 mins. between 30778 and 30779.

^{x} Omitted from average

Data analysed 7th November, 1984
Atmosphere pressure 1000 mbar

Table 5 TO5 High Level 1

File No	Sample	Protimeter Dew Pt/°C	Deviation /°C	Gas volume/ mbar.litre	Water sensitivity	% Water content
1	AIR	9.5	0.4	0.10	0.252[x]	
2	NITROGEN	9.8	0.4	0.10		
3	AIR	9.9	0.4	0.10	0.303[x]	
4	AIR	10.0	0.4	0.10	0.329	
5	Background	10.1	0.4	0.10		
6	AIR	10.2	0.4	0.10	0.329	
7	30791	10.4	0.6	0.217		0.419
8	AIR	10.4	0.5	0.10	0.362	
9	30794	10.4	0.5	0.209		0.439
10	30805	10.3	0.4	0.208		0.455
11	AIR	10.4	0.5	0.10	0.368	
12	30816	10.5	0.6	0.217		0.418
13	30826	10.5	0.6	0.210		0.414
14	AIR	10.7	0.6	0.10	0.370	
15	30836	10.6	0.5	0.213		0.415
16	30846	10.7	0.5	0.215		0.407
17	AIR	10.8	0.7	0.10	0.370	
18	30856	10.8	0.6	0.215		0.460
19	30866	10.8	0.5	0.215		0.427
20	AIR	10.7	0.3	0.10	0.371	
21	30876	11.0	0.6	0.216		0.423
22	30886	10.9	0.5	0.212		0.429
23	AIR	11.0	0.4	0.10	0.352	
24	30896	11.1	0.5	0.213		0.432
25	AIR	11.2	0.6	0.10	0.381	
			Average		0.359	0.428
			Std. deviation		0.018	0.015
			% deviation		4.9	3.5

Water content during filling = 0.44% (Michell dew point -16.2)

Data analysed 14th November, 1984
Atmosphere pressure 1002 mbar

[x] Omitted from average

Table 6 TO5 Low Level 2

File No	Sample	Protimeter Dew Pt/°C	Deviation /°C	Gas volume/ mbar.litre	Water sensitivity	% Water content
4	AIR	3.0	1.1	0.101	0.170[x]	
5	AIR	3.2	1.3	0.101	0.173[x]	
6	30583			0.200		0.165
7	AIR	3.5	1.1	0.0101	0.167[x]	
8	30595			0.197		0.138
9	AIR	3.9	1.1	0.0101	0.201	
10	30607			0.199		0.174
11	AIR	4.0	1.0	0.0101	0.226	
12	30618			0.195		0.155
13	AIR	4.4	1.2	0.0101	0.220	
14	30633			0.197		0.194
15	AIR	4.9	1.2	0.0101	0.237	
16	30645			0.197		0.152
17	AIR	4.3	0.8	0.0101	0.181	
18	30657			0.194		0.192
19	AIR	4.5	1.1	0.0101	0.216	
20	30669			0.194		0.192
21	AIR	4.3	1.1	0.0101	0.202	
22	30681			0.193		0.211
23	AIR	4.3	1.1	0.0101	0.183	
24	30693			0.195		0.195
25	AIR	4.0	0.9	0.0101	0.214	
26	30739			0.191		0.200
27	AIR	4.1	1.1	0.0101	0.209	
28	30752			0.194		0.207
29	AIR	3.8	0.7	0.0101	0.205	
			Average		0.209	0.181
			Std. deviation		0.016	0.023
			% deviation		7.7	13

[x] Omitted from average

Data analysed 18th December, 1984
Atmosphere pressure 1008 mbar

Table 7 TO5 High Level 2

File No	Sample	Protimeter Dew Pt/°C	Deviation /°C	Gas volume/ mbar.litre	Water sensitivity	% Water content
2	AIR	10.9	0.6	0.101	0.311[x]	
3	AIR	11.0	0.7	0.101	0.321[x]	
4	30793			0.211		0.418
5	AIR	11.0	0.3	0.101	0.335	
6	30804			0.228		0.468
7	AIR	11.4	0.7	0.101	0.321	
8	30815			0.218		0.420
9	AIR	11.3	0.6	0.101	0.310	
10	30825			0.222		0.412
11	AIR	11.2	0.5	0.101	0.317	
12	30835			0.215		0.420
13	AIR	11.1	0.4	0.101	0.324	
14	30845			0.221		0.409
15	AIR	11.4	0.5	0.101	0.301	
16	30855			0.219		0.426
17	AIR	11.7	0.5	0.101	0.323	
18	30865			0.215		0.396
19	AIR	11.8	0.5	0.101	0.337	
20	30875			0.217		0.426
21	AIR	11.7	0.6	0.101	0.325	
22	30885			0.222		0.374
23	AIR	11.5	0.4	0.101	0.317	
24	30895			0.215		0.401
25	AIR	11.5	0.5	0.101	0.331	
26	30906			0.215		0.388
27	AIR	11.4	0.6	0.101	0.311	
			Average		0.320	0.413
			Std. deviation		0.0097	0.023
			% deviation		3.04	5.7

[x] Omitted from average

Data analysed 20th December, 1984
Atmosphere pressure 1010 mbar

Table 8. Typical moisture data for each type of sample.

Sample	Output for Mass 18 in millivolts			Mass 18 Area
	Maximum	Final	Background	(Millivolt Seconds)
1.7% water in 0.1ml air	1620	320	48	114400
1.6% water in 0.01ml air	99	90	43	8600
High level moisture in TO5	620	210	49	58300
Low level moisture in TO5	136	114	39	16100
Typical mass 29 (all samples)	9500	60	32	310000

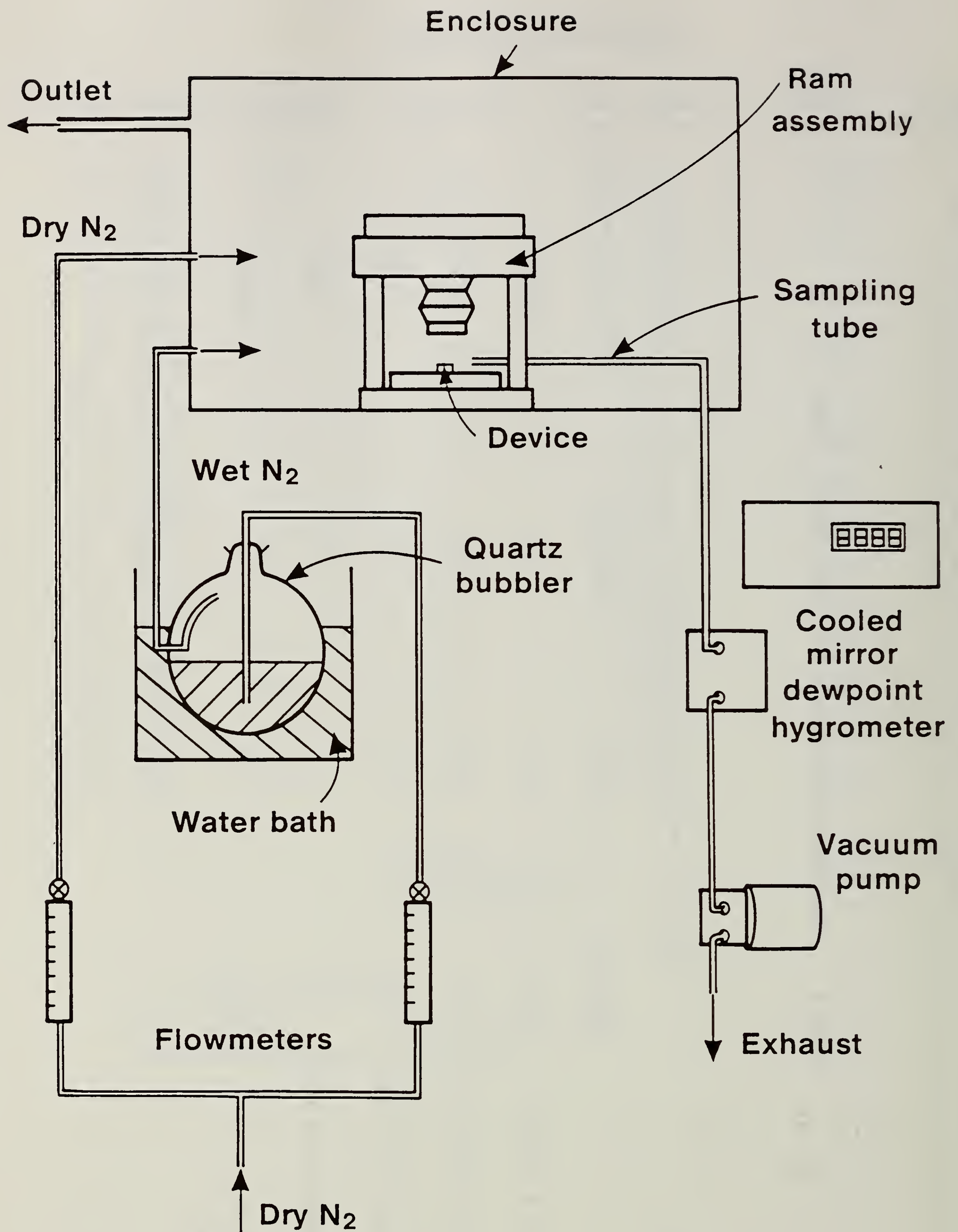

Fig.1 Encapsulation System

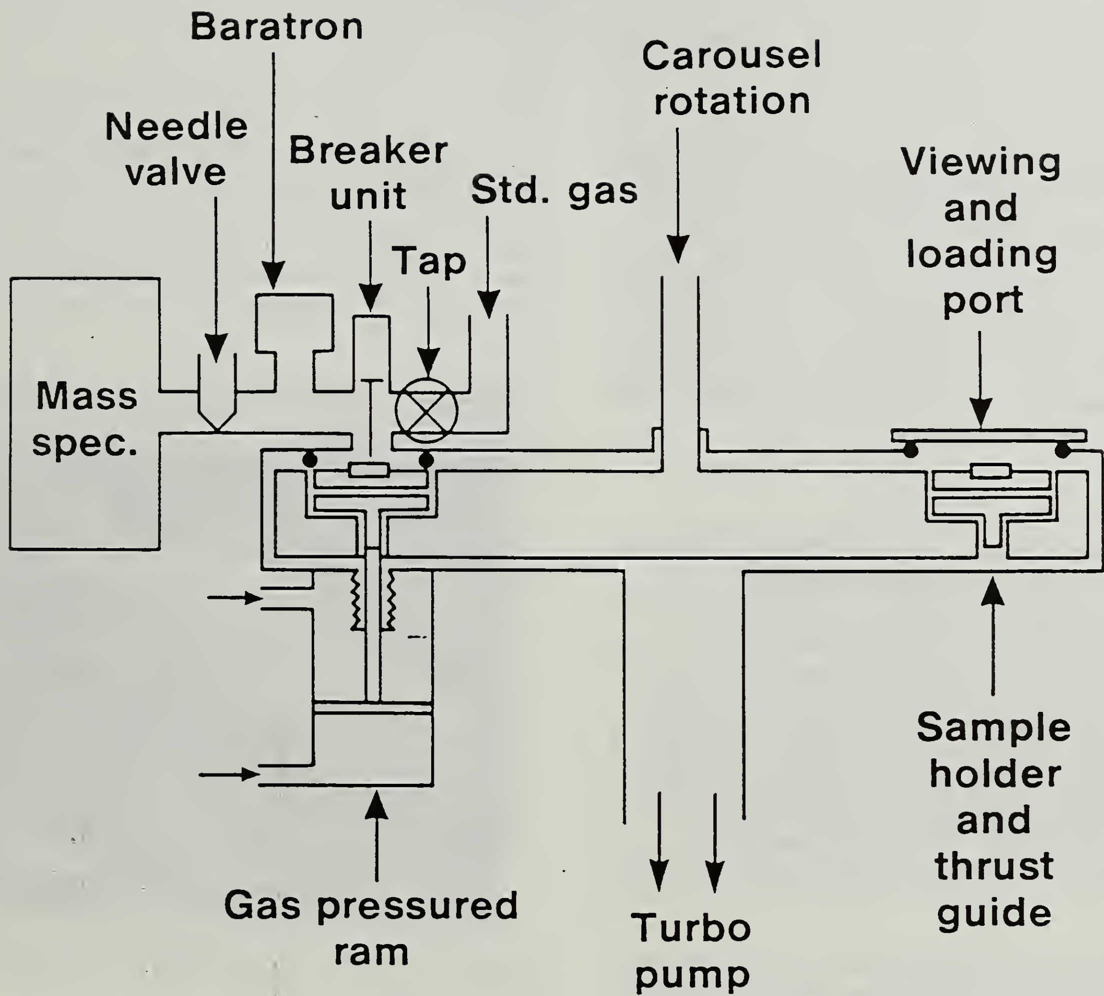

Fig.2 Schematic Diagram of External Carousel System

© 1986 IEEE, Reprinted with permission from the 36th Electronic Component Conference, May 5-7, Seattle, Washington.

3.1 NEW FAILURE MECHANISMS IN TEMPERATURE AND HUMIDITY STRESS

D. Y. Guan* ,T. F. Gukelberger, E. C. Cahoon,
T. W. Joseph, and J. M. Snowdon

International Business Machine Corporation
Dept. A28, Bldg. 908
P. O. Box 950
Poughkeepsie, New York 12602

Abstract

New failure mechanisms other than metal corrosion were observed in high-temperature, high-humidity testing of plastic encapsulated VLSI modules. The mechanisms were unique in that physical defects such as microcracks were associated with the failures. Failures appeared as single-bit, column, or row failures depending on circuit designs and process technology. Additionally, for one process design, ionic accumulation contributed to the failures. Electrical diagnosis, physical analysis, and failure kinetics along with the uniqueness of temperature and humidity (T/H) testing to the mechanisms will be discussed.

Introduction

Temperature/humidity stress testing is performed to assess the moisture resistance of plastic encapsulated integrated circuit (IC) modules. The most extensively reported failure mechanism to date is electrolytic corrosion of the chip metallization. With the advent of VLSI technology, however, increased circuit sensitivity has resulted in other T/H failure mechanisms. These have been attributed to the conductive or capacitive effects of the build-up of a layer of moisture on the surface of the chip [1-4]. However, this paper will describe new failure mechanisms characterized by physical defects in the interlevel dielectrics. Both leakage-induced and open-circuit failures have been observed.

Experiment

The test vehicles were vendor dynamic RAM (DRAM) chips encapsulated in plastic dual-in-line packages. Out of many vendors tested, two in particular, referred to as Vendors A and B, had extensive fails, and, therefore, will be discussed in detail.

Multiple T/H conditions (85°C/85%, 85°C/81%, 85°C/75%, 70°C/85%) were used in this evaluation. During the first 168 hours in the stress chamber no bias was applied. This allowed the modules to achieve equilibrium with the stress environment while exposing those "defect" fails which occurred in the absence of bias. After electrical readout the samples were returned to stress, with bias applied for 24 hours and subsequently removed again for readout. This stress methodology provided a means of separating the "defect" and intrinsic failure populations.

Conventional T/H tests were conducted for both Vendor A and Vendor B. Additionally, Vendor A samples were tested under Highly Accelerated Stress Test (HAST) conditions. These accelerated stresses (138°C/85%, 138°C/75%, 138°C/50%, and 127°C/85%) provided kinetic data in a relatively short stress time [5].

* Present address: IBM Corp., Rt. 52, Hopewell Junction, NY 12533.

Results

Most of the failures for Vendor A came from HAST stress and were predominantly row failures. Some single-bit failures were also observed. Physical analysis showed that the row failures were due to cracks in the word line and interlevel oxide at a step over a first level polysilicon edge (see Figure 1). The single-bit failures were due to a crack in the thin oxide under the transfer gate of the failing cell as shown in Figure 2. In both cases the cracks were isolated to the areas around the fail sites and no cracks were observed in the passivation above the fail sites.

Figure 1. Vendor A failing word line showing crack in refractory metal silicide line and interlevel oxide. SEM micrograph, 20,000x.

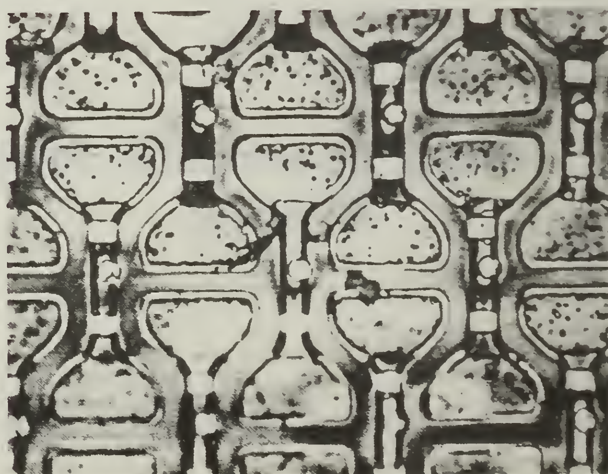

Figure 2. Vendor A failing bit showing area where transfer gate disappeared due to cracked thin oxide. Optical photograph, 2000x.

Since the failures for Vendor A were due to cracks causing added resistance or opens, they were not sensitive to test voltage or recoverable by baking at 150°C for 24 hrs.

Single-bit failures were the predominant failure mode for Vendor B's product subjected to T/H stress with bias. The failures were found to be voltage, timing, and pattern sensitive. Failures only occurred during long-cycle, low V_{dd}, and disturbed patterns. Electrical diagnostics indicated that the failures were due to leakage between the cell and the bit line or cell to cell. These failures demonstrated voltage sensitivity in that higher V_{cc} could make the failure recover. Physical analysis found a crack in the passivation and interlevel oxide along the edge of a metal line running over the failing cell (see Figures 3 and 4). One single column fail was also observed. In this case, a crack was found in the active restore circuitry, resulting in leakage between bit line and V_{cc}. These microcracks could not be seen until after a light glass etch, due to their narrow dimension and the severe chip topology. The cracks always extended down to one of the polysilicon layers and in some cases to the Si surface.

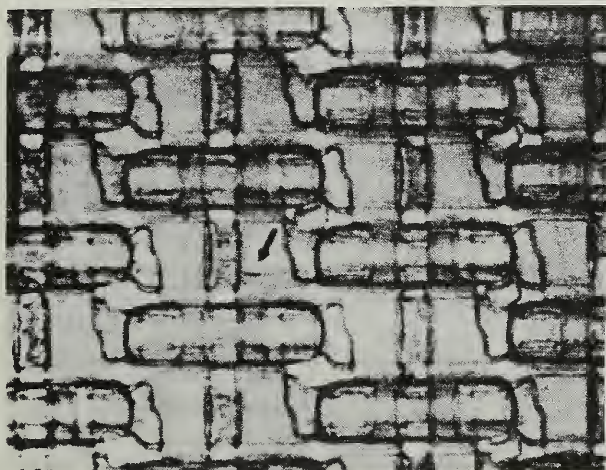

Figure 3. Vendor B failing bit showing crack in interlevel oxide over cell plate and transfer gate. Optical micrograph, 2000x.

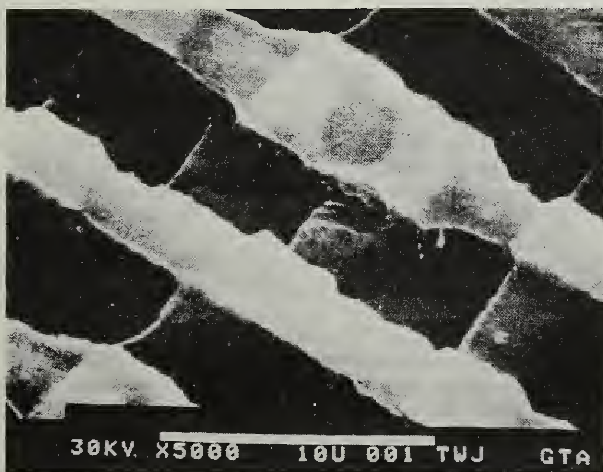

Figure 4. Vendor B failing bit showing crack in passivation glass along metal edge. SEM micrograph, 5000x.

Subjecting Vendor B single-bit failures to a bake often produced recovery. Physical analysis of recovered single-bit failures always revealed a microcrack at the fail site, indicating that the crack alone was not enough to cause failure, and that moisture and/or ionic build-up were necessary for the leakage to occur.

Kinetic Study

The failure population of Vendor B was bi-modal. One group of fails occurred early in stress (with and without bias), whereas the second group, which required bias, failed later in stress. Statistical analysis of the data clearly indicated two populations, that is, defect, and intrinsic. The latter population fit well to a lognormal distribution as shown in Figure 5. For Vendor A. no defect population was observed. Analysis of the data, T/H and HAST likewise indicated a lognormal fit as shown in Figure 6.

The activation energy ΔH was estimated to be 0.7 eV for Vendor A (Figure 7) and 1.0 eV for Vendor B. Recall that the failure modes were correspondingly different, that is, single-bit failures (short) for Vendor B; row fails (open) for Vendor A. Analysis of the data is consistent with the following dependency for the mean time to failure:

$$t_{50} \sim \exp\left(\beta / RH + \Delta H / kT \right) \qquad (1)$$

where, RH = relative humidity in fraction

T = absolute temperature in Kelvin

k = Boltzmann constant

then the humidity dependency value, β, is estimated as 1 for Vendor A and Vendor B (see Figure 8). This RH dependency is supported by the absence of intrinsic failures in high-temperature bias (HTB) stress for both Vendors A and B within a reasonable time.

Given the strong temperature dependence and the occurrence of failures relatively late in stress, the intrinsic failure mode posed no field reliability concern for either vendor.

Discussion

The uniqueness of this study is the finding of microcracks at the fail sites of modules subjected to T/H stress. If cracks are initially present in the passivation, as in Vendor B, failure can occur during stress at the location of the defect. Alternatively, cracking could be induced by T/H/B stress alone. Swelling of the plastic and/or organic layers through moisture absorption could lead to crack generation and propagation in the areas of high stress [6,7]. Due to high cell densities, DRAM technologies often employ narrow structures in multiple layers resulting in severe topology. This topology produces both horizontal and vertical stresses in and between layers. Another source of stress in DRAM technology is refractory metal silicide lines. These silicides are an attractive alternative to polysilicon due to their low resistivity, however, high formation temperatures result in high tensile stress on the order of 10E9 dynes/cm^2 [8].

In Vendor A, stress in the refractory metal silicide line caused a crack in both the line and the underlying oxide. This happened at a very steep 2000Å step, directly under the edge of a metal line, contributing to localized stresses. These cracks occurred only after tests subjecting the parts to high humidity, indicating that the increased stress due to swelling

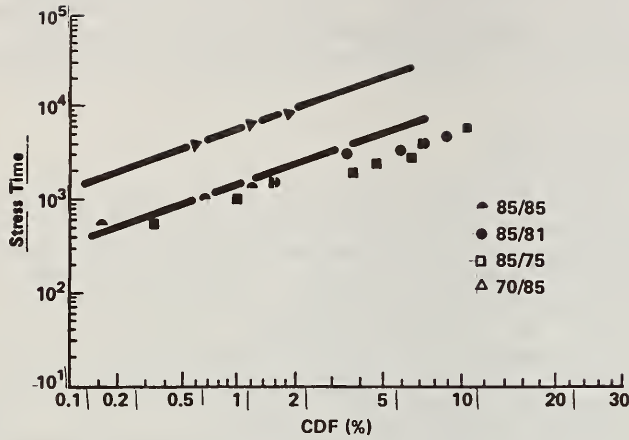

Figure 5. Vendor B stress data.

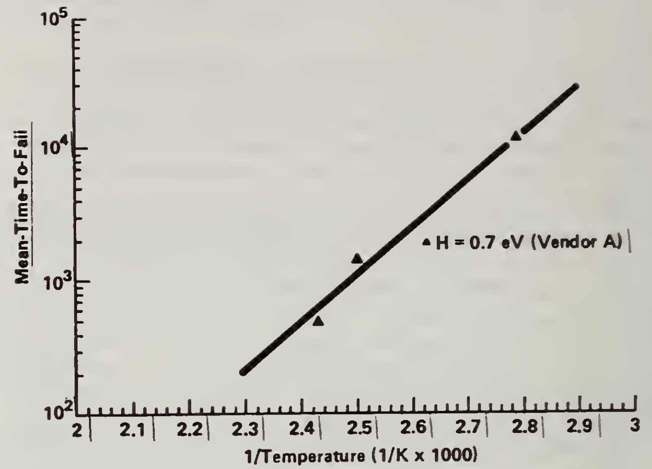

Figure 7. Delta H determination.

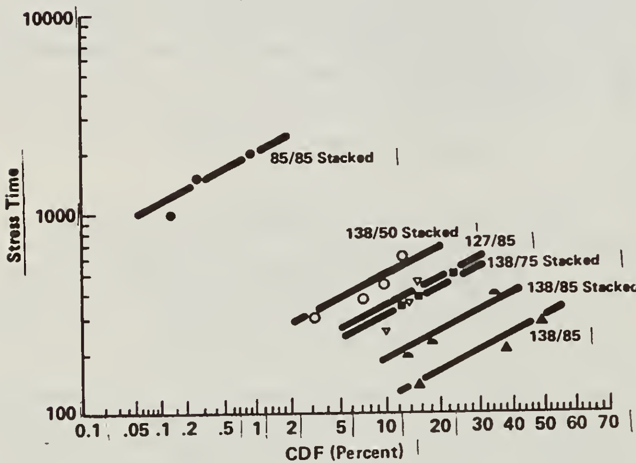

Figure 6. Vendor A stress data.

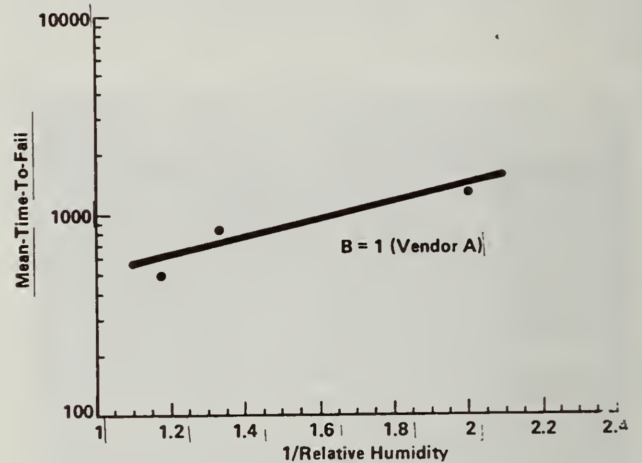

Figure 8. Beta determination.

caused the lines to crack, resulting in failures. None of these failures were bake recoverable as the cracks caused high resistance or opens.

In the case of Vendor B, during THB stress, cracks occurred in passivation layers between dynamically isolated nodes. Failure was due to leakage between these nodes. The microcracks were always found in the area of the most severe topology along the edge of a metal line and over two layers of polysilicon. The fact that a defect population was observed in Vendor B tends to indicate that the stress alone in this structure was enough to cause a crack. Voltage was required to induce failure during T/H stress indicating the possibility of ionic accumulation in the crack [9]. These failures were extremely sensitive to voltage, temperature, and extended timings when being tested. The fact that most of these fails were recoverable after baking may depend on the size of the crack and the amount of ionic accumulation.

For both vendors the microcracks were found to be along a metal edge, but the orientation of the metal line with respect to the cell was 90 degrees different for the two vendors, leading to the different failure modes.

t_{50} depends strongly on temperature and only weakly on humidity as indicated by small value of β in Equation (1). However, the presence of moisture is necessary for failure to occur as no intrinsic failures occurred on HTB and temperature cycling tests. The results of this study also indicate that moisture transport through the package was not the rate determining factor for failure as implied by the relatively higher activation energy [10-12].

The Vendor B population defect failures occurred early in stress, indicating that T/H testing is an effective way to screen out this failure mode. An equilibrium "soak" period, coupled with a frequent early readout schedule, provided for a clear separation of the defect and intrinsic populations.

Conclusion

New failure mechanisms other than metal corrosion and migration were found in THB testing of plastic encapsulated VLSI modules. The fails appear as single bit, partial column, or partial row failures depending on circuit designs, defect locations, and process technology. Microcracks induced by T/H stress with and without subsequent ionic accumulation were found to be two major causes for the failures. The high stress areas such as silicide lines and severe topological points are more susceptible to cracking. Additional stress from moisture absorption during T/H stress seems to be critical to crack generation and propagation. The defect could also be present before stressing, in which case the failure would occur after exposure to T/H, without bias, as observed.

The kinetic study indicated that the intrinsic population followed lognormal distribution. The data indicated a strong t_{50} dependence on temperature with

an activation energy of 1 eV for one vendor and 0.7 eV for the other. The humidity dependency was found to be relatively small, however failure only occurred when moisture was present.

Finally, no field reliability problem was projected with the intrinsic mode for either of the vendor products tested.

Acknowledgements

The authors wish to thank J. Gunn for providing HAST, P. Tasi for his excellent failure analysis, and G. Dauser and R. Bellin for electrical diagnostics.

References

1. S. Shabde, J. Edwards, and W. Meuli, "Moisture Induced Failure Mode in a Plastic Encapsulated Dynamic Timing Circuit," Proc. Rel. Phys. (1977) 33.

2. H. Gunther, H. Muller, J. R. Goetz, and D. Kantz, "Moisture Induced Failure in Plastic Encapsulated Dynamic RAMs," Proc. Electronic Components Conference, (1983), 344.

3. D. Stoehle, "Influence of the Chip Excess Temperature on the Moisture Induced Failure Rate of Plastic Encapsulated Devices," Proc. Electronic Component Conference, (1983), 253.

4. M. Noyuri, T. Ishihara, and H. Higuchi, "Secondary Slow Trapping - A New Moisture Induced Instability Phenomenon in Scaled CMOS Devices," Proc. Rel. Phys. (1982), 113.

5. J. E. Gunn, R. E. Camenga and S. Malik, "Rapid Assessment of the Humidity Dependence of IC Failure Modes by Use of HAST," Proc. Rel. Phys., (1983) 66.

6. N. Nagasima, H. Suzuki, K. Tanaka and S. Nishida, "Interaction Between Phosphosilicate Glass Films and Water," J. Electrochemical Society: Solid Science and Technology Vol. 121, No.3, (1974), 434.

7. R. F. Fedors, "Cracking in a Glassy Epoxy Resin Induced by Water Absorption," Polymer, Vol. 21, (1980), 713.

8. S. P. Murarka, Silicides for VLSI Applications, Academic Press, NY, (1983) p.60.

9. K. Watanable, T. Tanigaki, and S. Wakayama, "The Properties of LPCVD SiO_2 Film Deposited by SiH_2Cl_2 and N_{20} Mixtures," J. Electrochemical Society: Solid State Science and Technology, Vol. 128, No. 12 (1981), 2630.

10. R. M. Levin, "Water Absorption and Densification of Phosphosilicate Glass Films," J. Electrochemical Society: Solid State Science and Technology, Vol. 129, No. 9,(1982), 1765.

11. A. Apicella, L. Nicolais, G. Astarita, and E. Drioli, "Hygrothermal History Dependence of Moisture Sorption Kinetics in Epoxy Resins," Polymer Eng. and Science, Vol. 21, No. 1, (1981), 18.

12. E.J. McInerney and P. A. Flinn, "Diffusivity of Moisture in Thin Films," Proc. Rel. Phys. (1982), 265.

3.2 STUDIES OF MOISTURE IN POLYIMIDE: A SUMMARY

Stephen D. Senturia
Microsystems Technology Laboratories
Department of Electrical Engineering and Computer Science
Massachusetts Institute of Technology
Cambridge MA 02139
(617) 253-6869

Polyimide is finding increased use in microelectronic devices as a passivant, interlevel insulator, and die-attach adhesive, in part because of its excellent electrical properties, chemical, mechanical, and thermal stability, ease of application, and its good planarization and etch properties [1]. Like all polymers, polyimide absorbs moisture, and because of the link between moisture absorption and potential reliability problems, the role of polyimide's moisture absorption in ultimate device reliability must be carefully assessed. On the one hand, published data indicate improved reliability if polyimide is used in conjunction with inorganic passivants, when compared with the inorganic passivants alone. Furthermore, the fact that polyimide does absorb moisture provides a degreee of moisture gettering in finite-volume hermetic packages, even in cases where total moisture content of the package might exceed the recommended minimum. On the other hand, the role of moisture in degrading polyimide adhesion is well documented, and in the event of adhesion loss, moisture absorbed in the polyimide could collect in unadhered regions, creating the potential for corrosion.

This paper summarizes the results of a series of our previous studies [2-11] of moisture uptake and diffusion in polyimide films in integrated circuit structures, and of the effects of moisture on polyimide properties. Because of the large number of literature citations contained in these papers (more than 80), they will not be repeated or discussed here. The reader is directed especially to References 3-5, 7, 8, and 11 both for the citations and for a discussion of the relation between our findings and other published work.

We have carried out both gravimetric [2-4, 6] and electrical [2-6,8] studies of moisture absorption. Sample structures are illustrated in Figures 1 and 2. The simplest structure is a polyimide film spin-cast

onto an aluminum-coated silicon wafer (Fig. 1a). In this case, the path for moisture uptake is normal to the surface of the as-deposited film; we call this a "vertical" sample. Alternatively, one can investigate samples in which a metal film is photolithographically patterned on top of the polyimide (Fig. 1b). If the polyimide is etched away as shown in Fig. 1b, the path for moisture uptake is parallel to the polyimide surface; we call this a "lateral" sample. Samples of both types have been used for gravimetric studies [4,6]. If the polyimide is not etched away, the moisture uptake path to the region beneath the metal stripes involves a combination of vertical and lateral diffusion. Much of our early electrical work [2,3,5] was done with unetched samples, and was analyzed assuming isotropic diffusion characteristics. We subsequently discovered that the kinetics of moisture uptake differed for vertical and lateral samples [6]. As a result, there remains a small quantitative uncertainty in the detailed intepretation of some of the electrical data from unetched samples, but this does not affect the general properties as described here.

Sample fabrication begins with evaporation of 1 μm of aluminum onto a cleaned silicon wafer. This aluminum layer is used even for the gravimetric samples so that rigorous comparison with the electrical samples, which require a conducting lower electrode, can be made. The polyimide is then spin deposited and cured. We have examined three basic polyimide chemistries, PMDA-ODA, BTDA-MPDA/ODA, and a fluorinated modification of the BTDA material. While there are some quantitative differences among the various polyimides, they are not the principal subject of our research; hence we report here primarily on the widely-used PMDA-ODA material. The polyimides were obtained from Dupont and IBM in the form of a polyamic acid precursor dissolved in NMP. Samples of various thickness are achieved either by dilution of the precursor in NMP, or by multiple coats. Following spinning of each coat, the film is partially imidized at a temperature of 180°C. After all coats have been applied, the film is cured in nitrogen at a final cure temperature which was varied between 250 and 400°C. Thicknesses in the range 2 - 15 μm have been studied, although most studies were for either 3 μm or 6 μm films. For samples with an upper metal layer, 1 μm of aluminum is evaporated after polyimide cure, and is patterned photolithographically to achieve a multiple-stripe electrode (Figure 2). Etching of the polyimide is done after aluminum patterning in an oxygen plasma, with the alumimum electrode serving as the etch mask.

Another approach to sample fabrication was to develop a complete polyimide test chip containing a variety of test devices [8], including parallel-plate and interdigital capacitor structures specifically designed for the moisture studies. While this approach requires a much more elaborate mask set and process specification (because some of the measurement techniques involve MOS transistors), it has the advantage of permitting tightly correlated in-situ measurements of a wide variety of properties (ion transport, conduction, and moisture uptake) on the same polyimide sample.

We now review experimental findings. Figure 3 shows a typical gravimetric moisture-uptake transient, plotted as mass change against time starting from a point at which the ambient moisture is suddenly increased. To make these measurements, the coated wafer is hung in a Cahn 1000 microbalance, tared against a similar uncoated wafer. The moisture ambient of the test wafer is varied by control of the dew point of an air stream which enters the microbalance chamber through a baffle above the wafer position and exits from the same side of the microbalance below the wafer position. The dew point is monitored with a General Eastern dew-point hygrometer. By piecing together mass-change transients like those of Figure 3, it is possible to determine the total mass change with relative humidity over the entire range to about 85% RH. Above 85% RH, surface condensation appears to affect the microbalance measurement. Below 85% RH, the moisture uptake is proportional to sample thickness, hence is a bulk effect, and is approximately linear in RH. By extrapolating to 100%, we find a total moisture uptake that varies from 2 - 3%. Interestingly, we usually find a higher moisture uptake than that reported for free-standing bulk samples. A possible explanation is that the as-deposited films are under tensile stress [9-11], which can increase the moisture absorption. From the shape of the moisture-uptake transient, it is also possible to extract the diffusion constant based on a Fickian model. These results are discussed later.

Moisture uptake can also be studied by measuring the change in capacitance of a parallel-plate [2-6, 8] or interdigital [5,8] capacitor in which the polyimide serves as the dielectric. Figure 4 shows typical normalized capacitance vs. RH for a parallel-plate capacitor structure with a stripe-electrode upper plate. The data include room temperature points for which the dew point of the ambient air was varied, and points for temperatures in the range of 20 - 80°C measured with fixed-dew-point air. Both sets of data are consistent with the basic observation that the dielectric constant of the polyimide varies approximately linearly with relative humidity.

The correlation between the gravimetric and dielectric measurements of moisture uptake permit the extraction of the effective dipole moment of the absorbed water molecule [4]. The molecular polarizability of the absorbed water is extracted from the change in dielectric constant using the Clausius-Mossotti relation, and is plotted in Figure 5 against the concentration of absorbed moisture molecules, obtained from the gravimetric data. The solid curves are calculated for various values of dipole moment. It is seen that the absorbed water molecule has a moment equal to about 0.9 of that of the free water molecule (p_o). This indicates that the absorbed moisture is extemely weakly bound, possibly residing in microvoids that result from the removal of water during the condensation cure reaction which converts the polyamic acid precursor into the polyimide. This conclusion is supported by a decrease both in moisture absorption and diffusion constant with increased cure of the polyimide film [5].

Analysis of the moisture-uptake transients with a linear Fickian model can be used to extract the diffusion constant and the surface equilibration rate. In the earliest work [3], it was assumed that the diffusion was effectively one-dimensional, and that the equilibration of the film surface with the change in ambient moisture was instantaneous. Figure 6 shows an Arrhenius plot of the resulting moisture diffusion constant against temperature. The diffusion constant is on the order of 5×10^{-9} cm^2/sec at room temperature, and is weakly temperature dependent, having an activation energy of about 0.3 eV. We also find that the diffusion constant is 35% greater for absorption than for desorption at room temperature; this asymmetry, however, decreases with increasing temperature, approaching equal absorption and desorption rates at 100^oC (see Figure 7). These values may have to be modified slightly by our more recent discovery [6] that a better model for the moisture transient is the so-called "evaporation" boundary condition, and, further, that the surface equilibration rate which enters this boundary condition is about a factor of 9 faster for the sidewall of the lateral sample than for the as-deposited surface of the vertical sample. We also find that the diffusion constant is 50% greater in lateral samples. Further studies are in progress to determine whether this difference is due to the presence of an etched sidewall, to an intrinsic anisotropy in the diffusion characteristics of the film, or to enhanced diffusion at the metal-polyimide interface.

The effects of moisture on electrical conduction in polyimide aredifficult to document quantitatively, because when a voltage is applied to a sample, the resulting current exhibits very long-lived transients at ordinary device temperatures. We denote the shortest transient, which typically exhibits a power-law decay with time, as the "polarization" current, and the value of current that results after settling of the polarization current as the "transport" current, although both currents may in fact be transients on the time scale of actual device use. Figure 8 illustrates how moisture increases both components of the current [7]. However, the increase is not considered to be large enough to pose a significant reliability problem as long as the polyimide remains well-adhered to the substrate. Hence, the critical issue is maintenance of adhesion, which, in turn, may be affected by residual stress.

We have recently developed a suspended-membrane technology using microfabrication methods to create test site with which the residual stress, modulus, adhesion, and elongation at break of thin polymer films can be studied [9-11]. Figure 9 illustrates the simplest type of sample in schematic form. To make the sample, a diaphragm is first etched in a silicon wafer using micromachining techniques; then the polyimide is spin-deposited and cured; finally, the diaphragm is etched away leaving a free-standing membrane. To date, the principal use of these structures for moisture studies has been the demonstration of the well-known result that moisture exposure severely the adhesion of polyimide to silicon dioxide. However, we plan a more detailed study of this adhesion degradation by combining in-situ measurements of residual stress and modulus in conjunction with the peel adhesion experiment.

ACKNOWLEDGEMENT

This work was support in part by IBM, E. Fishkill, NY, and in part by E. I. DuPont de Nemours & Company, Wilmington, DE. The author is indebted to Denice D. Denton for her assistance in providing a critical reading of the manuscript.

REFERENCES

[1] For a review of recent literature, see "Polyimide and VLSI: A Research Perspective", S. D. Senturia, R. A. Miller, D. D. Denton, F. W. Smith, III, and H. J. Neuhaus, Proc. Second Intl. Conf. on Polyimides, Ellenville, NY, October 1985, pp. 107-118, and additional review articles cited therein.

[2] "Moisture Transport in Polyimide Films: Implications for Moisture Measurement in IC Packages", D. D. Denton, D. R. Day, and S. D. Senturia, Proc. RADC/NBS Workshop on Moisture Measurement and Control for Semiconductor Devices III, Gaithersburg, MD, November 1983; NBS Report NBSIR 84-2852, pp. 279-287.

[3] "Moisture Diffusion in Polyimide Films in Integrated Circuits", D. D. Denton, D. R. Day, D. F. Priore, S. D. Senturia, E. S. Anolick, and D. Scheider, Journal of Electronic Materials, 14, 119-136 (1985).

[4] "Effects of Moisture Uptake on the Dielectric Permittivity of Polyimide Films", D. D. Denton, J. B. Camou, and S. D. Senturia, Proc. ISA Moisture and Humidity Conference, Washington, DC, April 1985, pp. 505-513.

[5] "Fundamental Issues in the Design of Polymeric Capacitive Moisture Sensors" , D. D. Denton, S. D. Senturia, E. S. Anolick, and D. Scheider, Proc. 3rd International Conf. on Solid-State Transducers, Philadelphia, June 1985, pp. 202-205.

[6] "Vertical and Lateral Moisture Transport in Polyimide Films", D. D. Denton, J. B. Camou, and S. D. Senturia, Electronic Materials Conference, Boulder, CO, June 1985; manuscript in preparation for Journal of Electronic Materials.

[7] "Conduction in Polyimide Between 20 and 300 C", F. W. Smith, III, Z. Feit, D. R. Day, and T. J. Lewis, H. J. Neuhaus, and S. D. Senturia, Electronic Materials Conference, Boulder, CO, June 1985; Journal of Electronic Materials, in press.

[8] "An Integrated MOS Test Chip for Study of the Electrical Properties of Polyimide Films", D. D. Denton, D. F. Priore, H. J. Neuhaus, S. D. Senturia, E. S. Anolick, and D. Scheider, Proc. Second Intl. Conf. on Polyimides, Ellenville, NY, October 1985, pp. 521-528.

[9] "The Use of Micromachined Structures for the Measurement of Mechanical Properties and Adhesion of Thin Films", M. Mehregany, M. G. Allen, and S. D. Senturia, Proc. IEEE Workshop on Solid-State Sensors, Hilton Head, S. C., June 1986.

[10] "Novel Microstructures for the Study of Residual Stress in Polyimide Films", M. Mehregany, M. G. Allen, R. T. Howe, and S. D. Senturia, Electronic Materials Conference, Amherst, MA, June 1986.

[11] "Microfabricated Structures for the In-Situ Measurement of Residual Stress, Young's Modulus, and Ultimate Strain of Thin Films", Mark G. Allen, Mehran Mehregany, Roger T. Howe, and Stephen D. Senturia, submitted to Applied Physics Letters.

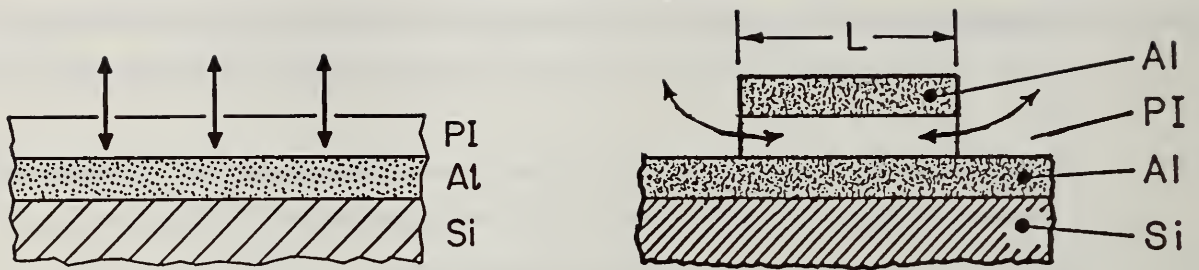

Figure 1 Schematic cross sections of (a) vertical and (b) lateral moisture-uptake samples.

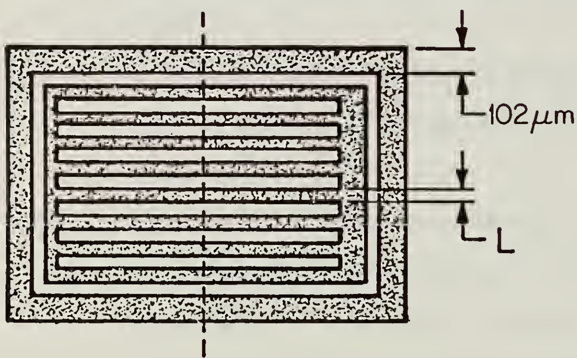

Figure 2 Schematic top view of a lateral moisture-uptake sample.

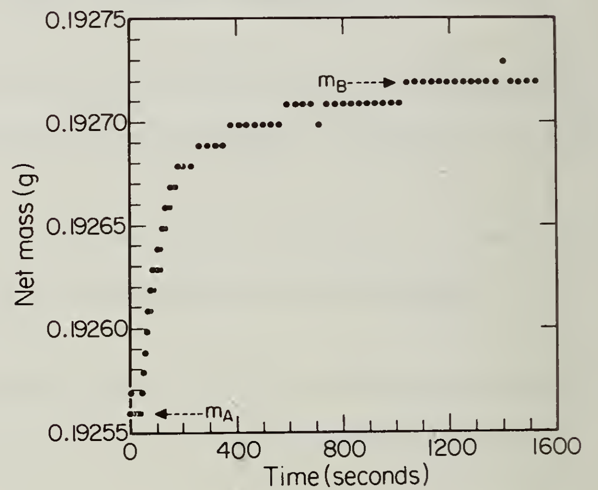

Figure 3 Typical gravimetric moisture-uptake transient. M_A and M_B are the steady state values before and after the change in ambient humidity.

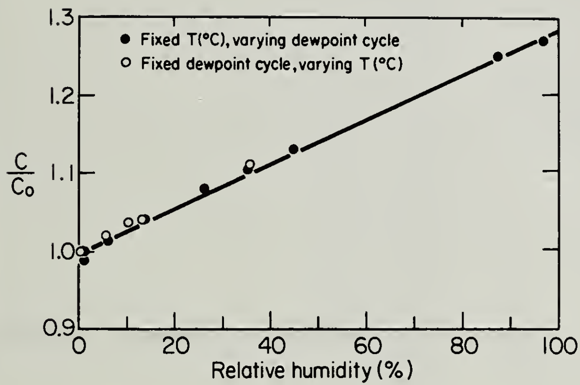

Figure 4 Steady-state normalized capacitance vs. relative humidity.

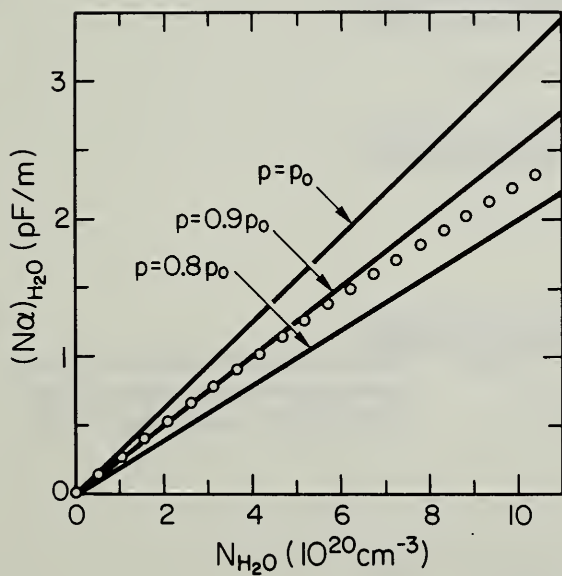

Figure 5 Correlation of capacitance and gravimetric moisture-uptake data.

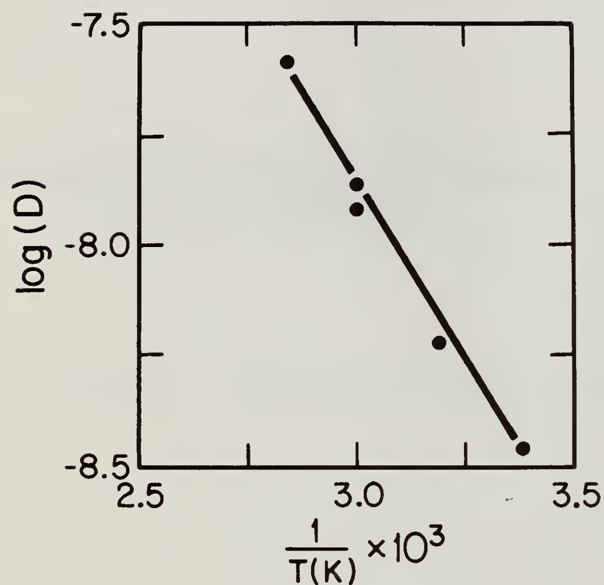

Figure 6 Arrhenius plot of diffusion constant.

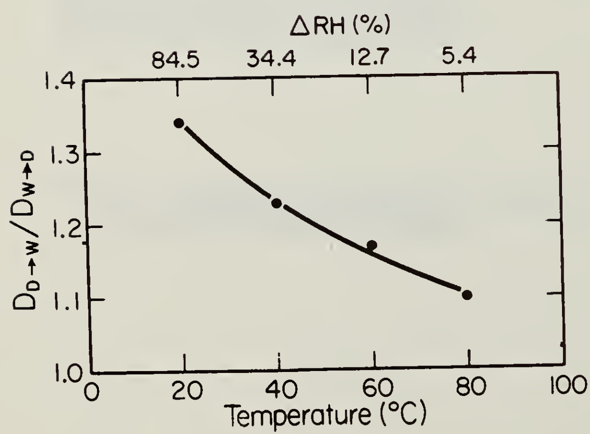

Figure 7 Ratio of diffusion constant (D→W) measured for absorption to that measured for desorption (W→D).

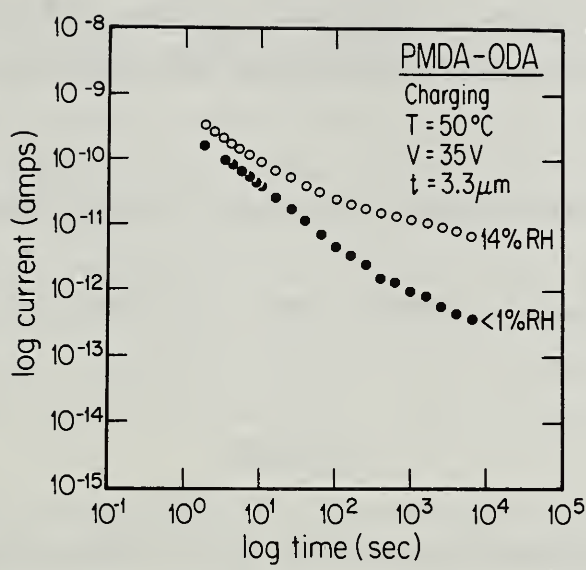

Figure 8 Effect of moisture on polarization power-law region) and transport current.

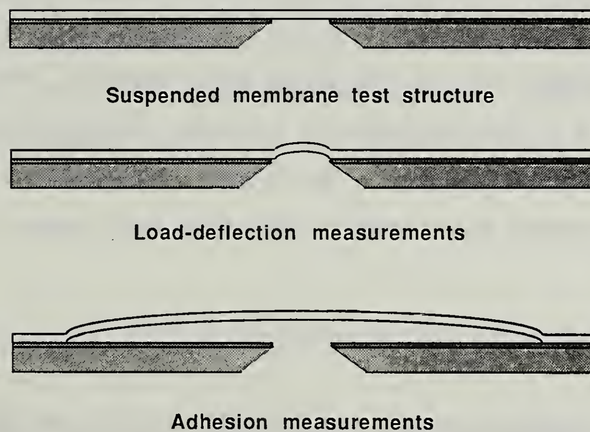

Figure 9 Schematic cross-section of membrane used for mechanical property and adhesion (end-point) studies.

Reprinted with permission from RCA Review, Vol 45, June 1984.

3.3 MOISTURE CONTROL IN HERMETIC LEADLESS CHIP CARRIERS WITH SILVER EPOXY DIE ATTACH ADHESIVE

D.R.Carley and R.W.Nearhoof, RCA Solid State Divion, Somerville ,N.J. 08876

R. Denning, RCA Laboratories, Princeton, N.J. 08540

ABSTRACT

This paper describes package design and process changes in the development of an improved system for controlling internal water vapor levels below 5000 ppmv in hermetically-sealed leadless chip carriers with silver-epoxy die attached silicon devices.

It is shown by mass spectrometry that the silver-epoxy die attach material releases water and unreacted monomers at about 300°C.

The high-temperature braze seal design and process originally used in manufacturing was changed to a controlled-environment low-temperature seam-welded design. A high-temperature preseal furnace bake-out and epoxy cure process was also incorporated. Moisture levels measured for the new package design and process have been below the 1000 ppmv level.

INTRODUCTION

An excessively high moisture level was detected on some product that was being fabricated for a critical high-reliability program. The product, CMOS/SOS devices, was assembled in leadless chip carriers (LCC) using DuPont 6838 silver-filled epoxy die attach adhesive (1).

Over a period of three years, a number of engineering tests and experiments were made, only those considered most significant are reported.

Initial production of four universal gate arrays (UGAs) and one random access memory (RAM), all CMOS/SOS devices assembled in leadless chip carriers, commenced in the fourth quarter of 1980 at the Findlay, Ohio facility. The LCC packages were designed for braze seal, using a nickel-plated, gold-plated Kovar lid with a Au/Sn brazing preform tacked to the lid at each of the four corners. The assembled package and lid are pre-aligned in a jig and clamped together with spring tension clips. The clipped assembly is placed on a conveyor belt and passed through the furnace in a nitrogen atmosphere (20 ppmv moisture) at a maximum temperature of 310° - $315^{o}C$ (Figure 1).

The initial water vapor measurements on three production lots sealed from December 1980 to November 1981 ranged from 460 to 2250 ppmv (parts per million by volume). A maximum of 5000 ppmv moisture is allowable for qualification to Mil-Std-883, Test Method 1018.2, Proceedure 1 (2). These results were satisfactory and qualified production; however, moisture measurements made on engineering tests processed during the March and April 1982 period of time ranged from 5000 ppmv to 15000 ppmv. Further moisture measurements made on the product, after the production line at Findlay, Ohio was carefully checked and controlled, indicated some product with internal moisture levels greater than 5000 ppmv. Figure 2 indicates the moisture level distribution of product made during this time. An engineering investigation into the cause of these inconsistencies was initiated.

ANALYTICAL TESTS

Empty Packages vs. Packages with Silver-Epoxy Die Attached Devices

One of the first series of tests run compared empty packages and packages containing the silver-epoxy die-attached devices for moisture levels (Table 1). The mass spectrometer results indicated a significant increase in CO_2 for the packages containing the silver-epoxy die attached CMOS/SOS devices. The moisture levels, however, showed no significant differences. Hydrogen, generally present in hermetic packages due to the nickel plating or gold plating processes (3), was significantly lower for the package containing the silver-epoxy die-attached devices .

It was clearly evident that the organic silver-epoxy die attach material had an influence on the gases contained in the leadless chip carrier hermetic package. It was also evident that at the high temperature required to braze seal, additional degassing or moisture release could occur (Figure 3).

ANALYTICAL MEASUREMENTS

Die-Attach Silver-Epoxy Mass Spectrometry Analysis (4)

A sample of cured silver-epoxy die-attach material was inserted into a mass spectrometer ion source by means of a pyrolytic probe, and the mass spectrometer was scanned from 10 to 600 a.m.u. once a second. The sample was heated at 200°C per minute to 1100°C. In this manner, identification of the evolved gases was made as the sample was heated. Two distinct regions were observed (Figure 3). At about 300°C, unreacted monomers of the epoxy (epichlorohydrin and bisphenol A) were evolved, along with degradation products from these species, in particular water (Figure 3). These data indicate that one source of moisture can come from the silver-epoxy die attach material. It suggests that at the braze seal temperature of 310° - 315°C, the water released from the silver epoxy could be captured within the package cavity as the braze seal is made, resulting in packages with greater than 5000 ppmv moisture levels (5).

ENGINEERING TESTS

Pre-Seal High-Temperature Bake-Out and Epoxy Cure

A pre-seal furnace bake-out and epoxy cure step through the braze seal furnace at 330°C was tested. This pre-seal high-temperature process was considered advantageous, since it would compensate for any insufficiencies in the pre-seal bake, would ensure the elimination of absorbed and condensed moisture from the package components, and would further out-gas the epoxy die attach material and release some of the unreacted chemicals and water shown to be present from the mass spectrometry analysis (Figure 3). This process could also be easily implemented in production.

Although a significant improvement in the distribution of moisture vapor content was made, this process did not consistently produce product below the 5000 ppmv of moisture required (Figure 4).

Si/Au/Sn Preform for Moisture Control

The incorporation of an Si/Au/Sn alloy in a hermetic package was reported to reduce the high levels of moisture (6). Preliminary tests were conducted by merely dropping a 0.35% Si/Au/Sn preform (0.070 x 0.070 x0.001 inches) in the package with a silver-epoxy mounted chip and braze seal with no other precautions taken to reduce moisture. The mass spectrometer moisture analysis results are shown in Table 2. For these tests, the moisture level for the control units measured 13,000 - 16,000 ppmv of moisture; the test packages containing the 0.35% Si/Au/Sn preforms measured only 125 - 135 ppmv moisture. Also, the hydrogen content of the packages containing the Si/Au/Sn increased to 5000 - 8000 ppmv, compared to the control packages with 1700 - 1900 ppmv hydrogen. These results confirm the proposed mechanism of the reaction of the Si in the preform during the heat cycle, $Si + 2\ H_2O \quad = \quad SiO_2 + 2\ H_2$ (6).

The use of a Si/Au/Sn preform inside a package with an epoxy-mounted die provided the silicon for the reaction to produce a very dry package. Unfortunately, the method of placing the Si/Au/Sn preform inside the package, and control of the related processing were not compatible with production processes.

Neither the Si/Au/Sn preform nor a Si/Au preform could be used as a die attach since the device substrate is sapphire. All of the Si/Au/Sn experiments involved CMOS/SOS die and silver epoxy for die attach. The development of a process using the Si/Au/Sn approach to control moisture is considered possible. However, the results of the next series of experiments proved more satisfactory from a cost and implementation point of view, and work on the Si/Au/Sn preform approach was discontinued.

Seam Weld Seal

A modification of the braze seal package is required for seam welding. The top layer of ceramic is reduced in thickness to allow the weld ring to be brazed on top of it (Figures 5 and 6). The gold plating is removed from the lid and the lid thickness is reduced to insure seam welding quality. The seam-weld sealing is controlled under dry box conditions of less than 20 ppmv moisture and sealed at room temperature. Initial engineering weld-seal tests on 48-pin packages with silver-epoxy die attach measured between 0 - 410 ppmv for moisture. The first series of tests with 24-pin and 64-pin weld-seal leadless packages compared the weld-seal process and pre-seal furnace bake with the braze-seal process and pre-seal furnace bake (Figures 7 and 8). Moisture analysis results are compared in Tables 3 and 4 for the 64-pin leadless carriers. The results indicated a significant (10-20 times) improvement in moisture for the seam-weld IC's. Moisture levels of 100-300 ppmv for seam-welded IC's were measured versus 1700-2200 ppmv for the braze-seal product. Based on these results, production was re-started with weld-seal packages. A total of 109 seam-welded IC's were measured for moisture (Figure 9); 90% of the product was below 300 ppmv and 63% of the product was below 100 ppmv moisture, a significant and dramatic improvement over the pre-seal bake braze seal process (which had approximately 16% of the product above the 5000 ppmv moisture levels) (Figure 4).

Seam-Weld Seals - Internal Moisture Analysis at High-Temperature Stress Conditions

A series of experiments were conducted for the seam-welded IC's to test changes in the ambient gases under temperature stress.

The first series of tests were to qualify the process, and tests were conducted at the highest temperature the devices would be subjected to in the application. Ten cycles from 25°C to 200°C were used to simulate the solder board mounting process. The 64-pin seam-welded packages containing silver-epoxy die attached CMOS/SOS devices, pre-seal furnace baked at 330°C, were analyzed for internal gases before and after the ten-cycle temperature stress (Tables 3 and 5). Moisture levels of 100-300 ppmv were obtained before temperature stress, and of 100 - 385 ppmv were measured after stress, indicating a stable system under this type of stress.

A series of tests were next conducted with 125°C, 230°C and 313°C post-seal bakes for these 64-pin leadless seam-weld IC's (Table 6). Moisture analysis was also made for seam-weld IC's before and after 125°C, 11V, 240 hour burn-in (Table 7).

Mass spectrometer results indicated that at temperatures above 200°C, significant changes in the ambient gases resulted (Table 6). Moisture increases from 70-80 ppmv moisture at 125°C to 5000 - 9000 ppmv moisture at 313°C were observed. However no changes in internal moisture levels were observed for the 125°C temperature stresses.

DISCUSSION

It is shown that at approximately 300°C (Figure 3), the silver-epoxy die attach material chemically reacts, or decomposes, releasing water as a by-product of the reaction. It is this reaction and water release that makes it difficult to consistently obtain internal moisture levels of less than 5000 ppmv for the high-temperature brazed-seal leadless chip carrier. The addition of the pre-seal high-temperature degassing, desorption and cure bake process had an advantageous effect on moisture control (Figure 4), although levels below 5000 ppmv were not consistently maintained.

The seam-weld sealing process yielded product with internal moisture readings consistently below 1000 ppmv, and typically at 200 ppmv (Figure 9).

Weld-sealed silver-epoxy die attached IC's, when subjected to post-seal temperatures above 200°C, show significant changes in the ambient gases, and increases in moisture content in the package.

CONCLUSION

Silver-epoxy die attached devices hermetically packaged in ceramic leadless chip carriers can be successfully controlled for internal moisture levels with the incorporation of (1) a high temperature 330°C pre-seal bake and (2) the conversion from a high-temperature braze seal technique to a low-temperature seam-weld seal. These devices, when burned-in for 240 hours at 125°C, show no internal changes in moisture levels.

REFERENCES

1. E. I. DuPont DeNemours & Co. Inc., "Epoxy Bonding Adhesives for Microelectronic Applications", E-10682, 8/76

2. Robert W. Thomas, "Test Method 1018.2 - A Progress Report", NBS/RADC Workshop, Moisture Measurement Technology for Hermetic Semiconductor Devices,II, NBS Special Publication 400-72, 4/82 Pages 126-127.

3. R. K. Lowry, "Gaseous Compositions of Hermetic Cavity Ambients", NBS/RADC Workshop, Moisture Measurement Technology for Hermetic Semiconductor Devices,II, NBS Special Publication 400-72, 4/82 pages 64-75.

4. J. Gale and B. Betz, "Epoxy Die Attach Analysis", Private Communications February 1984

5. D.T. Somerville, "The Role of Hybrid Construction Techniques on Sealed Moisture Levels",15th Annual Proceedings Reliability Physics, 1977, pages 107-111.

6. M.L.White, K.M.Striny and R.E.Sammons, "Attaining Low Moisture in Hermetic Packages", 20th Annual Proceedings Reliability Physics, 1982, pages 253-259.

7. A Czanderna, R. Vasofsky and K. Czanderna, "Mass Changes of Adhesives During Curing", Proc. 1977 International Microelectronic Symposium, October 1977, pages 197-208.

ACKNOWLEDGMENTS

The authors gratefully thank G. L. Schnable for his interest and critical reading of this report. P. Jane Gale and B. L. Bentz of RCA, Princeton Laboratory for the analytical analysis; R. St. Amand and R. Erdman, for internal moisture measurements; and J. Nielsen, L. Nemeth, J. Morgan and D. Glovich for their technical support and assistance. We are also grateful to R. Zeien, J. Patel, A. Shaw, C. Blew and P. Dugan, of the Solid State Technology Center for their suggestions, discussions and interest in factors affecting internal moisture.

We also wish to acknowledge the financial support provided by the United States Air Force (AFAC) Aeronautical Division, Wright Patterson AFB, Ohio, Contract F33615-77-5158 for funding part of this engineering effort on heremetic leadless chip carrier packaging methods.

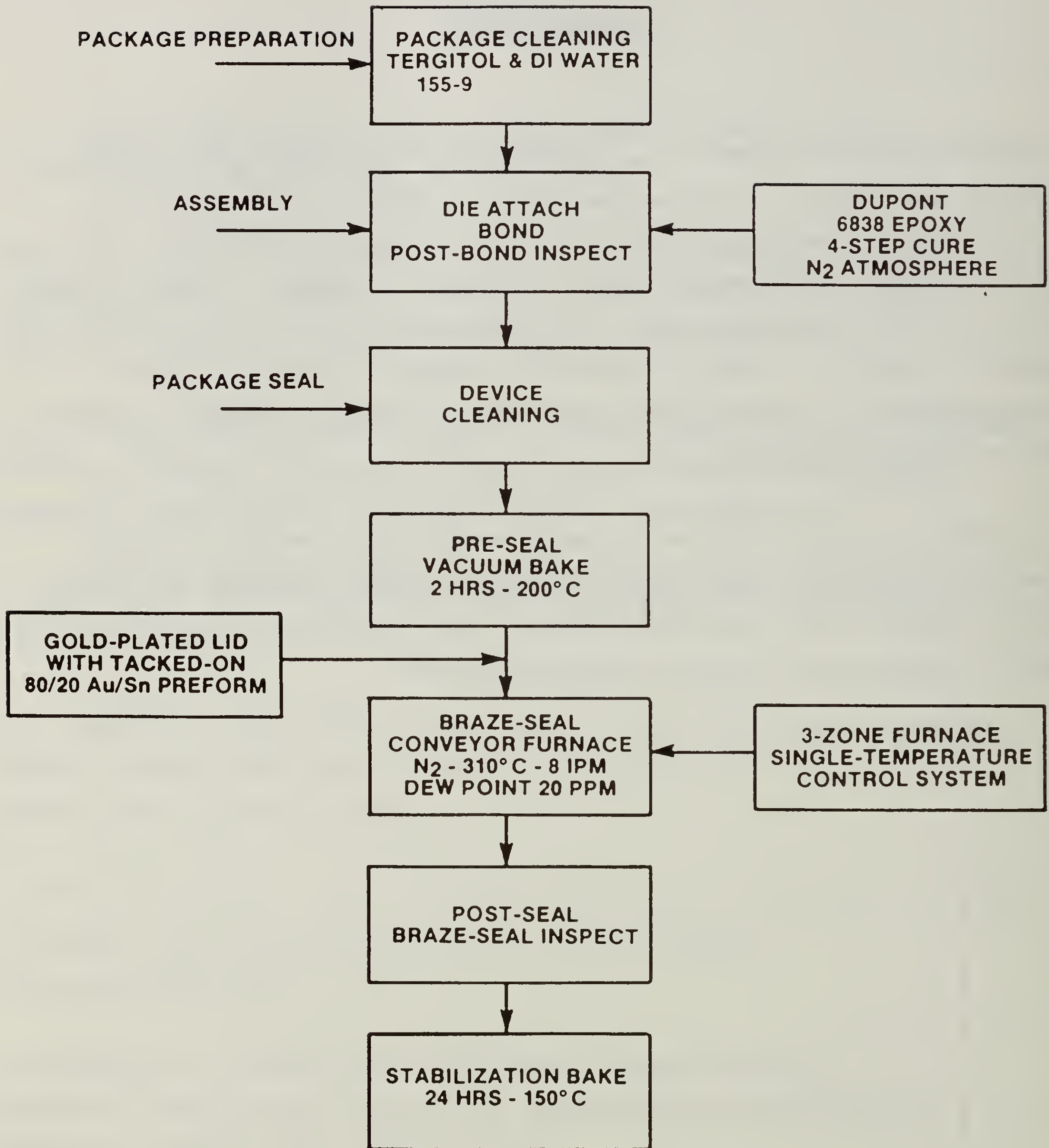

Fig. 1—Flow chart for braze-seal process with pre-seal vacuum bake.

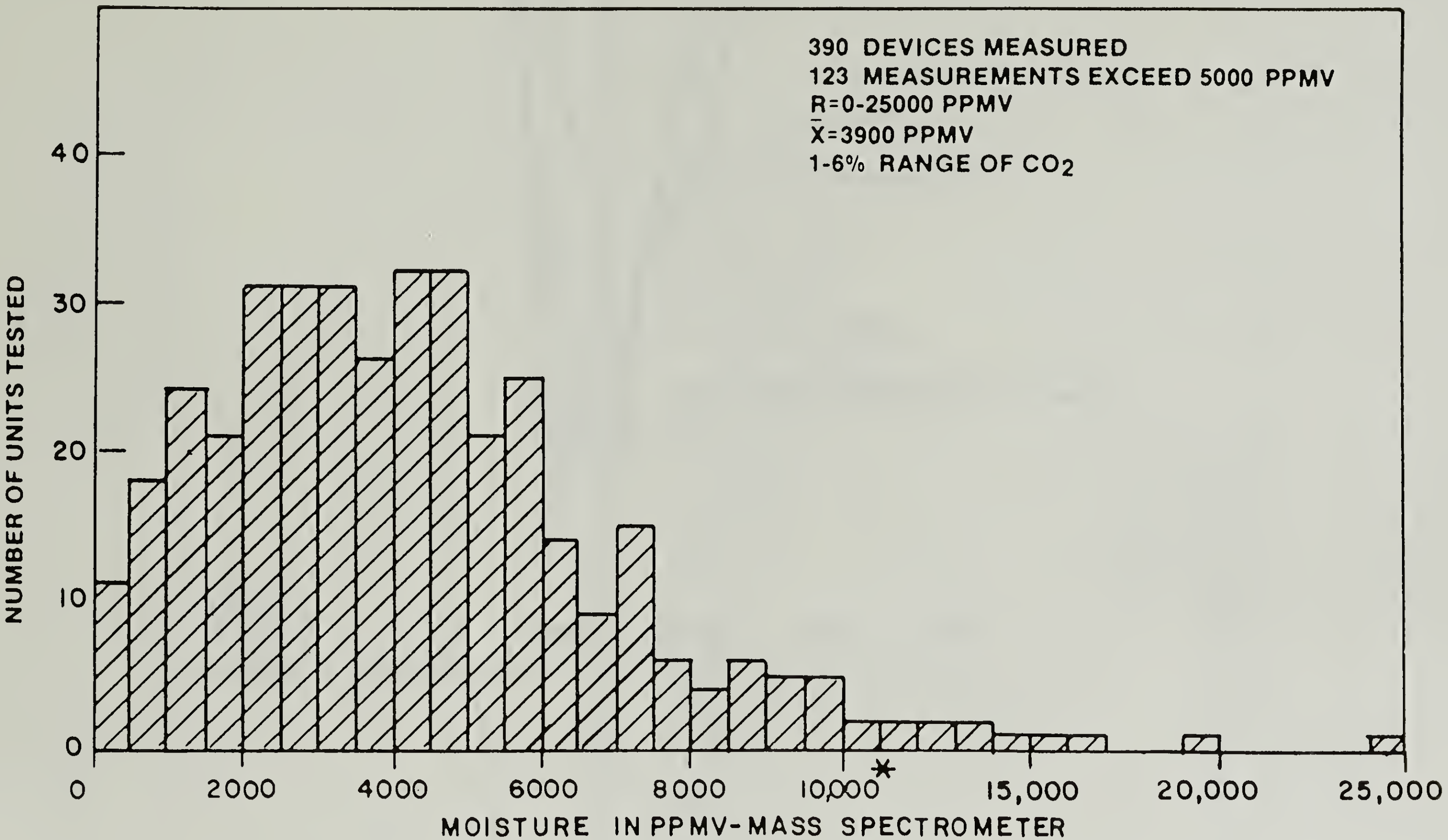

*SCALE CHANGES TO 1000 PPMV PER DIVISION

Fig. 2—Moisture-level distribution in early samples of devices made using braze-seal process.

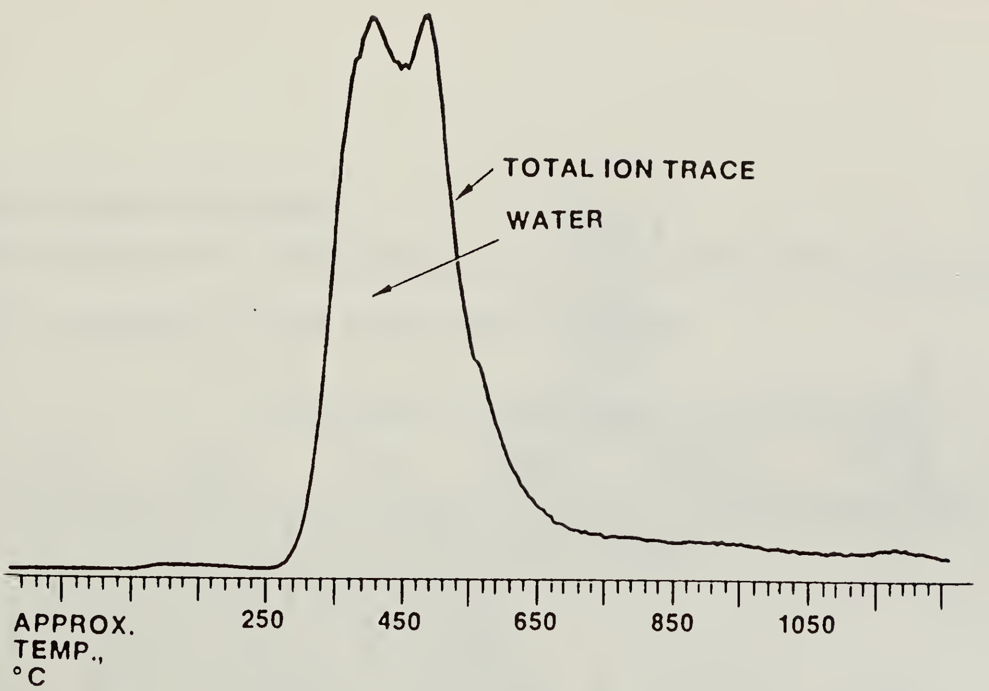

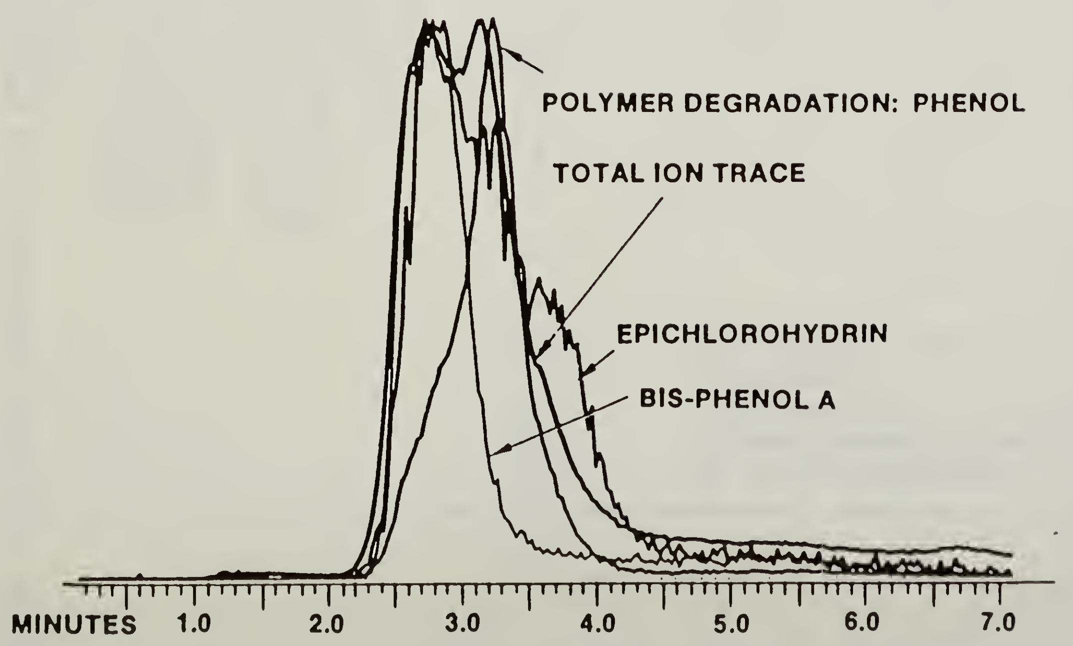

Fig. 3—Mass spectrometry analysis of silver epoxy versus temperature.

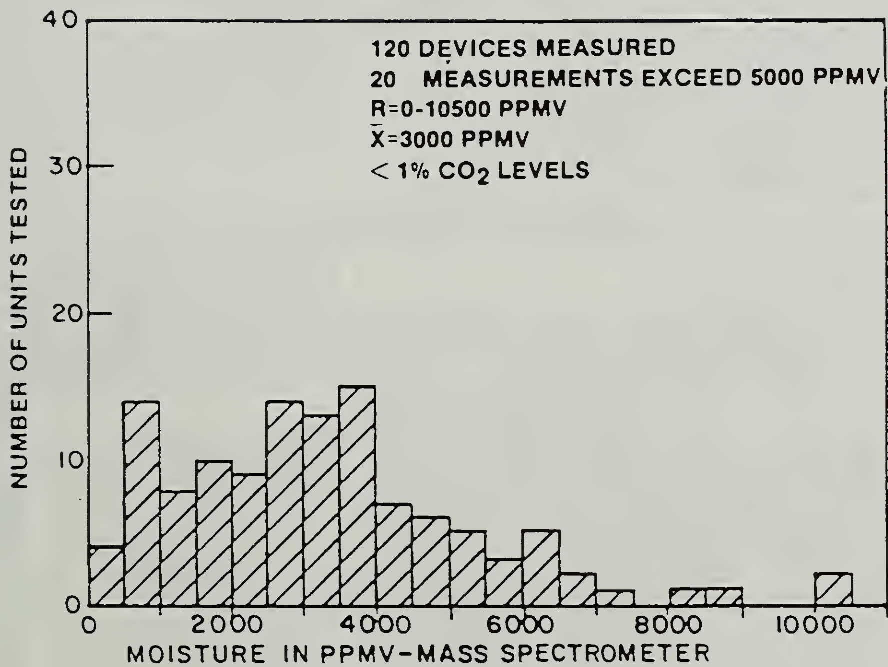

Fig. 4—Moisture-level distribution in sample of devices made using braze-seal process with pre-seal furnace bake.

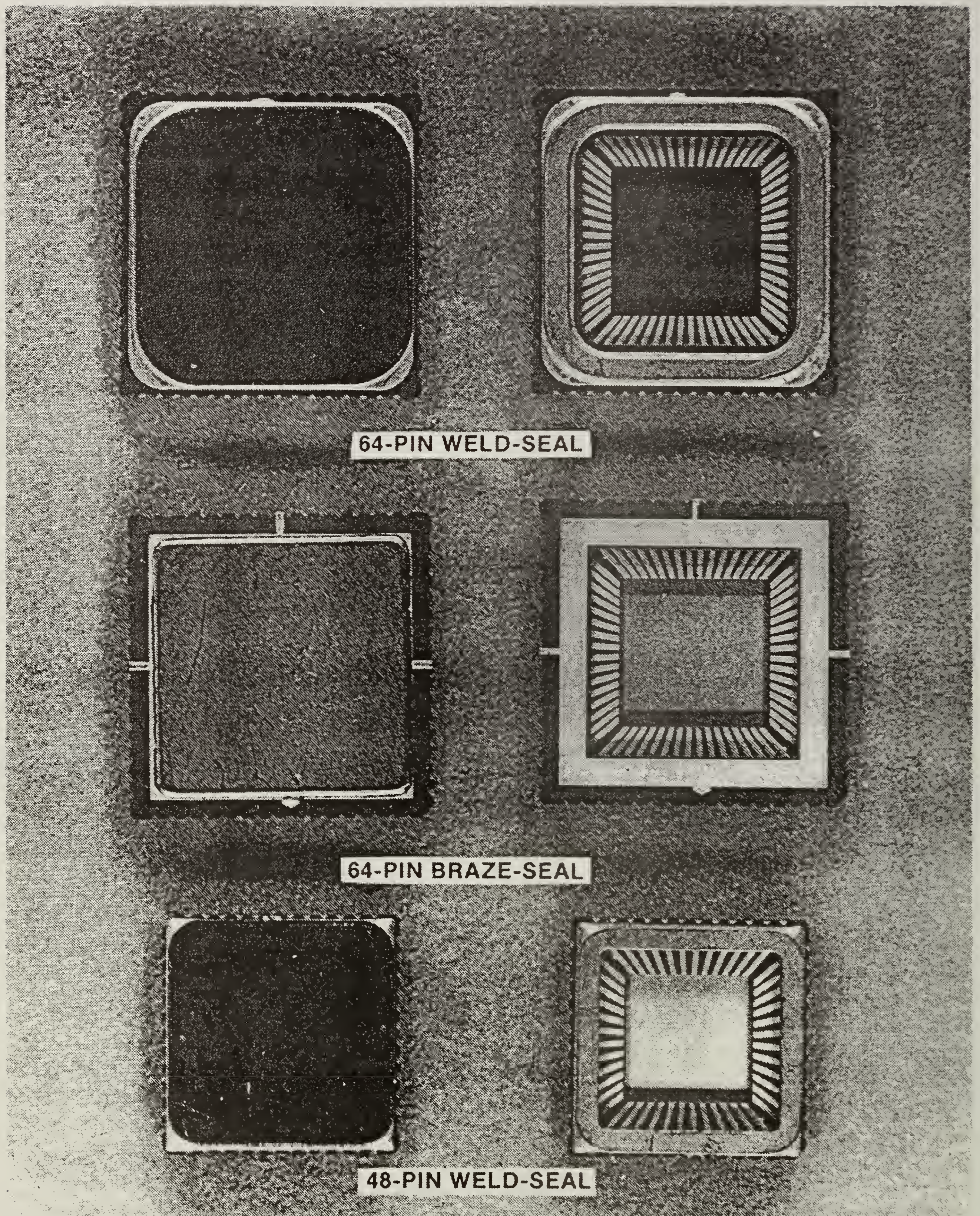

Fig. 5—Weld-seal and braze seal packages with and without lid attached. The 64-pin packages measure 0.720 inch square and the 48-pin package 0.560 inch square.

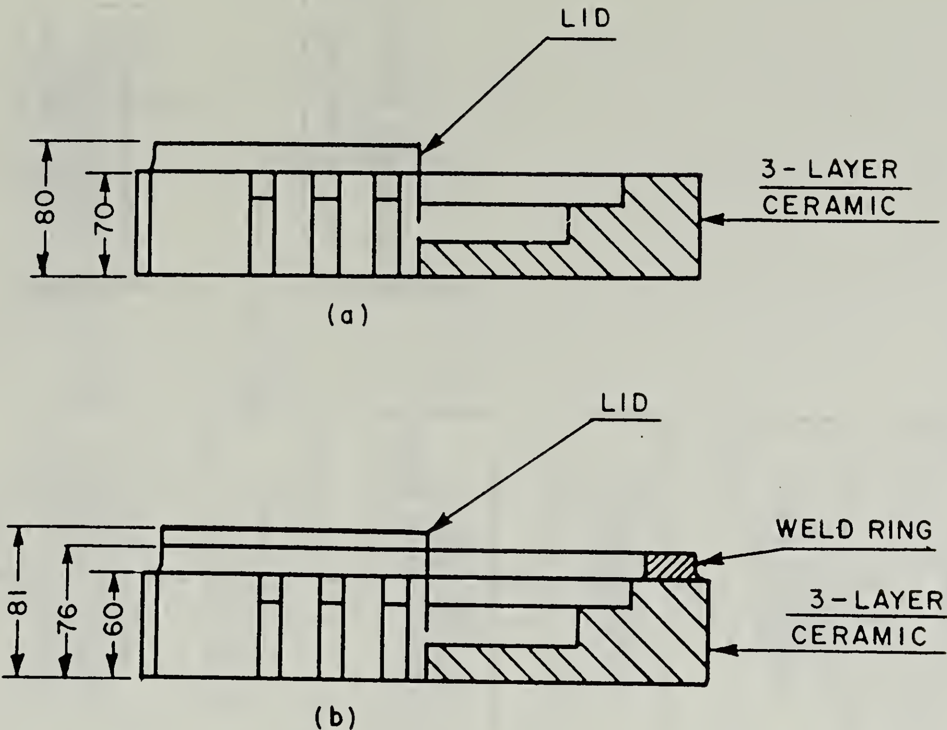

NOTE:
DIMENSIONS SHOWN ARE DESIGN CENTER VALUES

Fig. 6—Schematic of sections through braze-seal and weld-seal packages.

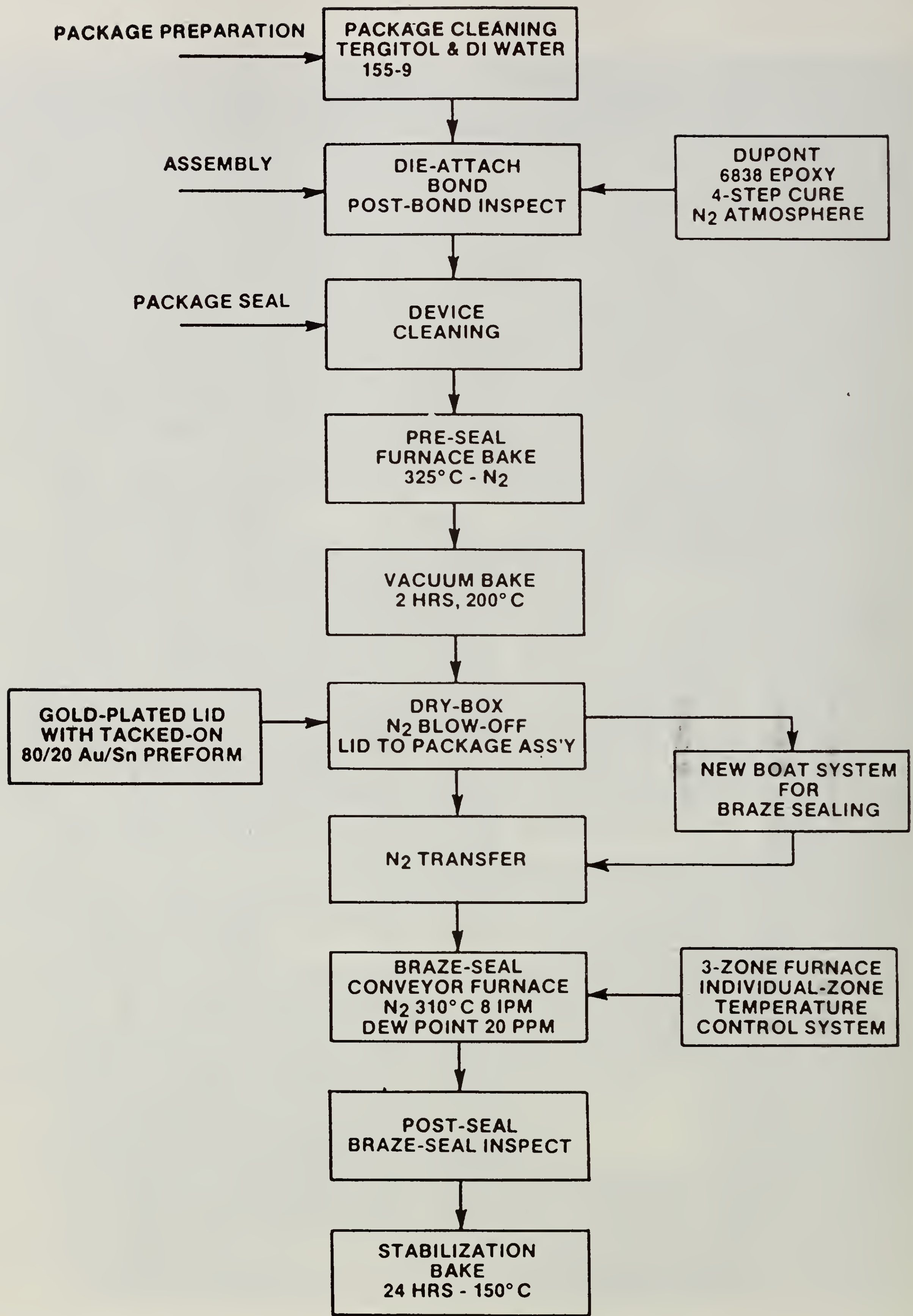

Fig. 7—Flow chart for braze-seal process with pre-seal furnace bake.

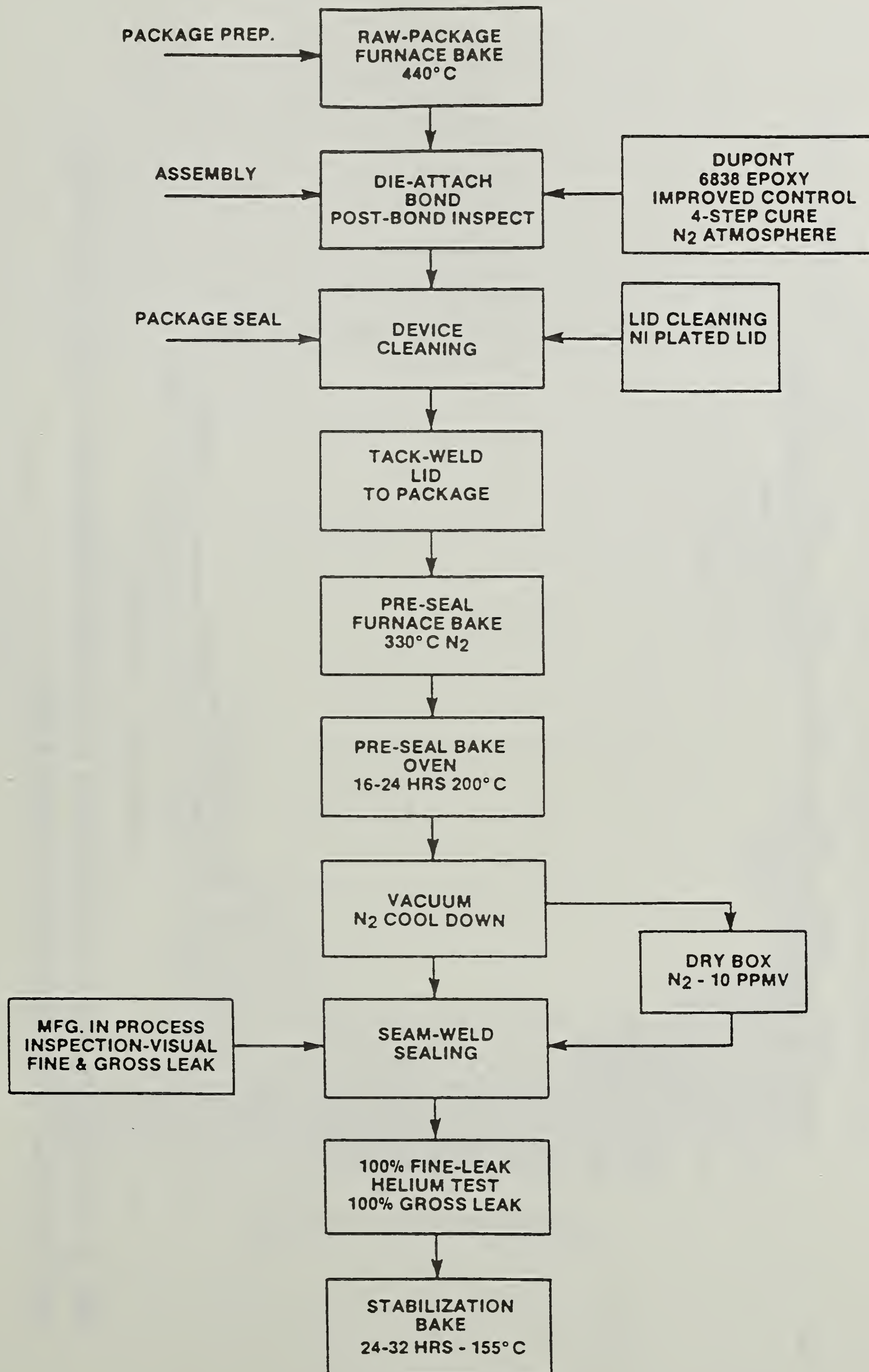

Fig. 8—Flow chart for weld-seal process with pre-seal furnace bake.

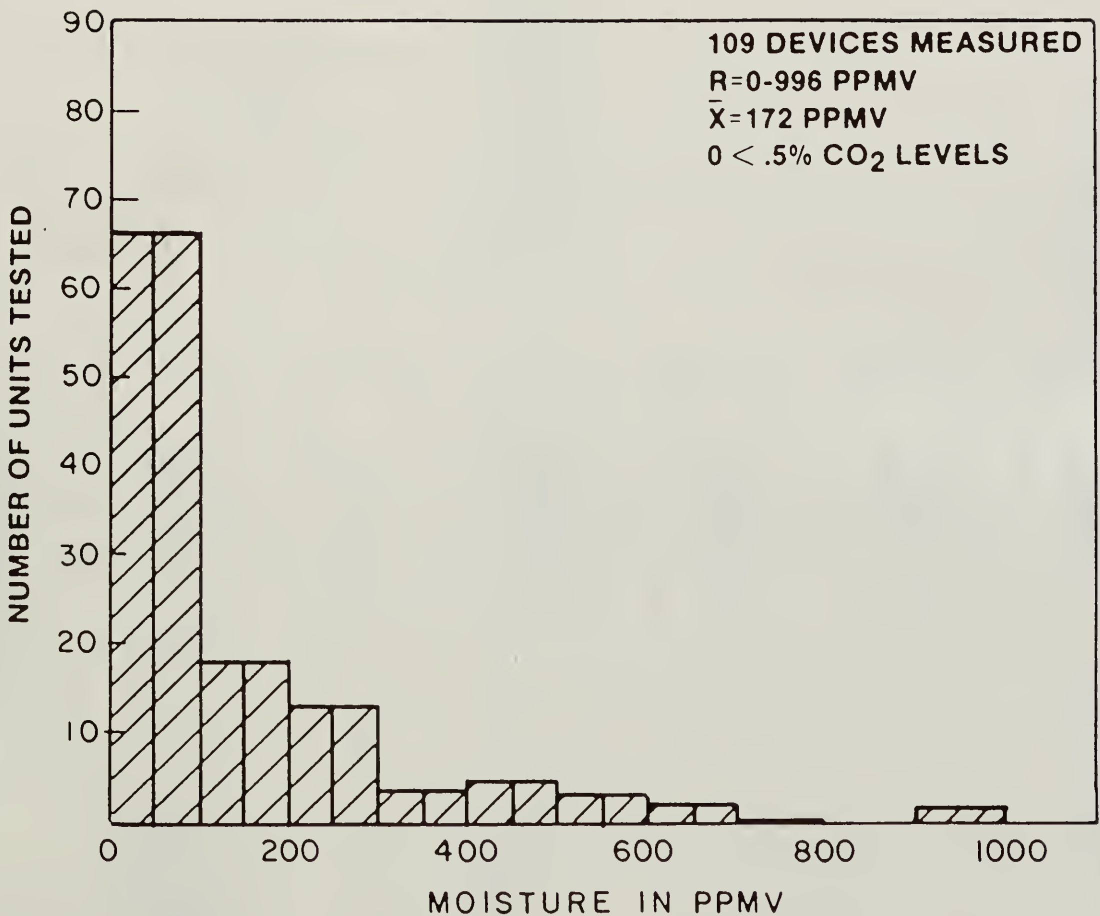

Fig. 9—Moisture-level distribution in sample of devices made using weld-seal process with pre-seal furnace bake.

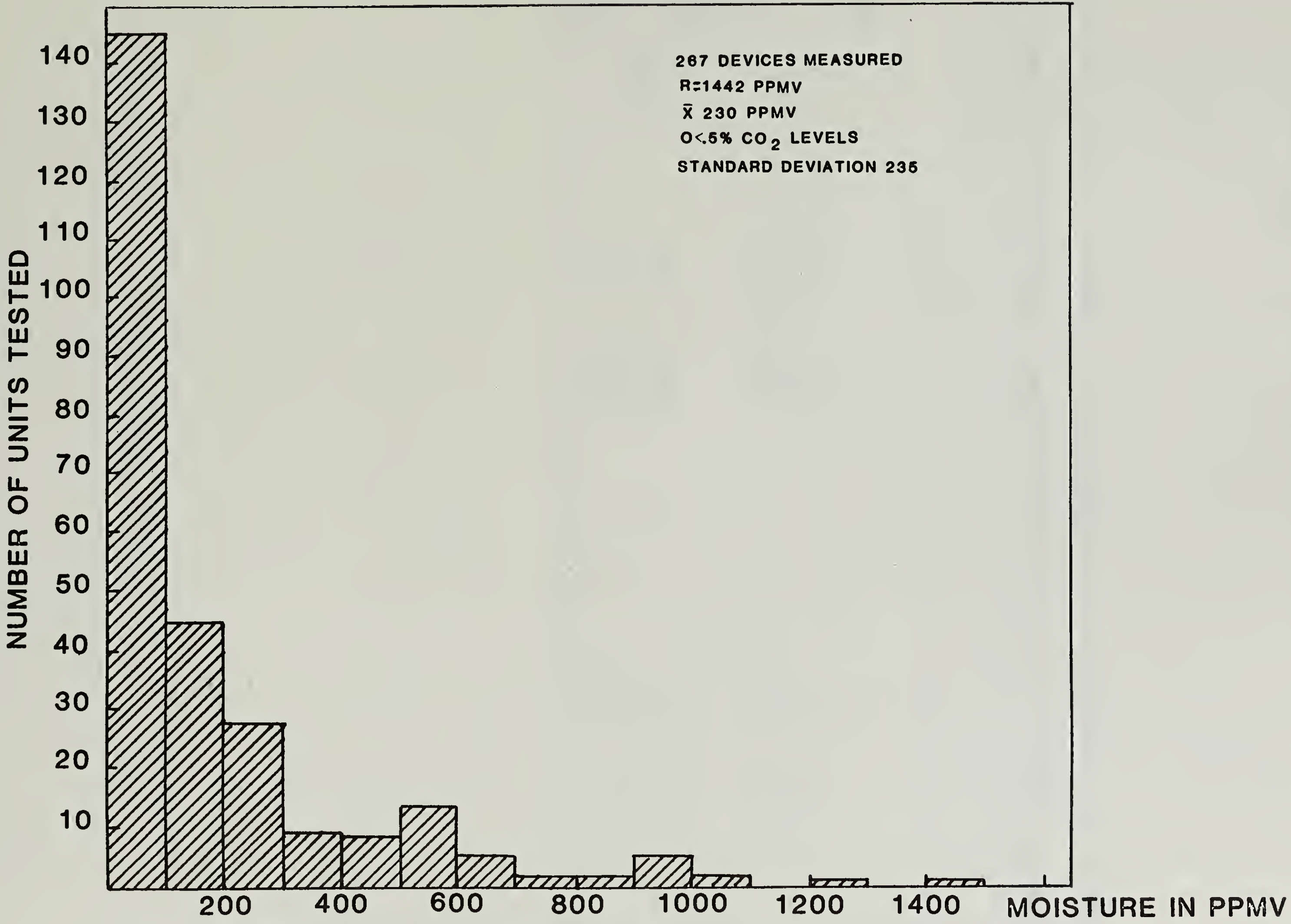

Fig. 9A Moisture-level distribution in sample of devices made using weld-seal process with pre-seal furnace bake

Additional Moisture Information

Figure 9A represents an updating of Figure 9 with 158 additional samples tested. All 267 samples were measured by the same Lab.

Table 1—IC Package Ambient Analysis (MIL STD 883, Method 1018, Proc. 1): Empty Packages Versus Packages Containing Silver-Epoxy Attached Devices

	Empty Packages	Packages with Standard Devices
64-Pin Leadless		
Moisture – ppmv	300 – 1100	100 – 1700
Hydrogen – ppmv	2000 – 4500	300 – 800
CO_2 – ppmv	30 – 200	4000 – 7000
24-Pin Leadless		
Moisture – ppmv	400 – 2700	200 – 2000
Hydrogen – ppmv	100 – 3000	300 – 900
CO_2 – ppmv	200 – 300	3000 – 14,000

Table 2—IC Package Ambient Analysis (MIL STD 883, Method 1018, Proc. 1): Control IC Package Versus Package with Si/Au/Sn Preform Insert

	Control	Si/Au/Sn Preforms
Moisture – ppmv	13,000 – 16,000	125 – 135
Hydrogen – ppmv	1,700 – 1,900	5,000 – 8,000
CO_2 – ppmv	18,000 – 22,000	19,000 – 25,000

Table 3—Moisture Level Tests for 64-Pin Packages: Weld-Seal Control Group, Braze-Seal Control Group, and Weld-Seal Group Subjected to Ten-Cycle Heat Stress Test*

Weld-Seal Control Group					
Part Identification	H1	H2	H3	H4	H5
Moisture – ppmv	300	263	129	<100	171
Hydrogen – ppmv	ND†	ND	ND	ND	ND
CO_2 – ppmv	1652	1609	1947	1972	1594
Braze-Seal Control Group					
Part Identification	J1	J2	J3	J4	J5
Moisture – ppmv	2024	1738	1862	2163	1887
Hydrogen – ppmv	1.17	0.209	0.532	0.426	0.565
CO_2 – ppmv	3418	5784	8325	6755	6689
Weld-Seal After Ten-Cycle Heat Stress Test					
Part Identification	E1	E2	E3	E4	E5
Moisture – ppmv	<100	133	203	385	356
Hydrogen – ppmv	ND	ND	ND	ND	ND
CO_2 – ppmv	2332	2512	3353	3546	4572

* Data reported by Oneida Research Services, Inc. IC package Ambient analysis (per MIL-STD 883, Method 1018, Procedure 1).

† ND = none detected.

Table 4—Moisture Analysis of Post-Seal Temperature Stressing 64-Pin Leadless Seam-Weld Seal

	Moisture Level (ppmv)
120°C – 16 Hours	70 – 80
230°C – 3 Hours	800 – 1,600
313°C – Furnace Bake – 3 Min.	5,000 – 9,000

3.4 POLYMERIC MATERIALS FOR MOISTURE PROTECTION OF MEDICAL IMPLANTS

Philip R. Troyk

Pritzker Institute of Medical Engineering
Illinois Institute of Technology
IIT Center, Chicago, Illinois, 60616

ABSTRACT

Within the past few years a number of devices known as "Smart Sensors" have been developed. These thin-film devices integrate a sensing element and processing electronics on the same die. Typically these sensors are not suitable for presently used methods of hermetic packaging such as welded cans due to their sub-miniature size, and need for exposure of the die to the sensed environment. Organic coatings have been considered as alternative packaging for these devices. The requirements for such coating materials depend upon the environment in which the sensor must operate, as well the method of lead attach. Techniques for interface from a flexible multi-conductor lead to a die protected by a polymeric coating have not been well researched. Sensors such as these will play an important role in the next generation of implanted medical electronic devices and technology for their non-hermetic protection in a saline submersed environment must be developed. We have examined addition-cure polysiloxanes in accelerated temperature-humidity tests and found them to be promising materials for this application.

INTRODUCTION

Various micro-sensors and stimulation arrays have been developed [1,2,3,4,5] for use in implanted medical electronic systems. Most of these devices take advantage of solid-state technology. In particular, photolithography and integrated circuit technology have been exploited in the design and fabrication of a number of subminiature structures specifically designed for use in neuroprostheses. Most of these devices are characterized by thin film technology and by a variety of metals and substrates not commonly used in the semi-conductor industry. The electrode arrays developed by Wise et.al. [2] require that part of the device actually protrude from the electronics/bond pad area since the electrode elements are distributed along a spear-like shank (fig. 1). Although considerable effort has been invested in the fabrication of such devices, less effort has gone into the definition of micro-packaging technologies which would permit their implanted use. To date, there exists no established packaging technology for use with implanted micro-prosthetic devices. The lack of package definition includes electrode array or sensor coating, micro-cable design and interconnection, interface of the cable with, and encapsulation of the main package. In related applications, the use of similar "Smart Sensors" has been suggested for use in robotic, automobile, military, and space assemblies. All of these devices are characterized by sub-miniature size and the need for all or part of the die to be exposed to the external environment.

Presently, the most widely used and generally accepted method of protection from body fluids for implanted electronic devices (and for electronic components in general) is the placement of an impermeable envelope around the device. The impermeable envelope usually takes the form of a welded hermetic can and this approach has been quite successful in pacemakers because it provides complete enclosure of the implant by the enveloping material. In spite of these advantages, the welded can is practical only in those devices which can afford a bulky case. Electrical connections through the wall of the can are usually provided by glass-on-metal feed-throughs. The implant's entering or exiting cables or wires are connected to the feed-throughs and the exterior of the metal can is sealed with an encapsulant or coating such as an epoxy resin or silicone polymer. As the size of the implant is reduced, and the number of exiting conductors increased, the number of feed-throughs become a determining factor in the size of the final package. For example, the feed-through and associated encapsulation for a pacemaker can account for as much as one-third the total package volume. Unlike a pacemaker, subminiature structures, such as the thin-film devices described above, depend upon the integration of electronics and transducer, and their primary performance advantages such as low noise and unique function are directly related to their size; the use of metal cans and similar conventional integrated circuit packaging technologies is precluded.

Encapsulants are an alternative to the welded can. A properly chosen encapsulation system can provide adequate corrosion protection for many types of electronic assemblies and a number of organic barrier coatings and encapsulants have been used to protect electronic systems from deleterious effects of water vapor including products based upon epoxy, imide, and silicone polymers. The latter, especially those polymerized by condensation mechanisms have gained wide acceptance for non-hermetic chips [6]. However, in implants the failure incidence of encapsulants (especially silicone polymers) for electronic devices is much greater than in nonmedical devices such as plastic-pak integrated circuits, even when the latter are subjected to accelerated stress tests. It is not clear whether this poor success rate is due to improper application and processing of the encapsulants or to material inadequacies. Silicone polymers are often misused in the sense that they are often inappropriately regarded as a vapor barrier. However for any system, the high failure rate, undoubtedly, is a result of the severe exposure conditions that exist in a physiological environment. Not only is the implant exposed to constant submersion in an aqueous system, but the electrolytic environment and ionic mobility present a milieu conducive to the electrical leakage currents which result in corrosion. One advantage of the implanted environment over other applications is the constant 37°C temperature.

Figure 2 illustrates the basic problem. The sensor device of figure 1 is shown using hermetic and non-hermetic packaging techniques. The arrows indicate the obvious locations of leakage of the hermetic package: at the flexible lead-out and at the exit of the sensor portion of the device. Using a non-hermetic approach, the die-coat might be made of the same material as the lead-out, eliminating one interface. The remaining exit can be protected by using a coating which can provide inactivation of the normally hydrophylic surface sites by chemical reaction with or maintained adhesion to the protected portion of the die.

Silicones are presently being investigated at our laboratory as candidate materials for integrated sensors. Our ongoing work is directed at the

identification of critical material parameters for the selection of existing, as well as the design of new materials. Based upon the theory that moisture protection by encapsulants is directly related to the adhesive bond between the encapsulant and the underlying surface, adhesion testing has emerged as the primary method of encapsulant qualification for implant use. Pacemaker manufacturers have performed lap-shear and butt-tensile testing of selected substrate/encapsulant combinations after high humidity exposure and these tests relate the bond strengths to the corrosion protective ability of the encapsulant [7]. Donaldson [8] has also investigated the effects parameters such as electric field strength [9], and tensile forces within actual implants. Data from tests upon silicones in our laboratory indicate that bond strength testing is necessary but insufficient to qualify an encapsulant for corrosion control of electronic devices [10]. Corrosion is an electrochemical process whose prevention depends upon the ability of the encapsulant to prevent the flow of electrical leakage currents. Electrical leakage current tests combined with bond strength tests provide not only a measure of the polymer's ability to remain in contact with the protected surface, but also act as an insulator to electrical leakage currents which inevitably will result in corrosion.

Previous applications of silicones for electronic encapsulation have, for the most part, been restricted to condensation-cure silicones. In this laboratory our preference has been for the addition-cure silicone materials. They can be cured very rapidly, in some cases a matter of minutes, and liberate no by-products making them useful for closed-container molding. In contrast, the condensation-cure products liberate a cure by-product, usually acetic acid or alcohol and cannot be cast into thick sections. In addition, acetic acid-evolving products have been implicated in the corrosion of numerous military encapsulated electronic assemblies.

METHODS

We evaluated 6 different silicone elastomers in conjunction with 3 surface primers in accelerated temperature-humidity tests. The materials and their designations are as follows:

Surface Primers

Designation	Name	Manufacturer	Formulation
Type A	Primecoat 1200	Dow Corning	Silane-Silicate Blend
Type B	Chemlok 607	Lord Chemical	Blended Silanes
Type C	SS 4155	General Electric	Ethylorthosilicate

Silicone Elastomers

Designation	Name	Manufacturer	Cured Hardness Durometer (Shore A)
Type 1	RTV-615	General Electric	45
Type 2	Sylgard 184	Dow Corning	35
Type 3	MDX-4-4210*	Dow Corning	25
Type 4	96-083	Dow Corning	63
Type 5	Sylgard 567	Dow Corning	38
Type 6	RTV-3140	Dow Corning	22

*MDX-4-4210 was blended with 10% Sylgard 527, by weight, to decrease viscosity for casting purposes.

The first 5 silicone elastomers are addition-cure products. The 6th material is a condensation-cure product which has been previously used for medical implant protection [11]. As verified by lap shear tests, (described below), the first 3 elastomers provide minimal adhesion in the absence of a surface primer. The last 3 are self-priming materials. To permit visual examination, we tried to select clear materials. All of the elastomers are clear except for types 5 and 6. Types 1, 2, and 3 were selected for test with each of the primers, types A, B, and C. In addition, type 4 elastomer was used as a primer for types 1, 2, and 3. All elastomers types 1-6 were also tested without primers.

Testing was performed by encapsulation of 4 PWB, G-10, epoxy-glass interdigitated test pattern substrates per test group. The patterns selected were taken from the IPC B-25 standard test board, patterns A and B. These patterns use interdigitated line widths and spacings of 0.006" and 0.012" respectively. Two single-sided A patterns (0.006" lines and spacings) and two single-sided B patterns (0.012" lines and spacings) were prepared for each elastomer-primer combination tested. Following encapsulation, each of the patterns was continuously submersed in 85° C water and placed under a continual voltage stress of 20VDC. Electrical leakage current (under 9VDC bias) was measured for each of the test substrates on a daily basis.

Preparation of each test substrate was performed as follows: A 10" long, 0.005" diameter Kynar (polyvinylidene fluoride) insulated wire was soldered to each electrical half of the substrate. The substrate was then completely grit-blasted (40 PSI) using 240 mesh (50um) aluminum oxide grit. Following grit-blasting, the substrate was cleaned in a series of solvents as follows: Methylene Chloride-1 min. wash, Isopropyl Alcohol rinse, Acetone-1 min. wash, Isopropyl Alcohol rinse, Freon TMS-2 min. ultrasonic clean in a Branson B-220 ultrasonic cleaner, Freon TF running rinse. During the cleaning procedure the substrate was handled, with gloves, only by the ends of the connecting wires. After cleaning, a vacuum-bakeout was performed for 12hrs at 120°C. Upon removal from the vacuum oven, designated substrates were primed with the appropriate primer according to the manufacturer's instructions. Each of the manufacturers was contacted directly in order to verify the procedure as outlined in the data sheet. A substrate ready for encapsulation was placed in a half-open mold which supported the substrate horizontally by its wires. The appropriate encapsulating elastomer was mixed and de-aired and poured into the mold under vacuum casting. This procedure produced encapsulated substrates with 0.100"$\pm$0.015" encapsulant thickness over and under the substrate. The diameter of the mold was such that a thickness of at least 0.3" of encapsulant covered the substrate's edge. As a result of the vacuum casting no bubbles were visible in the encapsulated substrates. Curing of the addition-cure elastomers was by forced-air convection at a prescribed temperature of 120°-165°C depending upon the particular elastomer cured. Curing of the type 6 material was done in a humidity chamber of >90%rh for 72hrs. The specific combinations of primers and elastomers tested are listed in table 1. Type 4 elastomer was used as a primer due its previously demonstrated high bond strength in experiments in our laboratory. It was applied in a very thin (<0.005") coat over the substrate and cured before elastomer casting.

A Keithley 610A electrometer with a shielded box and a 9VDC battery comprised the leakage current measurement apparatus. Resolution of the system was at least 0.1pA, however measurements less than 0.5pA were not recorded. Due to

the low levels of measured leakage current, a shielded box was essential to the measurement system. The volume resistivity of most silicones shows a strong temperature dependence. Therefore all leakage current measurements were made at room temperature. The substrates were removed from the water bath for a period of 1hr prior to measurement. Visual examination was done on a periodic basis, documenting visual evidence of discoloration, debonding, or corrosion. A dry lap shear bond test, as described in ASTM-D905 (modified), to G-10 for each of the tested materials was performed on an Instron Universal Testing Instrument. Double lap shear samples were prepared in the same manner as the test substrates.

RESULTS

The measured values of leakage current for each of the 72 test substrates over the initial 2 month test period are listed in table 1. In addition, visual test results are reported at days 30, 45 and 60. For each group of 4 samples, samples 1 and 2 are the A pattern (0.006" spacing), and samples 3 and 4 are the B pattern (0.012" spacing). The initial baseline leakage currents for each of the samples was in the low pA region, and for many of the samples, the measurement error below 0.5pA was probably greater than the actual leakage current. The Kynar insulated wire for connection to the substrates was a poor choice. Submicroscopic defects in the insulation resulted in discoloration and corrosion in the wires of a number of the samples. Some of the samples failed due to wire breakage. However, subsequent testing on specially prepared samples indicated that the measured values of leakage current were not affected by the wire discoloration; these samples continued to give consistent readings up to the day of wire breakage.

All samples primed with type B primer showed visible corrosion at a very early date. Within one week of water submersion, all of these samples showed some signs of deterioration. In each case, the side of the pattern maintained at positive potential was the first to discolor and then corrode. In contrast none of the samples primed with type 4 material showed visible deterioration at day 60. With the exception of the type B samples, all of the other samples failed to show any noticeable deterioration until one month into the test. At this time, most of the types A, B, and C primed samples showed discoloration and debonding. Correspondingly their leakage currents, at day 30, were an average of 35 times greater than those samples primed and encapsulated with the self-priming elastomer types 4, 5, and 6.

The samples on which no primer was used, and the encapsulating material was nonpriming are perhaps the most interesting. Their leakage currents were consistently lower than the types A, B, and C primed samples in spite of the fact that adhesion as tested in lap-shear tests was considerably less than the primed samples. Results from the lap shear bond tests are presented in table 2. Note that when used without surface primers, elastomer types 1, 2, and 3 demonstrated the lowest relative bond strengths when compared to the primed and self-priming samples. However, the leakage currents from the unprimed samples were an average of 50 times lower (day 45) than those primed with primer types A, B, and C, and their overall visual appearance was superior to that of the primed samples. The best performance was seen in types 4, 5, and 6 samples. None of these samples showed any signs of significant deterioration-visual or electrical, at day 60. Type 6 material consistently showed overall superior performance.

PRIMER	ENCAPSULANT	SAMPLE#	ELECTRICAL LEAKAGE IN AMPERES FOR ELAPSED TIME					
			0	6 hrs	day 15	day 30	day 45	day 60
TYPE A	TYPE 1	1	<0.5p	640n	700n	200n d	42n d,db	41n d,db
		2	3.0p	140n	360n	74n d,db	42n d,db	41n d,db
		3	3.0p	150n	120n	66n d,db	12n d,db	9.8n d,db
		4	2.0p	74n	100n	82n	9.4n	9.4n
	TYPE 2	1	<0.5p	20n	400n	260n d	62n d	39n d,db
		2	<0.5p	20n	540n	400n d	83n d	59n d
		3	<0.5p	5.8n	160n	86n c,db	24n c,db	18n c,db
		4	1.0p	20n	220n	82n	22n	22n db
	TYPE 3	1	1.0p	320n	3.2u	620n d	86n d,db	90n c,db
		2	64p	1.8u	2.0n	440n d	26n d	40n d
		3	3.0p	32n	620n	300n	86n	80n
		4	1.5p	120n	320n	510n	43n db	36n db
TYPE B	TYPE 1	1	2.9p	160n	8.8n	74n c,db	3.0n c,db	1.6n c,db
		2	1.0p	96n	32n	68n c,db	9.4n c,db	1.7n c,db
(note 1)		3	1.5p	6.4n	2.8n	2.2n c,db	960p c,db	290p c,db
		4	2.0p	700n	failed @ day 10, current >100uA			
	TYPE 2	1	<0.5p	7.4n	16n	9.4n c,db	1.8n c,db	620p c,db
		2	1.0p	7.2n	8.0n	8.0n c,db	2.8n c,db	1.8n c,db
		3	<0.5p	2.6n	2.0n	3.8n c,db	440p c,db	420p c,db
		4	2.5p	540p	3.0n	3.4n c,db	16n c,db	18n c,db
	TYPE 3	1	<0.5p	3.5n	5.4n	2.8n c,db	2.5n c,db	2.5n c,db
		2	<0.5p	140n	14n	4.0n c,db	540p c,db	420p c,db
		3	1.5p	4.0n	2.0n	420p c,db	150p c,db	180p c,db
		4	<0.5p	5.4n	2.2n	3.0n c,db	280p c,db	210p c,db
TYPE C	TYPE 1	1	7.0p	38n	140n	wire failure		
		2	5.0p	32n	220n	40n d	34n d	30n d
		3	<0.5p	14n	68n	24n d	8.8n d	8.6n d
		4	2.0p	7.8n	48n	28n d	7.6n d	6.2n d
	TYPE 2	1	<0.5p	28n	320n	44n	370n	wire failure
		2	<0.5p	540n	2.2u	550n c,db	360n c,db	200n c,db
		3	<0.5p	8.4n	120n	68n db	14n db	14n d,db
		4	2.5p	50n	220n	52n db	26n db	22n db
	TYPE 3	1	65p	1.2u	660n	140n db	18n db	22n db
		2	440p	190n	1.4u	160n d	180n d	160n d
		3	110p	840n	140n	24n	18n	16n
		4	40p	600n	900n	72n	160n c,db	140n c,db
TYPE 4	TYPE 1	1	<0.5p	50p	5.4n	3.4n	720p	520p
		2	<0.5p	60p	8.2n	1.4n	950p	280p
		3	<0.5p	4.0p	16p	50p	wire failure	
		4	1.0p	150p	120p	14n	120p	58p
	TYPE 2	1	<0.5p	80p	12n	6.0n	3.6n	560p
		2	<0.5p	20p	36p	8.8p	54p	60p
		3	<0.5p	220p	10n	440p	620p	2.9n
		4	<0.5p	64p	30p	5.4n	26p	38p
	TYPE 3	1	<0.5p	14p	260p	120p	39p	35p
		2	5.0p	46p	1.2n	1.6n	220p	200p
		3	8.5p	7.0p	32p	30p	22p	32p
		4	<0.5p	14p	30p	68p	18p	26p
NONE	TYPE 1	1	<0.5p	50p	5.6n	100n db	500p db	360p db
		2	<0.5p	220p	32n	5.4n db	2.9n db	2.7n db
		3	<0.5p	3.0p	40p	320p db	28p db	72p db
		4	1.0p	40p	32n	5.0n c,db	2.2n c,db	2.8n c,db
	TYPE 2	1	1.0p	1.2n	32n	400n db	2.1n db	7.2n db
		2	1.5p	1.2n	8.8n	84n db	320p db	600p db
		3	1.2p	4.2p	56p	66p	21p	47p
		4	<0.5p	3.0p	10p	30p	22p	19p
	TYPE 3	1	5.0p	8.0p	5.0n	24n	720p	840p
		2	1.0p	12p	300p	660p	380p	170p
		3	3.5p	14p	60p	40p	30p note 2	1.2u
		4	1.5p	4.5p	22p	60p	56p	50p
	TYPE 4	1	<0.5p	1.4u	7.2n	1.8n	710p note 2	4.0n
		2	<0.5p	56p	84n	12n	12n	wire failure
		3	<0.5p	3.0n	10n	840p	180p	200p
		4	<0.5p	1.8p	22p	25p	20p	23p
	TYPE 5	1	<0.5p	160p	3.0n	500p na	420p na	340p na
		2	<0.5p	52p	320p	500p na	600p na	580p na
		3	<0.5p	56p	2.2n	180p na	35p na	76p na
		4	<0.5p	14p	48p	200p na	45p na	46p na
	TYPE 6	1	<0.5p	22p	50p	40p na	35p na	38p na
		2	<0.5p	60p	120p	70p na	15p na	32p na
		3	<0.5p	6.0p	16p	40p na	18p na	38p na
		4	<0.5p	6.0p	28p	46p na	23p na	28p na

TABLE 1

Electrical leakage current measurements for interdigitated G-10 silicone encapsulated substrates over a 60 day period. Visual examinations made at day 30, 45 and 60 are coded as follows: d=discoloration of the conductors, db=debonding of the encapsulant, c=corrosion, na=not applicable. Note 1: All B-primed substrates showed corrosion at day 10. Note 2: Foil-pattern defect caused local metal bridge.

PRIMER	ENCAPSULANT	LAP SHEAR (PSI)	PRIMER	ENCAPSULANT	LAP SHEAR (PSI)
TYPE A	TYPE 1	451	TYPE C	TYPE 2	339
	TYPE 2	389		TYPE 3	163
	TYPE 3	149			
			NONE	TYPE 1	41
TYPE B	TYPE 1	512		TYPE 2	46
	TYPE 2	276		TYPE 3	80
	TYPE 3	111		TYPE 4	575
				TYPE 5	201
TYPE C	TYPE 1	292		TYPE 6	291

Table 2: Lap shear test results for G-10 substrates and various primer-elastomer combinations. (ASTM-D905 modified)

DISCUSSION

The rapid initial rise of leakage to steady-state values characteristic of most of the test samples was not surprising in light of the relatively high water vapor permeability of the silicones. Within 6hrs of water submersion most of the samples demonstrated currents of about the same order of magnitude as those which persisted throughout the test.

The lack of performance of all of the primed samples and the corresponding superior performance of the unprimed samples using types 1, 2, and 3 elastomers raises serious questions concerning the validity of adhesion testing in the selection of silicones for corrosion control of electronic assemblies. The poor performance of the primers A, B, and C, is perhaps easier to explain than the good performance of the unprimed samples. The manufacturers' original purpose of these primers was for bonding of silicones in non-electrical applications. The manufacturers presently provide no data concerning their electrical properties. One might postulate that these primers contain water-soluble contaminants, and that although they may remain bonded, their bulk and surface resistivities drop by orders of magnitude in the presence of moisture. There would seem to be no other reasonable explanation as to how groups such as type A-type 3 could sustain high levels of leakage current without early significant visible deterioration. Condensation of water at a debonded polymer-substrate interface sufficient to produce leakage currents in the near uA region would have to result in rapid conductor corrosion. Although we have not, as of yet, performed tests to determine the degree of possible contamination for each primer, the results of this study and others seem to support the concept that the primers degrade the performance of the elastomers from a corrosion control, and an electrical insulation standpoint. The use of primers such as type C in military high-voltage assemblies has been associated with drift of high resistance circuits such as high-voltage voltage dividers [12]. The degraded performance of materials such as types 1, 2, and 3 with the use of a primer cannot be more clearly seen that with type B primer. However, in spite of the rapid deterioration of the type B primed samples, they did not have the highest leakage currents. Although low electrical leakage is a necessary requirement for prolonged substrate survival, a weakness of leakage current measurements as a sufficient criteria of encapsulant acceptance is the difficulty in determining the current density across the substrate. Local sites of high current flow can result in local corrosion without causing correspondingly high values of <u>total</u> leakage. Low total current as well as a uniform current density is necessary for acceptance of an encapsulant. Note

that even for those samples which did not demonstrate early visible signs of corrosion, but did show elevated levels of leakage currents, the protecting primer-elastomer combination may not be acceptable for many high-impedance assemblies. An upper level of 60nA was chosen in this study as an acceptable total leakage current level. This represents a 5% error in the current which might flow in a 10Mohm resistor with a voltage differential of 12VDC. None of the primers A, B, or C could meet this limit, whereas the samples with types 4, 5, and 6 materials consistently met or exceeded this limit.

Perhaps the most surprising samples were the unprimed substrates encapsulated with types 1, 2, or 3 elastomers. The low bond strengths as seen in table 2 for these materials did not seem to be significant in their corrosion-protective ability. It may be that low substrate surface tension, with a correspondingly high degree of wetting by the protecting encapsulant is more important than the actual interfacial bond strength. Maintaining this surface wetting is obviously enhanced by strong adhesion, especially in assemblies with complex geometries and high local mechanical stresses. However, in certain assemblies adhesion is often lost due to the presence of sharp corners and close component spacings, characteristic of high-density PWBs. It may be that surface wetting could also be maintained by using a low durometer elastomer (not necessarily self-priming) as a "priming layer" with an overcoat of a more rigid elastomer. It is interesting to note that the materials which performed the best in this study were not only the self-priming ones, but also the ones characterized by low durometer readings. Both types 5 and 6 materials are self-priming, and of relatively low durometer (38 and 22) as compared with type 4 having a durometer of 63. Type 5 and 6 materials performed better than type 4, with type 6 (of lowest durometer) currents lower by approximately an order of magnitude. Type 6, however is a condensation-cure material and cannot be completely cured in closed molds or in thick sections. Most of our implant devices are cast, and addition-cure materials are preferred.

Rigid cleaning protocols are essential to low surface tension. Cleaning of the encapsulated surface prior to encapsulation may be the single most important process step in the use of any encapsulant. Contaminants present on the surface including non-polar organics (oils, grease), polar inorganics (water soluble salts, chlorides, etc), and insoluble particulate matter (dirt, dust), will not only interfere with the bonding of the encapsulant to the surface but are themselves sources of ionics which when put into solution will result in rapid deterioration. The presence of water soluble contaminants upon the encapsulated surface provides the ideal conditions for the initiation of corrosion. This is especially true when using the semi-permeable silicones. As a demonstration of this, we encapsulated a substrate (B pattern) using type 1 elastomer without any cleaning performed. Solder fluxes, finger prints, and other contaminants normally present during assembly were not cleaned off. This sample showed visible corrosion within 12hrs of water submersion. In contrast, the cleaned unprimed type 1 samples in this study survived over 60 days of exposure with comparatively little degradation.

The degree of life acceleration that this test represents is uncertain. Fitting data to a temperature dependent first-order exponential (Arrhenius) failure curve is often inaccurate due to initial model assumptions. Depending upon the estimate of activation energies used, and the criteria used to define failure, an acceleration factor in a range of 17-50 may result [13]. Based upon a frequently sited rule of thumb, that reaction rates double for every 10°C, an acceleration factor of 32 would be used. We have no evidence at this

time that a first-order exponential model is valid, nor that the 85°C accelerated test does not, in itself, induce stresses which would normally not be possible during the service life of the device. This is a criticism which is often sited against accelerated life tests. We do, however, have preliminary data from other humidity studies in our laboratory in which the time to corrosion for the type B primed substrates at 65°C was measured. Based upon these studies an acceleration factor of 25 was calculated for the 85°C test.

CONCLUSIONS

As part of our continuing program of evaluation of appropriate encapsulants for medical implants as well as non-medical electronic high-density assemblies, we shall pursue the question of surface wetting vs. strong adhesion as a criteria for selecting encapsulants suitable for corrosion control. We are investigating the use of silicone gels in place of surface primers in applications where a low-durometer material, with high wetting properties, may provide good humidity protection in the presence of high local mechanical stresses.

Low leakage current for the qualification of an encapsulant as a corrosion resistant coating is a necessary, but not sufficient, condition. The use of adhesion tests as a sole qualification of an encapsulant, used essentially as an insulator, is at minimum incomplete, and sometimes invalid. The bond strengths seen for types A, B, and C primer with their poor corrosion resistant performance demonstrate the inappropriate nature of classical bond strength tests. High bond strength accompanied by low leakage current is probably an indication of a high degree of surface wetting, good cleaning protocols, and low encapsulant contamination. All of these factors seem necessary for good corrosion control using silicone encapsulants.

REFERENCES

[1] K.D. Wise, "Multichannel multiplexed intracortical recording arrays," 9th Quarterly Report, NIH-NINCDS-NO1-NS-1-2384, 1984.

[2] K.D. Wise, J.B. Angell, and A. Starr, "An integrated-circuit approach to extracellular microelectrodes," IEEE Trans. Biomed. Eng., BME-17, pp.238-246, July 1970.

[3] M. Esashi, and T. Matsuo, "Integrated micro multi-ion sensor using field effect of semiconductor," IEEE Trans. Biomed. Eng., BME-25,pp.184-191, March 1978.

[4] S.D. Moss, C.C. Johnson, and J. Janata, "Hydrogen, calcium, and potassium ion-sensitive FET transducers: A preliminary report," IEEE Trans. Biomed. Eng., BME-25, pp.49-54, January 1978.

[5] H.D. Mercer, and R.L. White, "Photolithographic fabrication and physiological performance of microelectrode arrays for neural stimulation," IEEE Trans. Biomed. Eng., BME-25, pp.494-500, November 1978.

[6] D.S. Peck, and C.H. Zierdt, "The reliability of semiconductor devices in the Bell System," Proc. IEEE, 62, 2, pp.185-211, Feb. 1974.

[7] K.E. Cobian, et. al. "Epoxy adhesives for implantable medical devices," Adhesives Age, pp. 17-20, December 1984.

[8] P.E.K Donaldson, "The underwater life of joints between some adherend and adhesive materials in neurological prosthesis-making," Proc. Int. Conf. Biomed. Polymers, pp. 143-150, July 1982.

[9] P.E.K. Donaldson, and E. Sayer, "Silicone rubber adhesives as encapsulants for microelectronic implants," Med. Biol. Eng. Comput., 15, pp.712-715, 1977.
[10] P.R. Troyk, M.J. Watson, and J.J. Poyezdala, "Humidity testing of silicone polymers for the corrosion control of implanted medical electronic prostheses," Proc. ACS, Div. Polymeric Mat. Sci. & Eng., vol.53, pp.457-464, Chicago, Sept. 1985.
[11] P.E.K. Donaldson, and E. Sayer, "A technology for implantable hermetic packages. Part 1: Design and materials," Med. Biol. Eng. Comput., 19, pp.398-402, 1981.
[12] Personal communication with R. Swendsen, Northrop Corp. D.S.D., Rolling Meadows, IL.
[13] P.E.K. Donaldson, and E. Sayer, "A technology for implantable hermetic packages. Part 2: An implementation," Med. Biol. Eng. Comput., 19, pp.403-405, 1981.

CHARACTERIZATION OF IMPLANTED ENVIRONMENT

* AQUEOUS IONIC "SOUP" (Na, Cl, K, Macrophages)
* CONSTANT SUBMERSION
* CONSTANT TEMPERATURE: 37 DEGREES C.
* MINIMAL DIFFERENTIAL MECHANICAL STRESS

MATERIAL REQUIREMENTS FOR IMPLANTED ELECTRONICS

* PROVIDE NON-HERMETIC PROTECTION OF THICK AND THIN FILM DEVICES WITHOUT SIGNIFICANT VOLUME INCREASE.
* ABLE TO WITHSTAND "SALTWATER" ENVIRONMENT CONTINUOUSLY.
* PROCESSING ADAPTABLE TO FLEXIBLE LEAD-OUTS WITH MINIMAL BULK.
* BIOCOMPATIBLE, OR ABLE TO BE COATED.

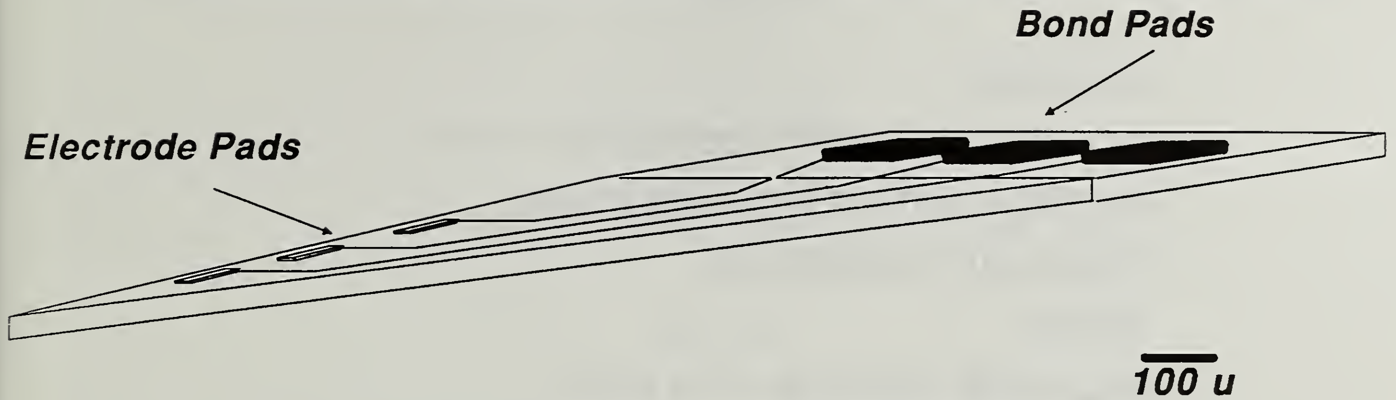

Figure 1. Silicon Probe for neural sensing as designed by Wise et. al. [2]. The bond pad area must be protected, however the electrode pads must be exposed to a saline environment.

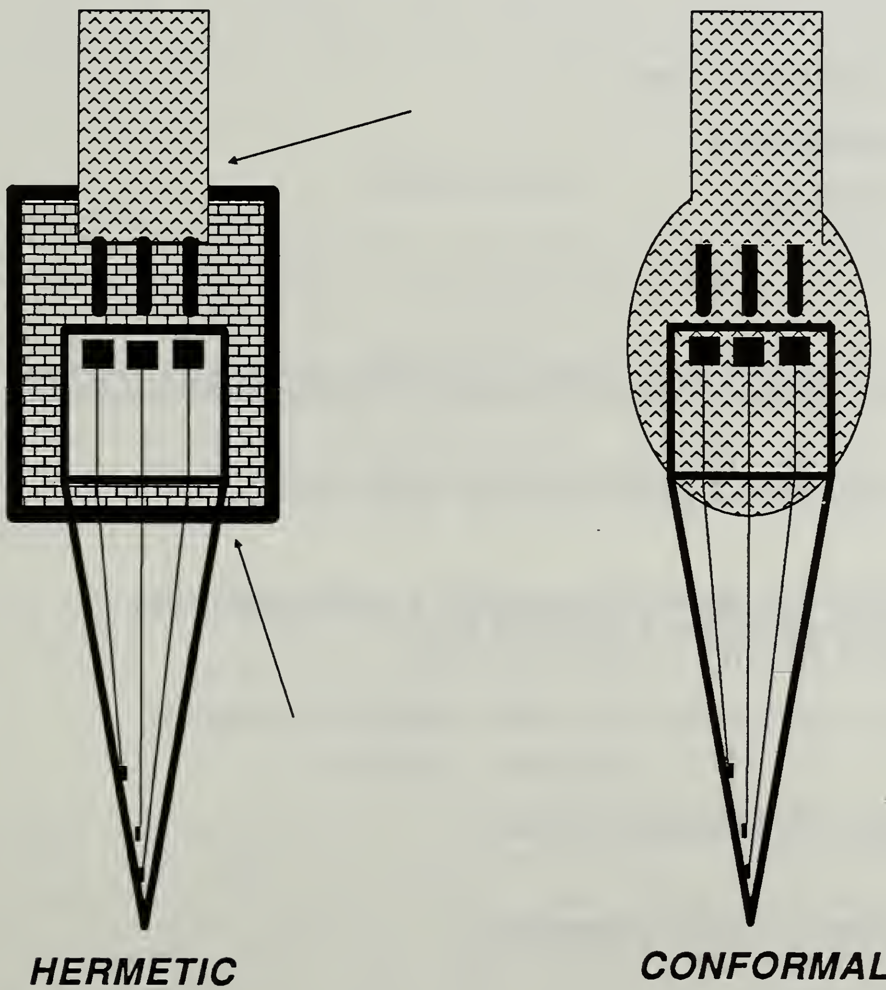

Figure 2. The sensor of figure 1 with hermetic and non-hermetic packaging. The Arrows indicate the probable sites of leakage for the hermetic package.

ELECTRONIC IMPLANT MOISTURE-PROOFING VARIATIONS

VARNISH
ACRYLIC WITH PVC COATING
ACRYLIC WITH EPOXY COATING
PMMA WITH BEESWAX
EPOXY
SILICONE RUBBER WITH WAX
GLASS WITH EPOXY COATING
PARYLENE C (GLOW DISCHARGE PRIMER)
POLYIMIDE
SILICONES
WELDED CAN
BEESWAX
TEFLON

IMPORTANT MATERIAL PARAMETERS FOR SILICONES

* ADHESION TO PROTECTED SURFACE
* LOW TO MODERATE SHORE A DUROMETER PREFERABLY ADJUSTABLE
* SMALL NUMBER OF LOW-ORDER CHAINS
* CLEAR OR TRANSPARENT
* CONTROL OVER PRIMING

4.1 PIN SELECTION CRITERIA FOR A.C. CONDUCTANCE TECHNIQUE

N.K. ANNAMALAI
RADC/ESR, Hanscom AFB, MA 01731

EUGENE BLACKBURNE
RADC/RBRE, Griffiss AFB, NY 13441

S.M.R. ISLAM
Clarkson University, Potsdam, NY 13676

ABSTRACT

An a.c. conductance technique used to determine the moisture in CERDIP packages is described. A circuit model is used to explain the observed experimental behavior. The conductance method measures the conductance between two pin pairs which have long parallel adjacent metallization runs. A description of the criteria for pin pair selection is given. The conductance method can be applied by selecting more than one set of pin pairs and connecting them in series or in parallel. The sensitivity of measurement is improved by using a series connection, and this is seen by employing a figure of merit for each connection.

INTRODUCTION

Moisture in hermetically sealed IC packages and hybrid packages is a known realibility hazard. An a.c. conductance method using a lock-in-amplifier (LIA) is superior to all the other available methods. The advantages of this method over other methods have been described in earlier works [1, 2]. The present conductance technique measures the conductance between any two pins of the chip which do not have any electrical component between them and which have long parallel adjacent metallization runs. An LIA is used to measure the conductance at 100 Hz and at 100 mV. The conductance is monitored as a function of temperature when the chip is taken through a cooling cycle followed by a heating cycle [1, 2].

Pin pair selection is important for the effective implementation of this technique. Further, the sensitivity (to measure low levels of moisture as low as 500 ppmv) can be increased by connecting a number of pin pairs in series.

MEASUREMENT PRINCIPLES

Conductance and capacitance of a device can be measured simultaneously by using an LIA. A voltage from a function generator is fed to the current-sensitive preamplifier and the device under test (DUT) connected in series. The voltage at the output terminals of the preamplifier is proportional to the current through the device. The magnitude and phase angle of the voltage are measured by using an LIA. Comparing this voltage with the reference applied signal, the LIA provides both the magnitude and phase angle. The LIA locks itself on the reference frequency provided by a function generator.

Two meters on the face of the LIA read either the magnitude and phase, or in-phase and quadrature phase voltages in equivalent d.c. form. The in-phase voltage is directly proportional to conductance, and the quadrature voltage is directly proportional to capacitance.

An input protective diode on the chip or a diode placed close to the package can be used for temperature measurement. A constant current is pumped through the diode, and the voltage drop across the diode is then given by a relationship of the form $V_D = AT+B$ where A and B are constants and T is the temperature in K. The calibration method used is descried in the latter part of this section.

Simultaneous measurement of temperature and conductance is not possible due to the common return path for both the signals. Hence time multiplexing of the temperature and conductance is essential for successful implementation of the conductance technique. To time-multiplex, a dummy device and the device to be tested were used to avoid meter transients during on/off cycles. In one time slot, when the temperature of the test device was measured, conductance of the dummy was measured, and at the next time slot measurements of the devices were reversed.

When a rapid cooling of the device is desired, the time-multiplexing procedure is not possible with the data acquisition unit we presently have. A rapid rate of cooling of the die was found to be essential to improve the sensitivity of the measurement. In such situations a thermocouple was attached to the bottom side of the package with thermal cement and used to monitor the temperature of the die. Due to the temperature gradient between the die and the bottom of the package, a calibration run for each type of package was performed. An additional calibration experiment was required to calibrate the diode to measure the temperature. The chamber was kept at a specific temperature, and the die was placed in the chamber and allowed to equilibrate with the chamber for a sufficiently long time. A voltage drop corresponding to the chamber temperature was noted when a constant current was pumped through the protective diode. The chamber temperture was read by a digital thermometer. The temperature of the chamber was varied and the corresponding diode voltage was obtained. From this set of readings, diode constants A and B were obtained. The die temperature was read by measuring the diode voltage V_D =AT+B when the current pumped through the diode was the same as in the calibration experiment. When a package was cooled rapidly, there was a temperature gradient between the die and the package. For each type of package, keeping the experimental conditions the same as that of the conductance method, the temperature at the bottom of the package was obtained by a thermocouple and the die temperature by the diode voltage. In the actual conductance technique, temperature was monitored at the bottom of the package by a thermocouple and the die temperature was thereby determined from the calibration experiment.

THEORY

The conductance is measured between two selected pins having a large impedance ($\geq$ 1000 MΩ) connected to metal tracks. The metallization tracks lie on top of silicon dioxide and connect silicon devices. A glassivation layer on top covers the tracks. These lines are separated from each other by silicon dioxide and through reverse biased p-n junctions on the

The LIA measures the conductance and capacitance between the two pins. G_3 includes the pin-to-pin leakage through the ceramic package and the leakage of all the connecting leads up to the LIA, and this conductance is less temperature sensitive and very small in practice. G_4 is the leakage between metallization tracks through SiO_2, and this is also very small. G_1 is the junction leakage conductance, and its value varies exponentially with the temperature. In the temperature range we are interested in (0 to -40°C), G_1 is large compared to G_3 and G_4. The capacitance C_1 is due to lead capacitance, plus the ceramic dielectric capacitance, and a substrate-to-metal track capacitance, and a depletion layer capacitance. All the capacitances are lumped together because they add in parallel. When moisture is present in the package, a conductance G_2 is added in parallel to G_1 due to dropwise condensation of moisture on cooling the die. These droplets also add a capacitance C_2 to the substrate, which is shown in parallel with G_2. The moisture-induced conductance and capacitance are connected through a switch S, closed only when moisture is present in the liquid form. The temperature at which the closing of switch occurs is also a function of the amount of moisture in the package. The switch closure occurs at a temperature T when water starts condensing on the die, and this temperature is taken as the dew point for our purpose. In a dry package condensation never occurs and hence the switch S is never closed. Further, even though the circuit components are shown as lumped quantities, they are really a distributed parameter system. Conductance G_2 and capacitance C_2 are there only when moisture is in liquid form. When moisture is in the solid or gaseous phase these conductance and capacitance components vanish and hence the switch is not closed under these conditions. The circuit is helpful in understanding the shape of the conductance characteristics as a function of temperature. The moisture-induced conductance G_4 should be at least 10% of the G_1 for the required sensitivity. Hence to improve sensitivity, a number of pins pairs can be selected and connected in series. The capacitance variation was not as sensitive as the conductance variation and hence this technique is termed a.c. conductance technique. Even though conductance and capacitance were measured simultaneously, the discussion pertains to conductance only.

INSTRUMENTATION

An LIA circuit setup was used for moisture measurement. For efficient data collection, control and recording of the results, a data acquisition setup was used. An HP 85 microcomputer, and HP 7475A plotter, and HP8290B printer, and an HP 3421A data acquisition unit with a multiplexer were used for data collection and control. The data acquisition was completely under computer control. The experimental data collected were displayed on the screen and a hard copy was obtained from the printer. Plots of conductance or capacitance and diode voltage as a function of time were made when desired from the computer memory after the completion of the experiment, with the help of the plotter. The data acquisition system HP3421A with a multiplexer permitted us to record the diode voltage (proportional to die temperature) and the conductance of the device under test (DUT) from the LIA, and to control the cooling and heating rate of the chip. Due to the common return path problems encountered in making temperature measurements using a protective diode on the die and conductance measurements using LIA simultaneously, the following scheme was used. Along with the device under test, a dummy device was selected. When temperature was measured on one, conductance was mesured on the other and vice versa. These measurements were computer controlled

silicon substrate. A leakage current of the order of nanoamperes was measured in the devices we tested. This current is due to leakage through the reverse biased junctions in the silicon substrate and the isolation islands. This conductance, when measured as a function of temperature, shows a positive slope in the absence of moisture. When the chip is cooled, a dropwise condensation of the water is seen by videotaping the process. These droplets on the top of the glassivation along with the condensed water in the capillaries provide an additional leakage conductance path. Therefore the conductance slope with the respect to temperature is changed from positive to negative when moisture is present. This sharp conductance change is marked as I in Figure 1. In this figure, the conductance variation is shown (by a thick solid line) as a function of time. Temperature of the chip, measured by a diode, is shown (by a dashed line) as a function of time. Water can be in a liquid state even well below 0°C and the temperature at which this transition occurs is a function of the amount of moisture in IC packages. The transition of water into ice is shown as a sharp drop in conductance (marked as II in Figure 1). If the device is taken through a heating cycle following the above cooling cycle, ice melts into water around 0°C. This results in a large increase of conductance (marked as III in Figure 1). Further heating results in water transforming into the gaseous state, and this is exhibited by a sharp drop in conductance value (marked as IV in Figure 1). The four sharp transitions in conductance value when the device is taken through a cooling cycle followed by a heating cycle are seen when moisture is present in the IC packages. If there is no moisture in the package then the conductance follows the short and long dashed lines in the conductance plot (also marked as "NO WATER PRESENT"). This characteristic does not show any sharp transition. Since the conductance of a dry package is due to junction leakage, it is given by

$$G \propto \exp(-E_g/kT)$$

where G = the conductance

E_g = the band gap energy

k = Boltzmann's constant

T = Temperature in °K

The conductance of a dry package therefore will decrease exponentially as temperature is decreased. This has been verified experimentally.

MODEL

A physical model is shown in Figure 2. The metallization tracks lie on SiO_2 at certain sections and make contact with the silicon devices at certain sections. These are shown in Figure 2. As the die is cooled, water condenses into the capillaries of the glassivation layer and condenses as droplets on top of the glassivation layer. An equivalent circuit was developed to explain the conductance characteristics seen in Figure 1 along with the physical model shown in Figure 2. The equivalent circuit is illustrated in Figure 3.

through multiplexer boxes and software programs. Further, software programs were developed to take data from the DUT only and the dummy device was used to avoid measurement transients. Data acquired were also stored on cassette tapes.

PIN SELECTION

Even though theoretically any pair of pins not electrically connected through internal components and having long parallel adjacent metallization runs is suitable, a scheme to select the best pin pairs is presented. Further the mode of connections to be used for increased sensitivity is also discussed.

The pin selection criterion is discussed using a chip layout diagram shown in Figure 4. The layout is for a three-input three-NAND gate TTL circuit. For the first NAND gate, 3, 4 and 5 are input leads and 6 is the output lead. The three input leads for the second NAND gate are 9, 10 and 11 and the output lead for it is 8. The third NAND gate input leads are 13, 1 and 2 and the output lead is 12. The pin numbered 7 is the ground lead and 14 is the lead for power supply Vcc.

For effective implementation of the a.c. conductance technique, select pin pairs (a) having lowest conductance value and (b) having a close and a long parallel metallization tracks. This is the pin-pair selection criterion. As a first step, conductance values between various pin-pairs were measured. Conductance values between all the possible pin pairs combinations of this CERDIP package are measured. Only a few measured values are shown in Table I. Let us consider pin pair combinations 1-2, 1-3,.... 1-14. The ground pin 7 has the longest metallization line (refer to Figure 4), but its leakage conductance is also very high with respect to any pin and hence it is rejected. In this case the conductance between pins 1 & 7 is 27.9×10^{-9}S. Pin pairs 1-3, 1-4, 1-5, 1-6, 1-8, 1-9, 1-10, 1-11, 1-12 are not suitable because there are no metallization tracks close by between these pin pairs. Pin 1-14 is dropped due to large leakage conductance between the pins. Pin pairs 1-2 and 1-13 are selected because they have a low leakage conductance and have a nearby metallization track (see Figure 4). Similarly, pin pair 2-13 is selected because of low measured leakage conductance and nearby metal tracks. By similar reasoning pin-pairs 3-4, 3-5, 4-5, 9-10, 9-11, and 10-11 are selected. All suitable pin pairs selected using the pin pair selection criterion for moisture measurement are highlighted in the table. The metal tracks need to be close by and should be long and parallel to register a high value of moisture-induced conductance. The pin pairs 3-4, 3-5 and 4-5 belong to gate I, pin pairs 9-10, 9-11 and 10-11 to gate II and 1-2, 1-13 and 2-13 to gate III. In the chip layout gate III is on the left lower end. The gates I & II are on the right side of the chip. The water condenses on the chip when it is cooled, but where it condenses on the chip is dependent on the way the chip is mounted in the package. If the chip is mounted slightly slanted to the package bottom, the surface closer to the bottom of the package will condense more water droplets. In this case, let us assume gate III is closer to the bottom of the package, and we are using pin pairs corresponding to gates I or II. The sensitivity will be poor and will vary from one package to the other, because chip mounting is not identical for every package even though we are considering exactly identical chips housed in each package. In other words, selecting the same set of pins will not provide the same sensitivity for all packages containing the same type of chips. Hence in

order to improve the sensitivity of measurement and to reduce the effect of chip mount variations a number of pin pairs are selected and are connected in series or parallel combination. These connection modes and their advantages measured by a figure of merit are discussed in the next section.

CONNECTION MODES

Pin pairs 1-2, 1-13, 2-13, 3-4, 3-5, 4-5, 9-10, 9-11 and 10-11 were selected as suitable pin pairs for moisture measurement using the pin pair selection criterion laid out in the previous section. Of these pin pairs, input pins belonging to each gate are shown in the layout diagram (Figure 4). Since the gates are presumably isolated from each other, pin-pairs from one gate can be connected to the pin pairs of another gate, in series or in parallel. The results of such a study are illustrated in Table II. In experiment 1 (marked as NO. 1 in the Table II), two pin pairs 1-2 and 9-10 were selected and were connected in series. Actual connections are given under mode of connection. In this case, it is shown as 2-10 < 1-9> under the mode of connection, and it implies that 1 and 9 are shorted and the conductance is measured between 2 and 10. The conductance of the above series connection and the diode voltage as a function of time are shown in Figure 5. The measured conductance is the wet conductance (G_W) and is shown by a solid line. When there is no moisture inside the package, the conductance will decrease continuously as the temperature of the chip is dropped, as shown by the solid line, then by a dashed line followed by a solid line (Figure 5). The dry conductance G_d shown in Table II is the value of the measured conductance just before the onset of condensation of moisture when the chip is being cooled. The difference between the wet conductance and dry conductance is ΔG and the figure of merit (M) is $\Delta G/G_d$. The figure of merit (M) is an important parameter to characterize the senstivity of a particular connection.

For this particular series connection G_d was measured to be 1.92×10^{-10} S, and ΔG was measured to be 0.37×10^{-10} S and the figure of merit (M) was determined to be 0.40. In experiment 2, only one set of pin pairs 1-2 was selected. The figure of merit for this connection was the lowest (M = 0.07). A parallel connection was adopted in experiment 3, pin pairs selected were 1-2 and 9-10. These pin pairs belong to gate III and II repsectively as shown in Figure 4. The conductance was measured between pins 1 and 2 when pin 1 was shorted to 9 and 2 was shorted to 10. This parallel connection yielded a figure of merit M of 0.18. Other series connections shown in 4 and 5 also yielded a high value of M, namely 0.46 and 0.54 repsectively. The series (experiments, 1, 4 and 5) always will yield a high value of M compared to the parallel connection (experiment 3) or a single pin-pair connection (experiment 2). This can be explained by the following arguments.

$$M = (G_W - G_d)/G_d = \Delta G/Gd$$

ΔG = conductance increase due to moisture condensation

G_W = wet conductance and G_d = dry conductance

When two pin pairs are connected in series, dry conductance decreases, and because the area of condensation increases, ΔG increases. Referring to the circuit model shown in Figure 3, when the two pin pairs are connected in series, the G_1's of the pin pairs are in series and the G_2's due to moisture condensation between metal tracks of the pin pairs are in parallel because the G_2's are in parallel, ΔG is high and because the G_1's are in series G_d is low and the value of M is high for a series connection.

When we connect two pin pairs in series a complete electrical isolation is assumed, and this is not true. When two pin pairs are connected in parallel ΔG increases and so does the dry conductance and hence M will not increase. When two pin pairs are connected in parallel, the M value is high (= 0.18) compared to a single pin pair 1-2 for the simple reason that there is electrical interaction between 1-2 and 9-10 and the conductance values 1-2 and 9-10 are not exactly identical. The figure of merit is high for a series connection provided one selects two or more pin pairs having minimal electrical interaction between them and connects them in series.

CONCLUSION

The a.c. conductance technique is a simple and a powerful method to determine the presence of moisture in an IC package. The conductance measured between two pins of a dry package shows a positive slope change with respect to temperature when the chip is taken through a cooling cycle followed by a heating cycle. When there is moisture present in the package, the slope changes from positive to negative at four distinct points; two during cooling cycle and two during heating cycle. The four sharp transitions occur (i) when water condenses on the chip (ii) when water freezes (iii) when ice melts and (iv) when water evaporates. The third transition was especially sharp and could be used as a positive identification of the presence of moisture in a package. But normally one is interested in the amount of moisture in a package. Hence the temperature at which the conductance slope changes is used for moisture determination. A criterion to select a pin pair is given by the following procedure:

1. Measure conductance between all pin pair combinations.

2. Select the pin pairs which have a low conductance value between them.

3. From the pin pairs selected in step 2, select the pin pairs that have nearby metal tracks and long parallel metallization runs. A layout diagram of the chip is necessary.

The pin pairs selected can be connected in series for increased sensitivity. The pairs to be connected in series are selected as follows:

a. A suitable set of pin pairs has been identified.

b. From the layout diagram, pick out pin pairs which are in different geographical locations on the chip. Make sure pin pairs are electrically isolated.

c. Connect the pin pairs in series to increase the dry conductance value.

d. The figure of merit of the connection should be high.

The previous procedures are useful in selecting proper pin pairs and a series mode of connnection which will yield an increased figure of merit.

References

1. N.K. Annamalai, and S.M.R. Islam, "Moisture Determination in IC Packages by Conductance Technique", Proceedings of the 24th International Reliability Physics Symposium, Anaheim, CA, April 1-3, 1986.

2. N.K. Annamalai, and R.W. Thomas, "Moisture Measurement in CERDIP Packages by Conductance Technique:, Proceedings of the Moisture and Humidity International Symposium, Washington, D.C., April 15-18, 1985.

CONDUCTANCE & TEMPERATURE AS A FUNCTION OF TIME WHEN AN IC PACKAGE IS COOLED AND HEATED AT A CONSTANT RATE

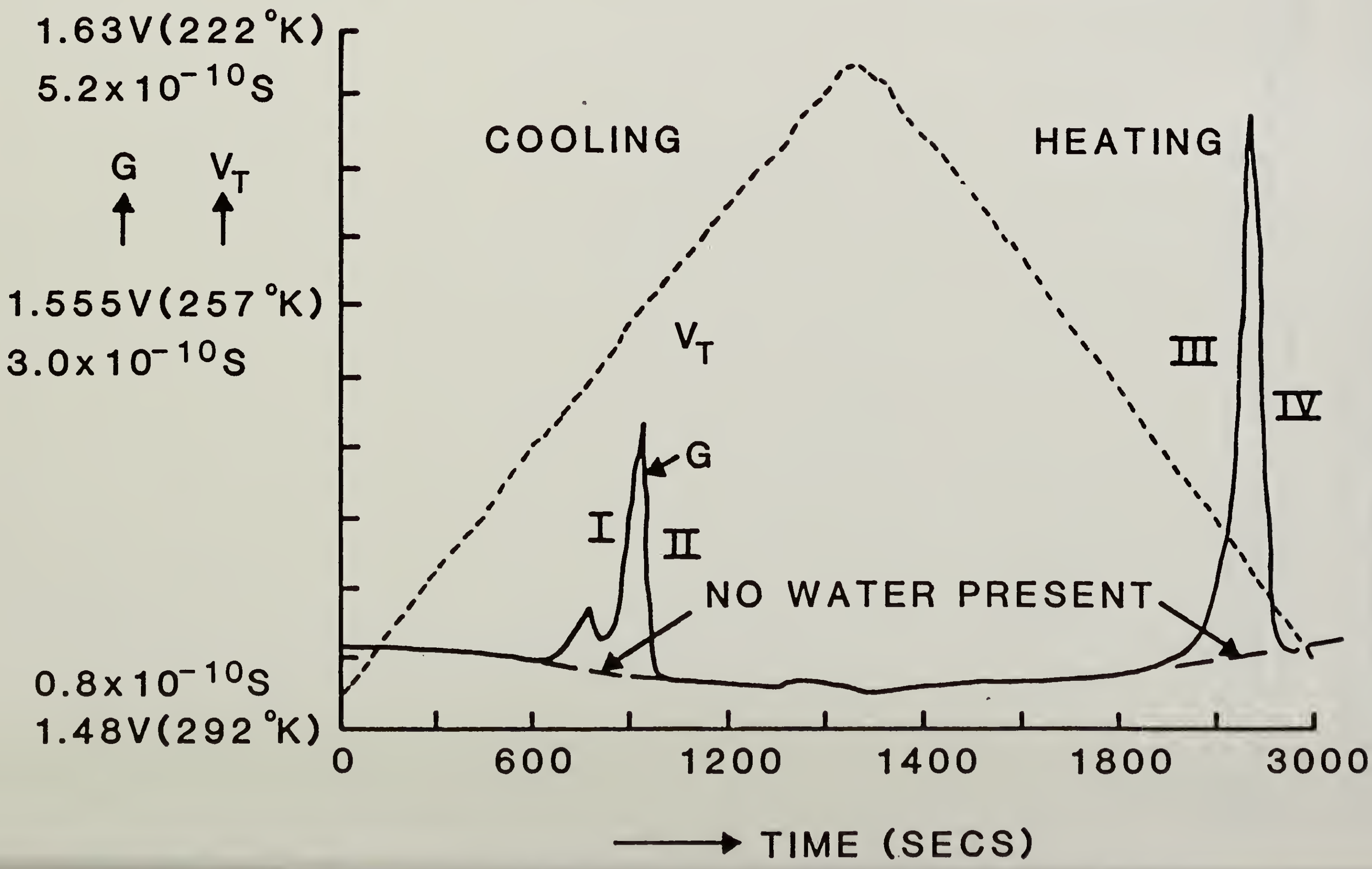

PHYSICAL MODEL

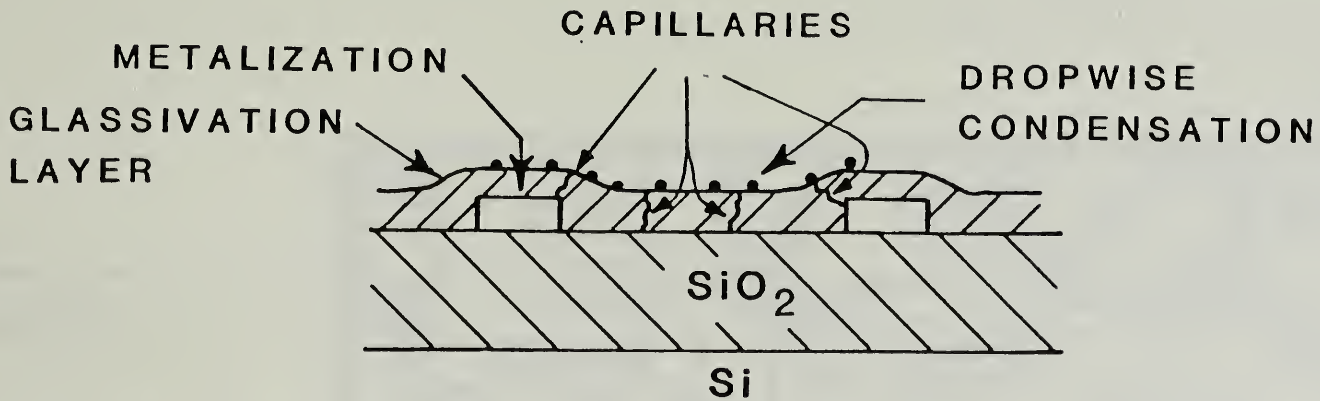

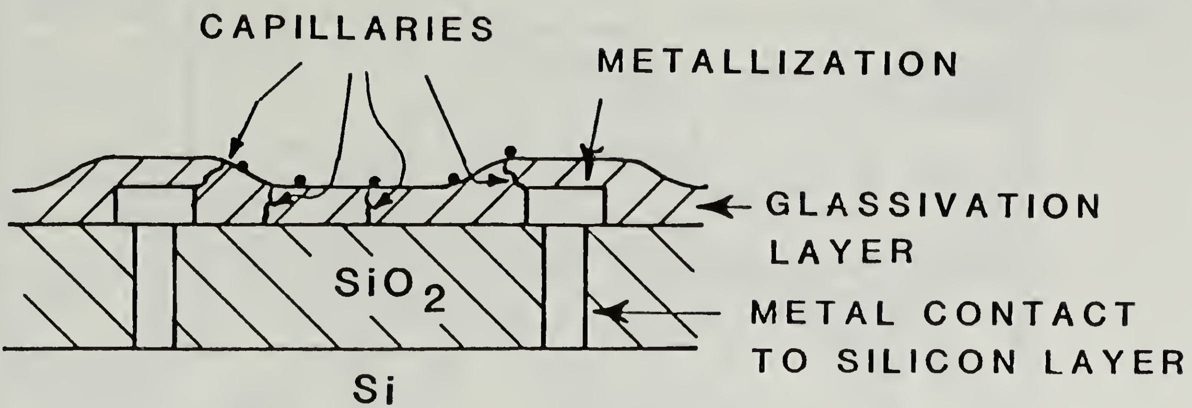

CIRCUIT REPRESENTATION OF THE MODEL

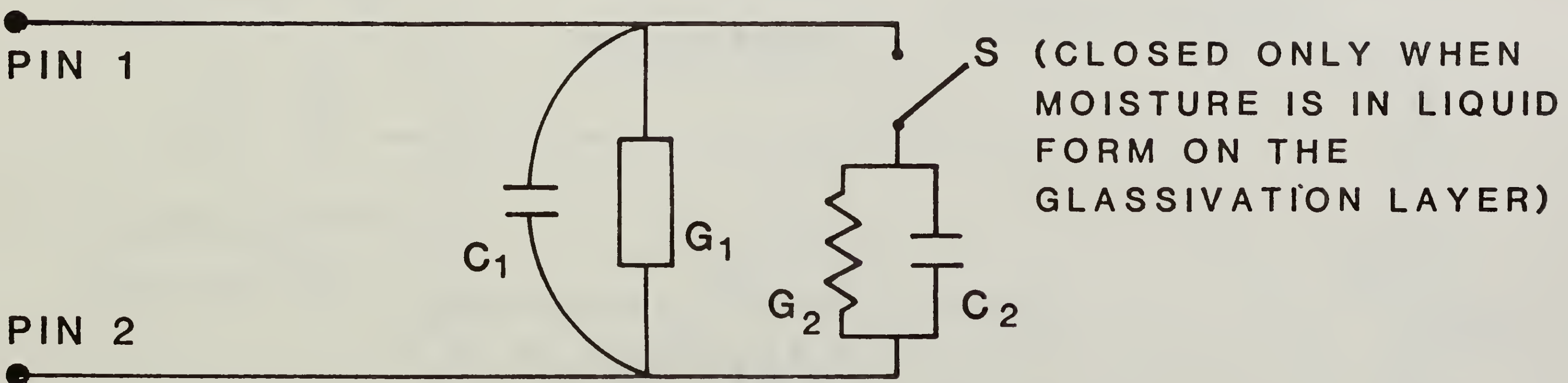

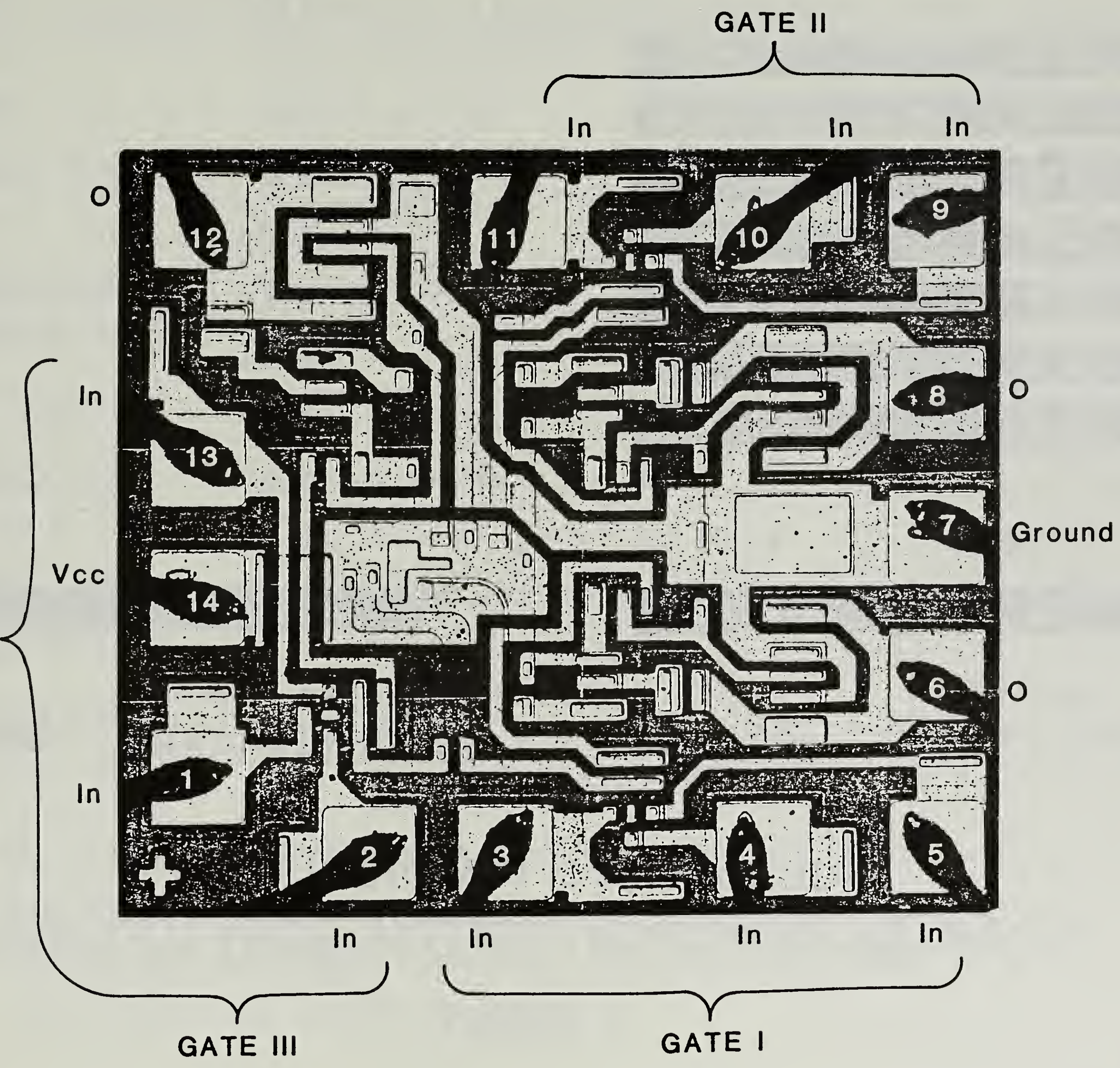

GATE II
In
In
In
O
O
Ground
O
In
Vcc
In
In
In
In
In
GATE III
GATE I

TABLE I

CONDUCTANCE VALUES MEASURED BETWEEN PIN PAIRS IN A 14PIN CERDIP

PIN PAIR	CONDUCTANCE $X10^{-9}S$	PIN PAIR	CONDUCTANCE $X10^{-9}S$
1–2	7.3	1–13	7.1
1–3	6.3	1–14	25.2
1–4	6.9		
1–5	7.5	2–13	6.9
1–6	12.7	3–4	9.2
1–7	27.9	3–5	6.9
1–8	13.5	4–5	8.1
1–9	9.6	9–10	8.5
1–10	3.2	9–11	8.0
1–11	7.2	10–11	7.7
1–12	27.7		

TABLE II

FIGURE OF MERIT (M) FOR VARIOUS CONNECTION MODES

NO.	PIN PAIRS	MODE OF CONNECTION	G_D $\times 10^{-10}$ S	$\Delta G = G_W - G_D$	$\left(M = \frac{\Delta G}{G_D}\right)$
1.	SERIES 1-2,9-10	2-10<1-9>	1.92	.37	0.40
2.	1-2		3.86	0.28	0.07
3.	PARALLEL 1-2,9-10	1-2<1-9,2-10>	4.0	0.72	0.18
4.	SERIES 1-2,4-5,9-10	2-5<1-9,10-4>	0.95	0.44	0.46
5.	SERIES 4-5,9-10	4-9<5-10>	1.7	0.92	0.54

- G_W = WET CONDUCTANCE, G_D = DRY CONDUCTANCE.
- PIN PAIR NOTATION A-B<C-D,E-F>: CONDUCTANCE IS MEASURED BETWEEN PINS A&B AND PIN C IS SHORTED TO D AND E IS SHORTED TO F.

CONDUCTANCE AND TEMPERATURE (MEASURED BY A DIODE) AS A FUNCTION OF TIME WHILE THE PACKAGE IS BEING COOLED & HEATED

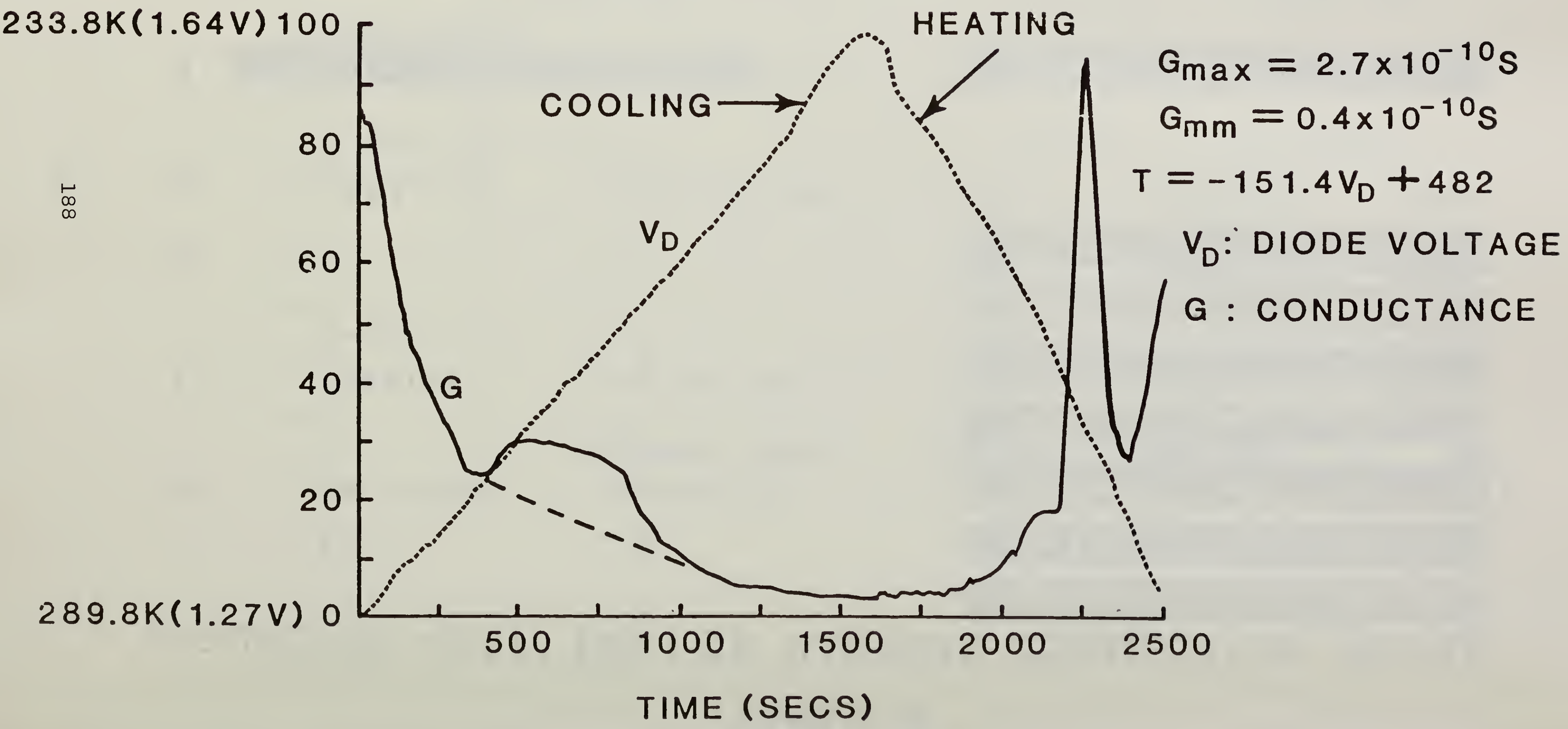

4.2 EVALUATION OF A PARASITIC CHARGE-SPREADING TRANSISTOR AS A MOISTURE SENSOR.

Karin Hultén and Örjan Hallberg
RIFA AB
S-163 81 STOCKHOLM Sweden
+46-8-757 49 20

ABSTRACT

This paper reports on a practical evaluation of a parasitic charge-spreading transistor (CST) as a moisture sensor. The device in question has a lateral PNP structure and operates as an MOS p-channel transistor where the gate charge is built up by charge-spreading over the oxide.

A model is proposed for the dependence of relative humidity (RH) on surface conductivity, which allows extrapolation to low values of RH. This model is evaluated by experiments using the CST device.

An estimate of the time it takes for water to permeate the bulk of a plastic IC package in different environments is made using the CST.

THE OBJECTIVE OF THIS WORK

This work aims at a better understanding of the parasitic phenomenon and its dependence on voltage, humidity, temperature and surface cleanliness.

The main purpose of this work was to evaluate the parasitic charge-spreading transistor as a humidity sensor in different applications. The device could possibly be used for monitoring moisture content inside hermetically sealed encapsulations. Another possible application is to use the CST for controlling hermeticity of the packages, something that so far has been tested with helium or krypton.

A third area to be investigated was the possibility of using the sensor for characterization of plastic enclosures, in the case of water penetrating the package.

THE TEST STRUCTURE AND TEST SPECIMENS

Special test chips were made that contained a lateral PNP structure (CST). They also contained a normal MOSFET for measuring the field threshold voltage (fig. 1). Some of the testchips had a 10.000 Å thick passivation layer on top of the thermal oxide. The passivation was a phosphosilicate glass (PSG), trading name Vapox, of sandwich type. The rest had only the 10.000 Å thermal oxide.

The devices were enclosed in different encapsulations; plastic, metal can and ceramic dual-in-line packages (CERDIP).

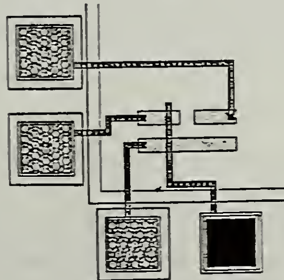

Figure 1 The CST test structure

THEORY

Charge spreading /1,2/

The voltage distribution on the oxide surface near a conductor can be described by the diffusion equation:

$$\frac{\partial^2 V}{\partial x^2} = /\sigma \frac{\partial V}{\partial t} \qquad \text{---(1)}$$

The solution given by:

$$V = V_0 \operatorname{erfc} \left(\frac{x^2 C}{4\sigma t}\right)^{\frac{1}{2}} \qquad \text{---(2)}$$

Where: Vo = applied bias
σ = surface conductivity
C = dielectric capacitance density
x = distance from conductor
t = time

Humidity dependence

The surface conductivity of Silicon Dioxide has been modelled and described according to the BET theory at this workshop in 1978 by R P Merrett and S P Sim. /2/ In summary the surface conductivity (s) according to the data in their report can be described by using the following expressions: (somewhat simplified)

```
m=cr/((1-r)(1+r(c-1)))                    ---(3)
s=am*exp(-11605*.82*(1-.09m)/T)           ---(4)
```

where m= proportional to the amount of adsorbed water
c= exp(Ø/kT)
a= constant , here 0.0001
r= relative humidity (0-1)
T= temperature (K)
Ø= difference between the latent heat of evaporation of water and the heat of adsorption of this water, here 0.035 eV

The water adsorption on SiO_2 is plotted in figure 2 from ref /4/. This S-shaped curve looks similar to a cumulative density function curve when drawn on a linear scale. By the use of a standard log normal distribution diagram this curve could be straightened out and thus helpful when extrapolating down to low values of RH.

Equation (4) was plotted in such a diagram to see if the expression would justify the use of it for linearisation purposes. The result is shown in figure 3 and it indicates that one should expect linear relations from roughly 60%RH down to at least 2%RH provided the expression is valid.

Figure 4 shows published data on surface conductivity replotted in a log normal diagram. These experimental findings form the basis of the humidity dependence used later for evaluating the moisture sensor readings.

In the literature on the related subject, corrosion, one can find several moisture models. Exp(a*(RH)2) by Lawson or a/(RH)2.67 by Peck have been used to linearise the data and to get moisture acceleration factors. /16,15/. Ref /5/ reported acceleration factors based upon a collection of moisture test results. In figure 5 that material has been updated with more recent data. The models are compared in figure 6.

Temperature dependence

In our computer model we have made use of the log-normal behaviour of the RH-dependence and assigned an Arrhenius function for the temperature dependence of the conductivity at 50% RH. As the activation energy varies from 0.35 to 0.8 eV depending on the RH /6/ this will result in different slopes in the log normal diagram. The lower the relative humidity the higher the activation energy. 0.35 eV is close to that of conduction in bulk water (0.34eV). Appendix A gives the fortran program that makes use of the model in order to estimate the ppm-level in a hermetic package with a CST device.

EXPERIMENTS WITH TEST CHIPS IN CERDIP PACKAGES

The time taken for the applied voltage to spread out on the oxide surface and eventually turn on the transistor was measured. (To be more precise, it was the time needed for the leakage current to reach a specified value.)

Humidity dependence

Tests were performed at room temperature with unsealed components in desiccators with different moisture contents.

12% RH: $LiCl.H_2O$; 32% RH: $MgCl_2.6H_2O$; 76% RH: NaCl

When the components to be tested had been placed in the vessel, they were left for 24 hours for equilibrium to be established before any measurements were conducted.

When measurements were made at room ambient, the occational great variations in the degree of humidity were monitored using a calibrated hygrometer.

The tests at 76% RH had to be abandoned since the turn-on time was too short for accurate measurements.

In fig 7 the turn-on time vs. relative humidity is plotted in a log-normal diagram for a few components. The results agree fairly well with the model, even though the spread between devices is relatively large.

A normal non-leaking Cerdip contains a total amount of moisture of about 1000 ppmv at 100°C according to mass spectrometric investigations. Taking into account the large surface-to-volume ratio of the ceramic package cavity, which leads to a large moisture uptake by the cavity walls, the water vapor that is free to absorb on the chip surface is around 200 ppmv /8,9,10/. This corresponds to approximately 0.4% RH at 22°C and as the pressure inside the die cavity of a Cerdip is approximately 0.5 atm this is equivalent to 0,2% at 1 atm. For this case, log normal linear extrapolation predicts a turn-on time of 200 hours for an applied voltage of 100 V. No leakage current was detected however, even though the test chips were kept under constant bias for 500 h.

There are two possible explanations for this; either the test structure is not sensitive enough for such low conductivities, or there exists a limit below which the model is no longer valid.

Voltage dependence

The voltage dependence was examined at constant humidity and temperature (22 C, 12%). The time elapsed until the leakage current reached -150 nA was measured. The results are shown in fig 8.

The theoretical values can be calculated by keeping one point fixed (e.g. 19s, -45 V in fig 8) while adjusting the threshold voltage for best fit. As can be seen, the theoretical and experimental curves are in excellent agreement. This also seems to be a way to estimate the threshold voltage for parasitic action.

Temperature dependence

A simple test was made in order to see if the CST device would show the same temperature dependence as surface conductivity has shown /6/. A device was stored at 30 % RH at varying temperatures. The turn-on time was recorded and is presented in figure 9. The device had vapox passivation. The activation energy was 0.62 eV that is very close to that reported by Koelmanns at 30% RH /Ref 6/.

EXPERIMENTS WITH "REAL" DEVICES

Instability mechanisms were reported from lifetesting of a particular circuit. It was thought to be due to parasitic action, which could be related to an unnecessary opening in the passivation layer. The chip layout is partly shown in fig 10. This device could have its input bonded to one of two pads in order to obtain two functions with only one chip. The input is on (a) in the first case and on (b) in the second case. In the circuit of interest the input is on (a) and (b) is not used.

When the emitter (c) is kept at a low potential, (b) ends up at about the same level. The distance from the contact-hole (b) to the pnp-transistor (d) is only about 25 um and if moisture is present the potential can spread out and possibly turn on the transistor.

According to equation (1), the turn-on delay has a quadratic dependence on the distance x. Theoretically, the turn-on should be delayed by a factor 100 if the distance was increased from 25u (b-d) to 250u (c-d).

Comparative tests were carried out on components with and without this bond-opening. The result is presented in fig 11. As can be seen, the predicted delay by a factor 100 is not reached but the improvement (by a factor of 33 using the median value) is clearly shown.

PLASTIC ENCAPSULATION

Diffusion times for water through the bulk of the plastic in different environments were studied and the acceleration factor between 85C, 85% RH and 120C, 100% RH was determined.

Components without PSG

The turn-on time for the test chips in autoclave (120/100) was measured once a day for five days and the components in 85/85-test were monitored continuously for a period of 3 weeks. The applied bias was -80 V.

Components with PSG

It was difficult to obtain any results at all from devices covered with passivation. The conductivity is greatly reduced by the plastic and the inversion threshold voltage is higher for components with Vapox, so in order to get any results within reasonable time the applied voltage would have to be raised above the breakdown voltage of the diodes. The only component that could be measured had a turn-on time of 80 minutes.

Results

For the components in saturated autoclave, water reached the chip surface after a little more than one day. The time needed for those tested in 85/85 was about 3 weeks. This gives the acceleration factor A.

$$A = (21 \text{days})/(1.6 \text{ days}) = 13$$

In one case, the plastic seemed to have been displaced from the chip surface. This gave rise to an increase in sheet conductivity with a factor of 80.

SENSOR STABILITY

In order to check the reproducibility, the test chips were measured directly after removal of the lid and then remeasured (after 30 seconds, 30 minutes, 1 day and 3 days). It was concluded that 30 seconds was too short a time for the outspreading surface potential to relax, and this resulted in shorter and shorter turn-on times. Waiting for 30 minutes or 1 day between measurements gave satisfactory reproducibility. The values differed about 10-20%.

After 3 days the turn-on time for the chips kept at 12% RH was increased by a factor of 3 compared with the first measurements, while the turn-on time for those kept at room ambient did not change. This was somewhat unexpected and needed of more thorough examination.

Cerdips

Directly after removal of the lid, Cerdips were extremely sensitive to variations in relative humidity, but this sensitivity became less and less pronounced with time.

This "aging process" turned out to be strongly dependent upon humidity, i.e. storage in a dry atmosphere had an accelerating effect (fig 12).

A certain difference between chips with and without Vapox was noted in the sense that devices with Vapox tended to have a slower loss of sensitivity. This might be due to the hygroscopic nature of Vapox.

Metal cans

Devices encapsulated in metal cans seemed to be completely insensitive to moisture. They showed no tendency whatsoever to leakage. This experience was not new, the same behavior had been observed before in connection with other measurements /12/.

Washing for a few seconds in dilute HF (10 sec. 1% HF) restored the surface of the chip and the behavior was then the same as for Cerdips.

Why a dry atmosphere increases the contamination rate

The decrease in sensitivity is thought to be due to organic vapor in the air. These impurities make the surface hydrophobic, which means that condensed water molecules on the surface form small droplets instead of a continuous film, thus reducing the surface-charge spreading to a great extent.

Tamai et.al./13/ have studied the effect of water vapor on the contamination of metallic oxide surfaces, using the contact angle of water as a criterion for surface cleanliness. Their results show that the contamination rates of the clean surfaces are reduced by the coexisting water vapor (fig 13). This can be explained by the fact that the organic contamination is to be regarded as an adsorption process, and not just due to material "falling out" onto a surface /14/.

An oxide surface is often strongly hydrophilic, which implies that it has a preferential bonding to water. This in turn means that the organic contaminants should adsorb onto the surface competing with water molecules. Consequently, a dry atmosphere means "free access" to the adsorption sites.

The difference between cerdips and metal cans

Metal encapsulated chips appear to be insensitive to moisture, while those in Cerdips are very sensitive. This would mean that some step in the Cerdip encapsulation process radically affects the surface.

An efficient method for cleaning surfaces that have been exposed to organic vapor involves heating to 400-500 C in an oxidizing atmosphere. Cerdips are sealed in dry artificial air and the temperature during this process is around 450 C. The surface can thus be cleaned as a result of the sealing process /9/.

When sealing metal cans, the temperature is much lower and the atmosphere is non-oxidizing, so the surface is still contaminated after the

previous encapsulation process. This explains the low sensitivity of metal can encapsulated CST devices.

CONCLUSIONS

*CST can be used for leakage testing of Cerdips immediately after the encapsulation when the surface is clean. Leakage testing at a later stage may give unreliable results because of the atmospheric contamination that will take place if the package is not hermetic. This will result in a hydrophobic surface and the CST will become less sensitive.

*It is difficult to use the CST-sensor in order to determin the exact moisture content inside a hermetic package because of the wide spreading between individual devices. Sorting out components with a water vapor content that exceeds a critical value of, say, 5000 ppmv may however be possible though.

*Measurements can be made in sample tests where each component must be calibrated in a desiccator with known relative humidity. (Appendix A)

*If different plastic package materials are to be evaluated regarding moisture resistance, the CST seems to be a good indicator of water penetrating the package. Acceleration factors for TH-studies (Temperature-Humidity) can also be determined. The field-inversion threshold voltage must be kept low in this application (no Vapox) because of the great reduction in surface conductivity when the plastic adheres well to the die.

ACKNOWLEDGEMENTS

This work was sponsored by the Swedish National Microelectronics Program Quality assurance project NMP-Q in cooperation with RIFA AB.

APPENDIX A. Program for calculating the moisture content inside hermetically sealed devices.

```
C      ***********************************************************
C      *                                                         *
C      *     PROGPAM FOR CALCULATING THE MOISTURE CONTENT INSIDE *
C      *     HERMETICALLY SEALED DEVICES (EXPRESSEO IN PPMV)     *
C      *                                                         *
C      ***********************************************************
C
C
C
C      READ VALUES FOR THRESHOLD VOLTAGE, OPERATING VOLTAGE, TURN-ON TIME
C      DURING OPERATION, OPERATING TEMPERATURE, TEST VOLTAGE, TURN-ON TIME
C      IN TEST, TEST TEMPERATURE, ACTIVATION ENERGY FOR TEMPERATURE OEPEN-
C      DENCE, RELATIVE HUMIDITY IN TEST.
C
         WRITE(*,*) 'THRESHOLD VOLTAGE'
         READ(*,*) VTH
         WRITE(*,*) 'OP.VOLTAGE, TURN-ON TIME DURING OP., OP.TEMPERATURE'
         REAO(*,*) VB0,TIME0,TEMP0
         WRITE(*,*) 'TEST VOLTAGE, TURN-ON TIME IN TEST, TEST TEMPERATURE'
         READ(*,*) VB1,TIME1,TEMP1
         WRITE(*,*) 'ACTIVATION ENERGY (EV)'
         REAO(*,*) EA
         WRITE(*,*) 'RELATIVE HUMIOITY IN TEST'
         REAO(*,*) RH
C
C
C      THE ZERO OF THE ERROR FUNCTION IS COMPUTED
C
         RES0=ERFX(VTH,VB0)
         RES1=ERFX(VTH,VB1)
         B7=(RES0/RES1)**2
C
C
C      THE ACCELERATIDN FACTDR FDR INCREASEO HUMIOITY IS CALCULATED
C
         B1=RHACC(RH,TEMP1)
C
C
C      THE ACCELERATIONFACTOR FDR INCREASEO TEMPERATURE IS COMPUTED
C
         B3=TEMPACC(TEMP0,TEMP1,EA)
         B8=TIME1/TIME0*B3*B1/B7
C
C
C      AN APPROXIMATIDN WITH THE NDRMAL DISTRIBUTION FUNCTION Q(X) IS OONE
C      AND THE ARGUMENT X IS CALCULATED.
C
         B9=QFUNC(TEMP0,B8)
         RES=B9*1E6/380*9.8E8*EXP(-5235/(273+TEMP0))
C
C
C      PRINT THE PPMV-VALUE
C
         WRITE(*,*) 'THE PPMV-VALUE IS',INT(RES)
         END
C
         FUNCTION ERFX(VTH,VB)
         ERF=1-VTH/VB
         XX=ERF+.17
         SLASK=ERFNOLL(XX,ERF)
         IF(SLASK.GT.0) GO TO 10
         UP=ERF-.04
         DOWN=XX
         GO TO 20
 10      UP=XX
         DOWN=ERF-.04
 20      IF(ABS(UP-DOWN).LT.0.005) GO TO 50
         XX=(UP+DOWN)/2
         SLASK=ERFNOLL(XX,ERF)
         IF(SLASK.LT.0) GO TO 30
         UP=XX
         GO TO 40
 30      DOWN=XX
 40      GO TO 20
 50      ERFX=XX
         RETURN
         ENO

         FUNCTION RHACC(RH,TEMP)
         SLASK=2.3-TEMP/75
         R=0
         IF(RH.LE.50) GO TO 100
         R=RH
         RH=100-R
 100     OS=SQRT(LOG(1E4/RH**2))
         ZZ=OS-(2.3075+0.2706*OS)/(1+0.9923*OS+0.0448*(OS**2))
         IF(R.GT.50) ZZ=-ZZ
         RHACC=10**(-SLASK*ZZ)
         RETURN
         END
C
         FUNCTION TEMPACC(T0,T1,EA)
         TEMPACC=EXP(11605*EA*(1/(273+T0)-1/(273+T1)))
         RETURN
         END
C
         FUNCTION QFUNC(T0,B)
         SS=2.3-T0/75
         XS=-LOG10(B)/SS
         YS=1/(1+0.3327*XS)
         QFUNC=SQRT(2/3.1416)/2*EXP(-(XS**2)/2)*(.4362*YS-.1202*(YS**2)+
         (.9373*(YS**3)))
         RETURN
         ENO
C
         FUNCTION ERFNOLL(U,V)
         ERFNOLL=(U**9/216-U**7/42+U**5/10-U**3/3+U)*2/SQRT(3.1416)-V
         RETURN
         END
```

References

1. Schroen, W., "Failure Analysis of Surface Inversion", Proceedings 11:th Reliability Physics Symposium, 1973.

2. Merrett,R.P., Sim,S.P., "Assessment of the Use of Measurement of Surface Conductivity as a Means of Determining Moisture Content of Hermetic Semiconductor Encapsulations", ARPA/NBS Workshop V, Moisture Measurement Technology for Hermetic Semiconductor Devices, 1978.

3. Kawasaki,K.,Hackerman,N., "On the Variation of Surface Conduction Current of Porous Vycor Glass by the Adsorption of Water Vapor", Surface Science 10, 1968.

4. Ammons,J.M.,Hoff,G.R.,Kovac,M., "The Physisorption of water onto Integrated Circuit Package Components", RADC/NBS Workshop, Moisture Mearurement and Control for Semiconductor Devices,III, 1984.

5. Hallberg,Ö., "Acceleration Factors for Temperature-Humidity Testing of Al-metallized Semiconductors", SINTOM, 1979.

6. Koelmans,H., "Metallization Corrosion in Silicon Devices by Moisture-induced Electrolysis", Proc. 12th Reliability Physics Symposium, 1974.

7. Sbar,N.L.,Kozakiewicz,R.P., "New Acceleration Factors for Temperature, Humidity, Bias Testing", Proc. 16th Reliability Physics Symposium, 1978.

8. Finn,J.B.,Fong,V., "Recent Advances in Al_2O_3 "in-situ" Moisture Monitoring Chips for Cerdip Package Applications", Proc. 18th Reliability Physics Symposium, 1980.

9. White,M.L.,Sammons,R.E., "A Procedure for Preparing Hermetic Packages with known Moisture Levels", NBS/RADC Workshop Moisture Measurement Technology for Hermetic Semiconductor Devices,II,1982.

10. Lowry,R.K.,Miller,L.A.,Jonas,A.,W.,Bird,J.M., "Characteristics of a Surface Conductivity Moisture Monitor for Hermetic Integrated Circuit Packages", Proc. 17th Reliability Physics Symposium,1979.

11. Morrison,S.R.,The Chemical Physics of Surfaces, Plenum Press NY, London,cop.1977.

12 Report RIFA Document No M/Z 83-39.

13. Tamai,Y.,Matonnaga,T.,Suzuki, K.,"The Effect of Water Vapor on Contamination of Metallic Oxide Surfaces", Bulletin of the Chemical Society of Japan, vol.50 (7), 1977.

14. White,M.L., "The Detection and Control of Organic Contaminants on Surfaces", Clean Surfaces, G.Goldfinger,ed., Marcel Dekker Inc.,NY 1970.

15. Lawson R.W., "A review of the status of plastic encapsulated semiconductor component reliability", Br Telecom Technol J Vol 2 No 2 April 1984.

16. Peck, D.S., "Comprehensive Model for Humidity Testing Correlation", IEEE IRPS 1986, pp 44-50.

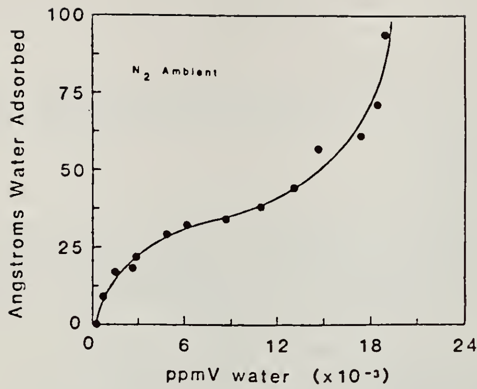

Figure 2 Water adsorption on SiO_2 /Ref 4/

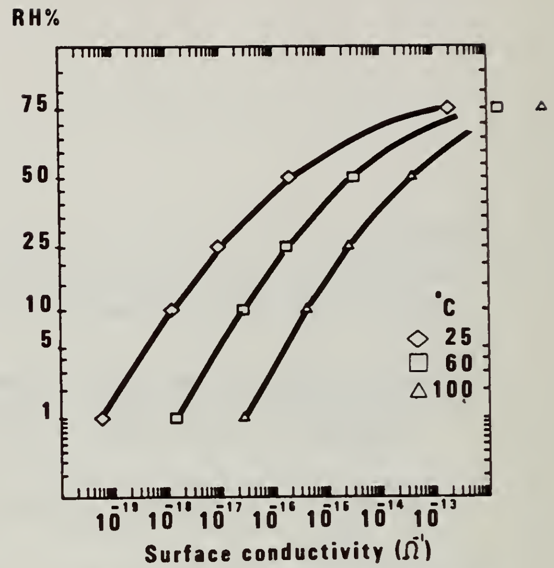

Figure 3 Calculated according to eqn (4)

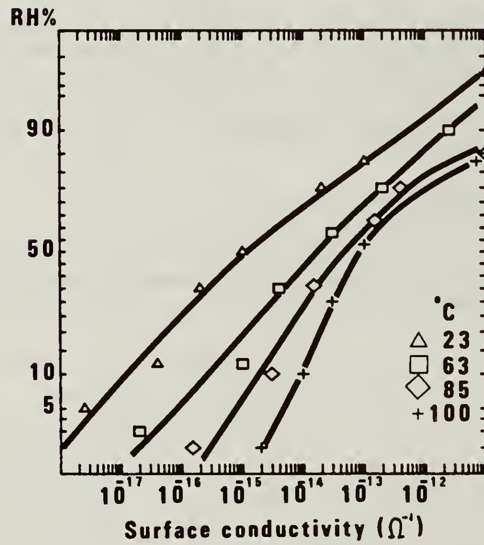

Figure 4 Data from Keelmans /6/

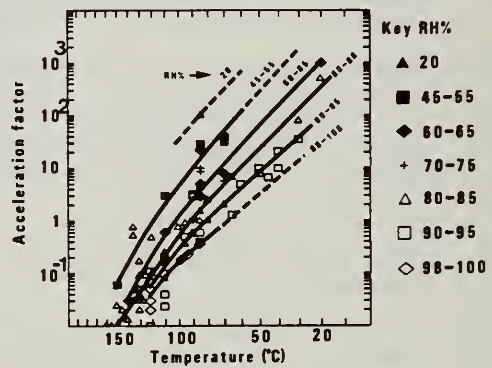

Figure 5 Corrosion acceleration factors from /5/ and other sources

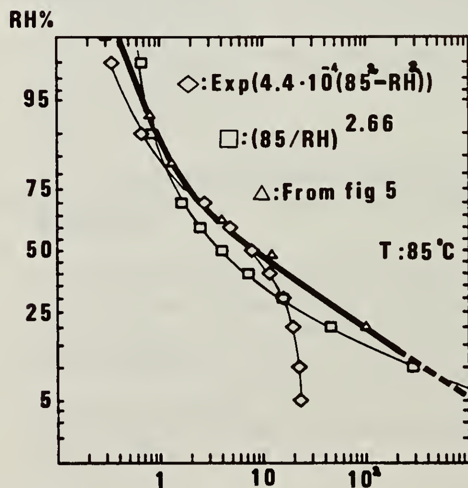

Figure 6 85%RH acceleration Different models

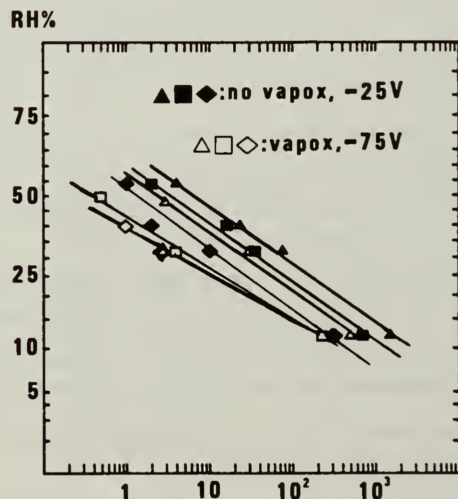

Figure 7 CST turn on time (s) vs RH

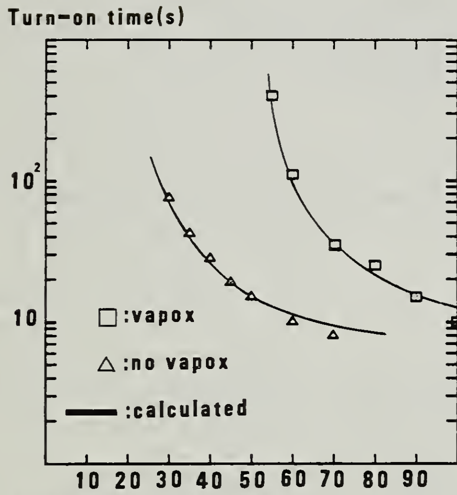

Figure 8 Turn-on time vs bias at 22C/12%RH

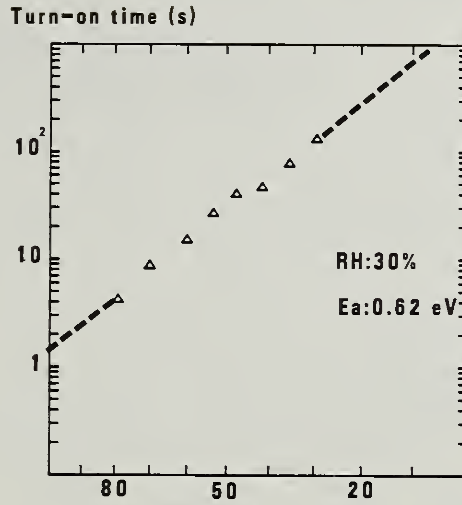

Figure 9 Temperature dependence of turn-on time

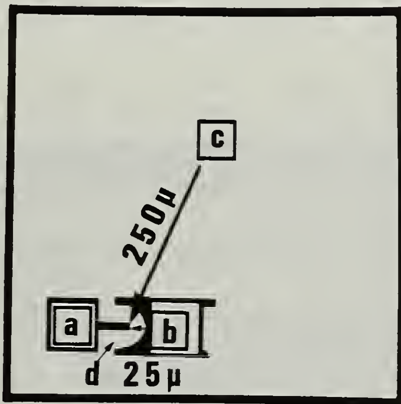

Figure 10 A pnp transistor with CST properties

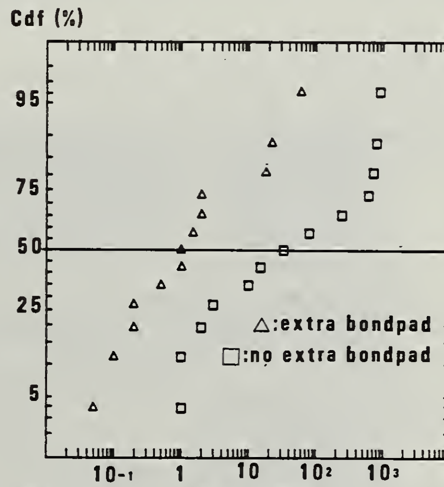

Figure 11 Distribution of values

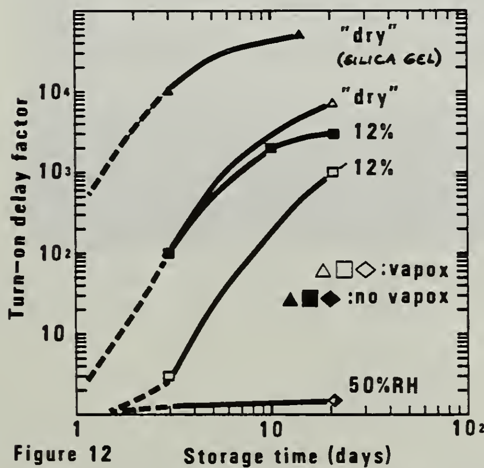

Figure 12 Loss of sensitivity at different ambients

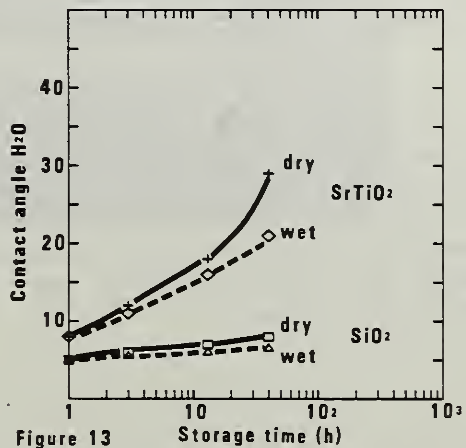

Figure 13 Change of contact angle by time. From ref /13/

4.3 MOISTURE MEASUREMENT BY AC-BIASED SURFACE CONDUCTIVITY SENSORS

Didier Kane* and Benjamin A. Moore
Rome Air Development Center (RBRE)
Griffiss AFB NY 13441-5700
(315) 330-4055

* Dr. Kane is a contractor from Clarkson University, Potsdam, NY

INTRODUCTION

Tomorrow's military and space electronic devices will cost thousands of dollars, not to speak of the overall cost of the systems in which they will be inserted, for which no risk of failure will be accepted.

Even though serious progress have been made in terms of moisture control, with the implementation of Method 1018 in MIL STD 883C, none of the techniques currently used can provide the insurance that a precise part selected for a given system will never experience a moisture related failure.

Among the non-destructive techniques, aluminum oxide sensors could be an answer for hybrid modules in which volume is not a major requirement, but the presence of an additional die will not be possible in most packages. The conductance technique using the die as a moisture sensor seems to be an ideal solution, but further evaluations are still necessary for determining the die-to-die reproducibility and sensitivity. Another possible solution that would probably be less dependent on the nature of the die would be the integration of surface conductivity sensing schemes as electrical test structures on the side of the die. This could be done with no additional mask, but would require four I/O, which might not be viable for some packaging approaches.

At the present time, RADC is still evaluating surface conductivity moisture sensing chips whose design might later be integrated on any die. Such sensors have been shown to be accurate but not reproducible when used with DC bias (1). The purpose of this paper is to present recent improvements brought to this technique by AC bias and to point out the importance of the adsorption on the cavity walls in any "dew-point" measurement technique.

DESCRIPTION OF THE TECHNIQUE

The sensor is made of an interdigited aluminum stripe pattern deposited on an insulating material (thermally grown thick silicon oxide) As shown in Figures 1 and 2, two different test structures have been used in this study; the main differences between these two structures are the shape and length of the aluminum electrodes and the existence of a diode on the later die itself, which enables more accurate temperature measurement. The sensing die is mounted in the package to be tested. The method consists of heating the package up to 100 C and maintaining this temperature for a given period of time to desorb the moisture fixed on the cavity walls in the same conditions as in a mass spectrometer. The package is then slowly cooled down, while the inter-electrode leakage current of the biased sensor is recorded versus temperature. Figure 3 represents the response curve that can be expected for an hermetically sealed package. It has been shown that the "dew-point" corresponds to the onset of conduction (change in slope), and not to the top of the peak (2). If the sealing pressure and temperature are known, some charts based on the application of the ideal gas law to the partial pressure of water in the package usually allow to convert the electrical "dew-point" into a moisture content in parts per million. However, these charts do not take into account the adsorption of moisture on the walls which makes it impossible to speak of a real dew-point in a closed package, and a model presented later in this paper will show how modified ideal gas law equations that take this effect into account can be writen.

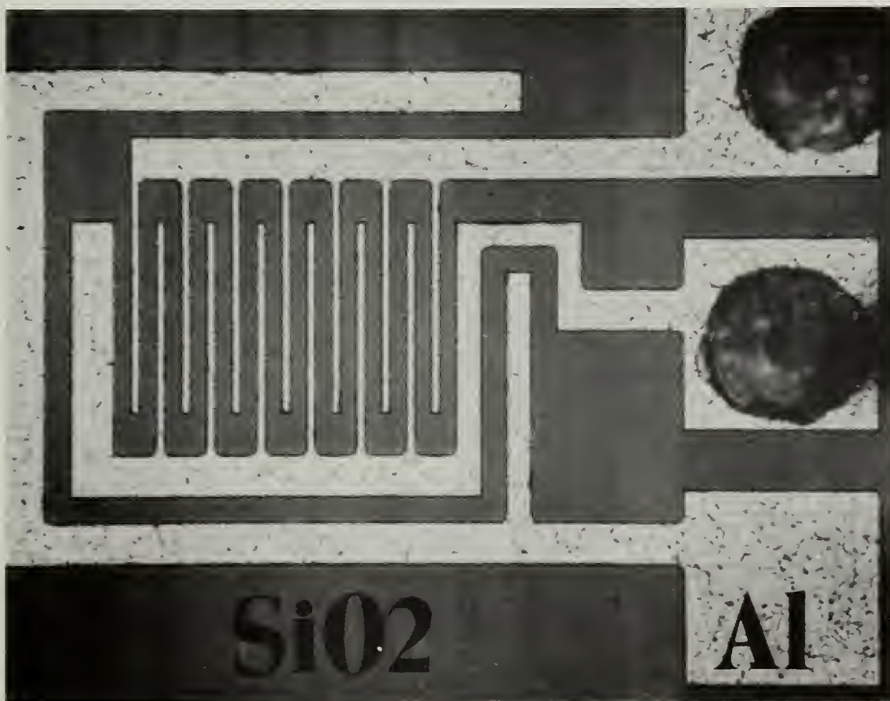

Figure 1

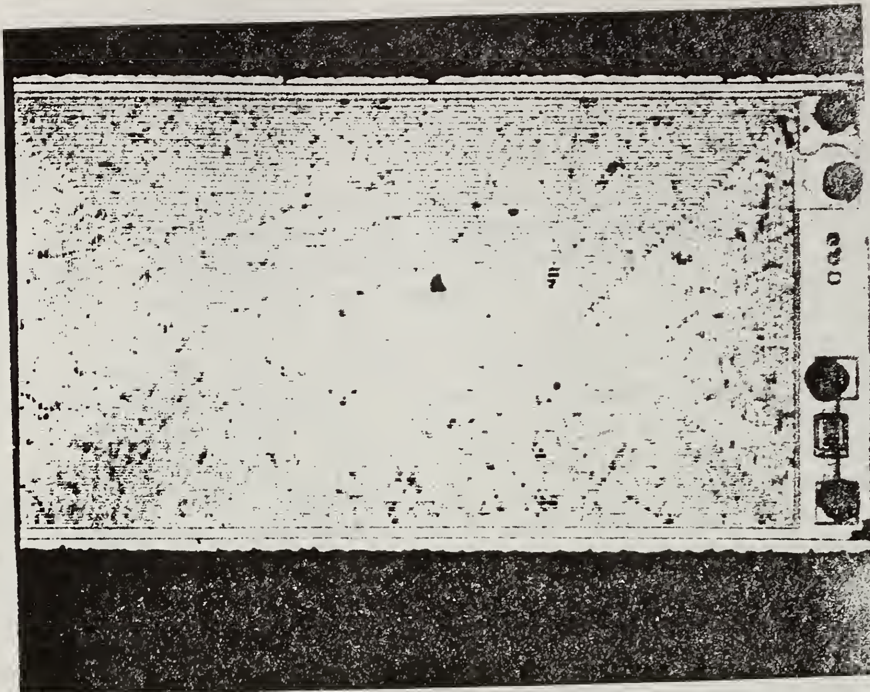

Figure 2

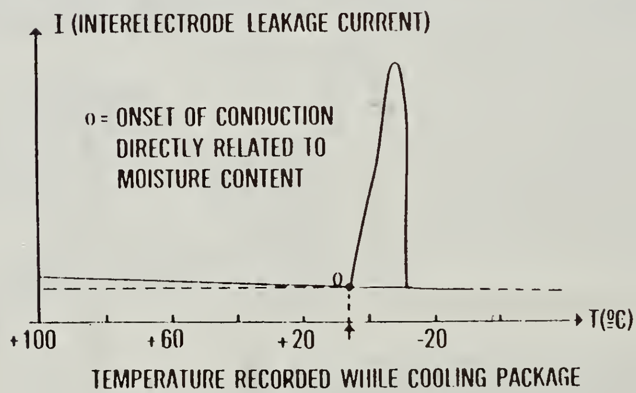

Figure 3

DESCRIPTION OF THE TEST SETUP

The test setup built at RADC includes a test chamber and an electrical measurement circuit. The test chamber, made of aluminum, is connected to a mechanical pump, allowing a primary vacuum (20 Pa.) inside the chamber. This design eliminates any possible condensation on the outside of the package, and minimizes the heat exchange with the surrounding medium. The pump is used for measurement on hermetically sealed packages only.

For calibrations and physical studies on delidded packages, the chamber also has an inlet and outlet for gas atmospheres. The inlet is connected to the RGA calibration system at RADC, which permits a continuous flow of controlled, humid gas in the chamber. The chamber has a removable top (fixed by O-ring), hermetic connectors and a power feed-through. A schematic representation of the test chamber is given in Figures 4 and 5.

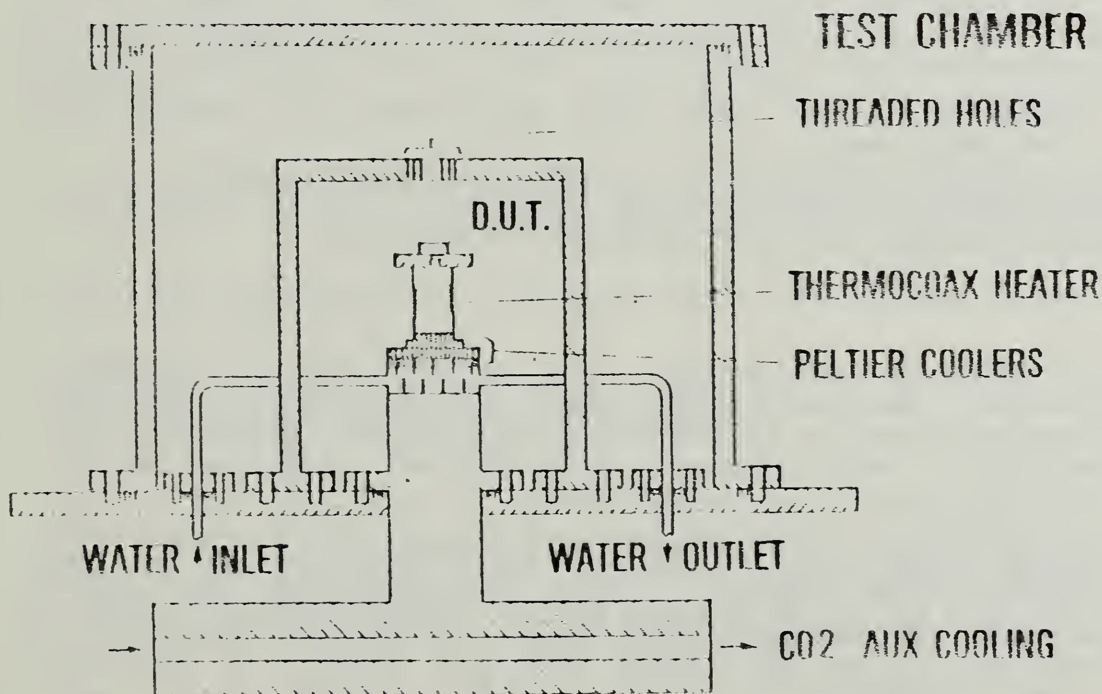

Figure 4

SCHEMATIC REPRESENTATION OF TEST SETUP

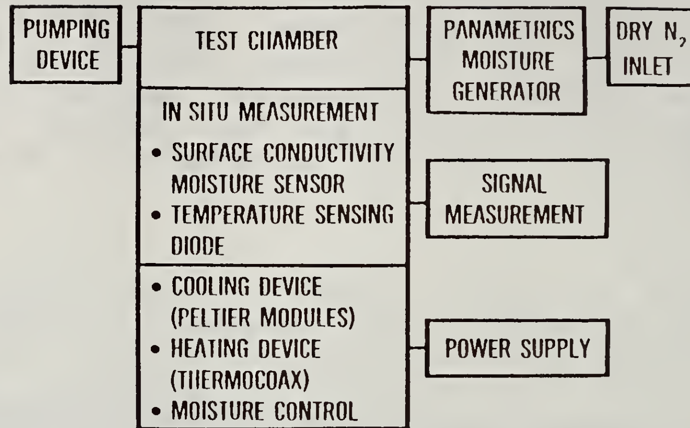

Figure 5

Thermoelectric heat pumps have been chosen for cooling the packages. The system uses :
- one heat pump module (MELCOR CP 1.4-127-06L) biased with 11V-4A
- three heat pumps in series biased with 11V-2.75V
  (MELCOR CP 1.4-31-06L + CP 1.4-71-06L + CP 1.4-125-06L)

Two sample holders have been designed for use with different kinds of packages. The first one is a copper cylinder with a groove in which a thermocoaxial heater (SODERN 1 Nc Ac 20) has been welded at both ends of the heater to avoid moisture related problems. Heat from the hot surface of the heat pumps is evacuated through a water circulation box. During the experiments, circulating water has been replaced by ethylene glycol, allowing a more efficient cooling. A cold finger on top of this copper piece allows a preferential cooling just underneath the sensor. This sample holder was used with TO-8 packages. An aluminum bracket with a large threaded hole on top was placed over the sample. A screw was inserted in this threaded hole. At the end of this screw, several heads could be adapted, according to the kind of device under test. These heads were made so that they could fit exactly around the top of the package to be tested. These heads have large openings on the sides, which allow a flow of gas to circulate freely around the sensor when a delidded package is being tested. A nichrome wire is wrapped around these heads and biased so that a thermal gradient of 1 to 2 C is always maintained between the top and the bottom of the DUT. This feature, together with the cold finger make sure that the sensor is always the coldest point of the package. Some TO-5 packages that had an insulating glass at the bottom of the package

between the leads, had to be tested. This glass was a very bad thermal conductor, and the previous sample holder could not be used : too much heat was lost in the thickness of the material,and the sample could not be properly cooled. A new sample holder was therefore designed.Its shape was a very thin copper pyramid with a ring (three quaters of a circle long) on top. This allowed cooling from the metal ring at the bottom side of the DUT. Moreover, some tiny holes in which were inserted the leads that were not used for the electrical measurements provided a second cooling source. A second nichrome resistor was wrapped around the appropriate screw-head in order to heat the DUT up to 100 C and to maintain it at this temperature at the beginning of each experiment. The screw-heads also permitted retention of a good thermal contact between the DUT and the sample holder. This was improved by the deposition of a thin layer of silicon grease between each surface involved in the cooling process.

An automated thermal cycling system, identical to the one described in reference 1, has been added to the test setup.

ELECTRICAL MEASUREMENT CIRCUIT

Some Auger analysis has been initially performed on sensors previously biased with 40 VDC and exposed to more than 50 temperature cycles in the range +110 C to -30 C, in a highly humid atmosphere, which permitted :

- verifying the presence of alumina on the anode, resulting from the oxidation of the electrode after electrolysis of the adsorbed water.
- confirming the presence of aluminum on top of the silicon oxide in the inter-electrode space.
- confirming the choice of AC bias instead of DC bias for a better reproducibility in the moisture measurement.

The non-reproducibility in the electrical response of a sensor mounted in a hermetic package and exposed to thermal cycling under DC bias had previously been observed, and may be explained (1) by a modification in the composition of the silicon oxide upper layers.

Consequently, it was decided to use a Lock-In-Amplifier (LIA) whose internal generator would be used for biasing the DUT with a low voltage AC signal and would also be used as a reference signal. A very sensitive digital microvoltmeter was used at the output of the LIA for detecting the voltage across a resistor in series with the DUT.

Optimizing the various settings on the LIA was a necessary condition in order to reach the required sensitivity in the measurements.

It implied selecting the appropriate time delay, bandwith, filters, and frequency. After many attempts, a frequency of 37.1 KHz was selected for providing the best signal to noise ratio. The choice of a high frequency was aimed at decreasing the 1/f noise, to which the device was very sensitive.

Figure 6 gives a schematic representation of the measurement circuit.

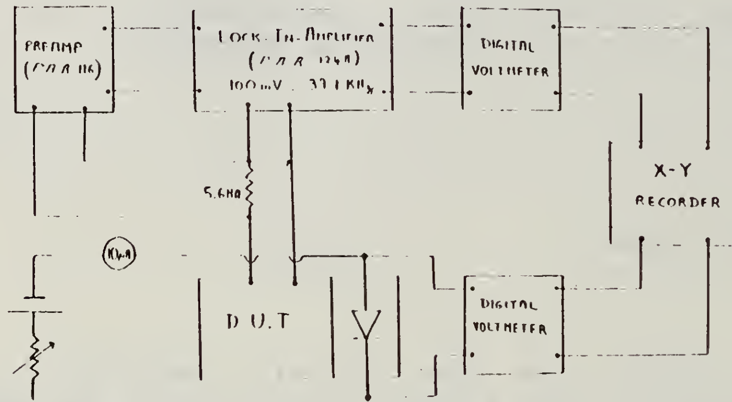

Figure 6

EXPERIMENTAL RESULTS

Successful results were obtained with biased sensors eutectically mounted in delidded TO cans and exposed to various controlled atmospheres. These sensors were AC biased (100 mV, 37.1 KHz), initially heated up to 100 C and maintained at this temperature for several hours, and then slowly cooled down to around -30 C. The temperature was measured with a diode eutectically mounted nearby the sensor. Very good accuracy could therefore not be expected because of the unknown thermal gradient between the temperature sensing diode and the sensor itself. The output signal of the Lock-In-Amplifier was monitored versus temperature during the cooling of the package.

The first experiment did consist of looking at the response of a sensor exposed to the room dew-point (controlled in flow conditions by a General Eastern mirror hygrometer). An onset of conduction (change in slope) could be very clearly detected within 1.5 degrees of the room dew-point. The experiment was repeatable. Each time, the detected dew-point temperature was slightly higher than the value indicated by the hygrometer. This had also been observed previously with DC bias. It might have two causes :

- The thermal gradient in the package
- The need for a certain amount of water to be adsorbed before a conduction can be electrically detected. This amount could be around three monolayers for ionic conduction, and probably a little less than one monolayer for electronic conduction. A theoretical study on conduction mechanisms in adsorbed layers between AC biased electrodes would be necessary for confirming this hypothesis.

The most important series of experiments consisted of studying the sensor response to a wide range of known dew-frost points. The test chamber was therefore connected to a gas generator that allows a flow of controlled humid gas to circulate. Several dew-frost points were generated in the range [0 C to -30 C] and the response of the sensor was recorded each time in the same conditions as for the first experiment described above. The results are summarized in Figure 7.

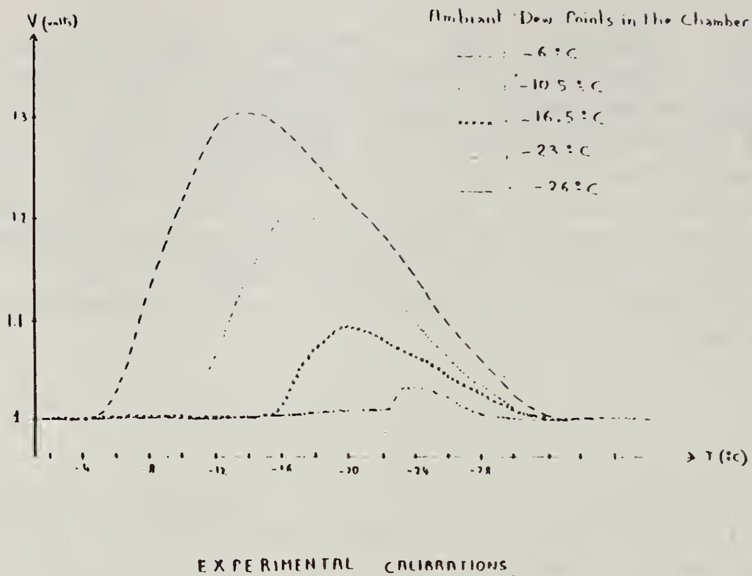

Figure 7

Several remarks can be made on this Figure :

1) The intensity of the leakage current total variation decreases with dew-frost point temperature. This means that the lower the moisture content, the lower the conduction. Therefore, the presence of water in the liquid phase and its abundance strongly affect AC conduction as it did for DC bias. This seems logical as water can be considered as a medium in which electronic and ionic conduction can occur, and as a source of ions.

2) There is an experimental limit (approximately -25 C) below which no conduction can be detected. This limit is the same as the one observed with DC bias. A physical model for explaining the existence of this limit has been proposed elsewhere (1).

3) It is difficult to correlate precisely the temperature at which an onset of conduction was detected and the generated dew-point temperature because of the thermal gradient in the package. Therefore it is important to be have to measure accurately the temperature on the sensor itself, if one wants to make a quantitative measurement.

As a possible answer to this problem, 13 new sensors were sent to us (courtesy of Harris Corporation), in which a diode was integrated in the chip itself. 12 of them passed a detailed visual inspection while 1 revealed a shortage between aluminum metal lines in one location. These parts were sent to Raytheon Co. for mounting (eutectic Au-Si), wire bonding and controlled sealing. The 12 "good" parts were divided in 4 groups of 3 devices, each group being sealed with a different moisture level (1,000 ppmv; 3,000 ppmv; 5000 ppmv and 8,000 ppmv). When the parts came back, it appeared that it was impossible to cool them down enough to reach a condensation point (the notion of dew-point is a closed package and the influence on the adsorption on the walls will be discussed later in this report), so that no measurement were possible. Some of them were open, which revealed that the dies were not properly attached. A failure analysis revealed that, even though a preform had be used, the eutectic did not stick to the die because its back surface had been previously etched. None of these dies could therefore be used, which would have given an answer to the accuracy of this measurement method.

PHYSICAL MODEL FOR QUANTIFYING THE EFFECT OF ADSORPTION ON THE CAVITY WALLS

The concept of dew-point has often been improperly used when reporting moisture measurements based on in-situ devices for which a cooling process is necessary. This is because one usually neglects the effect of adsorption on the cavity walls. Most tables and graphs giving a direct correlation between a dew-point temperature and a moisture content expressed in ppmv are based on the strict application of the ideal gas law. The intent of the following model is to develop a modified ideal gas law taht takes into account the adsorption on the cavity walls during the cooling of the package. This is very important when one tries to compare results obtained by two differentanalytical techniques, in which this contribution can be very different.

The ideal gas law applied to the partial pressure of water gives :

$$P\ V = n\ R\ T$$

where P is the partial pressure of water, V the volume of the package, n the total number of moles, R the constant of gas and T the temperature.

If one takes the adsorption into account, it becomes :

$$P\ V = (\ n_{100} - n_{ads}\ )\ R\ T$$

where n is the total number of moles of free water vapor at 100 C (neglecting what is adsorbed at this temperature) and n , the number of moles of water adsorbed on the walls at any temperatue T below 100 C.

The determination of n is the critical parameter that will enable a comparison between what can be measured by a technique working at 100 C (RGA, IR), a technique working at room temperature (Panametrics sensors) or a "dew-point" technique (surface conductivity, conductance technique). It is strongly dependant upon the surface areas of the materials involved, the surface to volume ratio and the thermal gradient in the package.

In the case of the samples on which the experimental study was performed, if one neglects the amount of water adsorbed on the sensor itself as compared to what is adsorbed on the gold-plated cavity walls during the cooling process, and the existence of a thermal gradient aimed at condensing moisture first on the sensor, n_{ads} can be determined by the BET model.

For this extremely simplified model, the number of water molecules adsorbed on the cavity walls at a given temperature and relative humidity can therefore be written :

$$n_{ads} = n_o \left(\frac{r}{1-r} \right) * \left(\frac{\exp(\emptyset/RT)}{1+r[-1 + \exp(\emptyset/RT)]} \right)$$

where $\emptyset$ = E1-El is the difference between the heat of evaporation of water and the heat of adsorption of water vapor on the adsorbate.
n_o is the number of water molecules necessary to cover the cavity internal surfaces with one monolayer.

n_o , E1 and El strongly depend on the materials inside the package (plating of the cavity walls, organic adhesives....), but can be found in literature for almost any material.

r is the relative humidity defined by : $r = \frac{P}{P^o}$

Where P is the partial pressure of water at a given temperature, and P^o the saturating vapor pressure of water at this temperature.

P^o can be determined by the Clapeyron equation :

$$P^o = Pseal \left(\frac{373}{Tseal} \right) * \exp \left[\frac{\Delta Hvap}{R} \left(\frac{1}{373} - \frac{1}{T} \right) \right]$$

n_{ico} is defined by the ideal gas law : $n_{ico} = \frac{P_{ico} * V}{373 * R}$

where P_{ico} = Ptotal at 100 C * Xppmv * 10^{-6}

This model has been applied to gold plated TO-8 packages; the results are summarized in the following table.

MOISTURE CONTENT at 100 C (in ppmv)	DEW-POINT (computed by Ideal Gas Law	DEW-POINT (computed by modified Ideal Gas Law)
1000	- 23 C	- 27 C
3000	- 9 C	- 13 C
5000	- 3 C	- 7 C
10000	+ 6 C	+ 2 C

RECOMMENDATIONS

The following recommendations can be made at the end of this study :

Surface conductivity moisture sensing chips can be used for performing measurements of any hermetic package moisture content provided that all the conditions listed below are fully satisfied :

- The chip must include a temperature sensing diode
- The die-attach material must be a good thermal conductor, and must not adsorbe more moisture than the other materials in the cavity.
- AC bias is required in order to avoid reproducibility problems.
- The bias frequency and voltage must be optimized according to the measurement circuit used. The use of a Lock-In-Amplifier is advised for obtaining the required sensitivity (signal to noise ratio).
- A thermal gradient must be maintained in the package, so that condensation can be assumed to occur first on the sensor.
- The adsorption properties of all the materials used in the package (plating, lid....) must be known precisely, if one wants to make a quantitative measurement, and correlate this result to other techniques such as RGA, for which the thermal conditions are different.
- A precise knowledge of the sealing conditions (temperature, pressure) is also necessary.

CONCLUSIONS

1) A new, original test setup has been developed at RADC, that allows measuring non-destructively the water vapor content of any integrated circuit hermetic package. This system allows working either in vacuum for measurements on hermetically sealed parts, or in a controlled humid atmosphere, for calibrations on delidded parts.

2) Calibrations have been succesfully performed on AC biased interdigited surface conductivity moisture sensors eutectically mounted in delidded TO- packages, for moisture levels corresponding to the range [0 C to -25 C] in "dew-frost" points.

3) A physical model has been developed that allows correlating the electrical "dew-point" measured by an in-situ surface conductivity sensor to the actual moisture content as measured by a mass spectrometer. This model is a modification of the ideal gas law applied to the partial pressure of water in the package, that takes into account the adsorption on the cavity walls during the cooling process. However,the accuracy of this model would be improved if one could quantify the influence of the thermal gradient in the package.

4) Several recommendations have been made that should allow potential users to become aware of this very promissing technique of its requirements and limitations.

REFERENCES :

(1) Recent Developments on Moisture Measurement by Surface Conductivity sensors
Didier Kane and Michel Brizoux
Proceedings of the 1986 International Reliability Physics Symposium

(2) Physical Characterization of Surface Conductivity Sensors in the Aim of an Absolute Moisture Measurement in Electronic Components
Didier Kane, Robert Gauthier, Michel Brizoux and Jacky Perdrigeat
Proceedings of the 1984 Electronic Components Conference

4.4 TUNABLE DIODE LASER SYSTEMS FOR MOISTURE MEASUREMENT IN INTEGRATED CIRCUIT PACKAGES

D. Wall, J. Sproul, and A. Mantz
Spectra-Physics, Inc., Laser Analytics Division
25 Wiggins Avenue
Bedford, MA 01730

Tunable diode laser techniques for moisture determination in IC packages developed by Mucha (Bell Labs, 1981) have been implemented in commercially available systems. This paper will discuss details of operation, system calibration, and performance specifications. Comparisons to existing mass spectrometric techniques and instrumentation will be drawn. Finally, data will be presented showing correlations between systems and techniques using prepared package standards.

Since the last RADC/NBS International Workshop on Moisture Measurement and Control for Microelectronics held in 1983, three prototype semi-automated tunable diode laser systems have been developed and constructed with two systems delivered to beta sites for evaluation. The measurement principles are those developed and described by J. Mucha (1-3). These systems are designed to be automated and except for loading of packages and puncturing operation, the systems are fully automated including long-term frequency stabilization (2) of the laser to insure that the diode laser is operating at the peak of the water line.

In this paper we describe the results from two extensive measurement programs utilizing one system installed at National Semiconductor (NSC) and one at Laser Analytics. In these experiments we attempted to statistically characterize the system performance. The first experiments were oriented toward establishing a correlation between Mass Spectroscopic results, measured under the method (MIL-STD Method 1018.2), and the tunable diode laser results obtained utilizing the method developed by J. Mucha (1). These results were obtained on production packages which were collected from production runs.

In the second experimental program, we performed a "round robin" experiment in which two independent sets of diode laser measurements were compared with Mass Spectrometric results measured by the MIL-STD Method 1018.2 Method. In this experiment large numbers of packages were sealed in a carefully controlled atmosphere in which humidity conditions were carefully adjusted and monitored.

CORRELATION EXPERIMENT RESULTS

Packages manufactured by National Semiconductor Corporation (NSC) were used in this experiment. Package sizes included TO-3 in which

fifteen packages were measured by the Mass Spectrometric (MS) method and fifteen packages were measured utilizing the tunable diode laser (TDL) system at NSC. Thirty-nine TO-5 packages were measured by the MS, and thirty-nine were measured by the TDL. For TO-46 packages, sixteen were measured by TDL, and ten were measured by MS.

The results are presented for each package size in Figures 1-3. In each figure the number of packages measured in a concentration range is plotted on the vertical axis, while the horizontal scale presents H_2O concentration. The width of each horizontal cell (in ppm) is presented in each figure. For example, in Figure 3 we present results for a TO-46 package, each cell width (vertical bar) is 500 ppm wide, and we measured three packages in the region 11500 to 12000 ppm utilizing the TDL method. TDL results are plotted with solid histograms while MS results are plotted utilizing open bars.

Figure 4 contains a weighted least squares fit to the TDL data presented in Figures 1-3. Error bars for each package size are presented as one standard deviation (1σ). The dashed curves represent 1σ limits on the slope and intercept values determined by fitting the data. Each package size is represented by its internal total surface area to internal volume ratio.

Figure 5 shows the Mass Spectroscopic results taken from Figures 1-3 and plotted in a similar manner.

Table I summarizes the surface area/volume ratio for each package type, accurately calculated from NSC package drawings, and the mean value of the measured concentration for each can type. These data are obtained from the data in Figures 1-3, as well as the numerical value for one standard deviation for both TDL and MS methods. Finally, calculated

concentrations for each can type are calculated from Figure 4 for TDL results and from Figure 5 for MS results. The calculated concentrations are presented in Table I.

From Table I it can be seen that, while TDL and MS results differ significantly for different can types, the standard deviations are essentially identical. This suggests that the error bars are determined from the statistical variability in the samples, or the two methods have similar error limits. The results from the second experiment will provide more insight to this point.

CORRELATION EXPERIMENT ANALYSIS

Referring to Figures 4 and 5, it appears that both TDL and MS results when plotted versus internal surface area to volume ratio are linear with different sensitivity to surface area to volume ratio (slope). In order to further analyze these results, we plotted the ratio of TDL to MS results for each package type as seen in Figure 6.

In relating our experiment to previous published measurements on similar metal packages, we utilized the results of the 1981 RADC TO-18 Round Robin which are included in Table II. In the 1981 Round Robin test four independent Mass Spectrometric measurements were reported as well as infrared measurements made with the package at 100C or 25C. Since our data were run with 100C conditions, we selected only the high temperature data for comparison.

Table III contains a summary of TDL/MS ratio results. MS values were selected to be the average value of the four reported MS measurements for a particular moisture concentration.

Figure 7 shows that the TDL/MS ratio, from the 1981 Round Robin results, is essentially constant over the entire range of concentrations tested. These data are the same data set presented in Table III, but presented in a graphical format.

From Figure 7 we conclude that, for a given package type, the TDL/MS ratio, once measured, is a constant which also tells us that a definite fixed correlation exists between the TDL and MS results for each package type.

Taking this analysis one step further, we calculated an internal surface area to volume ratio for a TO-18 package and plotted the Round Robin results (labelled Bell Labs TO-18) in Figure 6. The error bar on the Bell Labs TO-18 data point reflects the one standard deviation value of the ratio. From the least squares fit data, we calculated a TO-18 value (labelled National Semiconductor TO-18) which is well within the error bars for the Round Robin data, and which fits the weighted least squares fit function for TO series cans very well.

TUNABLE DIODE LASER (TDL) AND MASS SPECTROSCOPIC (MS) EXPERIMENT RESULTS

The purpose of this experiment was to produce a large number (3000) of standard hermetically sealed IC packages (TO-3, -5, -18, and -46) under known and well-controlled humidity conditions for subsequent testing utilizing both TDL and MS methods. The description of the procedure for filling the packages is described as follows:

1. The Moisture Generator

   A variable rate moisture generator was designed and constructed at LAD using a Valcor Model SV 515 metering pump as the water injector. Distilled H_2O was injected at a nominal

rate of 5-6 microliters/pulse onto a heated aluminum block capable of flash vaporizing the water. The vapor was then mixed with the flowing N_2 in a 20-gallon mixing chamber and carried to the sealing station. The pulse rate of the metering pump was controlled by a solid state timer and could be varied between 3 and 120 pulses/minute. The thermally large aluminum block was heated by two cartridge heaters and regulated by a thermocouple/temp. controller. In all cases, the block temperature was maintained at 150°C.

Using a 25mℓ Buret and a separatory funnel as a reservoir, the solid state timer could be calibrated by measuring the decrease in Buret water level versus time. The humidifier was capable of injecting up to 1000 microliters/minute into an N_2 purge. The complete humidifier is shown in Figure 8.

2. The Sealing Station

The two IC sealing stations were located at NSC. One station is designed specifically for sealing TO-3 packages while the other can accommodate TO-5, TO-18, and TO-46 IC packages. Using the glovebox mounted on each station, the operator could passes the samples into the sealing chamber via a "Bake-Out" oven or small purge chamber, both located at the ends of the main sealing chamber. During normal operation, dry N_2 flows through the box at a nominal rate of 600 SCFH. During that portion of the experiment where moisture was being added, the flow was reduced to 100 SCFH through the humidifier.

There are two inlets to the sealing chamber from the humidifier. Inside the chamber, the moisture level can be

monitored with two sampling lines. One line is held fixed near the welding area while the other can be placed at any location in the box to monitor moisture level gradients that may exist. Each line can be toggled on or off separately. In normal operation, both sampling lines are placed on opposite sides of the welding area to assume an average moisture concentration.

3. The Dew Point Hygrometers

Two EG & G Model 660 Dew Point Hygrometers were used to determine the moisture content in the sealing chamber. At a known pressure, the dew point of a gas is related to the H_2O concentration. Table IV shows this relation. For example, if the Dew Point Hygrometer reads -20^oC at 760mm Hg then the ppmV H_2O is 1020. One Dew Point Hygrometer was used to monitor an inlet line into the sealing chamber--effectively, the moisture level in the humidifier. The other Dew Point Hygrometer monitored either or both of the sampling lines. A small air pump drew the moist N_2 through each Dew Point Hygrometer at a rate of 3 SCFH. Cooling water was provided for the Dew Point Hygrometer sensors to relieve cooling requirements at low dew points at a non-critical flow of 1/2 GPM. The Dew Point Hygrometer's could be read to the nearest tenth of a degree C. Refer to Figure 9 for a schematic description of the experimental set-up.

THE EXPERIMENT:

As stated previously, two complete sealing stations were needed to seal all the samples. The procedure described is applicable to

both stations. At the termination of sealing packages at all concentrations on one station, the equipment was disconnected and reassembled on the other. Five package types: TO-3, TO-5 (flow 80), TO-5 (flow 85), TO-18, and TO-46 were sealed at four concentrations; dry, 3000 ppm, 6000 ppm, and 10000 ppmV H_2O target value. Initially, all caps and IC headers were baked at 150°C for one hour in the side purge oven to remove any trapped moisture. After baking, the units were transferred directly into the sealing chamber and allowed to cool. It was necessary to seal the packages at the driest level first and then increase the moisture level progressively. For dry N_2 sealing, the purge line bypassed the humidifier and was connected directly to the sealing chamber and the flow set at 600 SCFH. The dew points were monitored until a stable condition existed. Usually, the dew point reached a minimum around -48.0°C (approximately 50 ppmV H_2O). Welded packages were passed out through the side purge chamber. The next target valve was 3000 ppmV H_2O. It was necessary to reconnect the purge line to the humidifier and cap the fitting on the sealing chamber. The heater block in the humidifier was turned on and allowed to warm up. The purge flow was reduced to 100 SCFH. After ten minutes the metering pump was turned on and adjusted to the approximate pumping rate. The rate can be calculated as follows:

The metering pump timer is calibrated in microliters/minute. We know the target concentration of H_2O to be 3000 ppmV @ 100 SCFH dry N_2.

Use the rate equation: $r = \frac{FC}{K} \times 4.7195 \times 10^{-4}$

Where r = Rate, microliters/minute
F = Dilution Flow, SCFH
C = Concentration, ppmV
K = Molar Volume Constant @ 25° = 24.47/M.W.
M.W. H_2O = 18

$$\text{so } r(\text{microliters/minute}) = \frac{(100 \text{ SCFH})(3000 \text{ ppmV} \times 4.7195 \times 10^{-4}}{24.47/18}$$

$$= 104 \text{ microliters/minute}$$

After setting the pump to this value, the inlet Dew Point Hygrometer was monitored to attain the actual moisture level. At the same time the sampling line Dew Point Hygrometer came to an equilibrium value. Small changes were made to the pulse timer until the sealing chamber dew point reached its proper value. Equilibrium may take up to an hour or more depending on how much adsorption takes place. The inlet Dew Point Hygrometer could fluctuate by as much as $\pm$ 0.5°C due to large moisture fluctuations at each pump pulse. The dew point in the sealing area stabilized to within $\pm$ 0.1°C throughout the sealing time. This corresponded to a moisture level accurate to approximately $\pm$ 1%. Table V depicts the target values and actual data taken from the experiment.

At the end of one moisture concentration, the cycle was repeated. The humidifier was turned up, fine-tuned, and allowed to come to equilibrium before sealing began. In all, a total of 3000 packages were sealed: 150 of each type at each concentration.

RESULTS

Table VI summarizes the results we have measured on these packages. Results for each package type are grouped by target

concentration (50 ppmV, etc.) for each laboratory [Laser Analytics (LAD), National Semiconductor (NSC), and the Mass Spectroscopic facility (MS)] for each laboratory the number, n, in parentheses [i.e. (23)] represents the number of packages measured, the next number is the average concentration value, CBAR, and the third number in the group is the one standard deviation value, s.d., for that particular measurement.

Figures 10-13 also summarize the results obtained for TO-46 cans, TO-18 results are summarized in Figures 14-18, and TO-3 results are summarized in Figures 19-21. Data are presented as normal Gaussian distributions with one standard deviation representing the width in order to visually sense the overlap. Results for one set of concentrations are summarized in each graph.

CONCLUSIONS

Readings for 50 ppmV on all systems are suspect for several reasons. First, the values as well as the standard deviations determined decrease with increasing volume. Secondly, we do not have a model to explain the results. We do know that we can generate very reliable results in flowing gas systems. We have made infrared measurements on other TDL systems in the ppmV level. Additional work will be necessary to better understand what we see. This will probably require looking into different experimental configurations to determine the effect of injection volumes and surfaces as well as some attempt to better understand how much water is actually sealed in one of these packages under the conditions imposed by the sealing technique.

In general all techniques give rather large standard deviations in the TO-46 can results. These results suggest a S/N problem for the TDL systems, which were designed primarily to accommodate larger volume packages. The standard deviations for Table VI appear to support a system standard deviation (whether due actually to the system or to the package sealing process) which is smaller than the deviations measured in Table I.

In comparing the results from Table I with those from Table VI, it appears that the Table I packages were probably sealed with moisture concentrations of approximately 1500-2500 ppmV for TO-3, between 2000 and 3000 ppmV for TO-5, and something between 2000 and 6000 ppmV for the TO-46 cans. Most likely results suggest all moisture levels were sealed at approximately 2000 to 2500 ppmV.

The data in Table VII generally support the results of Figure 6 for all other packages.

GENERAL CONCLUSIONS

Surface area/volume ratio and TDL/MS ratio define a unique linear function for the TO series cans we checked over the range of moisture concentrations we were able to measure, with the exception of TO-46 cans. This is a particularly important result since the packages we tested were not prepared in any special way for the first experiment, and the second experiment results were supportive.

Additional research is required to better understand the physics and chemistry of the measurement process and the results for small packages, especially with low concentrations. At this point low concentrations (below 3000 ppmV) probably cannot be reliably performed with any method on small volume cans (similar to TO-46).

REFERENCES

1. J. A. Mucha and P. R. Bossard, "Measurements of Water Vapor in Integrated Circuit Packages using an IR Diode Laser," Moisture Measurement and Control for Semiconductor Devices, NBS (November, 1980).

2. P. R. Bossard and J. A. Mucha, IEEE Proceedings of the 19th Annual International Reliability Physics Symposium. p. 60. (1981).

3. J. A. Mucha, Appl. Spectroscopy. 36, 393 (1982).

TABLE I

H2O DATA

		LASER		MS	
PKG	S/V (CM-1)	$\bar{C}$ (MEAS) (S)	$\bar{C}$ (CALC)	$\bar{C}$ (MEAS) (S)	$\bar{C}$ (CALC)
TO-3	6.79	1019 (586)	1195	1484 (677)	1315
TO-5	17.26	4151 (1056)	3914	1938 (1156)	2167
TO-46	47.00	11575 (1610)	11637	4646 (1662)	4586
(TO-18	19.61	---	4524	---	2358)

TABLE II

Results* of R.A.D.C. TO-18 Round Robin (December, 1981)

	-MASS SPEC. AT 100°C-				-INFRARED-	
TARGET	RADC	LAB 1	LAB 2	LAB 3	100°C	25°C
1000	2663	2800	1981	3067	5420	2639
3000	4535	5730	3317	8690	8630	3724
5200	5327	5670	5631	4453	10,250	4753
6000	6040	7800	5417	6676	12,257	5460
10,000	10,060	9900	8301	9170	14,220	8897

*All values in ppm by volume moisture.

TABLE III

COMPARISON TO BELL LABS RESULTS

TARGET	$\bar{C}$ (ALL MS)	IR/MS	$\bar{C}$ (-H/L)	IR/MS	IR/RADC
1000	2628	2.06	2732	1.98	2.04
3000	5568	1.55	5133	1.68	1.90
5200	5270	1.94	5479	1.87	1.92
6000	6483	1.89	6358	1.93	2.03
10000	9358	1.52	9535	1.49	1.41
	$\overline{IR/MS}$	1.79 (0.24)		1.79 (0.20)	1.86 (0.26)

CALC. RATIO FOR NAT. SEMI. IR/MS
(CALC. FOR TO-18 PKG.) = 1.92
(RANGE 1.80-2.05
FOR +/- 100 PPM
SWING IN CONC'S)

TABLE IV

DEWPOINT °C	DEWPOINT °F	VAPOR PRESSURE (WATER/ICE IN EQUILBRIUM) mm OF MERCURY	PPM ON VOLUME BASIS AT 760 mm OF Hg PRESSURE	RELATIVE HUMIDITY AT 70°F%	PPM ON WEIGHT BASIS IN AIR
- 48	- 54	.0378	49.7	.202	30.9
- 42	- 44	.0768	101.	.410	62.7
- 26	- 15	.430	566.	2.30	351.
- 20	- 4	.776	1020.	4.13	633.
- 12	+ 10	1.632	2150.	8.69	1335.
- 8	+ 18	2.326	3060.	12.4	1900.
- 2	+ 28	3.880	5100.	20.7	3170.
+ 8	+ 46	8.045	10590.	42.9	6580.
+ 14	+ 57	11.99	15780.	63.9	9800.

TABLE V

TARGET VALUE	EXPERIMENTAL DEW POINT (DEGREES CENTIGRADE)	PPMV H_2O	$\pm \Delta$ PPMV @ $\pm$ 0.1°C
Dry	-48.0°C	49.7	$\pm$ 0.61 ppmV
3000 ppm	-8.2	2962	$\pm$ 25
6000 ppm	+0.35	6186	$\pm$ 48
10000 ppm	+7.6	10318	$\pm$ 68

TABLE VI

RESULTS TABULATED BY LABORATORY, PACKAGE TYPE, AND TARGET CONCENTRATION

PACKAGE TYPE/	50 PPMV			3000 PPMV			6200 PPMV			10300 PPMV		
LABORATORY	n	CBAR	±1 s.d.	n	CBAR	±1 s.d.	n	CBAR	±1 s.d.	n	CBAR	±1 s.d.
TO-46												
LAD	(20)	4976	±2084	(20)	6595	±2419	(20)	9204	±3665	(4)	11814	±1409
NSC	(10)	5273	±1802	(10)	10555	±3255	(10)	13048	±3871	(5)	17296	±2174
M. SP.	(4)	890	±332	(10)	5115	±1050	(10)	7624	±1184	(1)	12700	
TO-18												
LAD	(20)	2509	±894	(20)	4845	±950	(20)	6290	±1258	(8)	10244	±2570
NSC	(15)	4095	±1308	(15)	6523	±1481	(10)	10242	±654	(5)	12866	±1795
M. SP.	(10)	1782	±1389	(10)	4549	±1754	(10)	8641	±2111	(6)	13497	±7617
TO-5 F-80												
LAD	(23)	1952	±1254	(25)	5465	±2402	(24)	6605	±902	(24)	9711	±1615
NSC	(15)	2500	±662	(15)	6465	±1193	(20)	11381	±2900	(15)	13312	±1606
M. SP.	(9)	1114	±503	(10)	4868	±1062	(10)	10788	±5254	(9)	11756	±1266
TO-5 F-85												
LAD	(25)	2426	±1099	(25)	5568	±1006	(25)	7879	±1744	(26)	9910	±1499
NSC	(15)	3662	±739	(15)	7811	±1941	(15)	11505	±1754	(15)	14847	±1879
M. SP.	(10)	1164	±643	(10)	4778	±526	(10)	7957	±2016	(10)	14160	±2214
TO-3												
LAD	(25)	335	±192	(25)	2229	±521	(25)	4474	±698	(24)	7776	±842
NSC	(25)	184	±76	(20)	2615	±1007	(15)	6020	±1602	(10)	10117	±1717
M. SP.	(15)	133	±64	(15)	2393	±1074	(15)	5098	±827	(15)	11665	±2389

TABLE VII

IR/MS VALUES FOR PACKAGE RESULTS IN TABLE V

LABORATORY	50 PPMV	3000 PPMV	6200 PPMV	10300 PPMV	ENSEMBLE AVERAGE
TO-46					
LAD	5.59	1.28	1.20	0.93	<2.51>
NSC	5.92	2.06	1.71	1.36	
TO-18					
LAD	1.41	1.06	0.73	0.76	<1.23>
NSC	2.29	1.43	1.19	0.95	
TO-5 F-85					
LAD	2.08	1.17	0.99	0.70	<1.53>
NSC	3.15	1.63	1.44	1.05	
TO-5 F-80					
LAD	1.75	1.12	0.61	0.83	<1.26>
NSC	2.24	1.33	1.05	1.13	
TO-3					
LAD	2.52	0.93	0.88	0.67	<1.19>
NSC	1.38	1.09	1.18	0.87	

FIGURE 1

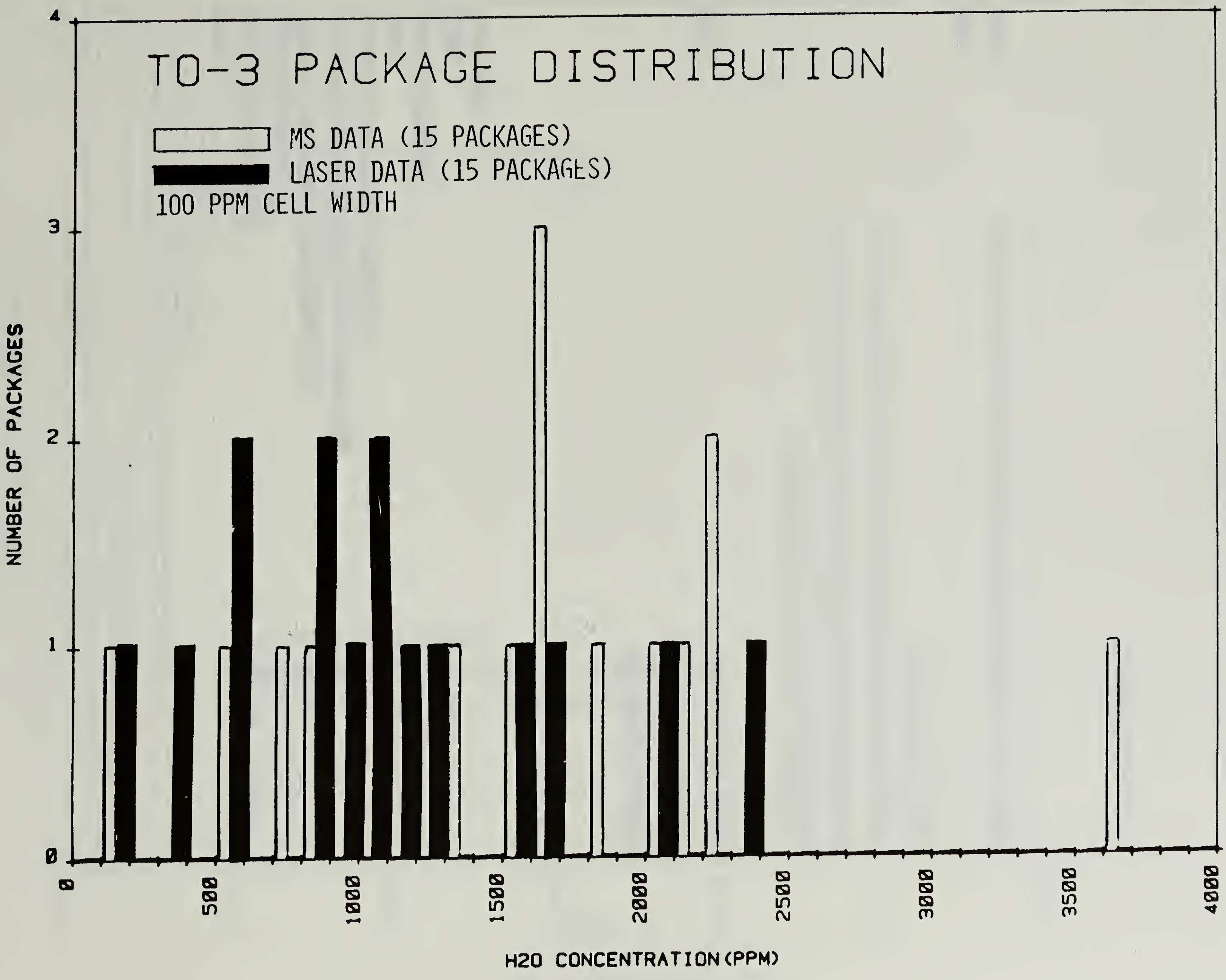

FIGURE 2

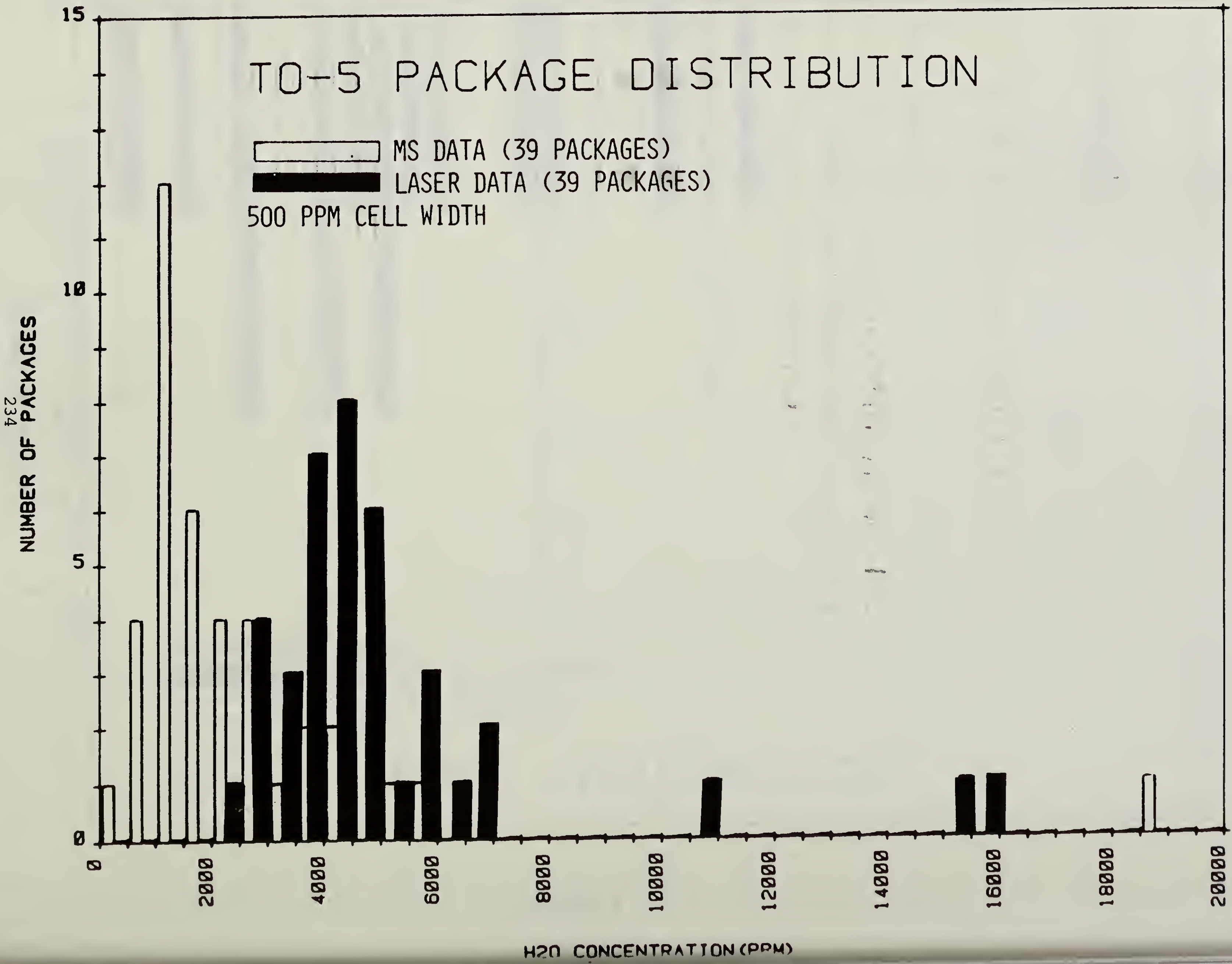

FIGURE 3

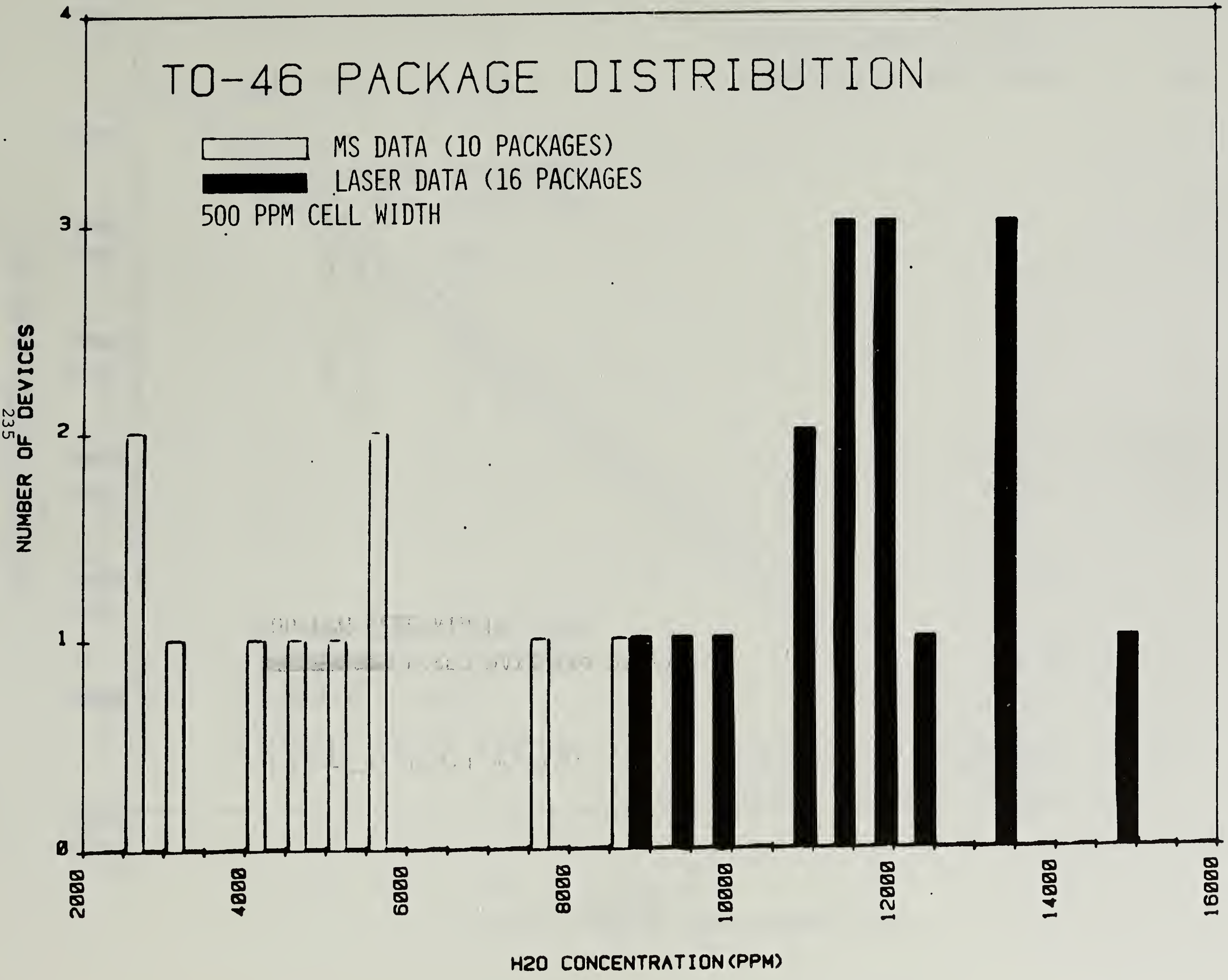

FIGURE 4

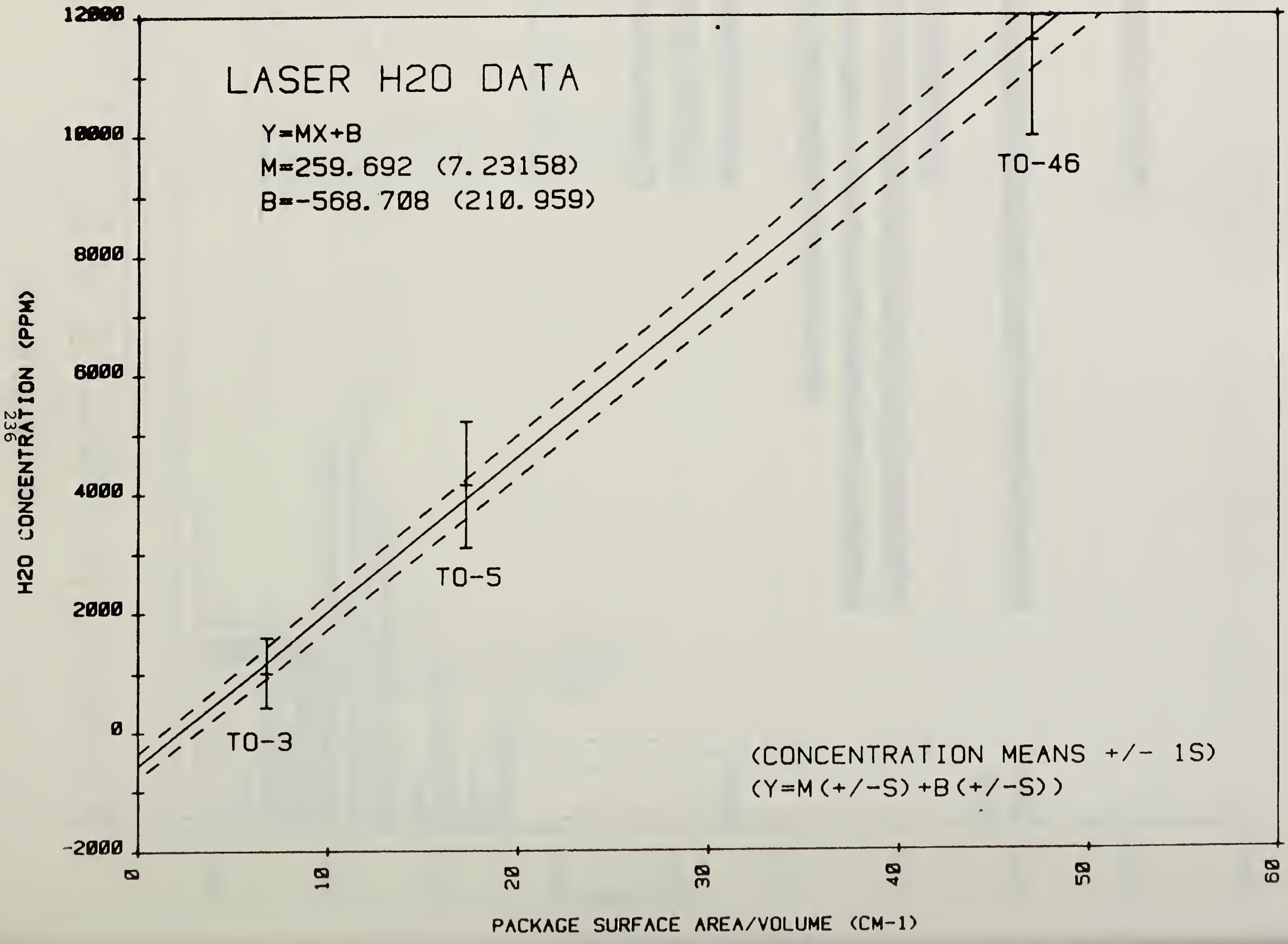

FIGURE 5

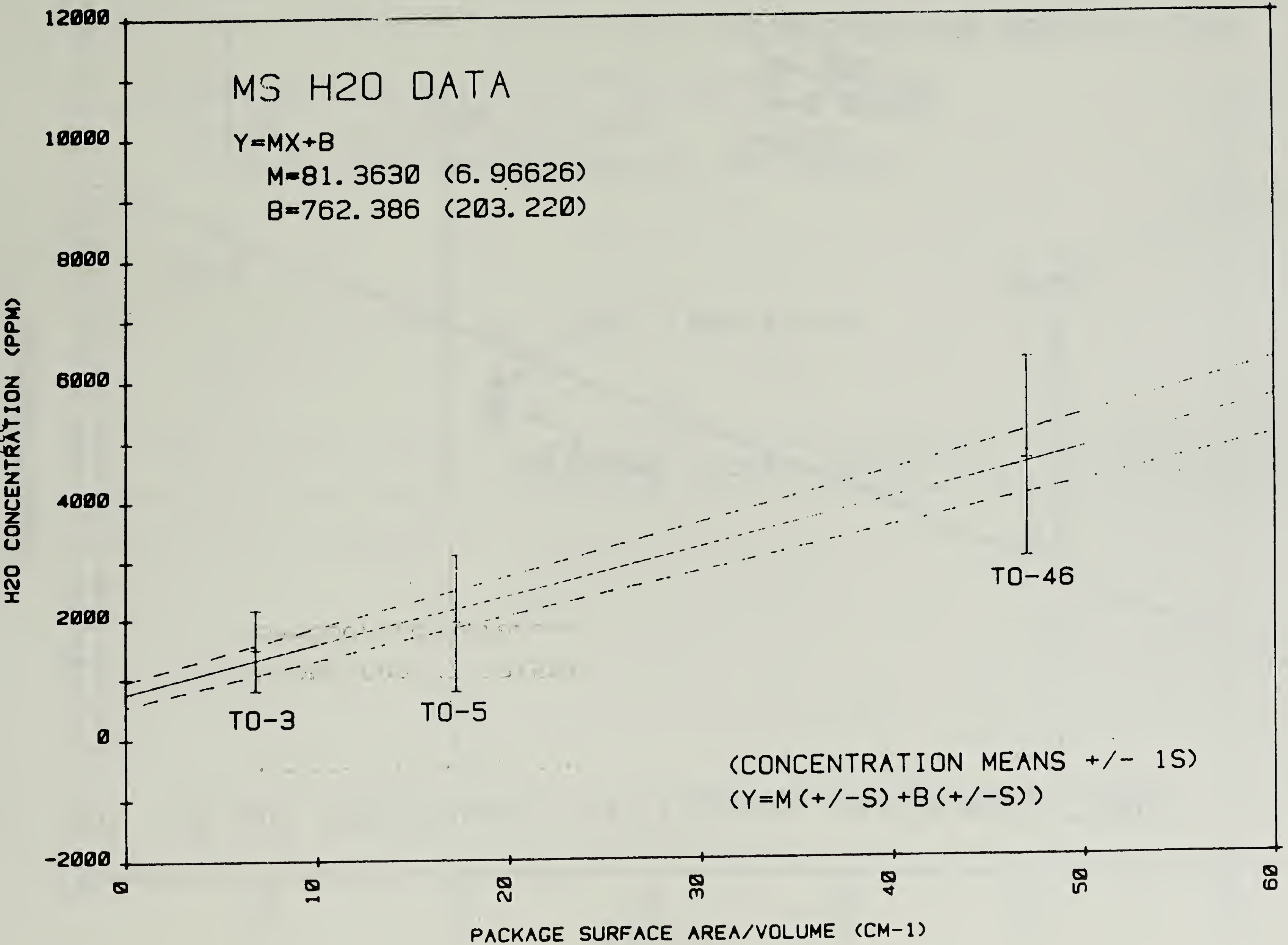

FIGURE 6

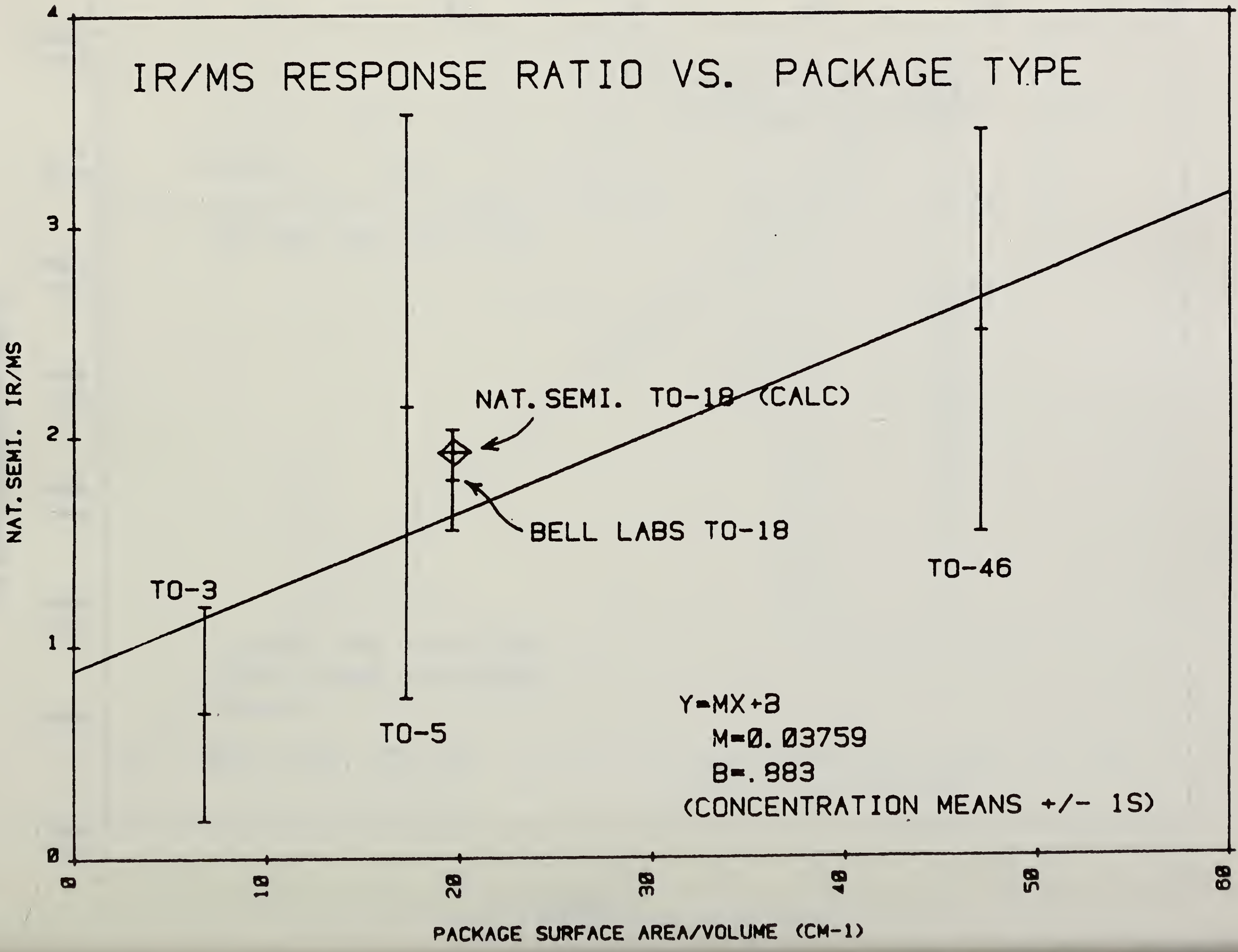

FIGURE 7

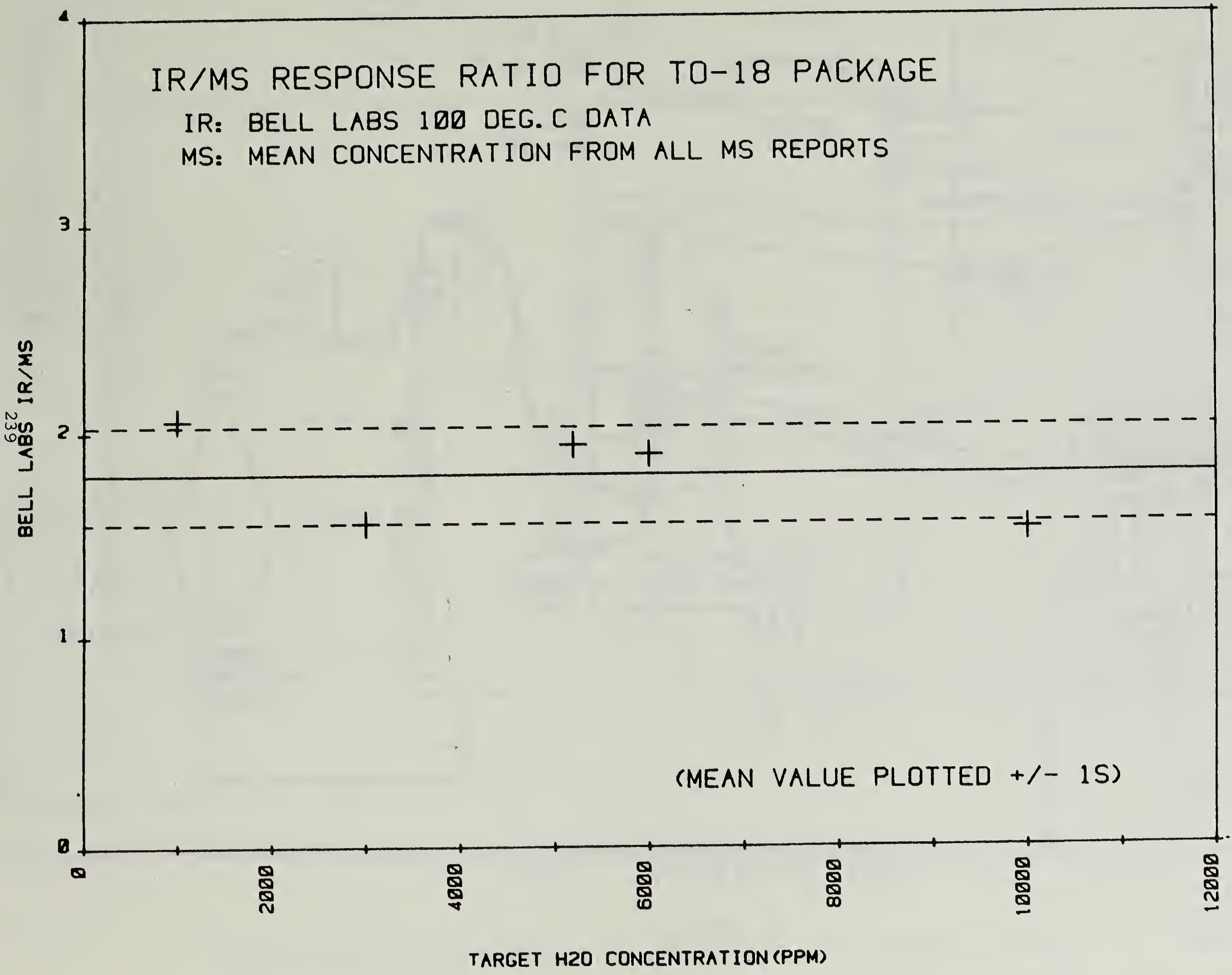

FIGURE 8

LAD HUMIDIFIER

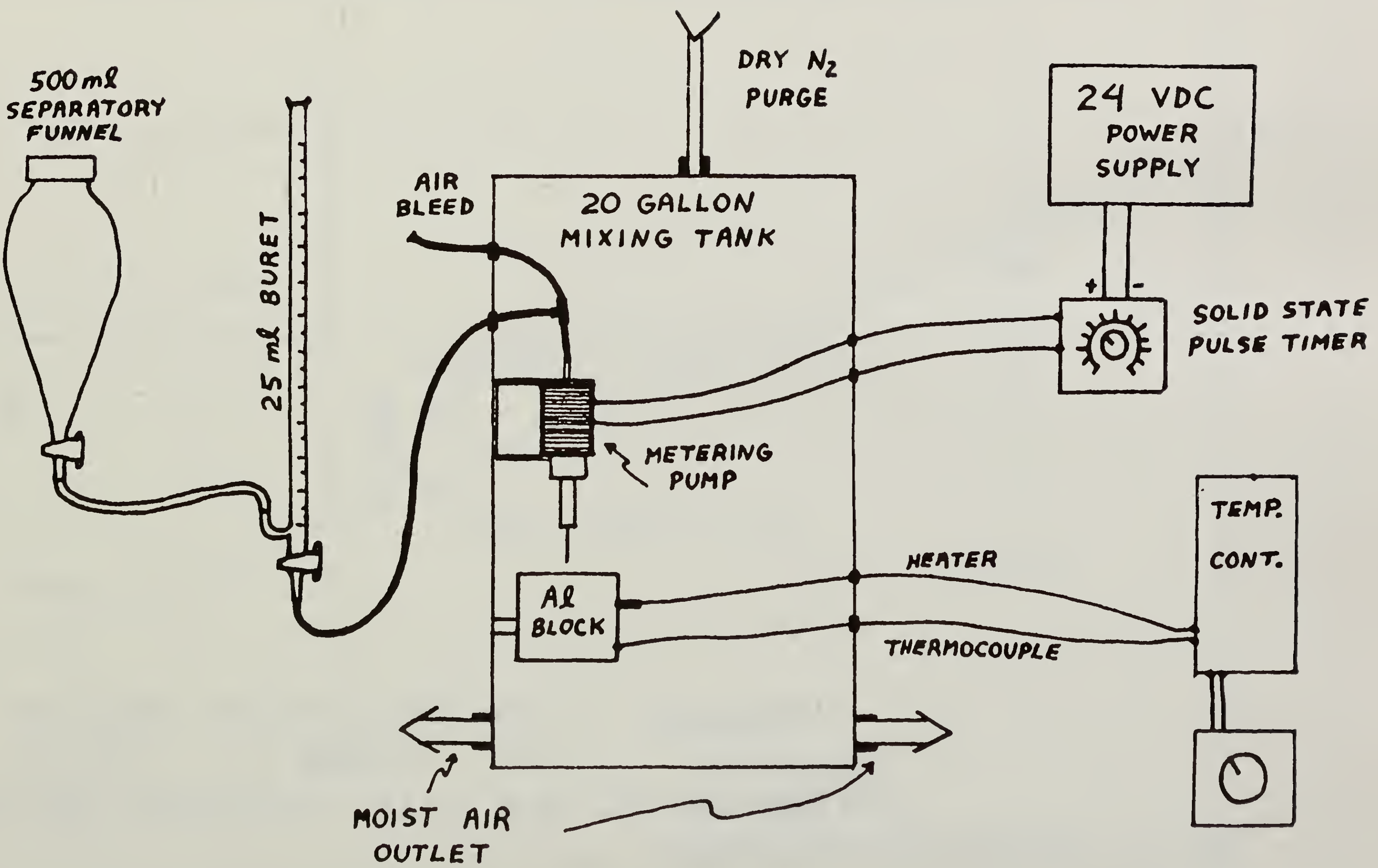

FIGURE 9

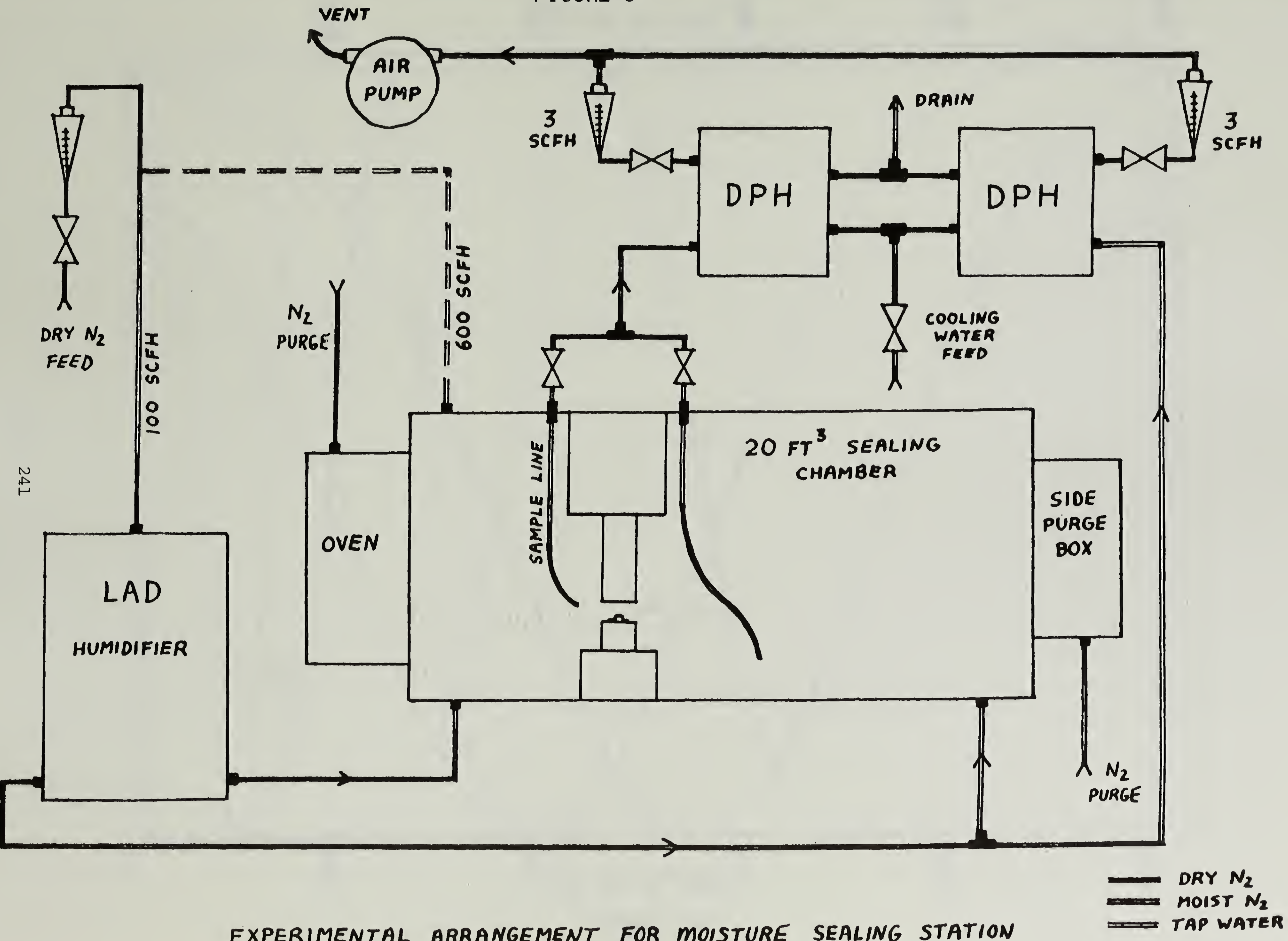

EXPERIMENTAL ARRANGEMENT FOR MOISTURE SEALING STATION

FIGURE 10

TO-46 50 PPM

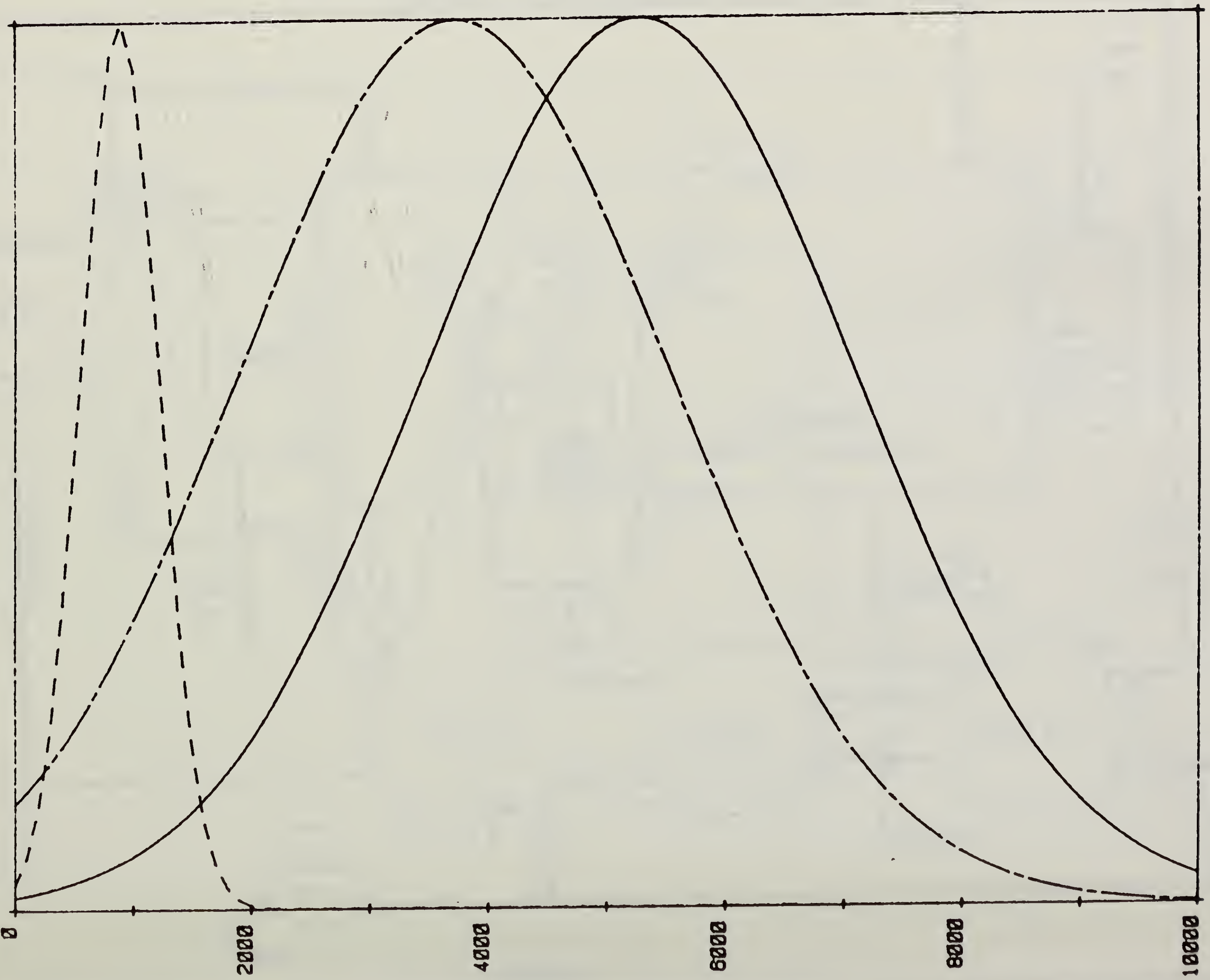

FIGURE 11
TO-46 3K PPM

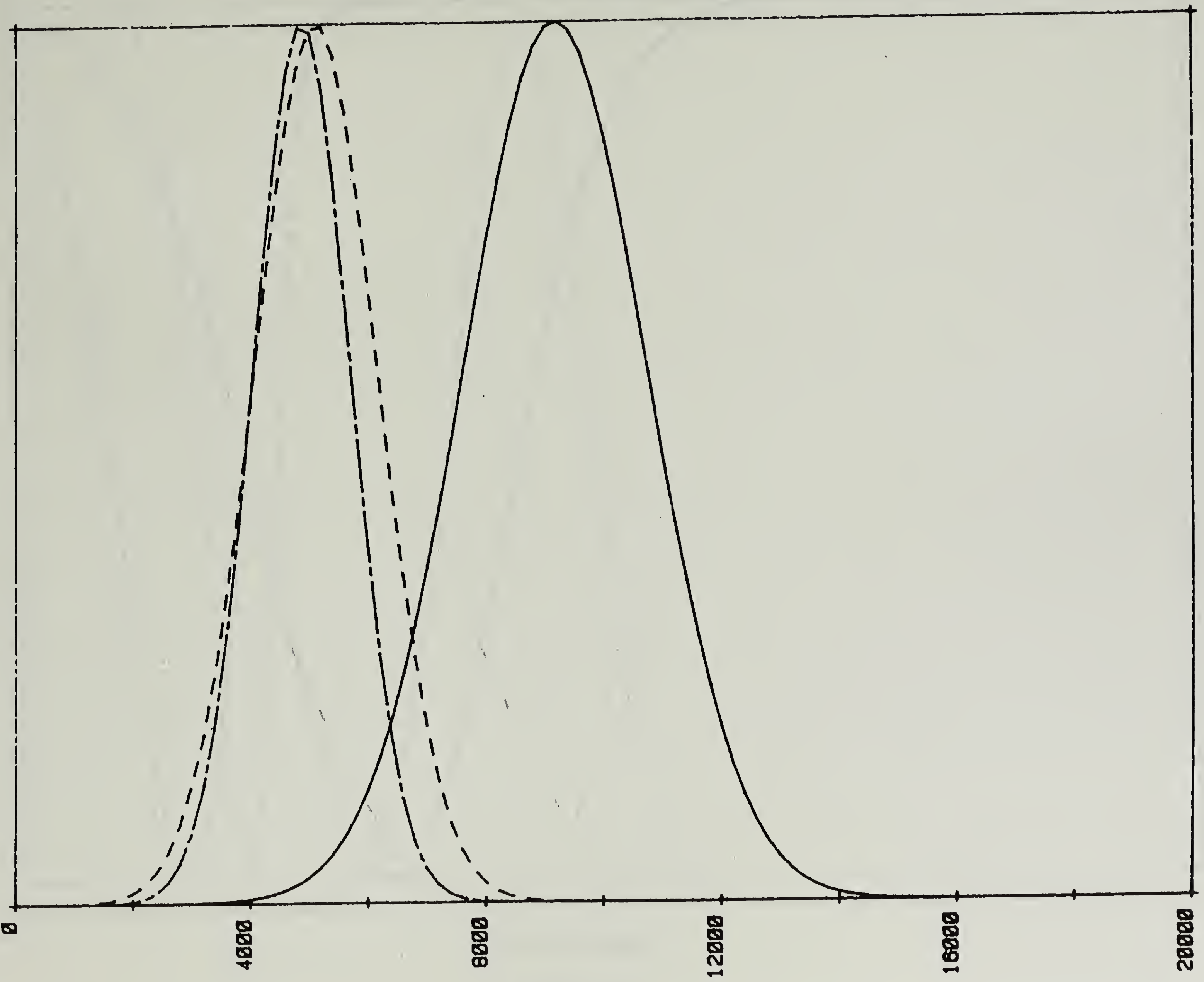

FIGURE 12
TO-46 6K PPM

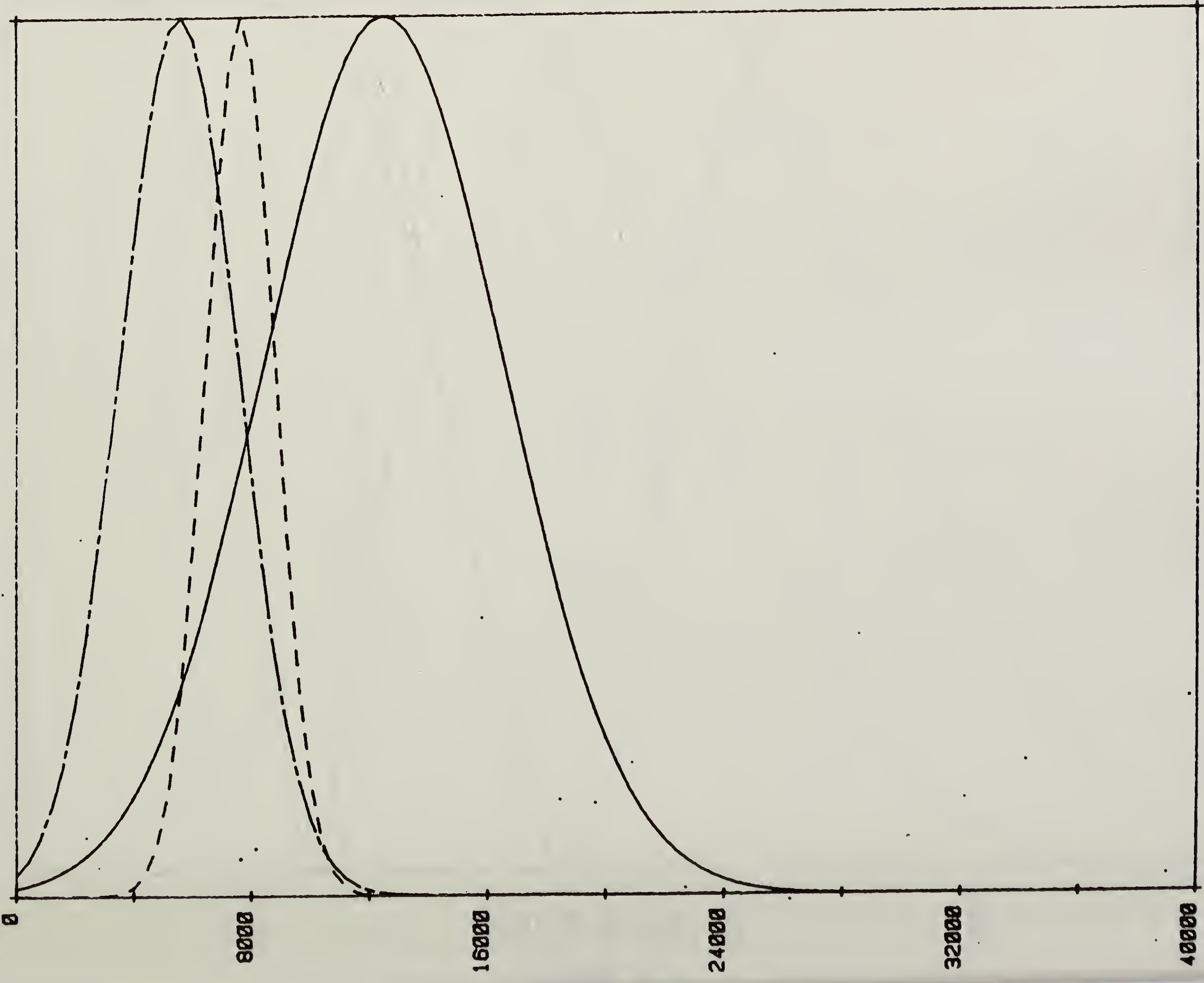

FIGURE 13
TO-46 10K PPM

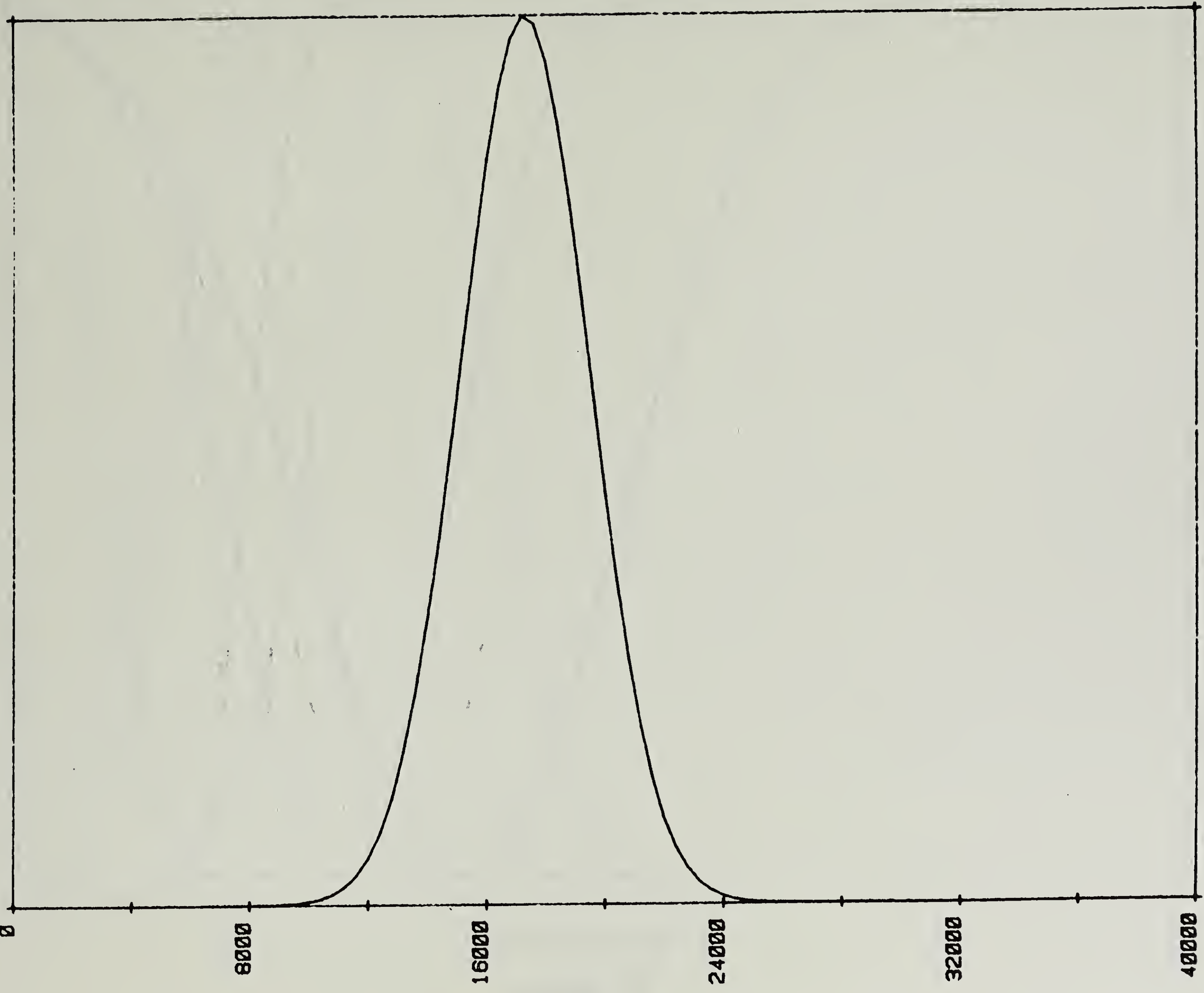

FIGURE 14
TO-18 50 PPM

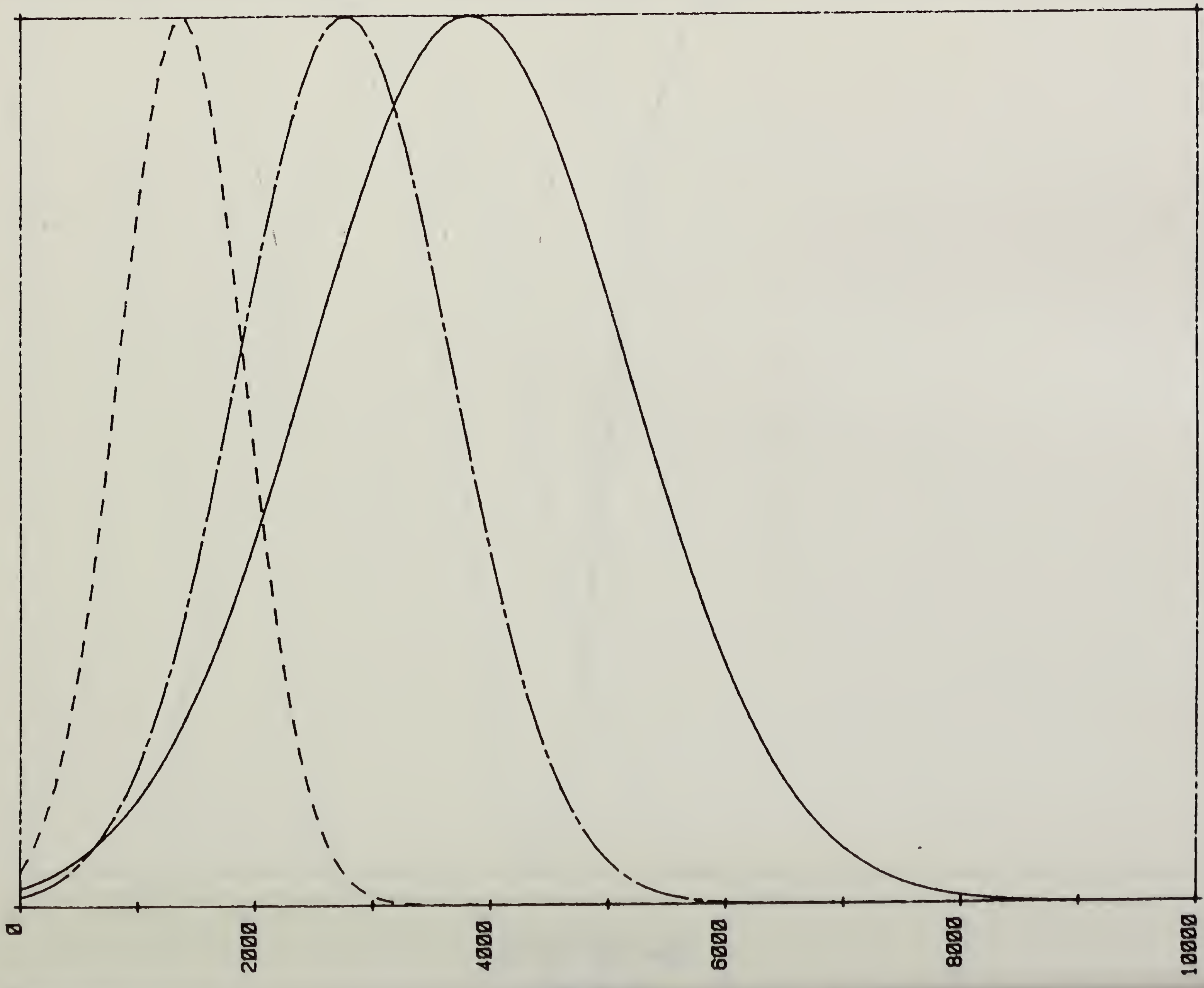

FIGURE 15
TO-18 3K PPM

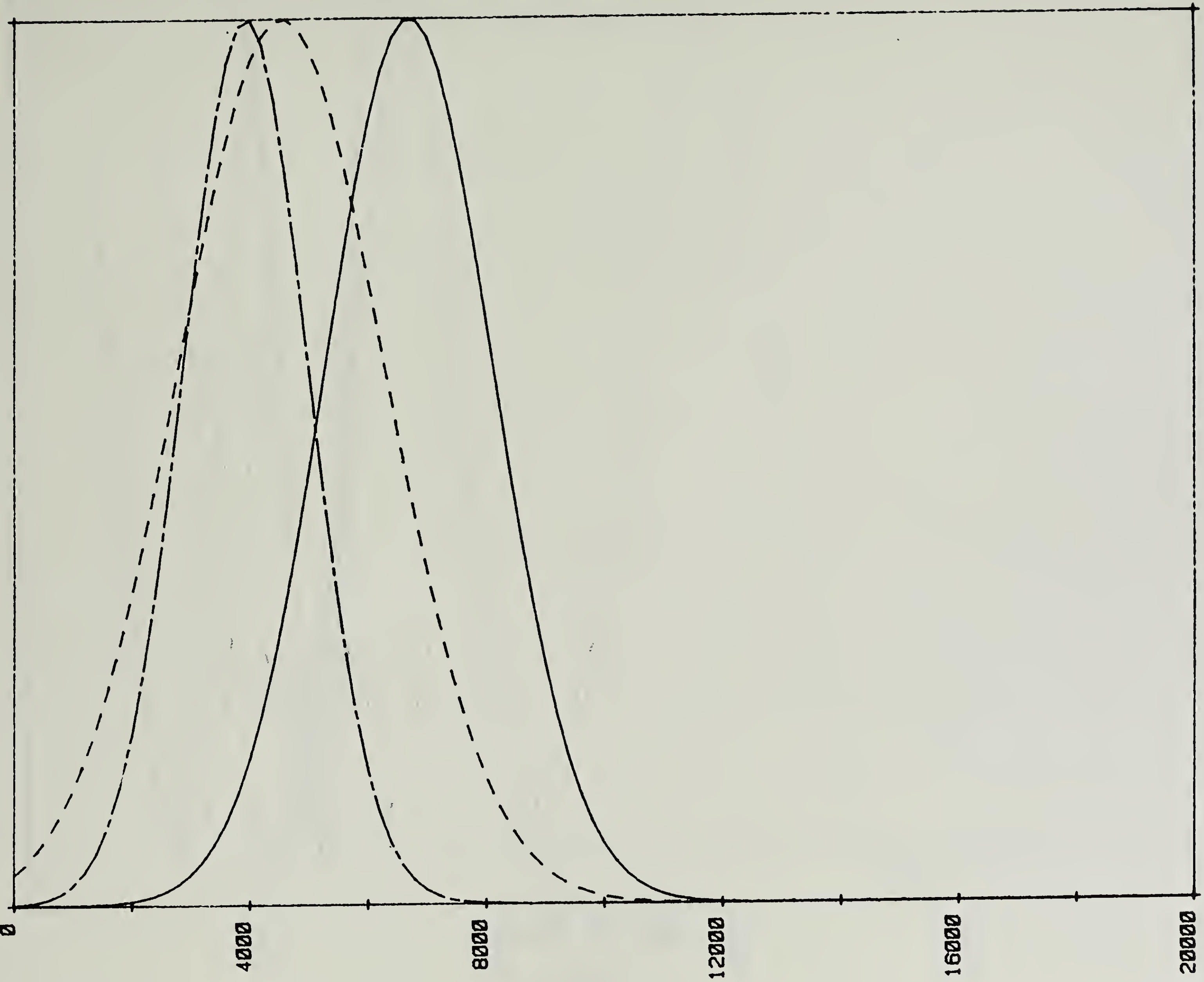

FIGURE 16
TO-18 6K PPM

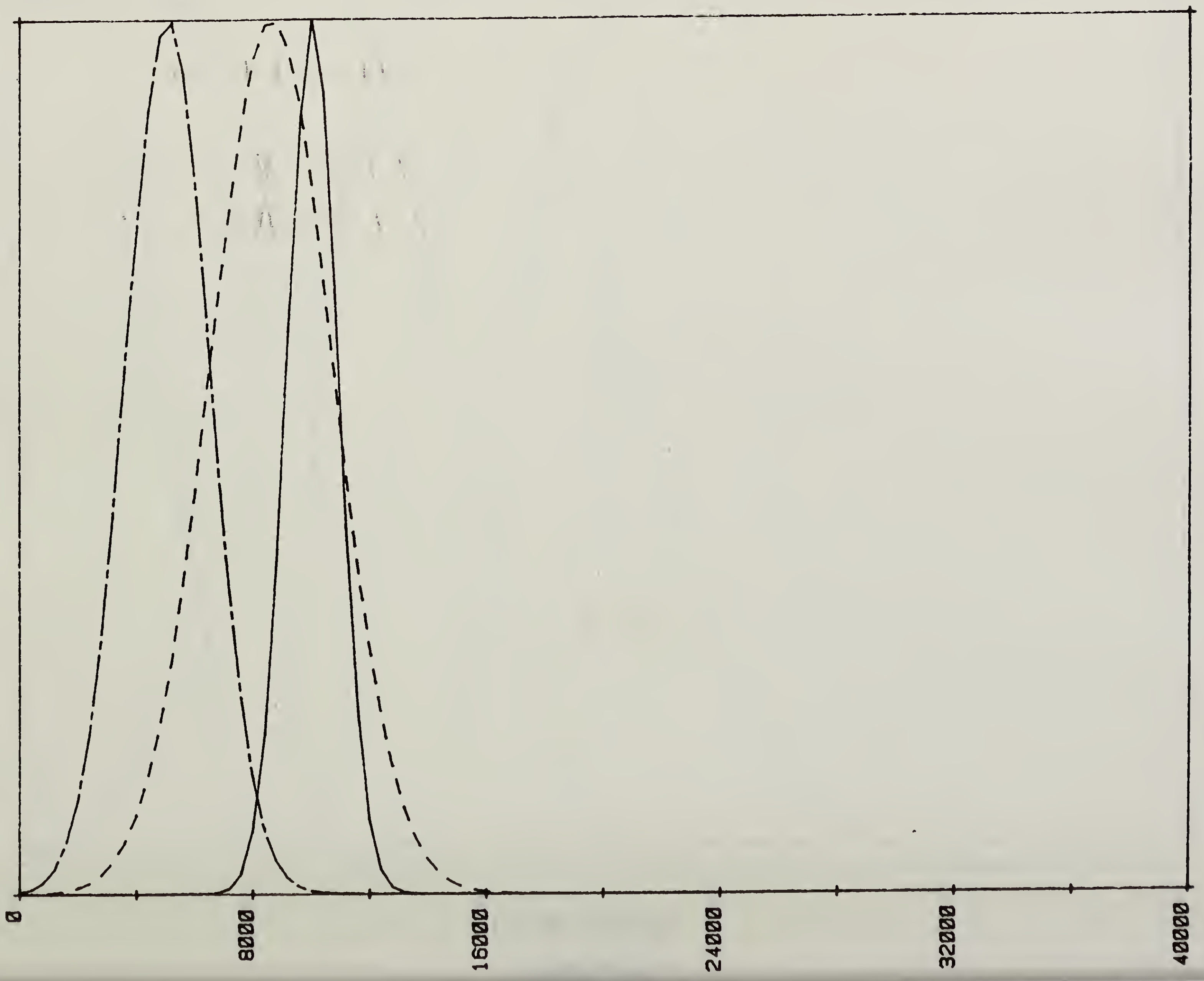

FIGURE 17
TO-18 10K PPM

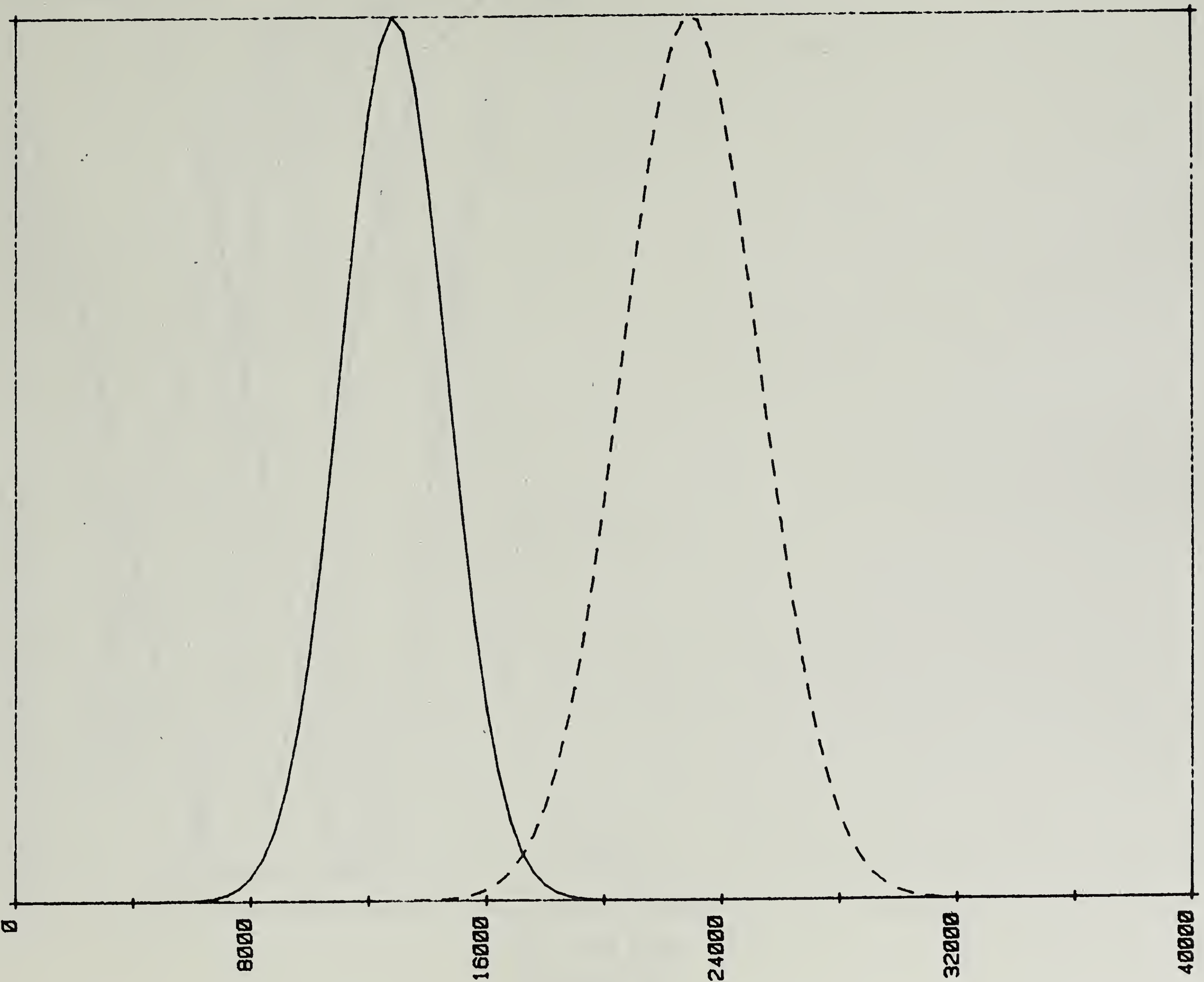

FIGURE 18
TO-3 50 PPM

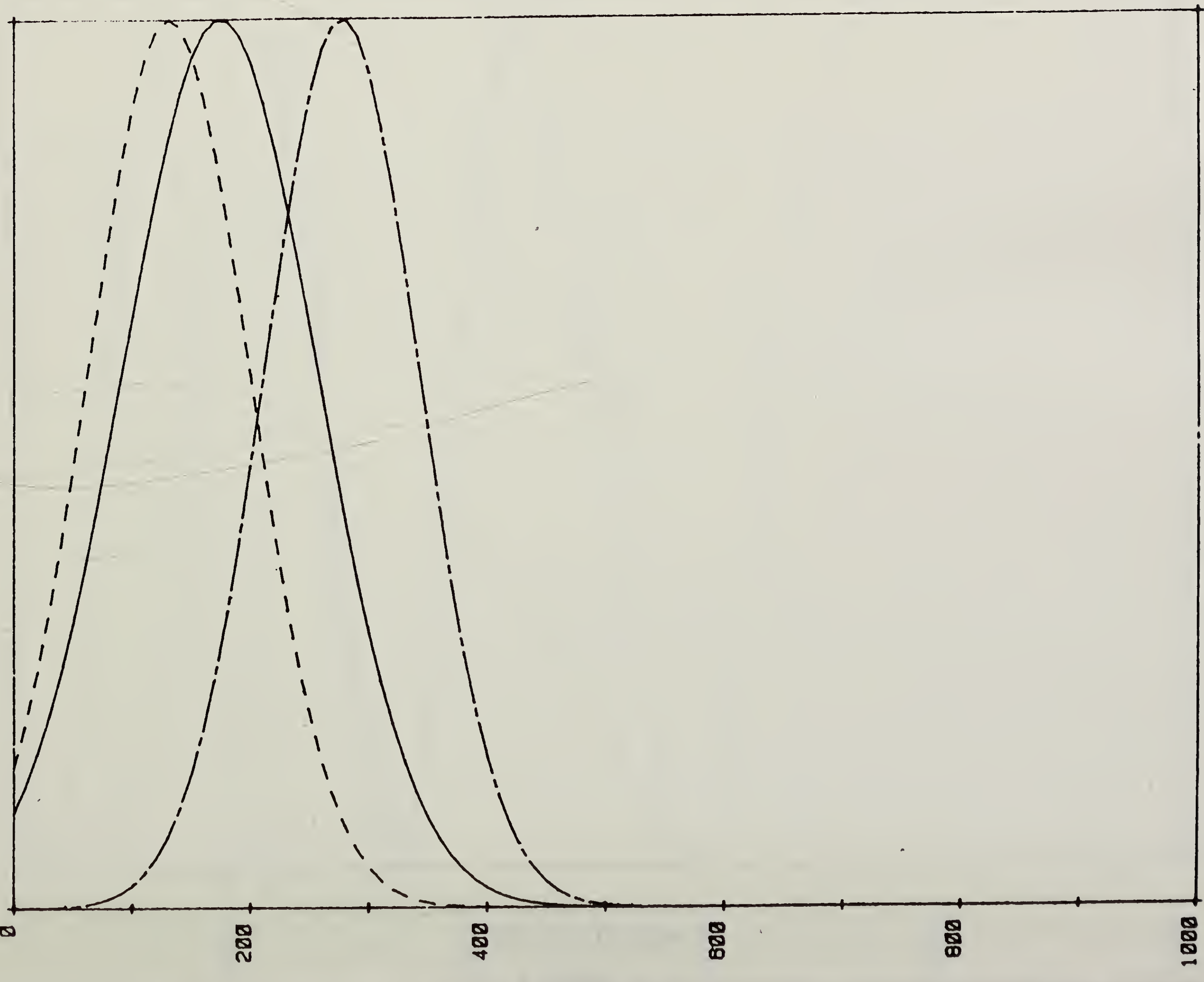

FIGURE 19
TO-3 3K PPM

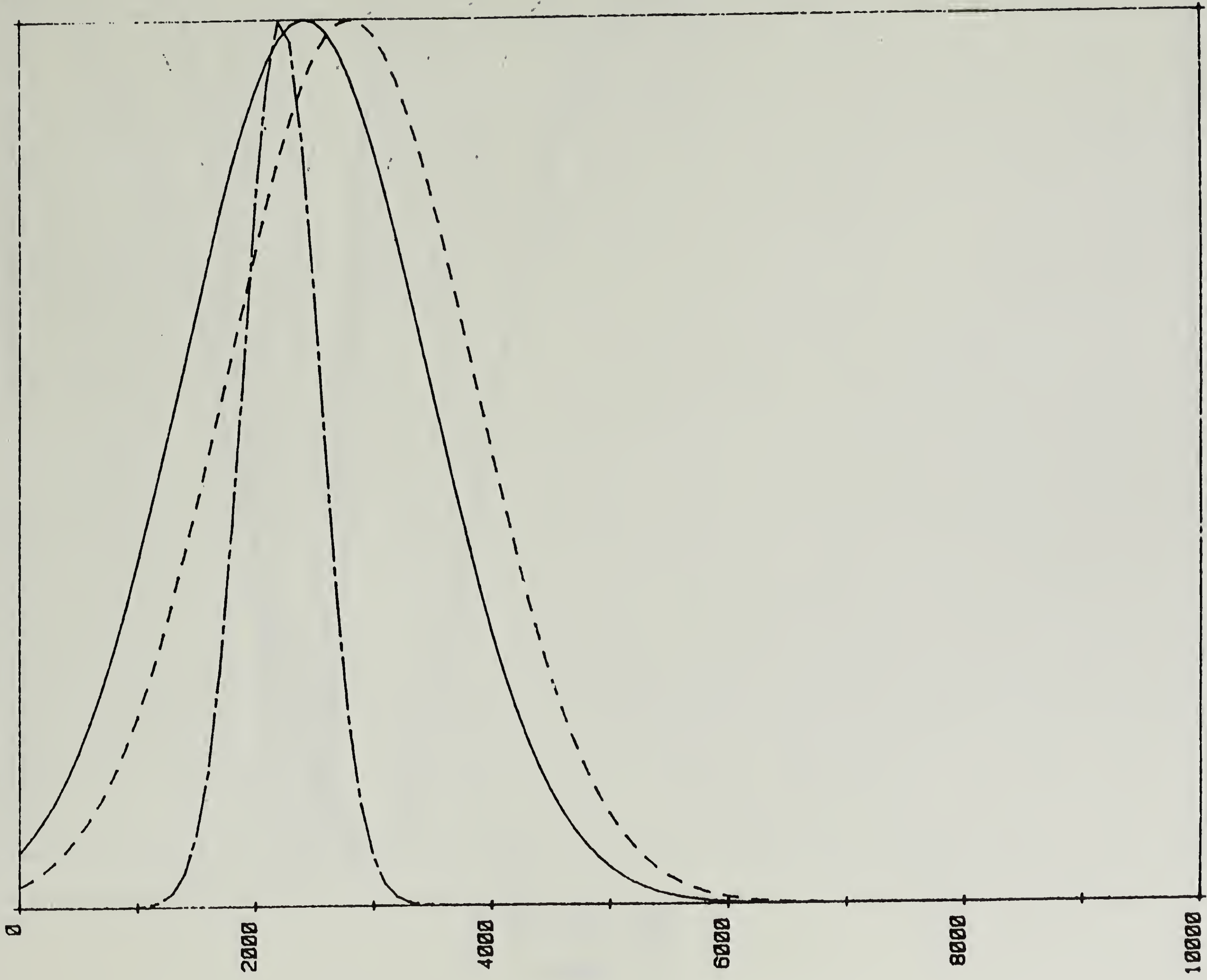

FIGURE 20
TO-3 6K PPM

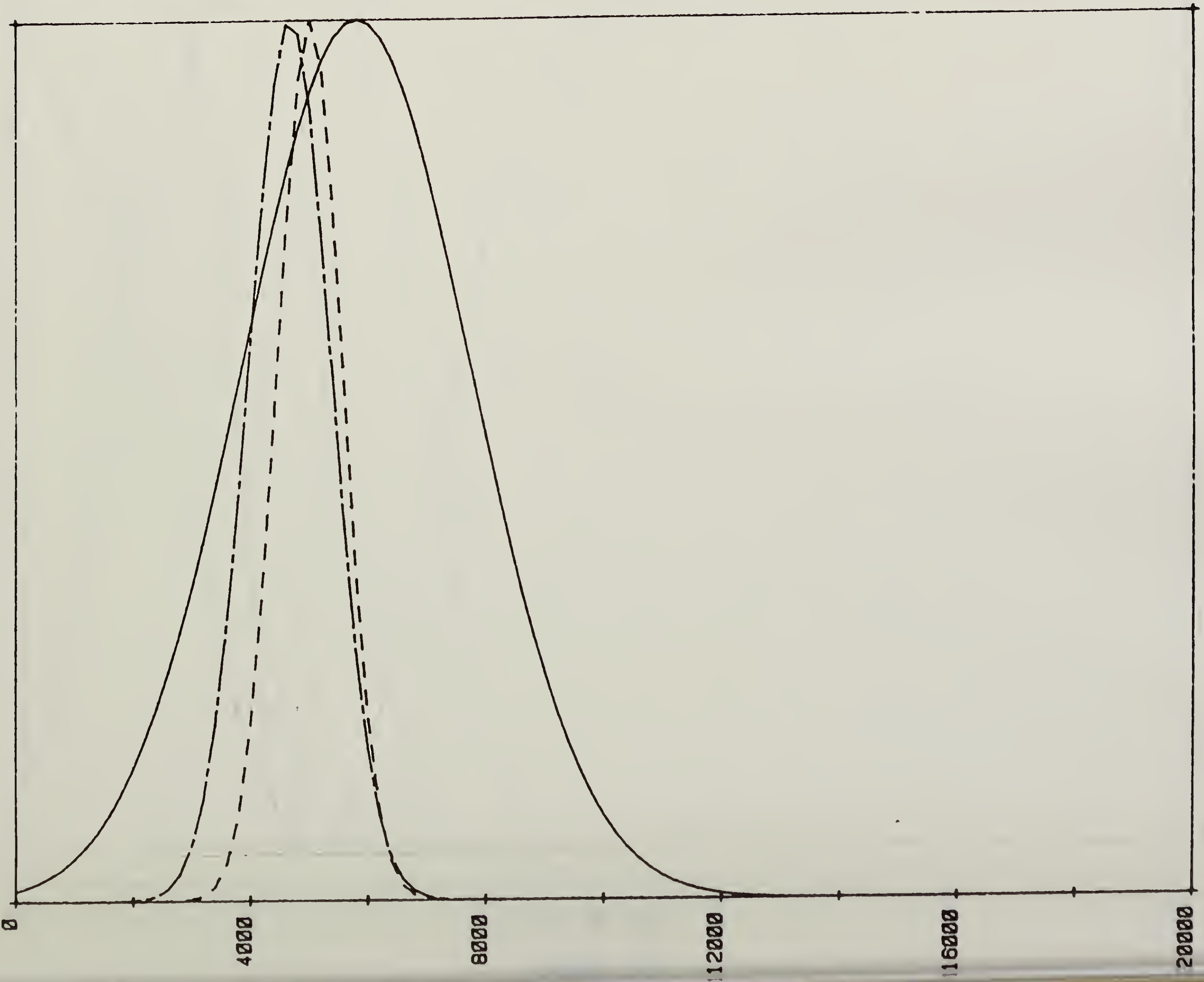

FIGURE 21

TO-3 10K PPM

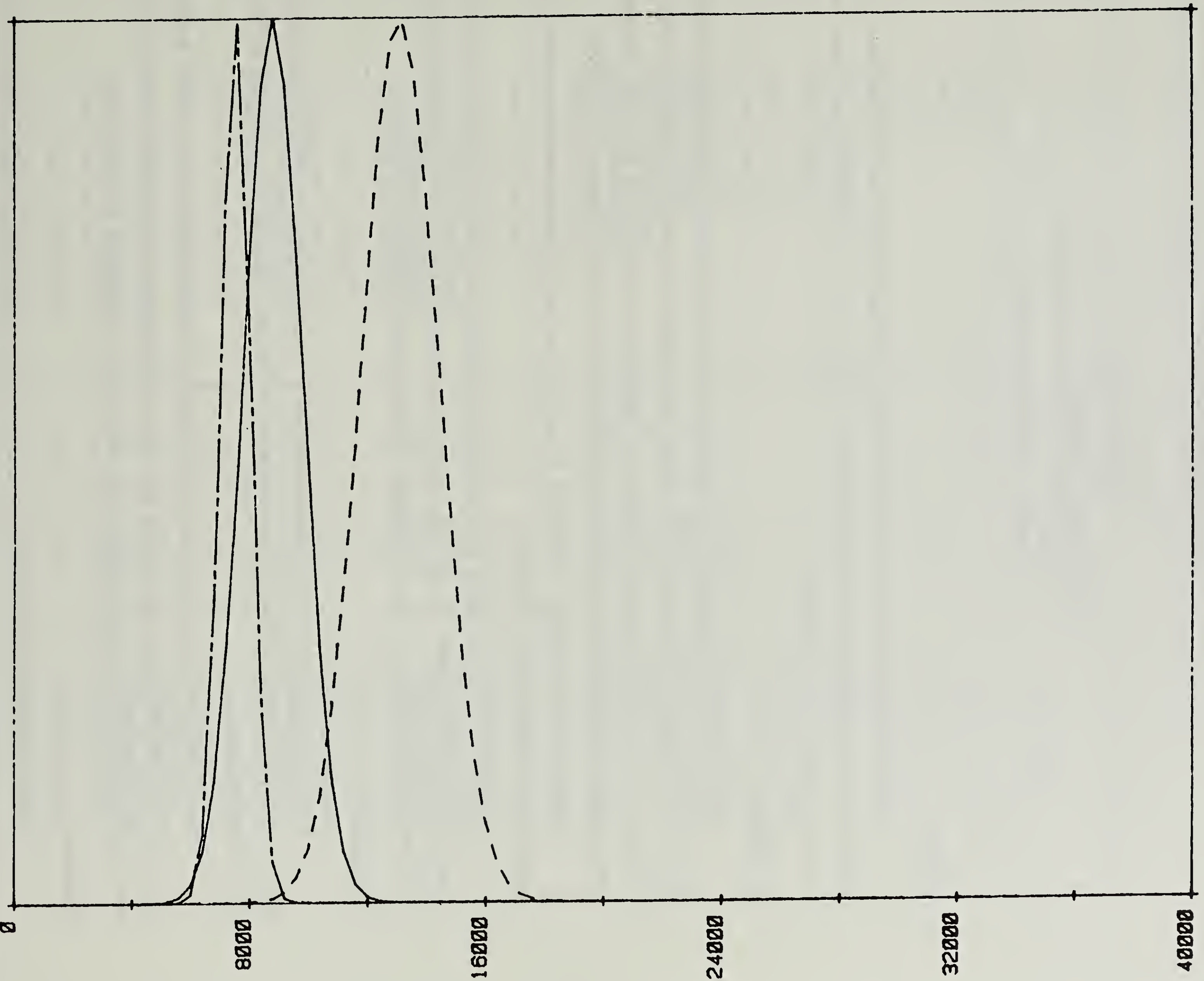

4.5 USING PANAMETRICS MINI-MOD MOISTURE SENSORS FOR MOISTURE MEASUREMENTS INSIDE SEALED MICROELECTRONIC PACKAGES

David A Pinsky

Raytheon Company Missile Systems Division

Bedford, Massachusetts 01730

(617) 274-4252

Abstract

The use of Panametrics MINI-MOD HT moisture sensor chips to measure moisture intrusion into sealed microelectronics packages is discussed. Limitations of these sensors and proper methods for their employment are defined.

Introduction

Moisture sensor chips provide an inviting technique for directly measuring the moisture level inside sealed packages. At first look, these devices seem capable of providing repeatable moisture data with ease. In fact, these devices are sensitive to temperature excursions so that their calibration becomes unstable. Experimenters who overlook this fact can be led to erroneous conclusions.

As recently as September 1986 (Ref. 1), a paper was published where experimenters mistook sensor drift for actual moisture data.

The intention of this paper is to describe the conditions under which good data can be obtained by using these sensors. In this way, the concerns raised in the last few years about hermeticity acceptance limits (Refs. 2-6) can be addressed directly by well designed experiments.

Background

A study was performed to evaluate hermeticity criteria for large microelectronic packages as part of an RADC funded contract to investigate the effects of VLSI/VHSIC technology of MIL-STD-883 test procedures.

The technique used for this work was to directly measure moisture levels inside sealed packages, and correlate these data with helium fine leak results obtained by MIL-STD-883 methods. Moisture contributions from internal organic materials was to be addressed as a side issue.

Packages

Thirty packages of four different styles were used in this study. A single Panametrics MINI-MOD HT moisture sensor chip was mounted in each. Chip-to-package interconnections were provided by 1-MIL aluminum wire.

Die attach was achieved by use of gold-silicon eutectric, non-conductive epoxy, or polyimide film.

Table I summarizes the information on the packages and die attach used.

TABLE I - TEST SAMPLES

S/N	Style	Number I/O	Internal Volume	Die Attach
1	Metal Can	58	5.24 cc	Gold-Silicon Eutectic
2	Metal Can	58	5.24 cc	Gold-Silicon Eutectic
3	Metal Can	58	5.24 cc	Non-Conductive Epoxy
4	Metal Can	58	5.24 cc	Non-Conductive Epoxy
5	Ceramic Leaded CC	132	0.26 cc	Polyimide
6	Ceramic Leaded CC	132	0.26 cc	Polyimide
7	Ceramic Leaded CC	132	0.26 cc	Non-Conductive Epoxy
8	Ceramic Leaded CC	132	0.26 cc	Non-Conductive Epoxy
9	Ceramic Leaded CC	132	0.26 cc	Gold-Silicon Eutectic
10	Ceramic Leaded CC	132	0.26 cc	Gold-Silicon Eutectic
11	Ceramic Pad Grid Array	180	0.31 cc	Polyimide
12	Ceramic Pad Grid Array	180	0.31 cc	Polyimide
13	Ceramic Pad Grid Array	180	0.31 cc	Non-Conductive Epoxy
14	Ceramic Pad Grid Array	180	0.31 cc	Non-Conductive Epoxy
15	Ceramic Pad Grid Array	180	0.31 cc	Gold-Silicon Eutectic
16	Ceramic Pad Grid Array	180	0.31 cc	Gold-Silicon Eutectic
17	Ceramic Leadless Chip Carrier	80	0.23 cc	Gold-Silicon Eutectic
18	Ceramic Leadless Chip Carrier	80	0.23 cc	Gold-Silicon Eutectic
19	Ceramic Leadless Chip Carrier	80	0.23 cc	Gold-Silicon Eutectic
20	Ceramic Leadless Chip Carrier	80	0.23 cc	Gold-Silicon Eutectic
21	Ceramic Leadless Chip Carrier	80	0.23 cc	Gold-Silicon Eutectic
22	Ceramic Leadless Chip Carrier	80	0.23 cc	Gold-Silicon Eutectic
23	Ceramic Leadless Chip Carrier	80	0.23 cc	Gold-Silicon Eutectic
24	Ceramic Leadless Chip Carrier	80	0.23 cc	Gold-Silicon Eutectic
25	Ceramic Leadless Chip Carrier	80	0.23 cc	Gold-Silicon Eutectic
26	Ceramic Leadless Chip Carrier	80	0.23 cc	Gold-Silicon Eutectic
27	Ceramic Leadless Chip Carrier	80	0.23 cc	Gold-Silicon Eutectic
28	Ceramic Leadless Chip Carrier	80	0.23 cc	Gold-Silicon Eutectic
29	Ceramic Leadless Chip Carrier	80	0.23 cc	Gold-Silicon Eutectic
30	Ceramic Leadless Chip Carrier	80	0.23 cc	Gold-Silicon Eutectic

Initial Calibration

Each of the thirty packages had a pair of wires soldered to the external I/O leads to provide access to the sensor signals. The packages were then placed in a dry-box with their leads passing through a formed-in-place silicone gasket.

Figure 1 is a schematic diagram showing the apparatus used for calibration (and subsequent testing). A Panametrics System I Hygrometer System was used to monitor the effluent from the dry box. The moisture level was controlled by adjusting the rate of dry nitrogen flow through the system.

Output signals from the sensors were fed into a panametrics model 771 hygrometer which is specially designed for this purpose. The voltage from the model 771 was read out on a separate digital voltmeter.

Calibration data was collected on each sensor. The dry box moisture level was varied from 4500 ppm_v to 25 ppm_v, as determined by the effluent.

Figure 2 is a plot of the calibration data taken from a single sensor over a period of several days. The dry-box moisture level was slowly raised and lowered from about 20 ppm_v up 500 ppm_v. No hysteresis effect was observed. These data indicated that the sensors can provide repeatable output. Two data points shared the same voltage only when the dry box readings were different by no more than 50 ppm_v.

Using this type of data a calibration slope was assigned to each sensor. These slopes are listed in Table II.

At this point in the study, expectations were high that very small changes in internal moisture levels could be measured over long periods of time.

Post-Seal Drift

Following calibration, every package was sealed by use of tin-lead solder preforms. (Sealing was performed in a dry nitrogen atmosphere held at about 50 ppm_v of moisture.) The sealed packages were then returned to the calibration dry box for testing. The moisture level was raised and lowered over a few days and the sensor outputs were recorded. Most of the sensors did not respond to changes in the dry box environment, indicating hermetic-like behavior. Nine sensors responded dramatically to the dry-box environmental changes, indicating leakage. These packages will be discussed in a later section.

The next part of the moisture intrusion study called for the packages to be monitored at room ambient conditions. Data obtained during the first weeks after sealing showed the output voltages steadily falling for all sensors. Quick calculations proved that this could not be due to an actual drop in moisture content unless negative moisture levels were assumed.

Data was taken on all the sensors for three months following seal. Figures 3 and 4 show sensor output voltage data for two packages. Both voltages exhibit an exponential decay to a new, lower val-

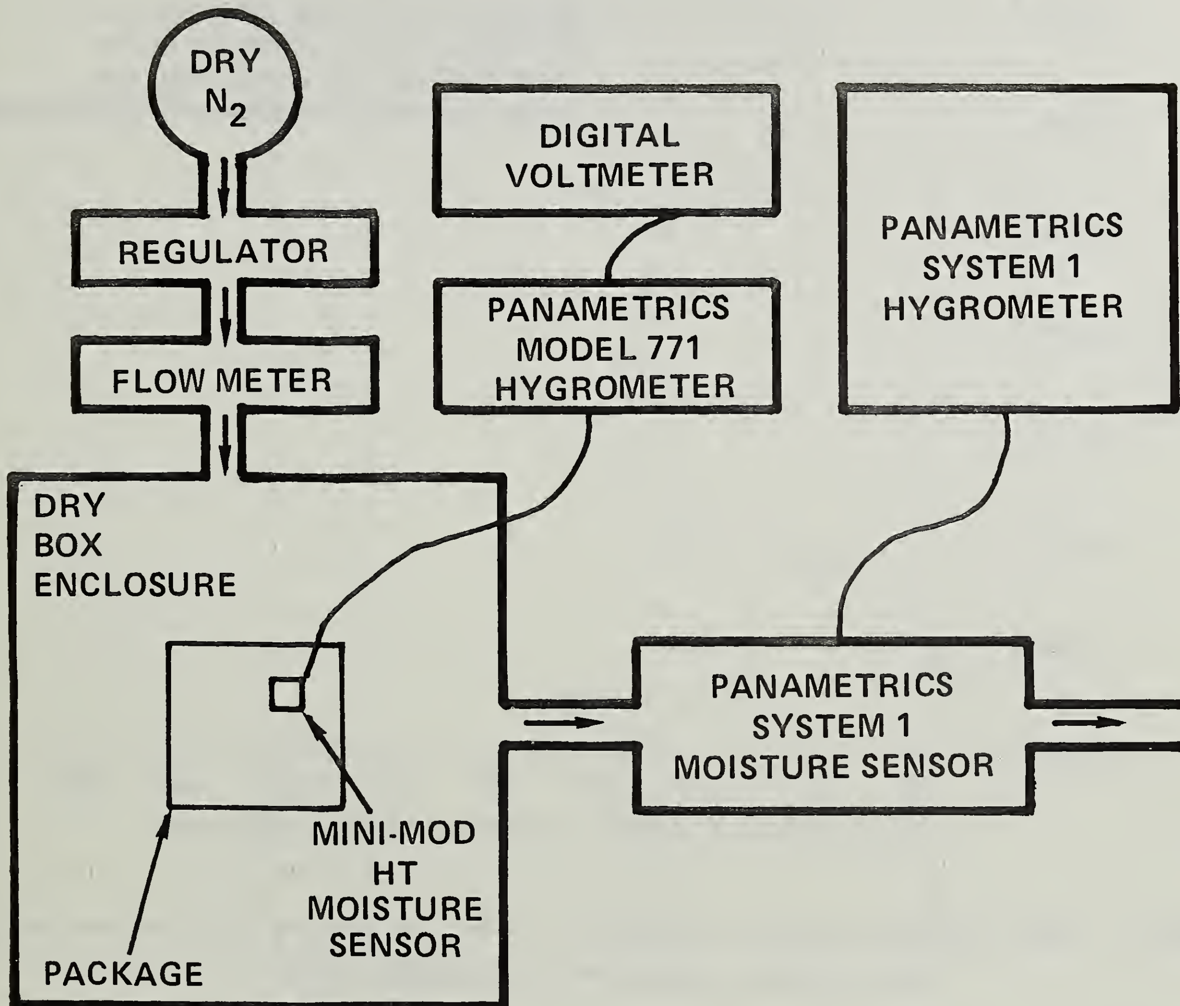

Figure 1 - Schematic Diagram of the Apparatus Used for Initial Sensor Calibration and Subsequent Testing

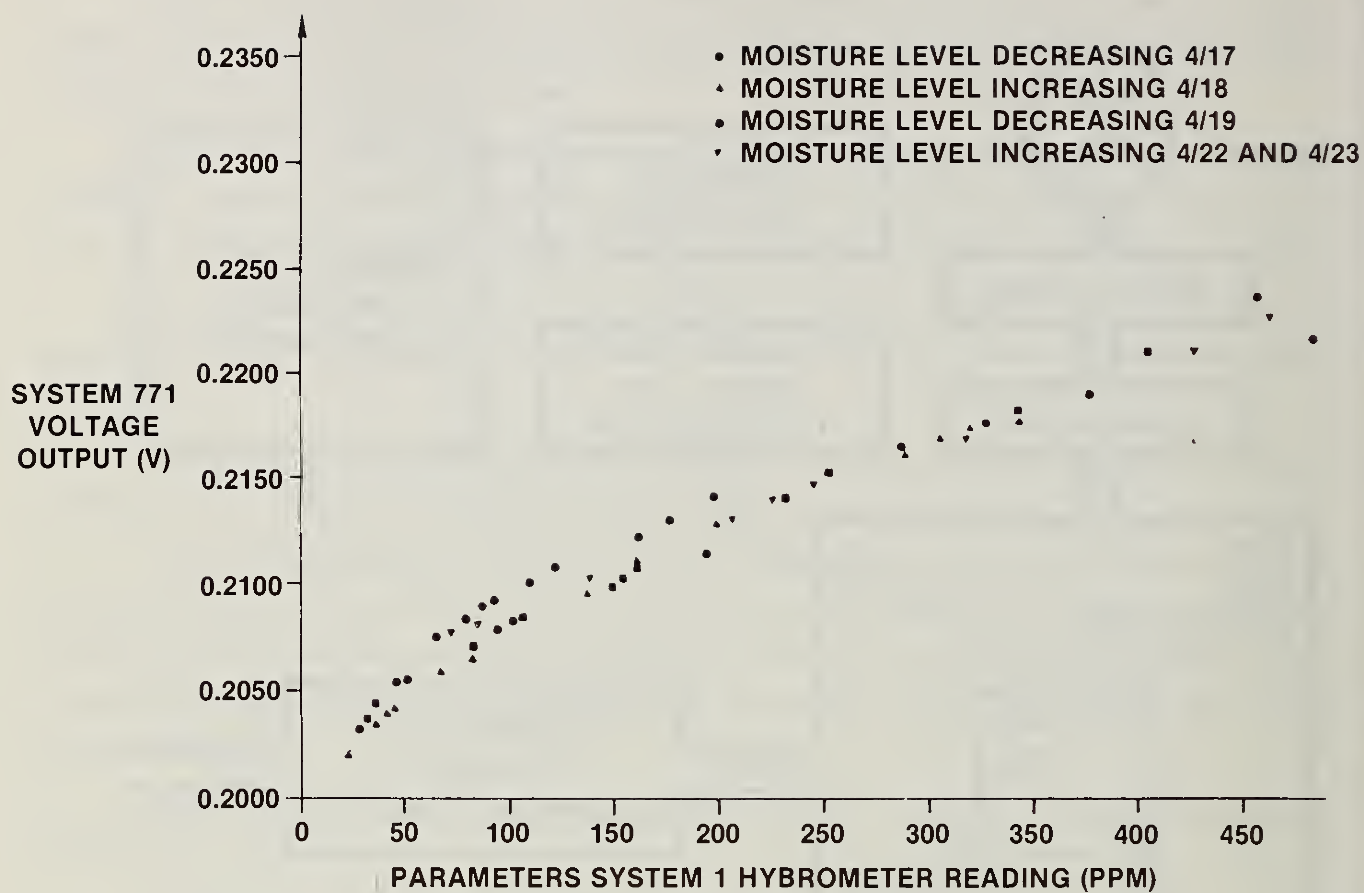

Figure 2 - Initial Calibration Response of Sensor S/N 25. Data was collected with slowly increasing and decreasing moisture levels on five different days.

TABLE II - INITIAL CALIBRATION SLOPES FOR ALL PACKAGES. SLOPES ARE FOR THE RANGE 100-500 ppm_v.

S/N	Calibration Slope in ppm_v/mV
1	5.8
2	5.8
3	No data - dead sensor
4	6.9
5	17.2
6	8.7
7	20.8
8	7.4
9	16.9
10	28.6
11	5.0
12	6.6
13	6.5
14	7.5
15	No data - dead sensor
16	22.7
17	21.4
18	30.3
19	24.7
20	26.3
21	28.6
22	31.3
23	53.7
24	25.3
25	26.3
26	20.8
27	22.4
28	27.0
29	24.3
30	26.6

ue. Figure 5 is the data from Figure 3 on a semi-logaryhmic plot. This slope indicates a time constant of about 33 days.

This type of drift data was collected on all sensors and is summarized in Table III. Some of the sensors did not achieve a stable output during the entire three month period.

TABLE III - DATA ON DRIFT FOR OPERABLE SENSORS MOUNTED IN APPARENTLY HERMETIC PACKAGES FOLLOWING PACKAGE SEALING

S/N	DC Voltage At Stabilization	Total Amount of Negative Drift As a % of Final Value	Approximate Time Constant For Drift Decay In Days
1	.2469	1.9	20
3	.2655	0.6	20
4	.3125	1.6	34
5	.2246	3.1	78
17	.2050	3.5	32
18	.2056	7.1	30
19	.2046	5.7	32
20	.2146	6.1	34
21	.2835	13.7	34
22	.2590	17.7	32
24	.2150	4.9	35
25*	.3138*	29.6*	>133*
26	.2099	4.4	33
27	.2500	12.3	34
28	.2160	6.2	32
29	.2134	3.3	32
30	.2030	6.0	37

* S/N 25 never stabilized. Data given is for 200 days after seal.

Another form of sensor failure also occurred during this investigation when some sensors suddenly provided very high or very low output voltages and would no longer respond. These failures may have been due to internal short or open circuits, or other problems.

Moisture Intrusion - Data

Despite these calibration difficulties, some interesting moisture intrusion data was obtained. For the purposes of obtaining qualitative results, the initial calibration data was used to convert voltages into apparent moisture values. These values can be used only to compare the relative moisture levels inside the packages used in this study.

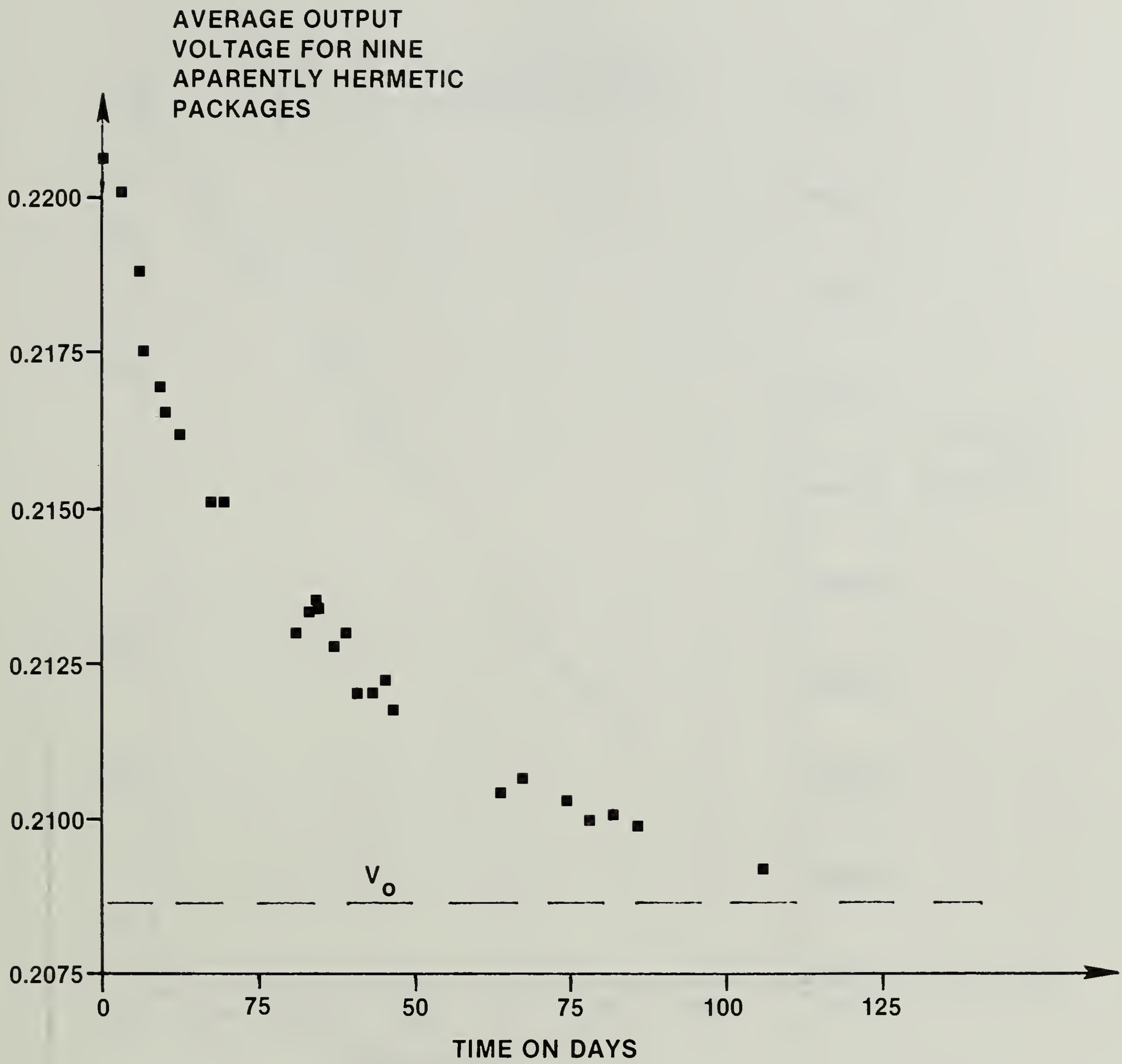

Figure 3 - Average Voltage from Nine Sensors with Apparently Hermetic Behavior Showing Post-Seal Drift which Assympototically Approaches the Value 0.2086

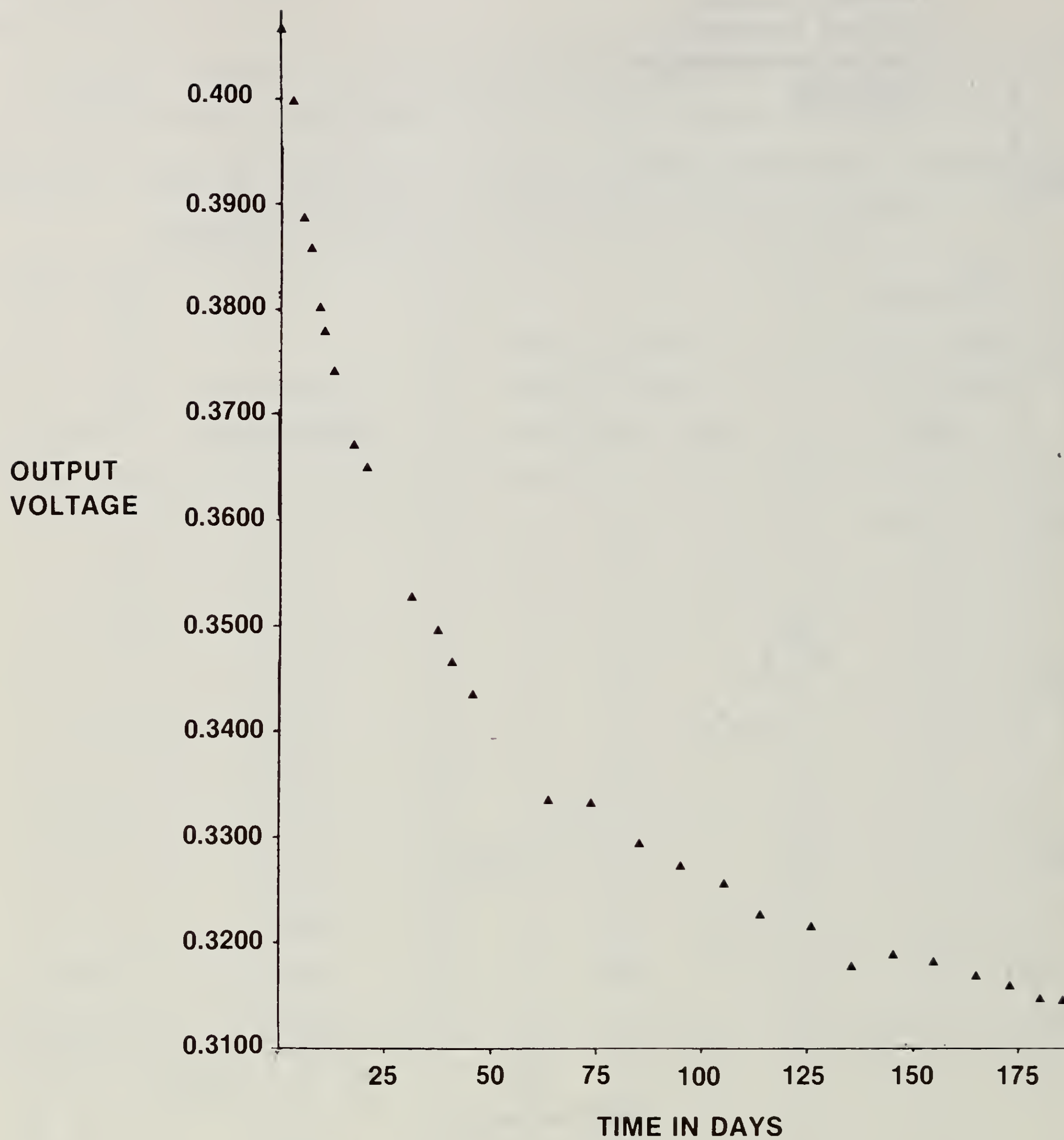

Figure 4 - Voltage from the Sensor in an Apparently Hermitic Package Showing Post-Seal Drift. Stabilization has not occurred within 175 days.

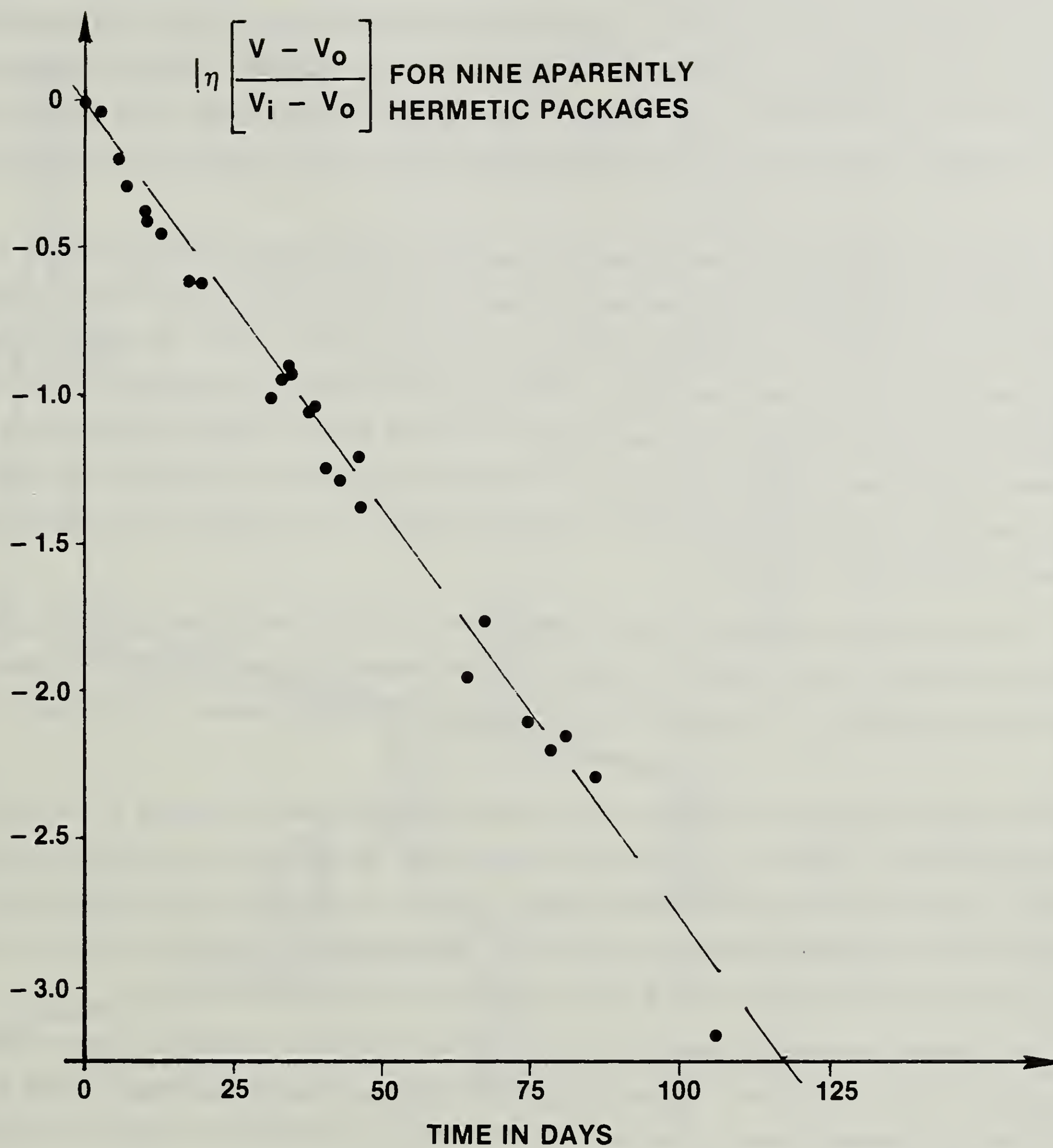

Figure 5 - Post-Seal Drift Data from Figure 3 Fit to the Curve: $V = V_o + (V_i - V_o)e^{-t/\tau}$ *with* $V_o = 0.2086$ *and* $V_i = 0.2207$

Figure 6 is a plot showing the apparent moisture levels in two packages which were cycled between room ambient and about 50 ppm_v in the dry box. These data clearly indicate the immediate effect of the dry box moisture on the apparent package moisture. Hereafter packages displaying this form of behavior will be referred to as "apparent gross leakers". Most of the other sealed packages showed no response to the dry box moisture level and therefore will be described as "apparently hermetic".

Figure 7 is a plot of the apparent moisture content in three packages during the three months at room ambient. Package S/N 28 is apparently hermetic. The sensor drift can be seen as a small drop in the apparent moisture content. Package S/N 8 is an apparent gross leaker. Its apparent moisture content immediately rises to between 2000 to 2500 ppm_v and remains there. Package S/N 7 exhibits a quite different behavior. Its apparent moisture level rises and asympototically approaches the apparent moisture level of package S/N 8. About seventy days are required for the moisture rise to be complete. This package will be referred to as the "borderline leaker", as it is clearly in the region between gross leakage and hermetic behavior.

At the end of three months at room ambient the remaining stabilized, apparently hermetic packages were divided into two groups. One group was maintained at room ambient. The other group was placed into a chamber at 95 percent RH. (Previous plans for temperature cycling had to be discarded.)

The apparent moisture content in most of these packages showed no signs of increase or decrease during this time. Figure 8 is a plot of the changes in the apparent moisture content of one package which was exposed to 95 percent RH (wet) and one which was exposed to room ambient (dry). Table IV provides the number of data points taken and their standard deviation in terms of apparent moisture content for all packages of both groups (except those discussed below).

Two packages held at high humidity did display large increases in moisture content. Both were metal packages which experienced corrosion at the seal. Figure 9 is a plot of the apparent moisture content in one such package showing two sharp increases in the moisture intrusion rate. This behavior is consistent with the effects of corrosion.

An apparent moisture intrusion rate was assigned to each package with a functioning sensor. Assignments for the apparently hermetic packages were made by assuming that the increase in apparent moisture level were less than 25 ppm_v, which is approximately equal to the standard deviation of their moisture level data. Table V summarizes these rates.

Moisture Intrusion versus Helium Leak Rates

A goal of this study was to correlate moisture intrusion rates with helium leak rates. To this end all but one of the packages were helium leak tested at the end of this study.

Gross leak testing was performed on all packages (except no. 2 which died early) per MIL-STD-883C, Method 1014, Test Condition C_1, Fluorocarbon Gross Leak, fixed. Parts were bombed at 60 psig for 2 hours.

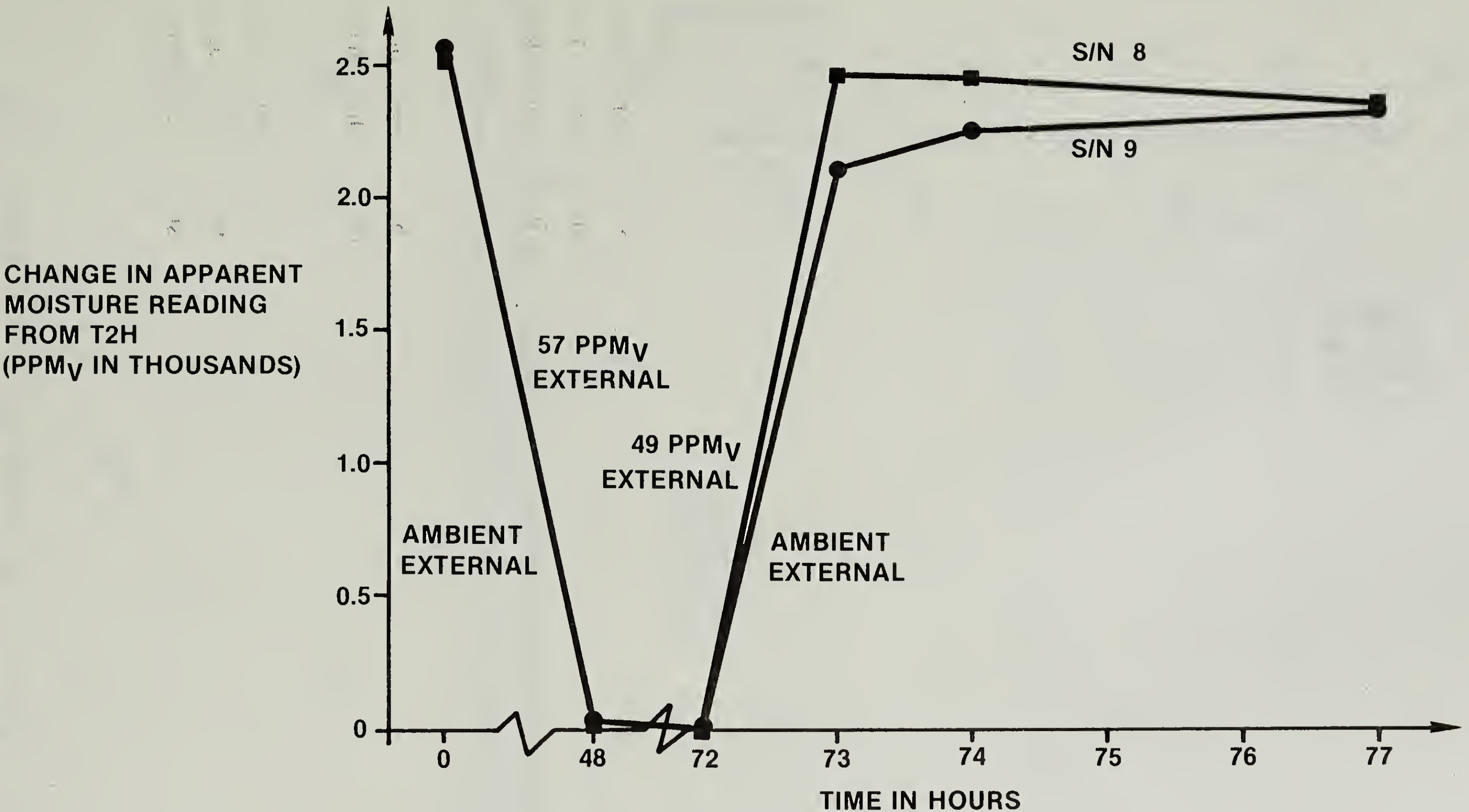

Figure 6 - Response of Two Sensors To Changes in Dry Box Conditions. Apparent Gross Leakage is Indicated

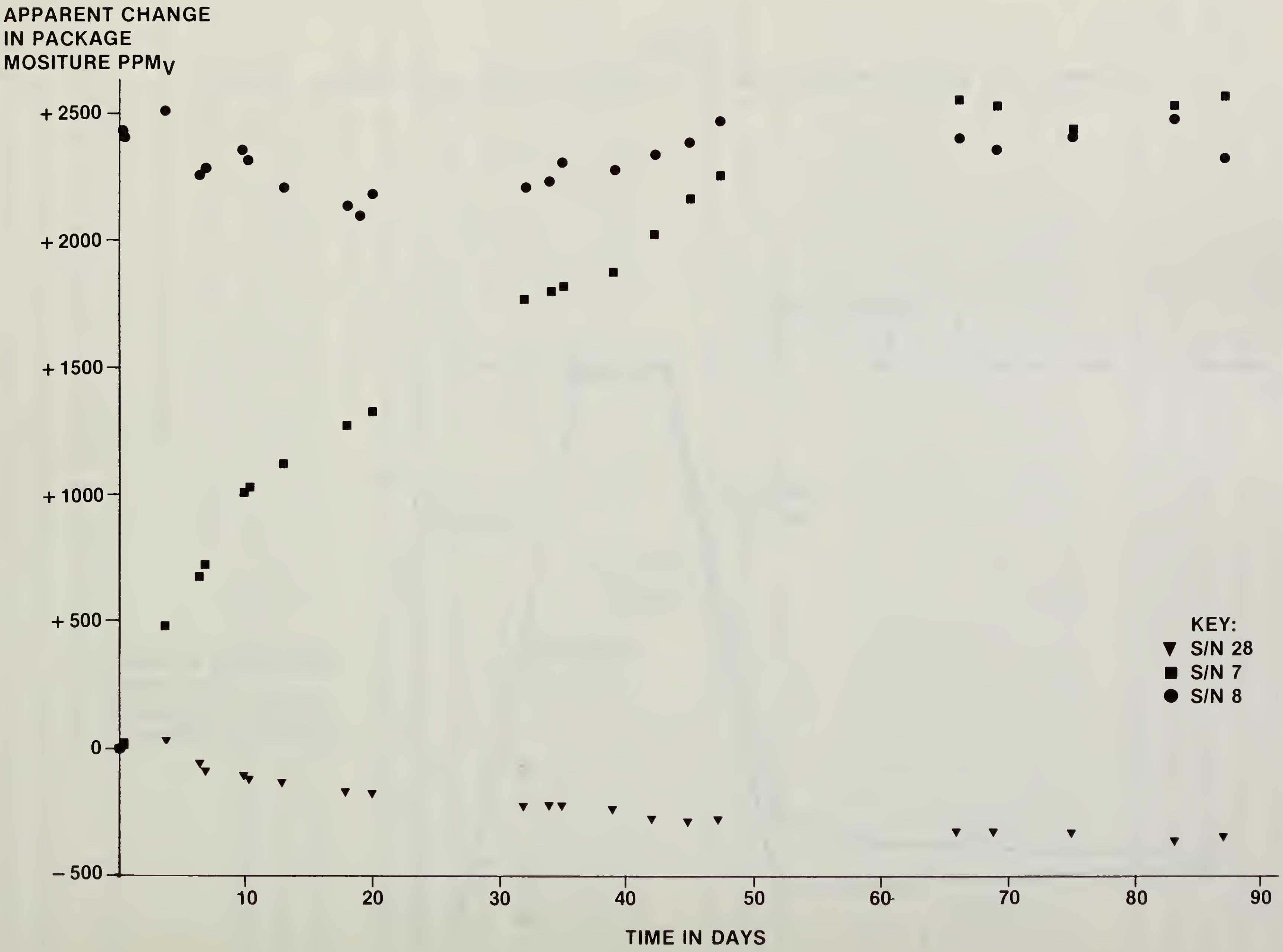

Figure 7 - Post-Seal Response of Three Sensors During 87 Days at Room Ambient. Package S/N 8 is an apparent gross leaker. Package S/N 28 is apparently hermetic. Package S/N 7 is the borderline leaker.

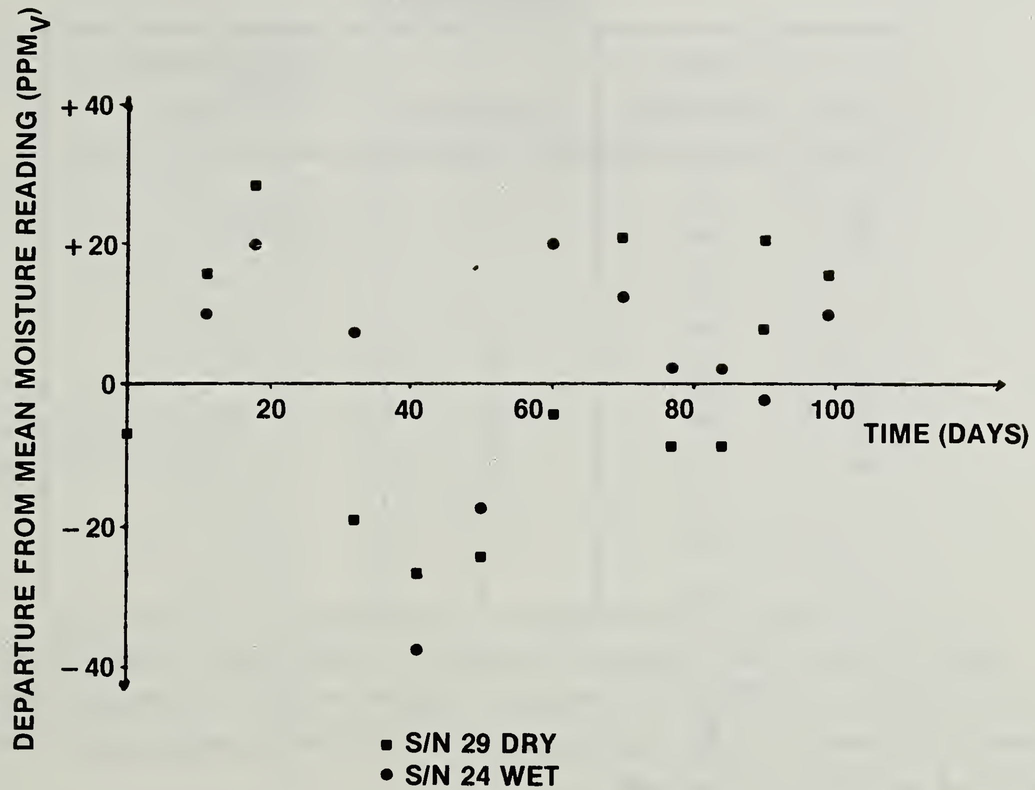

Figure 8 - Post Stabilization Behavior of Two Sensors in Apparently Hermetic Packages. One package, S/N 29, was held at room ambient, while S/N 24 was exposed to 95 percent relative humidity.

TABLE IV - APPARENT MOISTURE INTRUSION DATA FOR HERMETIC PACKAGES AFTER STABILIZATION

S/N	External Environment	Data Points	Standard Deviation in ppm_v
3	Dry	13	4
17	Wet	8	11.3
18	Wet	11	17.9
19	Wet	11	28.5
20	Wet	11	24
24	Wet	11	18.8
26	Dry	14	20.5
27	Dry	13	11.1
29	Dry	14	18
30	Wet	8	22.7

Eighteen packages which passed gross leak test were then tested per MIL-STD-883C, Method 1014, Test Condition A_1, Helium Fine Leak, fixed. A bomb pressure of 60 psig was used and the part was baked for 10 minutes at 100°C to accelerate the 1 hour allowed waiting period. Leak rates were measured and recorded for all packages.

To perform an analysis, all moisture intrusion data was converted to units of g/s intrusion of water. This absolute measure of moisture intrusion should relate directly to absolute helium leak rate expressed in atm-cc/s. All of the packages in this study were sealed with solder preforms, thus the effects of package geometry should not be significant. Though seal areas and package volumes may vary, any existing leakage path would exist for both helium and water. Thus, it is reasonable to expect a correlation between absolute helium leak rates and absolute moisture intrusion rates.

Table VI summarizes all of the helium leak rate data and the apparent moisture intrusion data converted into absolute units. Figure 10 is a plot of $\log_{10}$ of the apparent moisture intrusion rate versus $\log_{10}$ of the measured helium leak rate. Every gross leakers was assigned a helium leak rate of $>10^{-5}$ atm-cc/s because this is the upper limit of measurement on our equipment. Two vertical lines are drawn on Figure 10. The right hand line corresponds to a helium leak rate of 5×10^{-8} atm-cc/s and the left hand line to 1×10^{-8} atm-cc/s. The data point corresponding to package S/N 7 falls between these lines. This package is, therefore, considered to be hermetic by MIL-STD-883. However, moisture intrusion data shows that this package achieved ambient levels of moisture in just 70 days at room ambient, which is cause for some concern.

Sensor Performance - Discussion

The sensor instabilities resulting from a temperature excursion poses a serious difficulty for the experimenter. It is clear from the data that the calibration curves change not only in DC voltage offset, but also in slope. Thus, moisture changes cannot be determined absolutely.

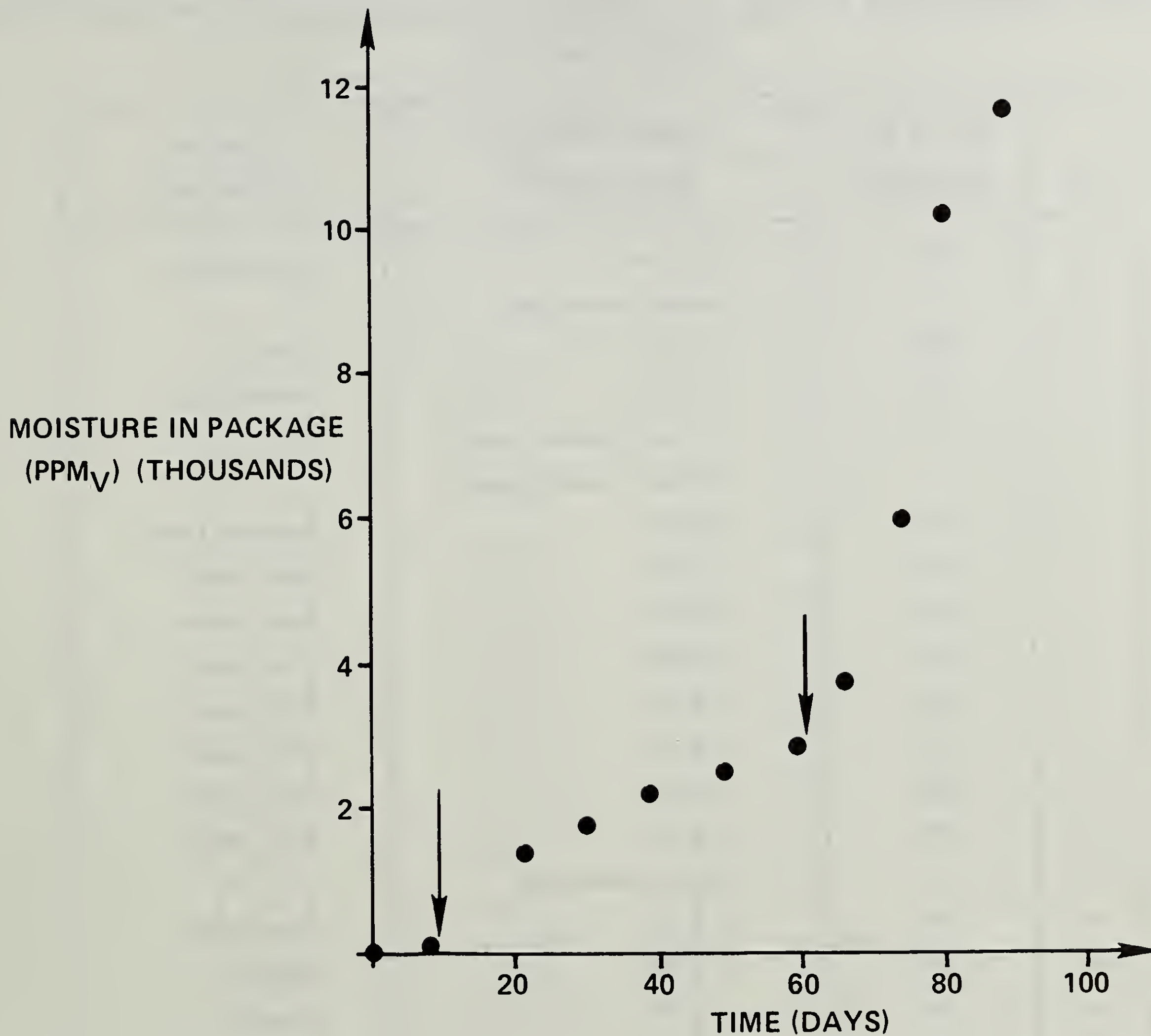

Figure 9 - Apparent Moisture Intrusion into S/N 1 (Induced Leaker) During Exposure to High Humidity. Arrows indicate times at which leak rate appears to increase. Moisture levels are for . comparison only. Absolute levels could not be determined due to sensor calibration shift.

TABLE V - POST-STABILIZATION ENVIRONMENT, APPARENT MOISTURE INTRUSION RATE OR FAILED SENSOR STATUS, AND HERMETICITY DESIGNATION FOR EACH OF THE THIRTY PACKAGES

S/N	Wet or Dry Environment	Moisture Intrusion Rate (ppm_v/S)	Apparent Hermeticity
1	Wet	$>5.4 \times 10^{-3}$	Induced Leaker
2	--	No Data - Sensor Died	—
3	Dry	$<3 \times 10^{-6}$	Hermetic
4	Wet	$>1.5 \times 10^{-2}$	Induced Leaker
5	--	No Data - Unstable Sensor	—
6	--	No Data - Unstable Sensor	—
7	Dry	4.6×10^{-4}	Borderline Leaker
8	Dry	$>6 \times 10^{-1}$	Gross Leaker
9	Dry	$>6 \times 10^{-1}$	Gross Leaker
10	Dry	$>6 \times 10^{-1}$	Gross Leaker
11	Dry	$>6 \times 10^{-1}$	Gross Leaker
12	Dry	$>6 \times 10^{-1}$	Gross Leaker
13	Dry	$>6 \times 10^{-1}$	Gross Leaker
14	Dry	$>6 \times 10^{-1}$	Gross Leaker
15	--	No Data - Sensor Died	—
16	Dry	$>6 \times 10^{-1}$	Gross Leaker
17	Dry	$<3 \times 10^{-6}$	Hermetic
18	Dry	$<3 \times 10^{-6}$	Hermetic
19	Dry	$<3 \times 10^{-6}$	Hermetic
20	Dry	$<3 \times 10^{-6}$	Hermetic
21	--	No Data - Unstable Sensor	—
22	--	No Data - Unstable Sensor	—
23	--	No Data - Sensor Died	—
24	Wet	$<3 \times 1^{-6}$	Hermetic
25	--	No Data - Unstable Sensor	—
26	Dry	$<3 \times 1^{-6}$	Hermetic
27	Dry	$<3 \times 1^{-6}$	Hermetic
28	--	No Data - Sensor Died	—
29	Dry	$<3 \times 1^{-6}$	Hermetic
30	Wet	$<3 \times 1^{-6}$	Hermetic

TABLE VI - APPARENT MOISTURE INTRUSION RATES CONVERTED TO UNITS OF g/S, AND MEASURED HELIUM LEAK RATES FOR ALL PACKAGES

S/N	Moisture Intrusion Rate (g/s)	Helium Leak Rate (atm-cc/s)
1	$>2.3 \times 10^{-11}$	$>10^{-5}$
2	No Data	No Data
3	$<1.3 \times 1\text{-}^{-14}$	6.2×10^{-9}
4	$>6.3 \times 10^{-11}$	$>10^{-5}$
5	No Data	2.7×10^{-9}
6	No Data	1.5×10^{-9}
7	9.6×10^{-14}	3.5×10^{-8}
8	$>1.3 \times 10^{-10}$	$>10^{-5}$
9	$>1.3 \times 10^{-10}$	$>10^{-5}$
10	$>1.3 \times 10^{-10}$	$>10^{-5}$
11	$>1.5 \times 10^{-10}$	$>10^{-5}$
12	$>1.5 \times 10^{-10}$	$>10^{-5}$
13	$>1.5 \times 10^{-10}$	$>10^{-5}$
14	$>1.5 \times 10^{-10}$	$>10^{-5}$
15	No Data	$>10^{-5}$
16	$>1.5 \times 10^{-10}$	$>10^{-5}$
17	$<5.6 \times 10^{-16}$	1.6×10^{-9}
18	$<5.6 \times 10^{-16}$	1.6×10^{-9}
19	$<5.6 \times 10^{-16}$	1.6×10^{-9}
20	$<5.6 \times 10^{-16}$	1.6×10^{-8}
21	No Data	1.9×10^{-9}
22	No Data	6.5×10^{-9}
23	No Data	$>10^{-5}$
24	$<5.6 \times 10^{-16}$	0.8×10^{-9}
25	No Data	1.3×10^{-9}
26	$<5.6 \times 10^{-16}$	1.5×10^{-9}
27	$<5.6 \times 10^{-16}$	0.7×10^{-9}
28	No Data	0.7×10^{-9}
29	$<5.6 \times 10^{-16}$	0.7×10^{-9}
30	$<5.6 \times 10^{-16}$	1.1×10^{-9}

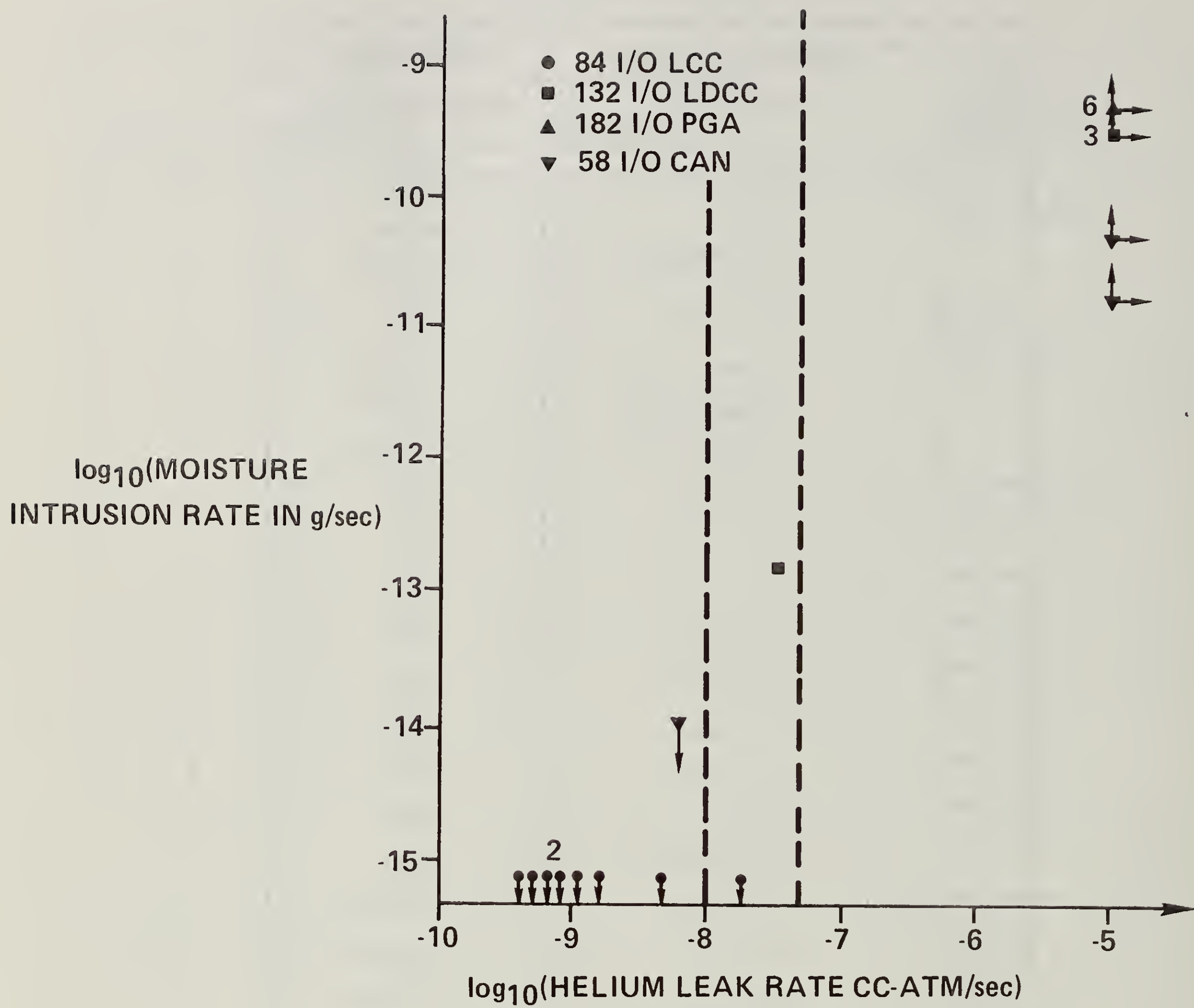

Figure 10 - Correlation of Apparent Moisture Intrusion Rates with Measured Helium Leak Rates. Small arrows indicate region bounded by each datum. Numerals indicate a number of data falling on the same location.

However, some information about the calibration shifts can be inferred from the existing data. The apparent moisture level corresponding to room ambient conditions always came out as about 2500 ppm_v. If room ambient is taken to be 40 percent RH at 20°C (which approximates our air conditioned lab in summertime), the actual moisture level was around 14,000 ppm_v. This implies that the new calibration slopes should be approximately 5.6 times their original values.

For the purposes of the analysis given in Figure 10, such a relative slope change is not very significant. Determination of actual leakage into apparently hermetic packages is, however, impossible.

Another factor affecting the sensor performance was the nature of the interconnections. Slight differences in output voltages (a few tenths of a millivolt) resulted from moving the location along the tinned-leads where the clips were attached from the model 771 hygrometer. Half a centimeter was enough of a movement to show in the output. All readings were taken with clips attached at the edge of the insulation to aid repeatability.

Sensor Utilization - Recommendations

The primary concern of the experimenter using these sensors is to avoid variations in temperature. Temperature excursions result in calibrations that change with time. Thus, the entire experimental sequence should be as isothermal as possible. Calibration should be performed at the end of the sequence.

The mounting of dice and sealing of packages almost always entails the use of elevated temperatures and this in turn results in unstable sensor responses that may take several months to stabilize. During this period of instability, precise measurements cannot be made - only changes of thousands of ppm_v can be inferred during this time.

One concept to get around this difficulty is to enclose sealed packages with mounted sensors in a dry box held at a constant, low moisture level equivalent to the seal atmosphere. This dry box should be held isothermally. The sensor outputs should be monitored until adequate stability is achieved. Once stability is reached the packages can be exposed to higher levels of external moisture (isothermally!). Data could then be obtained with leaking packages starting from a known moisture level.

This technique alone will not help to define the moisture contribution of organics sealed in a package. Outgassing that occurs within the first few months of sealing cannot be measured directly. Only through statistical methods can these sensors be used to determine moisture evolving inside a package.

The difficulties encountered with dying sensors could be avoided by mounting multiple sensors in a package. This could also help to reduce uncertainties associated with internal moisture determination. However, the experimenter must trade off the increased cost of additional sensors (about $50 each) against the use of additional packages.

Providing stable interconnections from the packages to the sensor bridge is important as soldering could result in sensor instability. The use of sockets are recommended.

One of the difficulties in performing experiments to determine optimum accept/reject criteria is the dearth of marginal packages. Both hermetic and gross leaking packages are fairly easily obtained. The marginal or borderline leakers are rarer. Out of thirty seals performed in this study only one was truly marginal, yet an entire distribution of marginal packages is required. The only way to insure that many marginally sealed packages are made is to seal large numbers of packages. The use of at least a few hundred packages will be needed if more than a few marginal leakers are desired.

Conclusions

Panametrics MINI-MOD HT moisture sensors have many crucial limitations which must be accounted for if optimum quantitative data is to be obtained. Qualitative data and relative quantitative data can be fairly easily obtained using these sensors.

Recommendations

Detailed recommendations are discussed above, but a short list of do's and don'ts for experimenters using these sensors follows:

Avoid all temperature excursions.

Allow sensor output to stabilize after any temperature excursions. This may require several months.

Calibrate sensors after stabilization.

Use sockets or other such devices to provide repeatable interconnections between packages and the sensor bridge.

Use enough sensors to provide reasonable statistics. Assume that 10-20 percent of all sensors will fail.

REFERENCES

1. A.D. Barany, et. al., "Hybrid Microcircuit Moisture Measurement Using Moisture Sensor Chips", Hybrid Circuit Technology, Sept. 1986.
2. D.A. Pinsky, "Hermeticity Measurements For Large Microelectronics Packages", Proc. of the Intl. Symp. on Microelectronics, ISHM 1986.
3. D.W. Swanson and J.J. Licari, "Effect Of Screen Tests And Burn-In On Moisture Content Of Hybrid Microcircuits", Solid State Technology, Sept. 1986.
4. David, R.F.S., "Testing Hybrids For Water Content", Test and Measurement World, Feb. 1986.
5. A. Dermarderosian and V. Gionet, "Water Vapor Penetration Into Enclosures With Known Air Leak Rates", IEEE Trans. on Electron Devices, Jan. 1979.
6. D. Stroehle, "On The Penetration Of Gases And Water Vapour Into Packages With Cavities And On The Maximum Allowable Leak Rates", IEEE Rel. Phys. Symp. Proc., 1977.

4.6: Aluminum Oxide Sensor: A Tutorial Update

V. Fong

Panametrics

PAPER NOT AVAILABLE

5.1 RELIABLE PLASTIC ICs FOR AUTOMOTIVE ELECTRONICS

Robert J. Straub
Ass't Staff Engineer, Parts Engineering
Delco Electronics Corporation
Mail Station R117
Kokomo, IN 46902
Phone (317) 451-7027

ABSTRACT

At Delco Electronics Corporation, we use almost one and one half million plastic-encapsulated integrated circuits per day. Many of the systems that use these ICs have a five-year or 50,000-mile warranty. To obtain this mandated high reliability required an effective parts program, complete specifications, adequate testing and a partnership with our key suppliers. This paper discusses some of the requirements to obtain these reliable integrated circuits. Some data is presented on what the warranty costs could be if a small percentage of parts would have to be replaced. Charts of plastic IC failure mechanisms observed during calendar years 1980 and 1985-86 are shown along with information showing significant improvements in reliability. Our suppliers have proven that we can work together to obtain the needed reliability utilizing plastic-encapsulated integrated circuits.

A CHALLENGE

In 1977, when Delco Electronics was given the charter to develop engine control computers for General Motors automobiles, a need for high-quality, reliable, low-cost integrated circuits (ICs) became a necessity. These engine controls must be reliable to support a minimum of a five-year or 50,000-mile warranty. For example, if one integrated circuit had a usage of one per automobile and, over a five-year period, there were 20 million automobiles made using this electronics system and 0.1% (1000 PPM) of this part had to be replaced, the warranty costs could be $2,600,000 because of a single, unreliable IC. This presumes there were no other failures.

At Delco Electronics, we use almost one and one half million plastic-encapsulated integrated circuits a day. That's an estimated 354 million for our 1987 Model Year. Thirty-eight (38) million of these are surface-mounted devices. We had to find ways to assure high quality and reliable ICs or customer dissatisfaction and warranty costs would severely damage our reputation and future business growth.

INVESTIGATION

During 1977 and 1978, we began a thorough investigation to find adequate integrated circuits to meet our goal of high-quality, reliable parts at cost-effective prices.

Military/Aerospace Parts

We reviewed the use of MIL-M-38510/MIL-STD-883 integrated circuits. They were not only too costly, but not enough capacity was available in the world to supply Delco Electronics' projected needs. Ceramic packages are also very fragile and, therefore, hard to handle in automatic assembly machines.

Commercial/Consumer Electronics Parts

Commercial plastic ICs were low cost, but the semiconductor industry did not provide specifications over the automotive temperature range of -40 to 85 or 125°C. These ICs had inadequate testing, even at room temperature. The thermal resistances of 24 and 40-pin plastic dual-in-line-packages (DIPs) were too high for use with complex high-power dissipation ICs in the high temperatures. Some manufacturers' ICs were unreliable in a humid environment, others would fail during the cycling of the ambient temperatures in the automotive environment; however, some manufacturers' ICs were good quality and were reliable in the automotive environment.

WHAT WE DID

Delco's approach to obtaining reliable plastic ICs was to have an effective parts program. It was based on previous experience in the automotive environment (primarily for radios, voltage regulators and ignitions) and knowledge obtained in the specification and use of integrated circuits in military and aerospace applications. This background allowed us to take a fresh approach to procuring extremely reliable ICs at cost-effective prices that would meet the demands of the automotive environment and the five-year or 50,000-mile warranty. This program began in 1977 with the transfer of some engineers from Delco's Santa Barbara, California Operation, where they had worked on military and aerospace ICs, to Kokomo, Indiana and the utilization of experienced automotive engineers from Kokomo.

Complete Specifications

Part Drawings

The IC part drawings were modeled after the military/aerospace drawings used in Santa Barbara, except they did not reference any military specifications because of the fear that if a military specification was used, our suppliers would feel that was an invitation to increase prices substantially.

The present IC part drawings contain:

Mechanical Requirements -
Mechanical requirements describe the plastic package outline and the thermal resistance junction to ambient as it is mounted on a printed circuit board in still air. We often cannot allow Alloy 42 lead frames because they do not achieve a low enough thermal resistance which is needed to meet the absolute maximum junction temperature restriction of 150°C for the power dissipations of the particular IC. Often copper lead frames are used to achieve the lower thermal resistance required.

Maximum Ratings -
- Storage Temperature Range
  - Typically -50 to +150°C.
- Operating Ambient Temperature Range
  - Typically -40 to either 85 or 125°C
- Maximum Voltages and Currents on Pins
- Absolute Maximum Junction Temperature
  - Never over 150°C for today's plastics.

Electrical Performance Requirements -
An outline of the voltages, currents and dynamic requirements that must be designed into the IC with process controls to assure they are met regularly.

Electrical Test Requirements -
- DC parametric
- AC (Switching times)
- Functional
- Adequate stuck-at-one and zero fault coverage of digital circuits.

Each of these electrical test requirements are specified at -40, 25 and a high ambient temperature (85 or 125°C) depending on if the system is mounted in the passenger compartment or under the hood.

High Test Temperature -
Based on the thermal resistance and the maximum specified power dissipation as the IC is used in the application.

The high test temperature is usually specified at a higher temperature than the maximum ambient operating temperature because the industry practice has been to test the ICs on automatic testers which test the parts in a very short time. This short time does not allow the IC die to reach thermal equilibrium and, therefore, does not assure that the part will work at steady-state conditions in the maximum ambient in the real world. An example is an IC that dissipates 400 milliwatts housed in a package that has a thermal resistance of 100°C per watt as soldered into the system circuit board which must operate in an ambient temperature up to 85°C.

The steady-state junction (die) temperature will be:

Tj = Ta + Pd*theta ja

where Tj - Junction temperature.
Ta - Ambient temperature within the system.
Pd - Power dissipation within the IC.
theta ja - Thermal resistance from junction to ambient as the IC is mounted in the application.

Tj = 85 + .400 * 100
= 125°C

The actual steady-state junction temperature in an 85°C ambient is 125°C. When tested on high-speed test equipment, the junction never reaches 125°C and, therefore, we are not assured the IC will function properly at the maximum operating ambient temperature.

The method of specifying the high test temperature utilizes an assumption that the test time is zero. It is obvious that a zero test time is impossible. This method provides a guardband. This is the high test temperature the handler or test chamber must be set at to measure the 85°C tests. This method only works where the test times are very short. The IC die does begin to warm up while being tested, but it never reaches thermal equilibrium if the test is quick. This high test temperature would not work for manual test equipment where test times are long. The time to reach thermal equilibrium for dual in-line packages is usually more than three minutes, but the rate of change is an exponential and quite complex, depending on the package thermal time constant, the method of heating the part, etc.

Lot Acceptance -

Delco requires every IC wafer lot to pass acceptance tests of autoclave and burn-in prior to being shipped for use in production. Our suppliers must do this lot acceptance at their facilities.

Autoclave
48 hours at 121°C, 15 psig. The sample plan is 22 samples with no defectives allowed. Every wafer lot must be sampled.

This is a test which replaces the test on hermetic ICs where 100% fine and gross seal screening is performed. There is no screen to eliminate ICs molded improperly. Autoclave is considered a destructive test. If the sample fails autoclave, the entire lot must be scrapped. The IC wafer fabrication, molding process and materials must be under good statistical process control to minimize losses.

Burn-in
48 hours at 125°C with bias applied.

Bias must be retained until the IC is cooled down. No high-temperature exposure is allowed between the time of bias removal and the endpoint testing at room temperature. The endpoint test must be made within 48 hours of the removal of bias. Burn-in lot acceptance evolved as follows:

100% burn-in was required on engine control ICs in 1979 while the volumes were low.

This gave us time to gather data which supported that a lot acceptance gate would be an effective means of preventing defective lots from being shipped to Delco. Refer to Figure 1 which shows the evolution of the burn-in lot acceptance sampling plans operating characteristic curves from before 1977 through 1986.

Electrostatic Discharge (ESD) Sensitive -
A Warning to treat all integrated circuits as Electrostatic Discharge Sensitive. Integrated circuits which were degraded at less than 2000 volts are treated as extremely ESD sensitive.

Common IC Specification -
A Reference to the Common IC Specification which contains added requirements.

FIGURE 1

BURN-IN LOT ACCEPTANCE SAMPLING PLAN OPERATING CHARACTERISTIC CURVES EVOLUTION

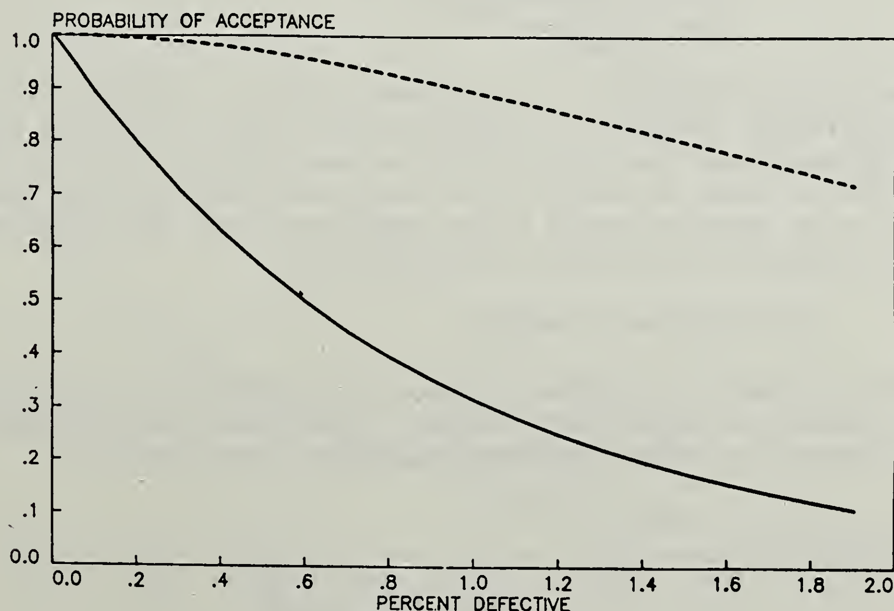

Integrated Circuit Specification

This integrated circuit specification is applicable to all integrated circuits. This specification defines the requirements common to all plastic ICs and also calls out the qualification specification which defines specific environmental test conditions. These specifications contain accelerated tests to assure the IC will operate reliably during the life of the vehicle.

Automotive and/or Manufacturing Environments -

- Temperature Cycle
  - 1000 cycles -40 to either 125°C or 150°C*
- Power and Temperature Cycling
  - 500 cycles with bias from -40 to either 85°C or 125°C*
- High Temperature Operating Life
  - 1000 hours with bias at 85°C or 125°C*

* Passenger compartment application uses lower temperature. Underhood uses higher temperature.

Automotive and/or Manufacturing Environments - (Continued)

- Autoclave
  - 48 hours, 121°C, 15 PSIG
- Bias Humidity
  - 1000 hours, cycled 30 to 65°C, 90 to 98% RH
- High-Temperature Storage Life
  - 1000 hours at 150°C
- Solderability
- Solder Heat
- Lead Bend/Pull
- Thermal Resistance
- Board Wash Test
- Solvent Resistance
- Test Grading

Test Grading/Fault Grading is a requirement that all digital ICs must have their test pattern "graded" to assure it will detect at least 99% of all the possible stuck-at-one and zero faults on every input and output of every gate on a gate-level model of the IC. We have found this grading necessary to assure our test patterns would catch defective ICs. This requirement has forced our suppliers to design in testability.

Test Software Control -

The IC test software is audited to assure the tests are actually performed as they are called out in the part drawing. The software, including the test graded patterns, are under Engineering Change Order control.

Electrostatic Discharge Capability Requirement -

a) 2000 volts, 100 pf, 1.5k ohm and
b) 200 volts, 200 pf, no resistor

Shipping Containers -

Requirement that all ICs must be shipped in antistat-coated conductive shipping tubes or conductive tape on reel. All ICs are treated as ESD sensitive within Delco.

Today, an average of 550-700 samples are used to qualify a surface-mounted integrated circuit. Refer to Figure 2 to observe the evolution of the operating characteristic curves for the sampling plans for each environmental qualification test. Each environmental test is usually run in parallel (i.e., temperature cycling on a single group of 77 ICs, operating life on another group of 77, etc.)

FIGURE 2

QUALIFICATION SAMPLING PLAN
OPERATING CHARACTERISTIC CURVES EVOLUTION

1983: N=31 A=1 (dashed line) 1986: N=77 A=0 (solid line)

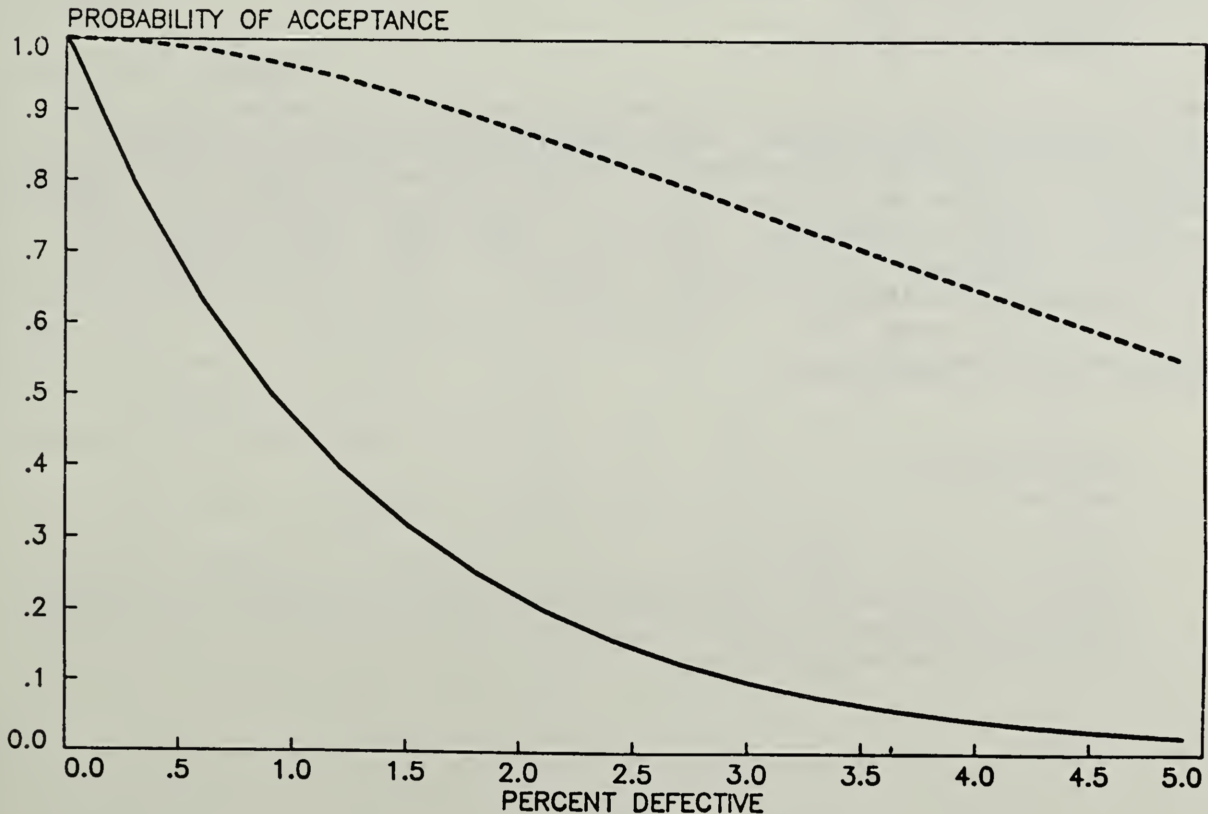

Changes -

We specify that no significant processes, design, or manufacturing wafer or assembly site changes are allowed without prior approval from Delco. When there are significant changes in design, processes, material, or manufacturing site which may degrade the reliability or impact the application of the IC, we may require a requalification plus assembly into over 1000 systems to assure compatibility and reliability prior to authorizing the change.

Qualification Program

We performed all the applicable environmental, mechanical, life and electrical transient tests at Delco until we were thoroughly familiar with the results on various types of parts. As we became experienced, we were able to do some qualification by similarity. We also have some of our key suppliers run qualification tests in parallel with Delco's tests and, if the supplier expressed a commitment, we correlated in our test results and, if the supplier passed our on-site survey, it may be certified to do self-qualification under Delco's directions.

Rigid Receiving Inspection Testing

0.1% AQL in 1979; today, no defects allowed
Testing at -40°C, Room, and Hot
Solderability Test
Mechanical Dimensions

Some suppliers' sites have been certified so that Delco no longer has to do incoming inspection verification. These suppliers have made a management commitment to be a partner with Delco, have had extremely successful results in incoming inspection, have avoided infant failures on the manufacturing line and have proven to have reliable parts from field experience. This program is called NIV (No Inspection Verification) at Delco. Delco still monitors the suppliers' quality performance in other ways.

Partnership With Our Suppliers:

No Inspection Verification (NIV). The no incoming inspection program described above.
The Certification to do Self-Qualification Testing as described earlier.
Failure Analysis performed by supplier on failures found at Delco.
Regular interface meetings between Delco Quality Control, Purchasing and Parts Engineering and the suppliers' Quality Control, Sales and Engineering representatives.

At these supplier interface meetings, held alternately at Delco and at our suppliers', the delivery performance, qualification testing data, incoming inspection results, line removal data, field performance, lot acceptance results, failure analysis findings and any problems are reviewed. We work together as teams to obtain optimum reliability.

Failure Analysis

Performed both at Delco and/or supplier.

- Receiving Inspection failures are analyzed.
- Line removals are studied.
- System level burn-in and reliability monitor failures are analyzed.
- Assembly plant part failures are evaluated.
- Warranty returns are analyzed.

We monitor these analyses for unacceptable trends and corrective action teams identify causes and implement corrective action.

RESULTS:

Qualification Testing

Over the last year, Delco tested 68,622 parts to qualify 263 new devices. Our suppliers tested 44,973 parts to qualify 95 new devices. In addition to qualification tests, Delco tested 11,131 parts to evaluate 73 new ICs under development.

Lot Acceptance Summary

During the last year, Delco's suppliers tested more than 219,000 ICs in autoclave at lot acceptance and they had an average fallout of 0.0407% (407 PPM). Those lots that failed the acceptance criteria were not shipped to Delco. During this same time, over 1.7 million ICs were subjected to the sample lot acceptance burn-in at our suppliers' with an average fallout of .0830% (830 PPM). Those lots that failed the burn-in sampling acceptance criteria had to be 100% screened at the supplier. These came from more than 10,500 lots from ten suppliers. Figure 3 shows the relative improvement over the last few years.

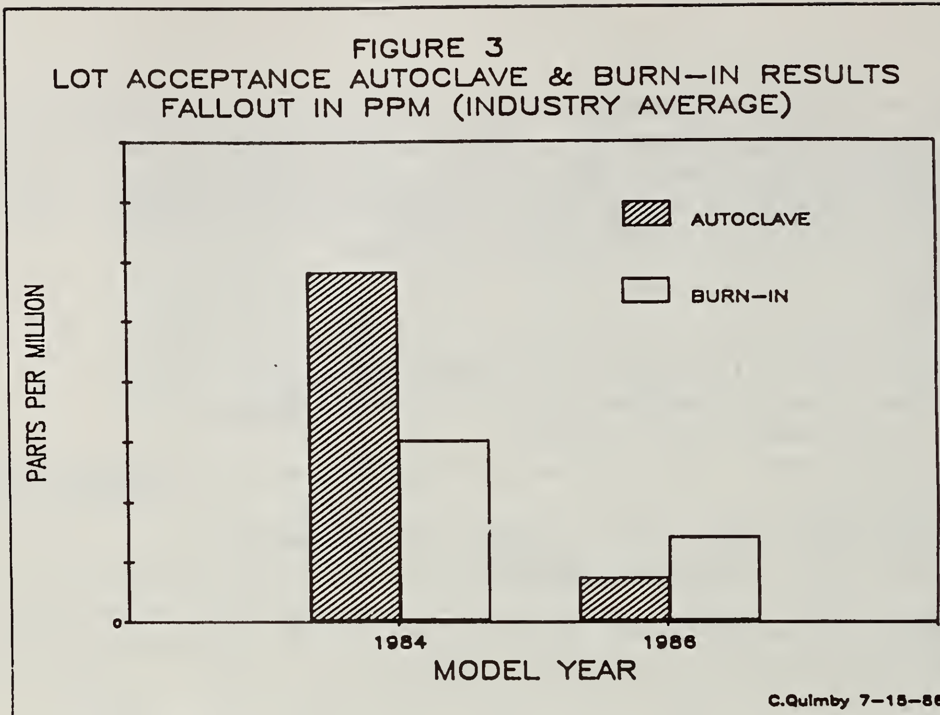

Receiving Inspection Electrical Results

Figure 4 shows the relative improvement observed in the Receiving Inspection electrical testing of the large scale integrated circuits (LSI) from Model Year 1980 to 1986.

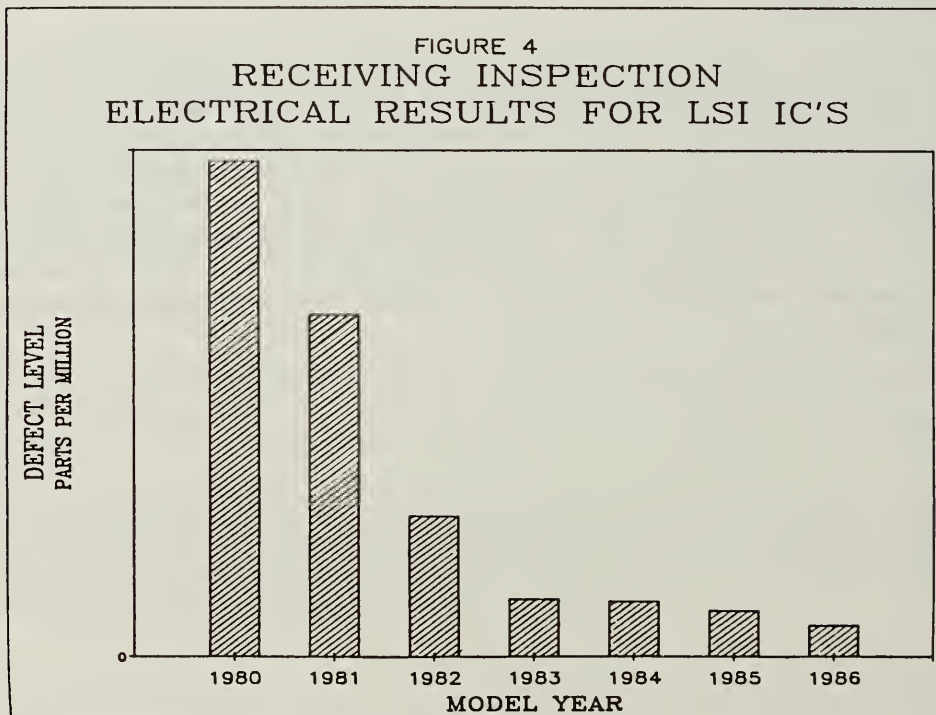

Manufacturing Line Removal Results

Figure 5 exhibits the relative improvement observed in the reduction of manufacturing line removals of complex LSI level ICs from Model Year 1979 through 1986.

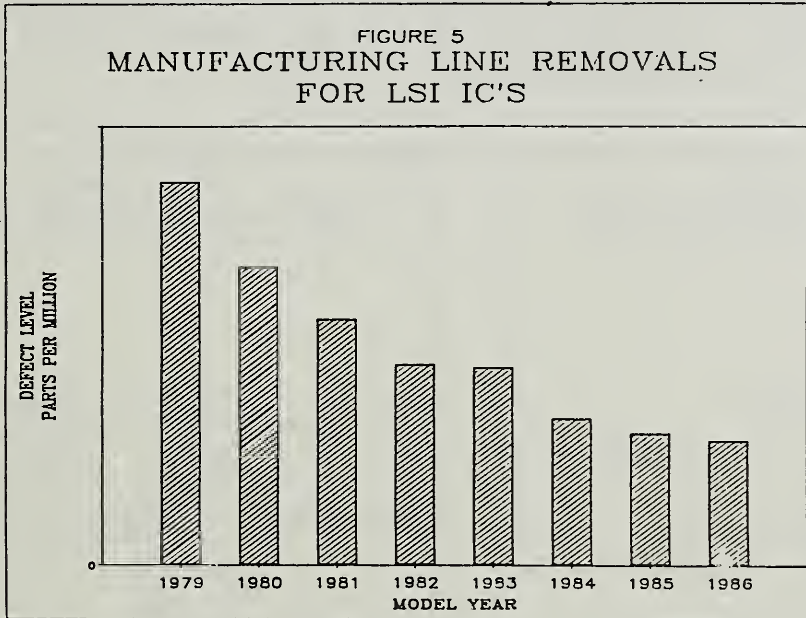

Integrated Circuit Warranty Return Results

Figure 6 shows the relative improvement in either the observed or predicted, depending on the age of the systems, 5-year/50,000-mile warranty returns for complex LSI integrated circuits.

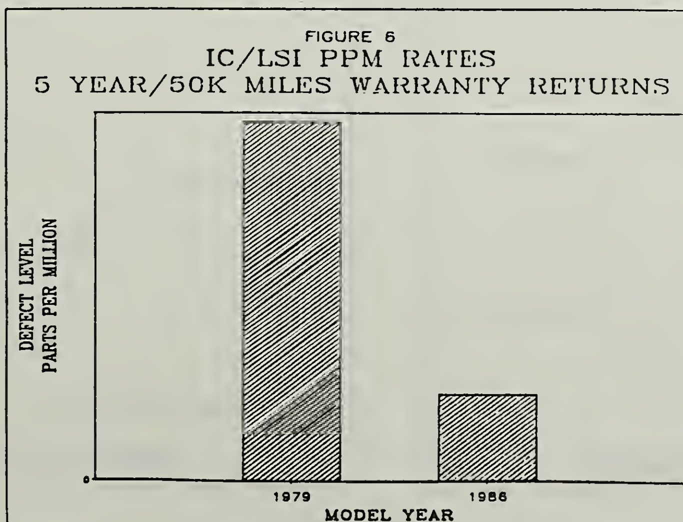

NMOS Failure Mechanisms 1980 Versus 1985-86

Figures 7 and 8 show the failure mechanisms we found during failure analysis of NMOS LSI manufactured in calendar year 1980 by two different suppliers. Note that each supplier has its own problems. Figures 9 and 10 show the failure mechanisms we found during failure analysis of NMOS LSI manufactured in 1985-86 by the same two suppliers as in Figures 7 and 8. Note how the failure mechanisms have evolved. Also keep in mind that the overall failure rates have become much lower during this time span.

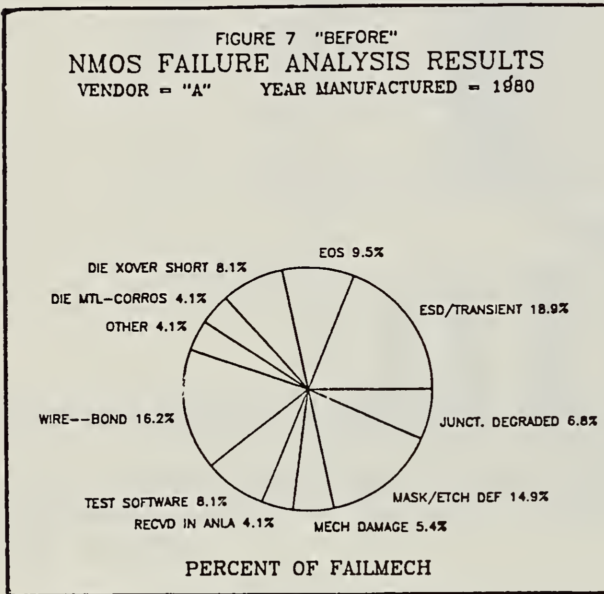

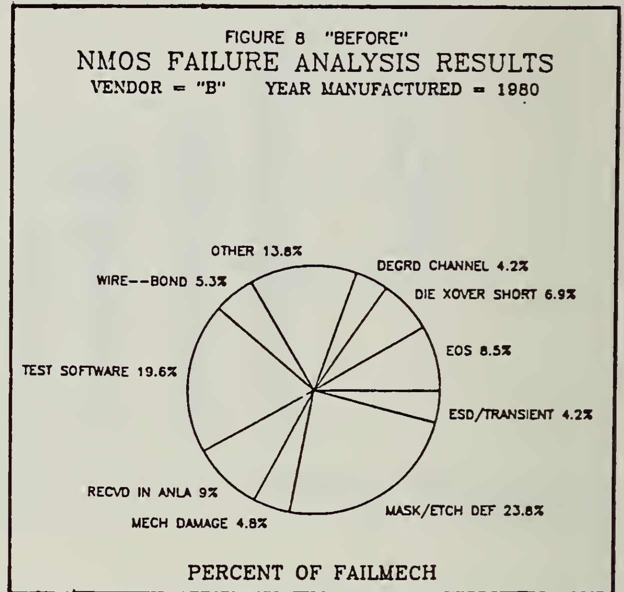

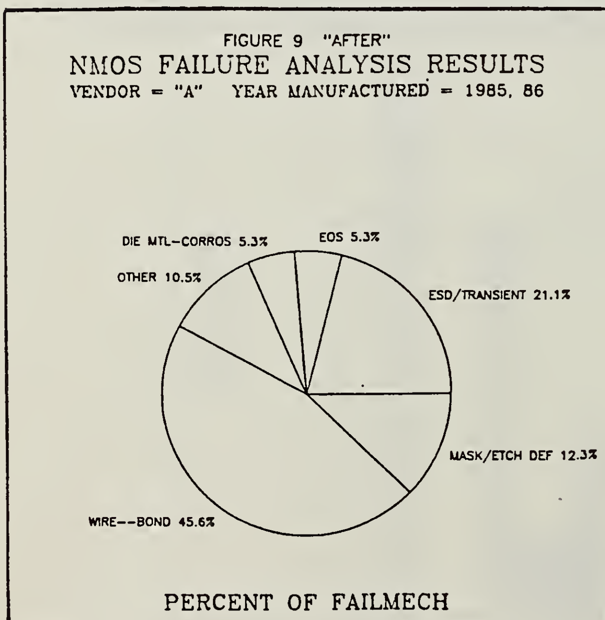

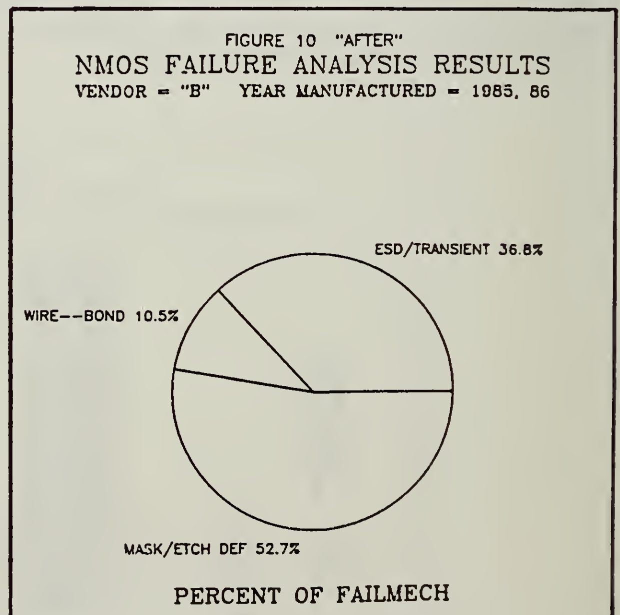

CONCLUSION:

Plastic-encapsulated integrated circuits are not inherently more or less reliable than hermetic ICs. A complete parts control program must be utilized to obtain highly reliable ICs. At Delco Electronics, we have proven that plastic ICs can meet our stringent reliability requirements.

The integrated circuit industry has made tremendous strides in improving reliability in the last few years. The reliability goal of Delco Electronics and General Motors is to continue this work and drive toward zero returns. Delco and our suppliers have strong programs to reach toward this goal.

5.2 A TEST PROGRAM TO ASSESS RELIABILITY OF PLASTIC PACKAGES AND GEL COATINGS FOR MILITARY ENVIRONMENTS

EUGENE C. BLACKBURN
Rome Air Development Center
Griffiss AFB NY 13441-5700
And
DR. DIDIER KANE
Clarkson University Contractor
Rome Air Development Center
Griffiss AFB NY 13441-5700

I. INTRODUCTION

The military microcircuit user community has through years of experience defined certain basic requirements that electronic devices must possess if they are to perform satisfactorily in their functional environment. The codification of this user experience is known as MIL-M-38510 (Specifications for Military Microcircuits) and MIL-STD-883 (Test Methods for Military Microcircuits). One measure of the appropriateness of these documents is the frequent citing of them by users in the automotive, industrial, and severe environment commercial applications. The requirements contained in these documents are based on the presumptions derived through historical evidence, that only hermetically sealed packages can adequately protect semiconductor devices. Over a period of many years, the Department of Defense (DOD)[1] and commercial organizations[2,3] have studied alternative packaging choices, including injection molded plastic, premolded plastic cavity, chip on board with conformal coating, combinations of organic and inorganic materials, and other options too numerous to mention. Each of these approaches shares the attribute that it replaces hermeticity with die protection designed to isolate the chip from its environment. This protection retards failures by slowing the speed with which corroding elements reach the die.

II. DOD INTEREST

Organic compounds are now available with higher levels of purity than were ever offered before. These materials are very low in ionic constituents and by their molecular design can limit the quantity of corrosion promoting materials that reach a silicon die. Test results have been reported by Hitachi[4] and internal studies have been conducted at AT&T [5] indicating that certain silicone coatings have achieved performance levels that may be sufficient for certain military applications. In view of this information, the Microcircuit Reliability Division of the Rome Air Development Center (RADC) has entered into participation with the IEEE Computer Society, Computer Packaging Committee, on the GEL Task Force.

III.GEL TASK FORCE

A consortium has been formed to investigate the state-of-the-art in GEL coatings. This group has an open membership policy that welcomes participation from any organization that has a contribution to make to the test program. The list of participating organizations is attached (Appendix 1). Five meetings have been held in nine months, plus two test subcommittee meetings. These discussions have produced a test program composed of: test methods, test plans, and assignments of responsibilities for achieving the task.

IV. THE TEST PROGRAM

The test program is composed of three test methods, three test plans, and a detailed logistic flow diagram to chart out the movements of the plastic packages under test.

The three test methods were selected by the test subcommittee. The intent of these tests is <u>not</u> to perform an extensive qualification of one or more GEL coatings and plastic packages for military use. The tests were chosen primarily to assess the coatings' ability to resist corrosion on the die. The first test is thermal shock as per

MIL-STD-883, Method 1011.6. The conditions are cycling from -65°C to +150°C with a five minute dwell at each extreme. The number of cycles will be given in the plan section that follows. The thermal shock temperature extremes were selected to match the most severe present military qualification range. The thermal shock procedure is the first in the test sequence in order to establish a path of ingress between the environment and the die. This will test for any weakness of the GEL coating adhesion to the passivated die. The second test is salt spray exposure from MIL-STD-883, Method 1009.6. The conditions of salt concentration, temperature, and pH are the ones contained in the test method. The number of hours will be given in the plan section which follows. The salt spray exposure is the second test performed in order to provide a ready supply of corroding ions to test the GEL coating integrity, primarily at the bonding pads where galvanic corrosion is likely to occur. The third is a steam autoclave exposure. The test condtions are taken from a standard General Electric plastic parts screening procedure.[6] The temperature is 130°C, the relative humidity is 85% and the parts are under bias during the test. This autoclave procedure has proven to be the single most consistent screen in assessing organic chip protection and serves to perform the function of the fine and gross leak tests which follow environmental test exposure of hermetic devices.

The three separate test plans were formulated in order to assess the validity of the test methods. It would serve no purpose if the first test destroyed all of the parts. All the time, money, and energy invested to date would be wasted. The pretest phase (P.T.) will perform a quick screen of just packaged parts without printed wiring boards to assure the three tests are appropriate. The P.T. phase includes 20 cycles of the thermal shock, 24 hours of the salt spray, and the autoclave test period is 96 hours. No failures are anticipated in these pretests which include only a small sample of the GELs. If a major failure mechanism appears, the task force will have to evaluate the materials under test, the assembly processes

used, and the test severity levels. Assuming no failures in the pretests, a selection of devices will be mounted to the specially designed printed wiring boards for the initial test phase (I.T.). This initial test is designed to assess the ability of the printed wiring boards, board connectors, conformal coating, and solder joints to survive the test environments. The stress levels for the I.T. phase are the same as for the pretest phase (20 cycles of shock, 24 hours of salt spray, and 96 hours of autoclave). The full test phase (F.T.) will follow assuming the boards and parts can survive the I.T phase. The F.T. will see the thermal cycles increased to 500, the salt spray raised to 96 hours, and the autoclave increased to 168 hours.

The chip test being used in this test is a triple-track resistor with 10 micron wide lines on 10 micron spaces. The center stripe has a series resistance of about 400 ohms. The resistance of the center track on each chip will be measured after packaging as well as before and after each environmental exposure. The leakage current between the center track and each of the parallel neighboring stripes will be measured also, with a 10 volt potential applied. The bias applied to the center stripe during the autoclave test will also be 10 volts.

There will be about eight printed wiring boards, each representing a GEL under test, with 15 experimental and three control packages on them. A set of "golden devices" will be held at the assembly point to assure all changes in the electrical measurements are due to the environmental exposures and not sample aging. Failure analysis will be performed on at least two devices per cell.

V. PRESENT STATUS

The specially designed triple-track resistor chips have been fabricated by Harris Semiconductor. Premolded cavity plastic packages have been provided by AMP. Prototype printed wiring boards are provided by Rockwell-Collins. Several candidate silicone gels will be applied by AT&T.

Estimates at this time place the completion of the test phases in the following time frame: P.T. phase Jan 87; I.T. phase Apr 87; and F.T. phase Dec 87. Results of the various tests will be made public after the data has been properly compiled.

VI. THE FUTURE

An obvious question that the task force activity raises must be: What would be a new task force activity? If one assumes for the moment that one or more of the GEL coatings performs well in the tests, then providers of microcircuits to the military would be expected to request procedures for qualifying coated devices. In the mean time, the task force will have provided industry and government a test sequence to assess non hermetic technology. The task force is discussing the extension of GEL coating use to injection molded packages. The process simplification derived from injection molded processes over premolded assembly could be very significant. The task force considered the testing of injection molded parts but found it would likely require substantial development time to establish a successful technique to mold over the GEL coatings. For this reason, the task force is now studying only the premolded package GEL coated chip option.

VII POSTSCRIPT

The considerations for exploring plastic package use in the military environment are many. Use of common processes from the commercial sector is an important one. The fusion of best commercial practices into the military procurement system could benefit both sectors of the market. Another potential benefit is better signal speed performance and a closer match between package and printed wiring board physical properties. Availability, competition between vendors, and possible faster insertion of newest technology into military equipment could result. However, the astute reader may have noticed the lack of a certain word or criteria in this postscript. That word is obviously cost. To understand why a deep

reduction in cost is not a likely result of success in using plastic packages, one must understand where the costs come from. Present commercial use plastic packaged devices are neither designed nor tested to operate over the full -55°C to +125°C temperature military environment. In addition to being required to meet tight electrical performance criteria over this temperature range, military devices must be able to be cooled conductively by a center core heat sink on the printed wiring board. In order to be designed to meet the substantially more severe testing and operating criteria necessary to satisfy military shipping, storage, handling, radiation, flight avionic, space repair, etc. environments, there may not exist a substantial cost differential between plastic and hermetic parts.[7] The valuable benefits would more likely be the increased speed performance, weight, and materials compatibility with the present glass-expoxy substrate technology.

ACKNOWLEDGEMENTS

To Mr. Jack Balde, IDC, the Chairman of the Task Force, who has made it possible for this consortium approach to work.

To Mr. Marty Freedman, AMP, the Coordinator of the Task Forces' actions.

To Mr. Al Sasaki, McDonnell Douglas, who has contributed extensively to the test plan.

VIII. REFERENCES

(1) Assessment of Silicone Encapsulation Materials: Screening Techniques; A. Christou and W. Wilkins, Proceedings of the 1977 IRPS.

(2) Moisture Resistive, Ultraviolet Transmissive Passivation for Plastic Encapsulated EPROM Devices, K. Alexander, J. Hicks and T. Soukup, Proceedings of the 1984 IRPS.

(3) Moisture Protective Coatings for Copper Thick Film Systems, J. P. Mannitt, Proceedings of the 1984 ISHM.

(4) Sealing Mechanism of Silicone Jelly Encapsulation with High Reliability, K. Otsuka, Y. Shirai, K. Okutani, Proceedings of the 1984 ECC.

(5) C. P. Wong, Private Communication.

(6) Accelerated Corrosion Testing in Pressure Cooker at 130°C, J. Burgess, A. Yerman, Proceedings of the 1986 ECC.

(7) IC Quality Grades: Impact on System Reliability and Life Cycle Cost, M. G. Priore, RADC/RAC Report NB SOAR-3 (1985-1986).

APPENDIX I

Organizational Membership List:

- Westinghouse Electric
- Hughes Aircraft
- Fairchild Camera and Instrument
- Microelectronics and Computer Technology Corp
- Loral Electronic Systems
- McDonnell Douglas
- Texas Instruments
- Interconnection Decision Consulting
- Boeing Electronics
- Dow Corning
- International Telephone and Telegraph
- Rome Air Development Center
- National Bureau of Standards
- Martin Marietta
- Rockwell Avionics
- AMP Inc.
- General Electric
- American Telephone and Telegraph
- Harris Semiconductor
- Lehigh University
- International Business Machine
- Naval Ocean Systems Center
- Rutgers University
- Aerospace Corporation

5.3 MOISTURE MONITOR FOR PLASTIC PACKAGED INTEGRATED CIRCUITS

HOWARD L. BLAZ

Harris Semiconductor

P.O. Box 883

Melbourne, FL. 32901

305 724-7128

ABSTRACT

The HARRIS Moisture Chip (H10-55001-6) designed for use in in-situ determination of internal water vapor content of hermetic integrated circuit packages can be used to monitor humidity performance of plastic encapsulated integrated circuits.

Tests run on the moisture cell in different brands of plastic from multiple assembly lots will repeatably distinguish between materials and processes.

This device provides a test structure to evaluate plastic packaging independent of wafer fabrication related variables. The data is simple and quickly obtained using inexpensive monitoring of leakage currents after stressing. Testing is non-destructive so parts can be returned to the stressing conditions for continued evaluations or until the onset of corrosion.

The experimental design and a statistical analysis of the data will be presented. This data demonstrates the effectiveness of this test structure in determining moisture penetration in different plastic compounds and the variability in the assembly process.

BACKGROUND

Conventional methods of evaluating the moisture resistance of packaged Semiconductors (temperature-humidity-bias and autoclave) are time consuming, labor intensive, and expensive. For these reasons the feasibility of using a moisture sensitive test cell was investigated. Moisture cells used in this study are unpassivated interdigitated aluminum combs on thermal oxide. The leakage current between interdigitated combs is used as an indicator of the presence of moisture.

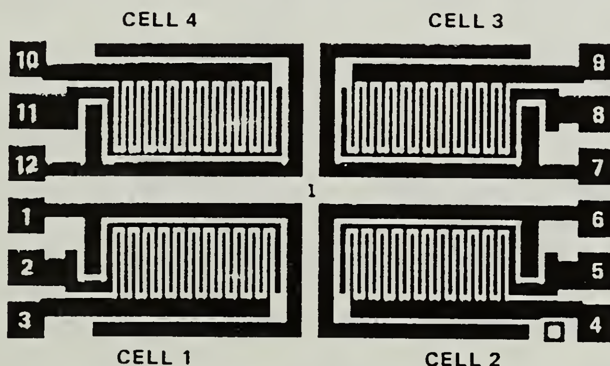

The HI-55001 has four electrically identical moisture sensing cells on chip. The user may apply any one cell or parallel combination of cells in a moisture measuring experiment. The individual cells are accessed as follows: Cell 1 – pads 2 & 3; Cell 2 – pads 4 & 5; Cell 3 – pads 8 & 9; Cell 4 – pads 10 & 11 respectively.

Chip Size: 95 mils by 50 mils.

Copyright © Harris Corporation 1979

The current flow to the cell is high initially and diminishes until the current reaches a steady state which is the leakage current (analogous to the charging of a capacitor). In this study leakage currents in the 10^{-13} amp range were observed in unstressed encapsulated cells. Steady states are attained rapidly enough to make measurements 1 minute after biasing parts with 5.0 volts. It is believed temperature and humidity stressing in autoclaves will eventually cause leakage currents to increase several orders of magnitude. In the following studies, leakage currents were observed to increase seven orders of magnitude.

The interval between test points (time on stress) must be carefully chosen since the leakage current measured is subject to a series of time ordered events (See below).

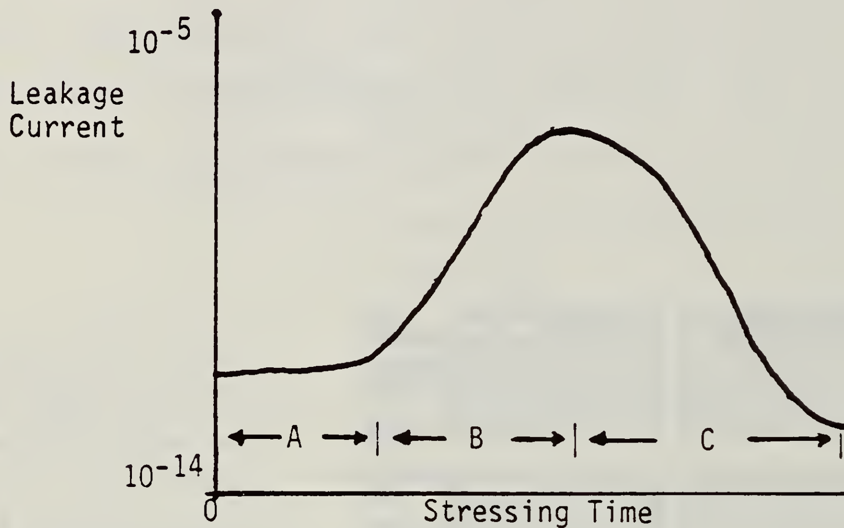

Segment A is zero hour to the onset of leakage current.

Segment B is the period of time in which the leakage current increases due to addition of electrolyte (ionics and moisture) to capacitor.

Segment C is the period of time in which the leakage current decreases due to corrosion (lowering of aluminum conductivity).

In addition measurements must be made quickly upon the removal of the part from stressing. The moisture driven to the cell surface by the thermal and pressure effects of the autoclave will leave the cell surface in the absence of these effects. This phenomenon is known as recovery. It takes place in fewer than 10 hours.

APPROACH

A preliminary study (Study #1) was conducted to determine a reasonable time for current measurement after removal from stress in order to reduce the effects of recovery.

Additionally a determination was made of the interval for interrupting stressing to make measurements in order to reduce the effects of corrosion. Three standard products of plastic molding compound manufacters were used to encapsulate moisture cells which had been specially doped with phosphorous in the thermal oxide beneath the metallization. The phosphorous dopant when combined with moisture penetrating the plastic would give a significantly higher electrolyte concentration at the die surface than would have been seen in the typical moisture cell. This doping made the cell so sensitive to moisture that all three plastics performed similarly without regard to ionics and/or lead lock. The time interval from hour zero to the end of segment B (see above) was approximately 15 hours. This study also confirmed the behavior of segment C (see above).

A second study was conducted to determine the feasibility of using the moisture cell to distinguish between different brands of plastic used for encapsulation.

A third study was then performed utilizing a statistically designed experiment to confirm the repeatability and seek to distinguish process variation. The experimental section discusses this third study.

EXPERIMENTAL

Five standard products of plastic molding compound manufacturers

were transfer molded onto 16 lead copper leadframes with moisture cells (all from same wafer lot) attached (polyimide die attach). This molding was conducted over a 5 day period with each plastic being 'shot' everyday; only the order of the 'shots' being varied. Between 'shots' the mold chase was cleaned with melamine and preconditioned with dummy 'shots' of the next plastic to be used.

On days 1 and 2 the cell/leadframe assemblies were spray cleaned with isopropyl alcohol (electronics grade) post wire bond. On days 3, 4, and 5 the assemblies were additionally cleaned with isopropyl alcohol prior to placing them on the hot chase. Molding was done 1 week post wire bond.

Stressing was performed in 24 hour intervals. Parts were grouped in 5 trays of 5 parts each (the five parts having one representative from each day/plastic combination). The parts were randomized as to position in the mold chase at time of molding. The order of measuring the parts in the trays and the order of the trays set for measurement was fully randomized using the latin square technique to block extraneous variables.

The parts were removed from stress and biased with 5.0 volts on a Hewlett Packard HP 4145A Semiconductor Parametric Analyser to measure the leakage current. This device was controlled by a HP 9836 computer to switch between 3 sets of interdigitated combs on each cell and to record the data. This setup was used to record zero hour stressing and 16 successive intervals of 24 hour stressing.

Statistical process control (SPC) was applied to the parametric analyzer using unstressed parts to assure the elevated current readings on stressed parts were not affected by drift in measurement.

$$\hat{\sigma} = 0.39 \quad \hat{\bar{x}} = 0.35 \text{ pA}$$

The samples were stressed in an unbiased condition using a National autoclave monitored with a Sensotec (SA) pressure transducer and a Doric (Trendicator 402A) thermocouple monitor. This equipment at 100% relative humidity (R.H.), saturated environment cycles on at 13.9 pounds, 120°C and off at 16.3 pounds, 122°C. Parts were removed from stress, tested/monitored, and returned to stress within 2 hours.

A general linear models procedure for statistical analysis utilizing the Bonnferroni (Dunn) T. tests for the variable log of measured current was applied to the data. The computer program used was S.A.S. (Version 79.6; SAS Institute Inc., Box 8000, Cary, N.C. 27511).

RESULTS AND FINDINGS

The following table contains the results of the studies.

Stressing Periods to achieve elevated leakage current	3rd Study (statistically designed)	2nd Study
Fewest (worst performance)	Compound A	Compound C
	Compound B	Compound A
	Compound C	Compound B
	Compound D	Compound D
Most (best performance)	Compound E	--

NOTE: 1) Compound E was not available for 2nd study.

2) Assembly lot variation of Compound C performance is consistant with historical reliability data gathered by Harris Semiconductor.

The following graph contains the time-leakage current relationship of the statistically designed (3rd) study.

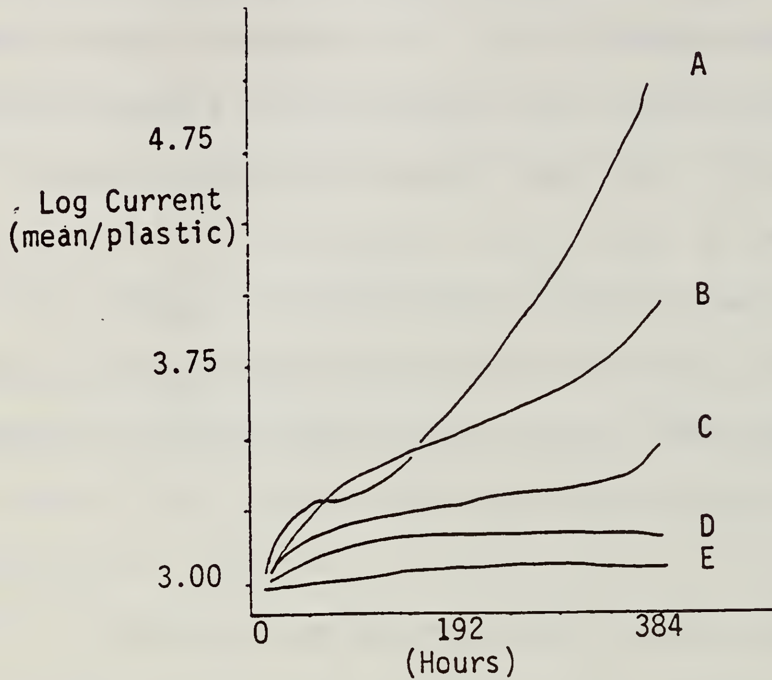

Additionally, those parts subjected to isopropyl alcohol rinse immediate prior to molding (indicated by *) showed a trend toward lower leakage currents than those not so rinsed.

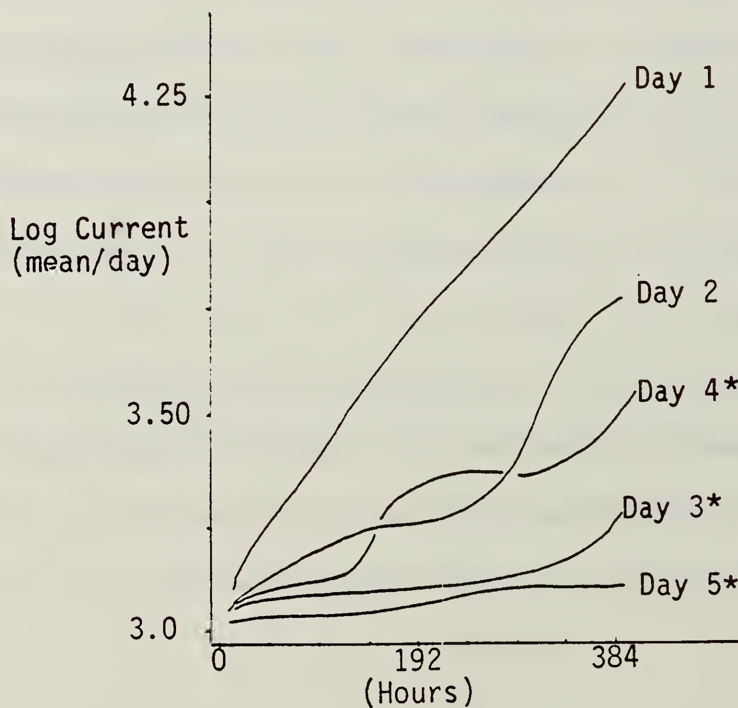

Position in the mold chase did not indicate any repeatable variance in moisture cell performance.

The onset of elevation of leakage current was a function of handling of stressed parts. The use of fingercots extended the time of the experiment from 5 days (2nd study) to 16 days (3rd study), demonstrating the effects of 'clean' handling. Further invesigations are planned to explain this phenomenon in detail. It is not known at this time if moisture ingress was by bulk diffusion or through the leadframe-plastic interface. It is not known at this time if the ionic content of the electrolyte reflects material solely available in the encapsulating plastic.

CONCLUSIONS

The interdigitated comb moisture cell provides a test vehicle for plastic mold compound T&H performance comparison. The response of the cell to stressing is repeatable. Measurements are performed utilizing any ammeter with a pA range.

The use of this cell as a performance probe eliminates lot to lot and/or wafer to wafer variability on production integrated circuits as a source of variation in a controlled experiment. Data can be gathered using simple equipment eliminating variability due to test handler situation. Parts need not be stressed to catastrophic failure. They can be stressed to the attainment of an arbitrarily determined leakage current; a great time saving.

Additionally, stressing can be accomplished in a relatively inexpensive autoclave chamber without bias. This will allow comparisons

in material and/or process performance to be evaluated. Stressing times are considerably less than in 85°C/85% R.H. chambers. At this time the issue of correlation with actual device life performance has not been investigated.

Lastly, the lack of passivation of this die allows it to be used as a strain gauge. Decapsulation should reveal shifting of portions of the aluminum interdigitated comb in high mechanical stress applications. Experiments are currently underway to assess this potential usage.

ACKNOWLEDGEMENTS

W. L. Schultz and H. A. Swasey for encouraging this work.

D. M. Andrews for encouraging my interest in semiconductor packaging.

5.4 HIGH RELIABILITY MOLDED PLASTIC PACKAGING (I) THROUGH A SYSTEMATIC APPROACH

LOUIS LIANG
LINEAR DIVISION
FAIRCHILD SEMICONDUCTOR CORP
313 Fairchild Drive
MOUNTAIN VIEW, CALIF 94039

I. INTRODUCTION

Traditionally plastic packages are known to be susceptible to moisture induced failures. This is particularly worrisome with some SMD such as SOIC which are subjected to severe temperature shock during board soldering.[1-3]

The industry customarily defines failure as non-recoverable corrosive defect on the chip. Test methods commonly used today are static pressure pot at 1 ATM; bias pressure pot from 2-8 ATM; and 85/85 THB. The user community, with the exception of only a few, specifies static pressure pot as the standard tool for HAST. The requirements for time to failure has been steadily increasing: from 24 HR in the early 70's to 96 HR in the early 80's; and now 168 HR appears to be a common requirement. Some users have begun to demand bias pressure pot as an incoming inspection method.

In order to meet the ever more stringent requirements and possible future acceptance of plastic packages in certain military applications, most semiconductor manufacturers have active programs to improve reliability performance of their plastic packages as a marketing edge. Some major IC producers even have programs addressing issues far beyond the present commercial applications. This report, however, is limited to the presentation of a "high reliability" conventional molded plastic package for commercial application. It should not be construed in any way to compare with "Gel Coated" plastic packages from AT&T, GM, Hitachi, etc.[4]

II. HIGH RELIABILITY DEFINITION FOR MOLDED PLASTIC PACKAGES

There is obviously no agreed upon industry standard for plastic packages reliability. Time to failure performance for pressure pot also varies significantly from vendor to vendor. In order to establish a reliability performance measurement, Fairchild's Linear Division has instituted a phase objective program as shown in Table I.

TABLE I.

FAIRCHILD LINEAR DIVISION MOLDED PLASTIC PACKAGE

RELIABILITY DEFINITION FOR MOSITURE RESISTANCE

(INTERNAL BENCH MARK FOR PRODUCTION PARTS)

TEST METHOD	OLD (pkg)	REL I '85	REL II	REL III
STATIC PR POT *1				
96 HR	0/45	--	--	--
168 HR	2/45	0/45	--	--
336 HR	--	0/45	--	--
500 HR	--	1/45	0/45	--
1000 HR	--	2/45	0/45	--
2000 HR	--	--	0/45	0/45
BIAS PR POT *2				
48 HR	--	0/15	--	--
168 HR	--	0/15	--	--
500 HR	--	--	0/15	--
1000	--	--	1/15	0/15
PARALLEL TESTS *3	YES	YES	YES	YES
SEQUENTIAL TESTS *3	NO	NO	YES	YES
85/85 THB *2				
1000 HR	< 1.0	--	--	--
2000 HR	--	< 0.1	0	0
CORROSION CRITERIA	YES	YES	YES	YES
PARAMETRIC CRITERIA	NO	NO	YES	YES

*1 Production Monitor Performed Twice Weekly.

*2 Reliability Monitor Performed Regularly.

*3 Thermal Shock; (Salt Spray); Autoclave or 85/85 THB

III. INVESTIGATIONS

In order to fully understand moisture induced failure mechanisms in conventional molded plastic package, detail experimental matrix was used to identify moisture path, contaminants, process conditions, design rules, and test methodology.

MOISTURE PATH

As shown on Figures 1 and 2 and photo slides.[5,6]

Key contributors to moisture path in terms of severity were found to be Trim/Form; Leadframe Design; Leadframe Material; Plating Material; Molding Compound; Lead Finish Operations; Flux; and Deflashing.

COMPATIBILITY OF MATERIALS

Contaminants in a molded plastic package were traced to three major sources: Flux Residual; Molding Compound; and Die Attach Paste. Although impurity level in the materials described above are crucial factors [7,8], material compatibility was found to be very important as shown in Figure 3. It was also found, during the final phase of the material selection process which involved a 3 X 3 matrix for die paste and molding compound materials, that 2 out of 9 elements consistently had superior results. Search of published literature however failed to uncover any similar report on this interesting and important phenomenon.

PROCESS CONDITIONS AND DESIGN RULE

To take maximum advantage of modern low impurity packaging materials and halide free flux, it was necessary to pay significant attention to design rules [9] (both chip layout and leadframe design), and assembly process conditions. Table II shows where improvements were made in the new plastic package at Fairchild's Linear Division in order to achieve the reported performance.

TABLE II. PROCESS IMPROVEMENT SUMMARY

AREA OF IMPROVEMENT	DESCRIPTION
Die Size Vs Pad Size	Maximum die size defined.
Wire Bond	Max length; loop height; and wire angle from bond pad to finger defined.
Plastic Locks and Moisture Trap	Incorporated.
Mold Grating	Redesigned.
Trim/Form	Redesigned.
Deflash Process	Changed.
Lead Finish	Re-tooled and Re-vamped.
Parts Handling	Eliminated all manual contacts with parts.

TEST METHODOLOGY AND PLASTIC MATERIAL QUALITY

A rigid test plan was found to be essential for post moisture environment tests because parametric shifts in some high precision Op Amp devices. They were, however, not at all apparent in logic and interface devices tested. Generally parametric shift and low level leakage were recoverable with time and may be a fact of life for high precision Linear devices in today's molded plastic packages. Fig. 4 shows a typical recovery curve for a sensitive high precision Op Amp

Packaging material consistency is another key variable for recoverable parametric failure (Fig. 5). Material supplier's ability to maintain quality consistency cost effectively in a high volume production environment, and our ability to implement a fast and effective incoming quality inspection method are yet to be developed.

Fig 4. Recovery Curve of an Op Amp

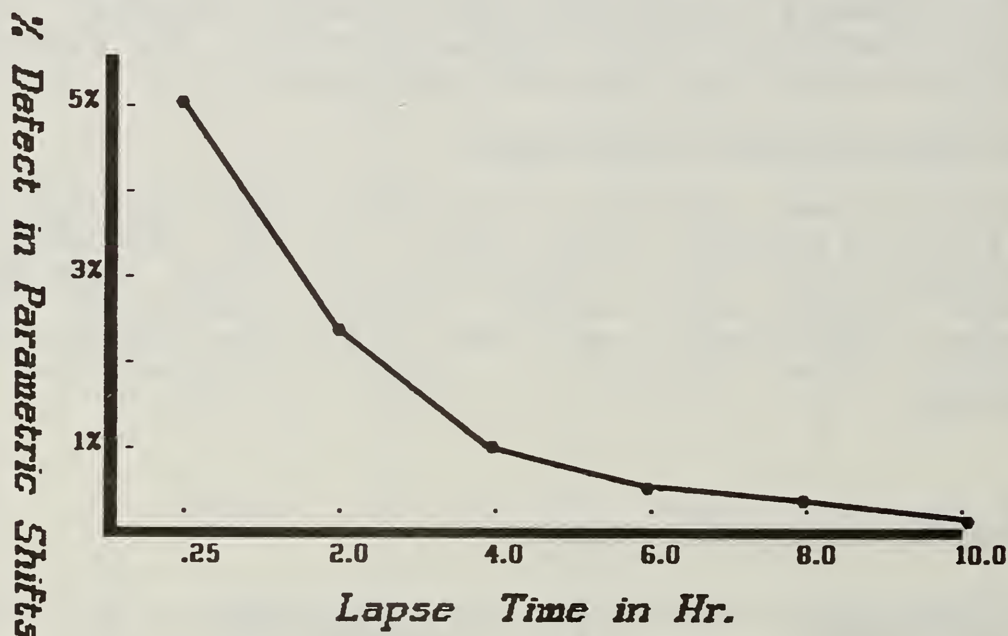

IV. RELIABILITY PERFORMANCE SUMMARY

TABLE III. PERFORMANCE COMPARISON OF "OLD" AND "NEW" PACKAGES (OP AMP

TEST COND.	OLD (CONTROL)		NEW (HI REL I)	
	ENGR.	PROD (MON)	ENGR	PROD (MON)
OP LIFE 125`C 1000 HR 2000 HR	.22% NA	0.7% NA	0/1000 + 0/1000 +	0% 0%
85/85 THB : 1000 HR 2000 HR	.8% NA	3.3% NA	0/1000 0/1000	0% 0.05%
121'C PR POT 168 HR 500 HR 1000 HR	2.0% NA	3.4% NA	0/6000 0/6000 1/6000	0% 0.01% 0.15%
BIAS PR POT 145`C 85% RH: 96 HR 168 HR 500 HR 700 HR 1000 HR	NA	NA	** 1/89 0/209 0/88 0/207 3/88 0/207 11/85 0/207 0/74 0/207	NA
THERMAL SHOCK -55`C - 125`C: 500CY 1500CY	0% NA	0% NA	0/1000 0/100	0% NA
TEMP CYCLE -65`C - 155`C 500CY 1500CY	0% NA	0% NA	(6/500)0/100 0/100	0% NA
SOLDERABILITY 1 HR 16 HR	0% NA	0% NA	0% 2/50	0% NA

REMARKS: Interface and logic devices typically have much better performance than precision Op Amp.

** Interface device.

V. DISCUSSION AND CONCLUSION

With modern low impurity plastic packaging materials, it is now possible to produce high reliability (I) molded plastic package for commercial applications. However, material technology alone is far from adequate. A systematic approach encompassing design, process, and carefully matching packaging materials was necessary to obtain the high performance reported. The biggest challenge, to date, is our ability to implement effective process control in production environment to hold the gain consistently without having to resort to exotic total automation in material manufacturing and package assembly.

The audience must be reminded that conventional molded plastic package may never achieve the same "hermeticity" performance we have so taken for granted with ceramic packages. This may be particularly true for some extremely sensitive high precision Linear devices. There is still a long road ahead of us before we are capable of producing a "High Reliability III" molded plastic package which could be universally acceptable by military applications while still being cost competitive with the present commercial molded plastic package. We may need to develop new passivation and molding technology in order to reach the next plateau. We are, nevertheless, encouraged by the preliminary results of our "Rel II" development project that cost effective solution is not entirely elusive.

ACKNOWLEDGEMENT

The author wishes to thank A. Sezen and J. Taylor for performing almost all the tests and failure analysis in the study; G. Chu and Linear's Korea Assembly and Test Plant for preparing many thousands of samples and data analysis used in this report.

REFERENCES

1. L. Feistein, "Failure Mechanism in Molded Microelectronic Packages"; Int'l Microelectronics Conf pp.49-57, (1979)
2. R. Larson, "A Review of the Status of Plastic Encapsulated Semi. Component Reliability"; Br. Telecom Tech J. V.2, No.2, (1984)
3. S. Ito, et. al, "Special Properites of Molding Compound for SO Packaged Devices" ECC (36) Proc, PP. 360-365, (1986)
4. A. Otsuka, et. al, "A new Gel Sealing Mechanism for High Reliability Encapsulation"; IEEE CHMT-7, No.3, PP.249-256 (1984)
5. M. Murtuea, et. al "Flux Penetration and Pressure Cooker Fail Mechanism in Plastic IC Packages" ECC (36) PP. 616-621 (1986)
6. R. Stroehle, "Influence of the Chip Temp. on the Moisture Induced Failure for Assessing Plastic Encapsulated Semi. Components"; IEEE CHMT-6, No.4, pp.537-543 (1983)
7. M. Iannuzzi, "Reliability and Failure Mechanisms of Nonhermetic Aluminum SIC's: Literature Review and Bias Humidity Performance" IEEE CHMT-6, No.2, pp.181-201, (1984)
8. W. Collins, et. al, "Improved Moisture Resistance in Plastic Package" ECC (35) PP. 14-17, (1985)
9. R. Thomas, "Stress Induced Deformation of Al. Metalization in Plastic Molded Semi. Devices"; CHMT-8, No.4, pp.427-439, (1985)

FAIRCHILD
A Schlumberger Company

Fig 1. Moisture Path in a SOIC Package

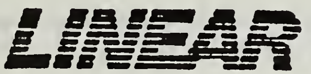

Number	Leads Pitch	Tip to Tip	Length	Body Width	Height
14	.050	.236	.340	.154	.061
16	.050	.236	.390	.154	.061

LINEAR

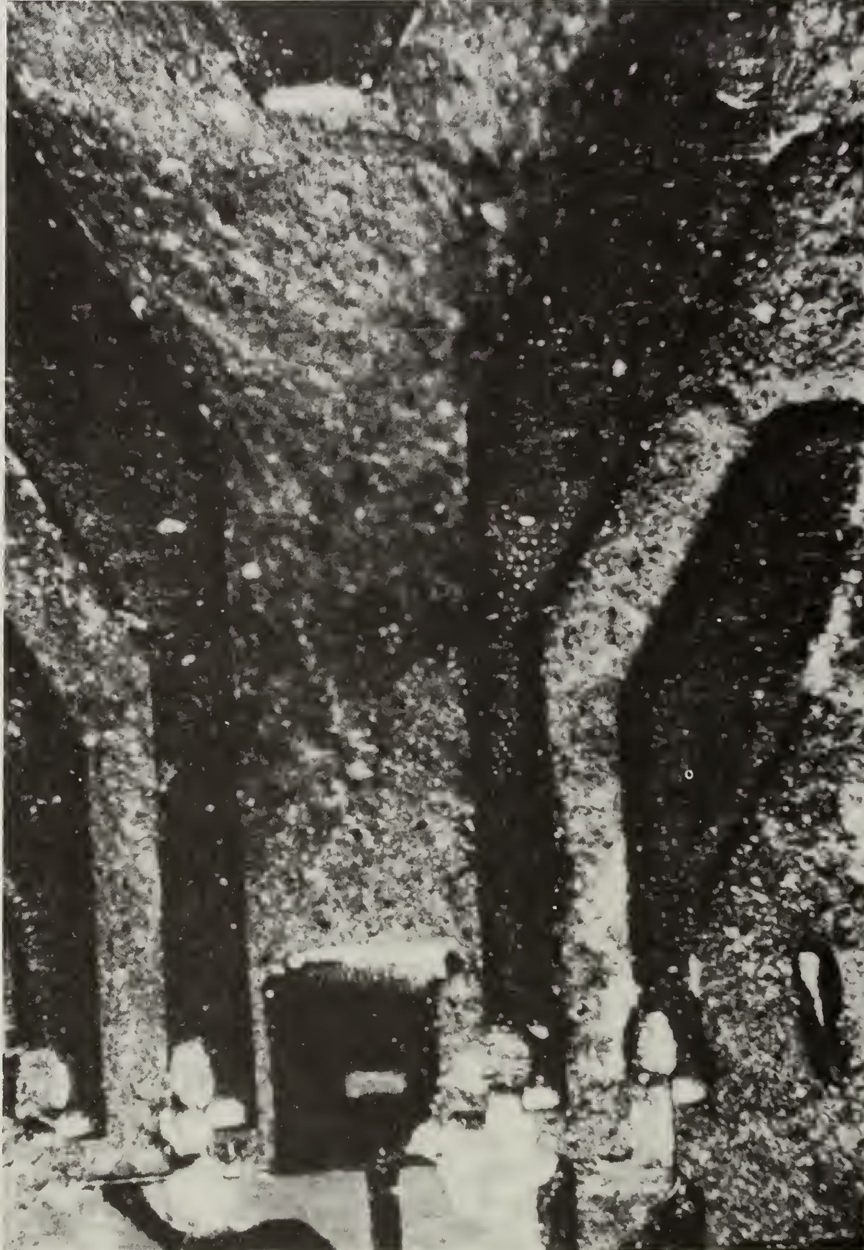

Fig 2. Flux Residual in a Plastic Dip

FAIRCHILD
A Schlumberger Company

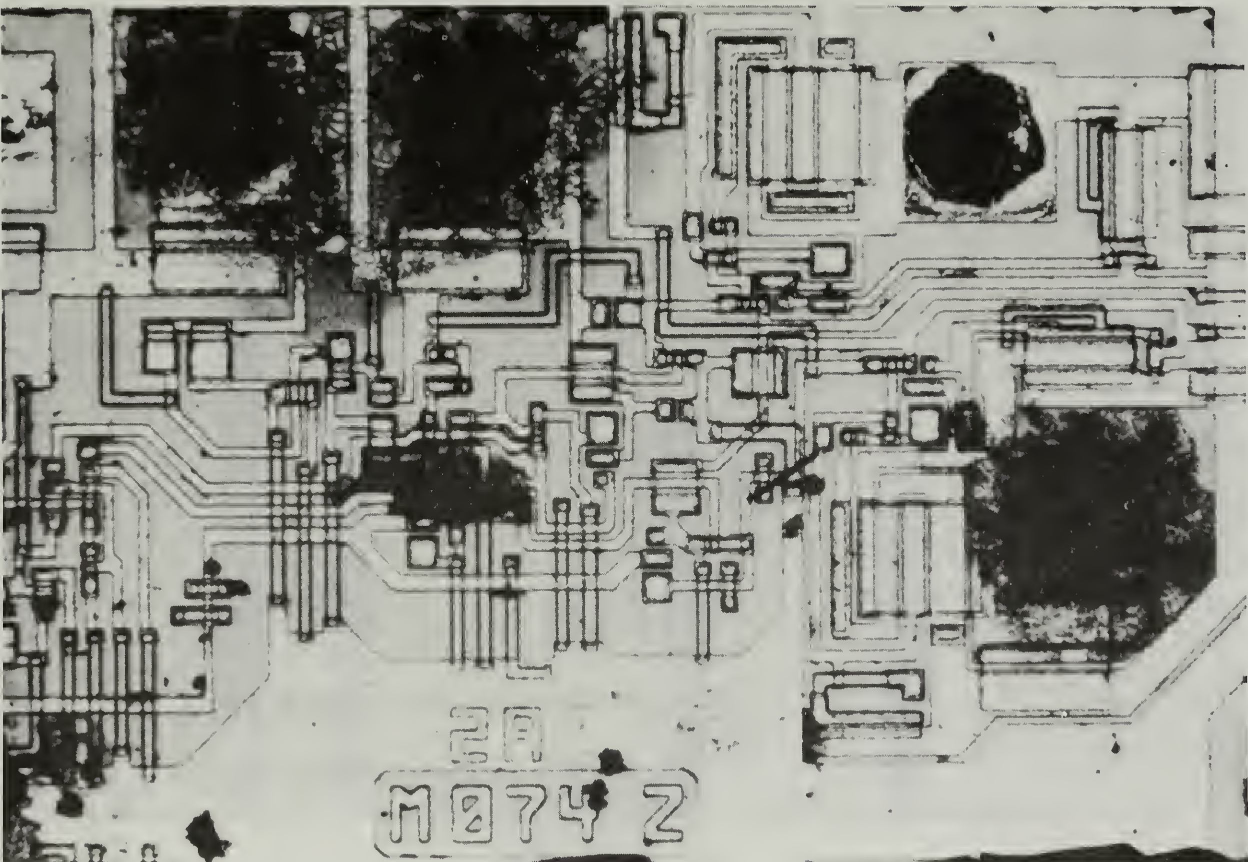

Fig 2.a Die Corrosion due to Flux

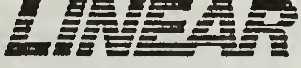

September 24, 1984

PRESSURE POT 121 DEG C

CUMULATIVE PERCENT FAILURE RATE

VS.

WEEKS IN PRESSURE POT

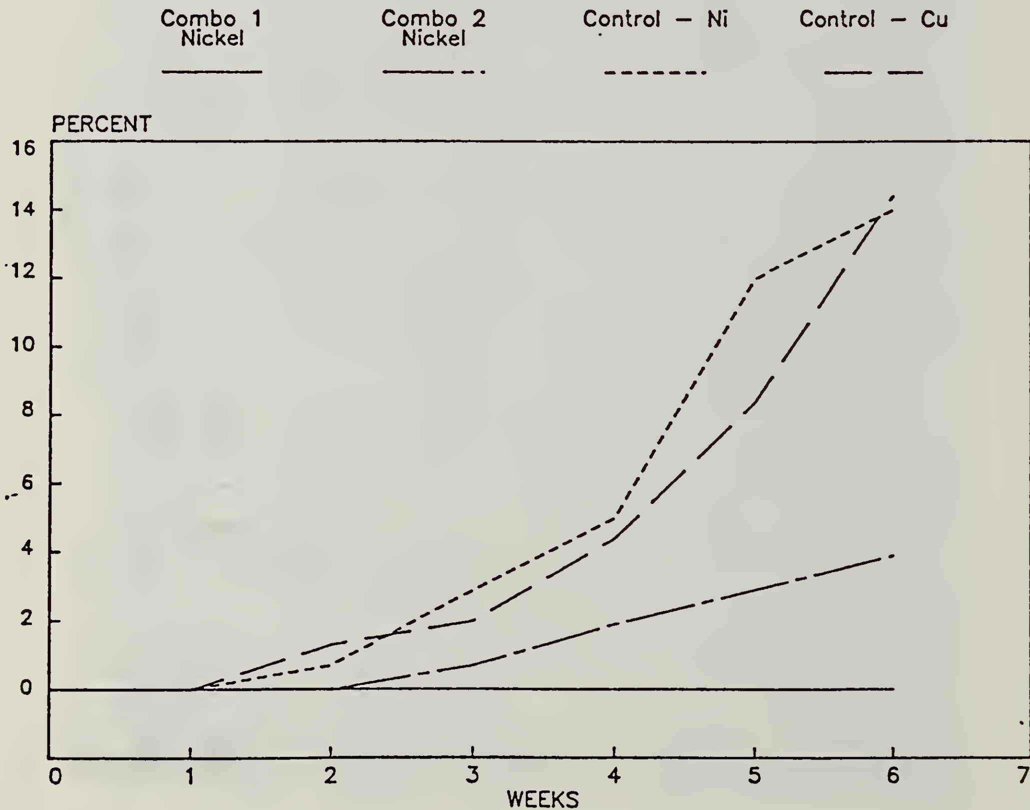

Fig 3. Packaging Material Compatibility

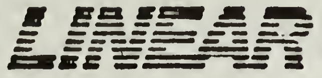

Fig.3a Compound to Metal Adhesion Strength

Fig 5. Filler Size Variation in a Molding Compound (Lot)

5.5 HIGH LEAD COUNT / HIGH RELIABILITY PLASTIC PACKAGING: ISSUES AND APPROACHES

Greg Pitts
Microelectronics and Computer Technology Corporation
12100 Technology Blvd.
Austin, TX 78727
(512)-331-6200

Abstract

Microelectronics and Computer Technology Corporation (MCC) is a research consortium developing both multi-chip and single chip packaging technology for high speed, high lead count integrated circuits on behalf of ten major U.S. companies. Approaches for both plastic and hermetic packaging in single chip applications are being developed.

The research in plastic technology is aimed at addressing applications from low lead count to those in excess of 300 I/O. The reliability of these packages depends upon a number of factors, including die size and moisture sensitivity, leadframe and package design, molding compound, material properties, and processing method and parameters. Unfortunately, the larger the die size and the higher the lead count, the more difficult it becomes to meet high reliability requirements.

This paper will describe some of the experiences with these and other factors. It will also outline some of the research and testing steps which will be needed before high lead count plastic packages can be considered for demanding commercial and military environments.

Introduction

The trend in semiconductor manufacturing has been towards integrating more and more functions into the same area of silicon. Unfortunately, the advances in integrated circuit manufacturing have outgrown the industry's ability to package these new devices effectively. The demands are for better electrical and environmental performance. At the same time, the silicon size and I/O are increasing, and the package body and lead pitch are decreasing.

The basic issues to be addressed, however, are not lead count dependent. The requirements of the commercial, industrial and military markets are not lead count specific. The same factors that are important in packaging low lead count devices are simply amplified by the smaller spaces between the leads and large die size. The desire to shrink the package while increasing the silicon area means that there is less plastic to protect the device. As a result, plastic packages are much more likely to crack and permit rapid moisture and ionic contaminant ingression. Even in a "good" package, the moisture path is shorter than with a conventional DIP because of the thinner walls. As the pitch between the leads gets tighter, the lead thickness gets thinner and manufacturability suffers due to handling problems.

These trends toward higher lead count and smaller packages make it more difficult to achieve reliability, but reliability is relative to the application. Reliability implies longevity, the ability to perform as specified in an appropriate environment for a given length of time. But

references to "high reliability" are generally understood to be synonymous with extreme military requirements, i.e. meeting the requirements of MIL-STD-883 and the likes. These specifications call for survival in severe environments with wide temperature extremes, situations in which plastic packages have not performed well. Plastic packages are highly reliable, but to date that has been limited to commercial and industrial type environments.

Current Status

Acceptance of plastic packages into severe military environments requires an extension of the current industrial testing beyond current levels. Typically, commercial applications require more cycles of a particular test, but with relaxed conditions. For example, in temperature cycling, the test may be from -40° C to +70° C for 1000 cycles instead of -55° C to 125° C for 10 cycles. In a sense then, the required reliability of the commercial environment is more severe than the military in the case of extended cycling. It is the low end of the cycle, the excursion below -40° C, that is particularly difficult for a plastic package to survive without cracking.

The difficulty in meeting military requirements comes not from the extended cycling but from the greater temperature extremes of the environment and harshness of the atmosphere. Conventional thermoset molding materials have a thermal expansion rate significantly higher than silicon and impart a great deal of stress to the silicon device and it's attachments. Any lack of cleanliness in the process or impurity in the molding compound which provides mobile ionic species will lead to corrosion with the ingress of moisture into the plastic. But although some new materials and processes show some promise in alleviating these problems, there are no specifications written for them to meet these "high reliability" requirements.

What is needed is a specification similar in scope to MIL-STD-883 and MIL-STD-38510 for plastic packages. The demands of a specification such as this would of course be specific to plastics and would need some unique features. At present, it is not possible to get sufficient feedback during the manufacturing process about the reliability of the package. There is no non-destructive test equivalent to the seal test for hermetic packages. Pressure cooker, temperature cycling, and other accelerated tests are destructive and time consuming in nature. Because of this, the most effective way to control the reliability of plastic packages is through emphasis on control of processes and materials, including incoming inspection. A comprehensive specification for plastic packages should require these controls.

Primary Packaging Concerns

There are a number of technical considerations in producing a reliable plastic package, particularly in attempting to meet the severe environment requirements of a military type application. The four most important concerns—device susceptibility, package design, material control, and process control—are described below:

Device Susceptibility

The most significant failure mechanism with plastic packages is corrosion. Conventional devices have exposed aluminum bond pads with only microns of thickness. Stress relief may come in the form of passivation cracks which expose the underlying metallization. In the presence of moisture and mobile ions, such as Na^{++}, K^{++}, Cl^{-}, or Ca^{++}, electrochemical cells

are formed during use which can destroy the metallization and the functionality of the device.

The trend today is towards producing a "bulletproof" structure that is resistant to moisture and corrosion. Passivation technology, using plasma nitride and other approaches, has improved the reliability of devices through increased crack resistance and elimination of pinholes.

More important, however, is the use of a bumping technology to protect the bonding areas. One way to do this is to use gold bumps with a barrier layer between the gold and the underlying pad metallization. Gold is much less susceptible to corrosion than aluminum. Bumps are also typically on the order of 1 mil in thickness, much thicker than the aluminum pad it is protecting which also enhances survivability. This type of bump is most often used for TAB (tape automated bonding). Other systems used for TAB include solder, where solder bumps are reflowed to hold the lead, and copper, both of which provide the same kind of volume improvement and protection of the aluminum as does gold.

The intended result in combining a state of the art passivation technique with bumping technology is the creation of a "hermetic" device, one which doesn't have the susceptibility to corrosion whether packaged or not. This would relieve much of the requirement of the package to protect the device. The package could then become a vehicle for mechanical protection.

Package Design

The package design becomes more significant as the die gets larger and the package becomes smaller while the lead pitch gets tighter. Intelligent decisions must be made to keep the dimensions within reason. Equally important, the selection of appropriate molding materials and manufacturing processes is critical. Plastic materials shrink upon cooling and can distort lead geometries, particularly important for the smaller leads found in high lead count devices. With more fragile leads coming out of the package, a scheme for maintaining the integrity of these leads is mandatory.

Material Control

Plastic materials with the appropriate properties must be developed and maintained. A thorough knowledge of the parameters which influence reliability is necessary so that a dependable incoming inspection procedure can be developed. Since it is impossible to monitor "reliability" during manufacture, lot to lot variations must be controlled within defined limits through incoming inspection testing and supplier process control. Of particular concern is the amount of ionic impurities inherent in the molding material, lot by lot.

Process Control

Process control is an equally as important factor in maintaining high reliability in plastic packages. There are no 100 % screening test for plastic packaged parts, no non-destructive tests that can be used to weed out the potentially defective parts. Plastic parts can be destructively evaluated on a sample basis only and these tests are typically time consuming. There is no room for a manufacturing process to be out of control until reliability predictions are made on manufactured packages. Reliability must be built in, not tested and inspected in.

MCC Concept

This research and development consortium was founded to cooperatively advance the state of the art of the U.S. computer industry. Of the four major programs in progress at MCC, three of them are aimed directly at computer technology, software and architecture. The fourth, the Packaging/Interconnect program, is concerned with the component and sub-system level hardware and the results, although proprietary, are applicable to the electronics industry in general. Funding for each of the programs is independent, so the participation in each specific program is unique. The Packaging/Interconnect program currently has ten shareholders, which are the following:

Advanced Micro Devices	**Harris**
Allied	**Hewlett-Packard**
Boeing	**Kodak**
Control Data Corp.	**3M**
Digital Equipment Corp.	**Unisys (Sperry-Burroughs)**

MCC Efforts

Generate a High Reliability Package Concept Incorporating TAB Technology

MCC has developed a plastic package concept which is based on the use of TAB instead of wire bonding. In this package, the volume ratio of plastic to die has been reduced from 90:1 for a conventional 40 lead DIP to 11:1 while providing the capability of 300 or more I/O.

TAB technology has been around for quite some time, but never fully utilized for high lead count devices. Only recently has the industry embraced TAB and attempted to put it into volume production. There are a number of performance issues which are driving this acceptance of TAB, including improved electrical performance. It is the mechanical features, however, which are relevant to reliability.

Bonds formed with a TAB process have significantly increased bond pull strengths over wire bonds. Typical bond pull strengths are greater than 30 to 40 grams, whereas comparable wire bond pulls over 15 grams are unusual. In addition, the incorporation of TAB allows the elimination of one interconnect level by using the TAB tape as the leadframe. In this situation, the lead which bonds to the device is also the lead soldered to the substrate. When these features are combined with state of the art bumping and passivation technology, reliability of a plastic package can be significantly improved.

In order for this concept to be applicable to high lead counts, the problem of thermoset material flashing must be addressed. Thermoset materials have very high flow properties and will pass through openings as small as 0.5 mils (0.0005"). This means that material will flow in between the leads and beyond the desired package body. In the conventional package, this is controlled through the use of dam bars, metal strips shorting the leads together. These strips prevent the plastic from being extruded between the leads and are removed in subsequent steps. With high I/O packages, the spacing between the leads becomes very small, potentially less than even 5 mils. In this case, it becomes uneconomical if not impossible to remove the dam bars mechanically. It would be better to eliminate the need for them.

Center on a Process Geared toward full Automation

TAB has been identified as an approach which lends itself well to automation and can be processed in a reel to reel format with little human intervention. It has been criticized for lack of flexibility, but this can be overcome, however, by developing tape families and normalizing the locations of bond pads. In this fashion, many different devices can be bonded using the same tape, minimizing set up times and facilitating high product mix situations.

Strive to Eliminate Manufacturing Steps

By using TAB, the tape becomes the leadframe and the bond wires are eliminated. In addition, there is no need for a die paddle to hold the die in position. Correct die position is provided during the inner lead bonding process when the die is presented on a pedestal. The inherent stiffness of the leads eliminates the need for additional mechanical support so the die attach process can be eliminated except when needed for electrical or thermal reasons.

Dejunk and deflash processes are where the excess plastic and resin material from molding are removed. These steps are required in conventional molding operations because of the high flow properties of the thermoset materials. Wire bonds are very fragile, so if the materials were not high flow (low viscosity), wire sweep would damage the device. With TAB, the structure is more rigid, and the interconnect is all in one plane and therefore much less likely to suffer damage from the molding process. As a result, new materials have been and can be developed to take advantage of this situation which may not require dejunk, deflash or dam bar removal, because there may not be any dam bars to remove.

Investigate Material Options

In addition to the opportunities that TAB affords (as mentioned above), something must be done to reduce the stress inherent in plastic packaging. Molding occurs at high temperatures, typically around 170° C. At this point, the package could be considered stress free. At any temperature below this point, stress will build up on the device due to the plastic shrinking faster than the silicon. The worst case, then, is the low end of a temperature cycle, and most plastics aren't cycled below -40° C (while the military requires -55° C). With the devices growing in size, this problem is amplified and new material options must be pursued.

Mechanical stress is a result of a combination of factors, the most important of which are the differential thermal expansion and the elastic modulus (Young's modulus). Stress can therefore be controlled by developing a material with a lower expansion coefficient, preferably as low as the thermal expansion of silicon, around 5 ppm/° C. An alternate approach is to modify the elastic modulus so that the differential expansion does not result in stress. Typical thermosets have an elastic modulus of around 2×10^6 PSI. An elastomeric material or a thermoset combined with an elastomeric can have a much lower modulus and impart less stress. The problem with many of the elastomers is that although they have a lower modulus, their thermal expansion rate is much higher and stress buildup still occurs.

The other potential opportunity is through the use of thermoplastic materials which are injection molded. Thermoplastic materials have not been used in the past for a number of reasons. Most thermoplastics do not have the high temperature stability required for electronics applications. In addition, there have been very few materials with a low enough

melt viscosity to not exhibit excessive wire sweep. A few "highly engineered" thermoplastics have improved the situation; Phillips Ryton™ and liquid crystal polymers from Celanese and Dartco are available specifically for semiconductor molding. The Phillips material, chemically known as polyphenylene sulfide has been around several years but has not been fully explored as of yet, particularly for TAB applications. The liquid crystal polymers look very good on paper. They exhibit very low melt viscosities despite fairly high molecular weights because the molecules orient themselves in the flow direction. The thermal expansion rate of these materials has the potential to be the lowest of any known molding material, at least in the axis of flow.

Develop Molding Processes

Conventional transfer molding of semiconductors requires the use of a leadframe with dam bars. Although the need for these may be eliminated with material modifications, it is conceivable to alter the molding process so that dam bars are not needed. In the past, attempts were made to use compliant materials within the mold to seal around the leadframe. The main criticism of this approach is that the seals don't seem to last very long. Grooving the mold presents tolerancing problems, particularly with high lead counts. Perhaps using a laser would simplify the mechanical problems of removing the dam bars.

Another likely approach is to use dam bars that are non-conductive and therefore would not need to be removed. With TAB, the leads are typically held in place by a polyimide film. Without this film, the leads could not span any reasonable length. Unfortunately, this polyimide is not desirable inside of a plastic package. Instead, an epoxy window frame could be used which would double as the support for the leads and provide the seal for the mold. Since it is of comparable material, if not identical to the molding material, it should not be incompatible with the package and would not be removed.

The use of thermoplastic materials opens up the possible processing options. Thermoplastics are injection molded, a more common molding method outside the semiconductor industry. The equipment available for injection molding today offers significantly higher speed as well as greater control of the process through closed loop feedback of the molding parameters. Thermoplastic materials do not require a curing step, so cycle times can be much faster, down to 20-30 seconds instead of several minutes. Tooling expenses can be minimized while maintaining the same throughput as a conventional thermoset transfer process since fewer cavities are needed.

Verification of Concepts

An internal specification has been generated, based on inputs from the MCC shareholders, for verifying the feasibility of these concepts. It includes much of the type of testing seen in MIL-STD-883 and is intended to stress the plastic packages to the same levels as would be required of a hermetic package for the military, if not more severe. Incorporation of TAB and state of the art materials and processes can accomplish this goal.

Additional Research Needed

A great deal of research is required before many of these concepts and approaches will be seen in the field. It is possible today, however, to build devices in the front end that cannot be

packaged and therefore cannot be used, so the need to make improvements in packaging is real. The following identifies some of the more obvious areas:

Material Studies, Development and Characterization

More materials need to be evaluated, particularly the new exotic materials that may offer significant improvements over conventional thermosets. The thermoplastics mentioned above show some promise, but they are only a starting point. Thermoset materials are continually improving, although typically not in leaps and bounds. Careful characterization of any new material will be required to develop comprehensive incoming specifications.

Process Development and Evaluation

The emphasis needs to be on fully automatable processes for two reasons: reduced high volume manufacturing cost and control of the process. A more thorough investigation of injection molding is necessary before this process can be fully utilized in a production environment, with the limits of the processing window well defined. Other approaches such as compression molding, or reaction injection molding (RIM) may also become applicable with some of the new exotic materials.

Definition and Implementation of True Statistical Process Control

The key to maintaining low failure rates in plastic packages is in effective use of process control. The lack of immediate feedback on reliability and the inability to screen plastic packages 100% with non-destructive testing requires that the process be under control. The definition and implementation of a true statistical process control procedure is essential.

Development of New Test Methods for Plastic Packages

New tests methods are needed to provide rapid feedback on reliability for the most effective process control. The incorporation of HAST (Highly Accelerated Stress Test) as an accelerated autoclave test would at least speed the return of reliability data, but again, this is a destructive test. Effort should be expended to develop effective, non-destructive test methods.

Generation of the Standards and Specifications for Plastics for Harsh Environments

A cooperative effort is required to generate the standards for plastic packages for military type harsh environments. A great deal of field testing and documentation of the test methods and conditions will assure reliability. To be effective, this will have to go beyond the typical scope of a qualification specification, and incorporate manufacturing process control practices.

6:1 List of Speakers

RADC/NBS Workshop

November 12-14, 1986

M. Andrews
Microelectronics and Computer Technology Corp.
12100 Technology Blvd.
Austin, TX 78727
(512) 331-6200

N. K. Annamalai
RADC/ESR
Hanscom AFB, MA 01731
(617) 377-3047

Lyle E. Bergquist
Martin Marietta Denver Aerospace
Dept. 0560, P.O. Box 179
Denver, CO 80201
(303) 977-4519

E. C. Blackburn
Rome Air Development Center
Mail Stop RBRE
Griffiss AFB, NY 13441-5700
(315) 330-4029

H. L. Blaz
Harris Semiconductor
P.O. Box 883
Melbourne, FL 32901
(305) 727-7128

E. C. Cahoon
IBM
Dept. A28, Bldg. 908
P. O. Box 950
Poughkeepsie, NY 12602
(914) 732-7238

D. R. Carley
RCA/Solid State Division
Somerville, NJ 08876
(201) 685-6465

Aaron DerMarderosian*
Raytheon Co.
Equipment Division
Sudbury, MA 01776
(617) 440-2791

Bill Evan
WEB Technology, Inc.
Dallas, TX

V. Fong
Panametrics
221 Crescent Street
Waltham, MA 02254
(617) 288-2719

D.Y. Guan
IBM
Dept. A28, Bldg. 908
P.O. Box 950
Poughkeepsie, NY 12602
(914) 732-7238

T.F. Gukelberger
IBM
Dept. A28, Bldg. 908
P.O. Box 950
Poughkeepsie, NY 12602
(914) 732-7238

Ray F. Haack
California Institute of Technology/JPL
M/S 125-214
4800 Oak Grove Drive
Pasadena, CA 91109
(818) 354-6568

Orjan Hallberg
RIFA AB
S16381
Stockholm, Sweden S1681
(08) 757-4626

* Session Chairman

Karin Hulten
MIMX, IC-Division, RIFA AB
Isafjordsgatan 10-16, Kista
S-16381 Stockholm, Sweden
(08) 747-4920

M.S.R. Islam
Clarkson University
Potsdam, NY 13676

T.W. Joseph
IBM
Dept. A28, Bldg. 908
P.O. Box 950
Poughkeepsie, NY 12602
(914) 732-7238

Didier Kane
Rome Air Development Center
RBRE
Griffiss AFB, NY 13441-5700
(315) 330-4055

Louis Liang
Fairchild Semiconductor
313 Fairchild Drive; M/S 4-390
Mtn. View, CA 94039
(415) 962-4164 or 4166

Robert K. Lowry*
Harris Semiconductor
Box 883, MS 62-07
Melbourne, FL 32901
(305) 724-7566

A. Mantz
Spectra-Physics, Inc.
Laser Analytics Division
25 Wiggins Avenue
Bedford, MA 01730

Benjamin Moore
Rome Air Development Center
RBRE
Griffiss AFB, NY 13440-5770
(315) 330-4055

R.W. Nearhoff
RCA/Solid State Division
Route 202
Somerville, NY 08876
(201) 685-6465

John Pernicka
Pernicka Corp.
112 Racquette Drive
Fort Collins, CO 80524
(303) 224-0220

David Pinsky
Raytheon Company
Hartwell Road
Bedford, MA 01730
(617) 274-4252

G. Pitts
MCC
12100 Technology Blvd.
Austin, TX 78727
(512) 331-6200

L.J. Rigby
STC Technology Limited
London Road, Harlow, Essex, CM17 9NA
United Kingdom

Stephen R. Schertz
Martin Marietta Denver Aerospace
Dept. 0560, P.O. Box 179
Denver, CO 80201
(303) 977-4519

Stephen D. Senturia*
Massachusetts Institute of Technology
77 Massachusetts Avenue, Room 39-567
Cambridge, MA 02139
(617) 253-6869

J.M. Snowdon
IBM
Dept. A28, Bldg. 908
P.O. Box 950
Poughkeepsie, NY 12602
(914) 732-7238

J. Sproul
Spectra-Physics, Inc.
Laser Analytics Division
25 Wiggins Avenue
Bedford, MA 01730

R.J. Straub
Delco Electronics Corp.
1800 E. Lincoln
Kokomo, IN 46902
(317) 451-7027

Philip R. Troyk
IIT
10 W. 32nd Street
Chicago, Il 60616
(312) 567-5324

D. Wall
Spectra-Physics, Inc.
Laser Analytics Division
25 Wiggins Avenue
Bedford, MA 01730

6.2 Attendees to RADC/NBS Moisture Measurement Workshop

Mr. Don Allen
Motorola
Mail Drop H1023
8201 E. McDowell Road
Scottsdale, AZ 85252
(602) 949-2386

Mr. Naga Annamalai
RADC/ESR
Hanscom AFB, MA 01731
(617) 377-3047

Mr. Dan Anderson
Bendix
1721 SE 5th Terrace
Lees Summit, MO 64063
(816) 524-9610

Dr. James Anderson
Ford Motor Company
Scientific Research Staff
Dearborn, MI 48121
(313) 594-1187

Mr. David L. Angst
AT&T Bell Laboratories
555 Union Blvd.
Allentown, PA 18103
(215) 439-5676

Mr. John L. Barchi
Cordis Corporation
10555 W. Flagler Street
Miami, FL 33172
(305) 551-2520

Mr. Richard Benson
Johns Hopkins Applied Physics Lab
Johns Hopkins Road
Laurel, MD 20707
(301) 953-6241

Mr. Lyle E. Bergquist
Martin Marietta Denver Aerospace
Dept. 0560, P.O. Box 179
Denver, CO 80201
(303) 977-4519

Mr. Eugene C. Blackburn
Rome Air Development Center
Mail Stop RBRE
Griffiss AFB, NY 13441-5700
(315) 330-4029

Mr. Colin B. Blakemore
Du Pont Company
Glasgow Site
Wilmington, DE 19898
(302) 453-2382

Mr. Daryl R. Brunswick
Allied Bendix
K.C. Division D/834 2A36
P.O. Box 419159
Kansas City, MO 64141-6154
(816) 997-4328

Mr. Stephen Bryant
Fairchild Inc.
20301 Century Blvd.
Germantown, MD 20879
(301) 428-6170

Mr. Stephen P. Carvellas
Gollob Analytical Service
47 Industrial Road
Beckeley Heights, NJ 07922
(201) 464-3331

Mr. Bill Collins
M&T Chemicals
P.O. Box 1104
Rahway, NJ 07065
(201) 499-2534

Mr. Kevin D. Cluff
Sperry Corporation
M/S L24C4
21111 N. 19th Avenue
Phoenix, AZ 85027
(602) 869-2869

Mr. David J. Daley
I.T. Corp., Cerritos
17605 Fabrica Way
Cerritos, CA 90701
(213) 921-9831

Mr. Ray Denton
Mail Code 6051
Naval Weapons Support Center
Crane, IN 47522
(812) 854-3828)

Mr. Robert Edelman
M&T Chemicals
Randolph Avenue
Rahway, NJ 07901
(201) 499-2316

Mr. William Ege
Struthers-Dunn, Inc.
Lambs Road
Pitman, NJ 08071
(609) 589-7500

Mr. Edward Etess
WEB Technology, Inc.
10520 Plaro Road, Suite 104
Dallas, TX 75238
(214) 343-9238

Mr. John E. Fennimore
Martin Marietta Corp.
P.O. Box 5837, MP 184
Orlando, FL 32855
(305) 356-2086

Ms. Diane Feliciano-Welpe
Oneida Research Services, Inc.
One Halsey Road
Whitesboro, NY 13492
(315) 736-3050

Mr. Victor Fong
Panametrics
221 Crescent Street
Waltham, MA 02254
(617) 899-2719

Ms. Kathleen V. Frisbie
DOD, Attn: YZ53
9800 Savage Road
Ft. Meade, MD 20755
(301) 688-7739

Ms. P. Jane Gale
RCA Laboratories
P.O. Box 432
Princeton, NJ 08543-0432
(609) 734-3053

Mr. Richard Gerber
Aerospace Corp.
Box 92957, M4/996
Los Angeles, CA 90009
(213) 336-1535

Mr. Graham Gibson
VG Instruments
4 Elena Court
Medford, NJ 08055
(609) 654-1862

Mr. John F. Graves
Allied/Bendix Communications Division
1300 E. Joppa Road
Towson, MD 21204
(301) 583-4133

Mr. Hal Greenhouse
Allied Bendix Aerospace
1300 E. Joppa Road
Baltimore, MD 21204
(301) 583-4102

Mr. Thomas F. Gukelberger
IBM
B/908
Poughneepsie, NY 12601
(914) 432-7238

Mr. I. Macit Gurol
Vishay Intertechnology, Inc.
63 Lincoln Highway
Malvern, PA 19355
(215) 644-1300, x371

Mr. James W. Guthrie
Sandia National Laboratories
Division 7551, P.O. Box 5800
Albuquerque, NM 87185
(505) 846-4266

Mr. Ray F. Haack
Jet Propulsion Laboratory
California Institute of Technology
M/S 125-214
4800 Oak Grove Drive
Pasadena, CA 91109
(818) 354-6568

Mr. Orjan Hallberg
RIFA AB
S16381
Stockholm, Sweden S1681
(08) 757-4626

Mr. George Harman
National Bureau of Standards
Building 225, Room A331
Gaithersburg, MD 20899
(301) 975-2097

Mr. William L. Harrington
RCA Laboratories
David Sarnoff Research Center
Princeton, NJ 08540
(609) 734-2415

Mr. Sab Hasegawa
National Bureau of Standards
Building 221, Room B312
Gaithersburg, MD 20899
(301) 975-2620

Mr. Howard J. Herzog
Spectra-Physics, Laser Analytic Div.
25 Wiggins Avenue
Bedford, MA 01730
(617) 275-2650

Ms. Laura A. Hughes
Rockwell International
3370 Miraloma Ave (DF03)
Anaheim, CA 92803-4192
(714) 762-2357

Ms. Karin Hulten
MIMX, IC-Division, RIFA AB
Isafjordsgatan 10-16, Kista
S-16381 Stockholm, Sweden
(08) 747-4920

Mr. Ronald Hunadi
Furane/Rohm & Haas
5121 San Fernando Road W.
Los Angeles, CA 90039
(818) 247-6210

Mr. Douglas K. Ishio
Litton/Amecom
5115 Calvert Road
College Park, MD 20740
(301) 864-5600, x1066

Ms. Charlotte Jackson
Northrop Electronics
P.O. Box 5032
Hawthorne, CA 90251-5032
(213) 600-7196

Mr. Kevin Jewett
ILC Data Device Corp.
105 Wilbur Place
Bohemia, NY 11716
(516) 567-5600

Mr. Robert J. Kalin
Medtronic, Inc.
7000 Central Ave., N.E.
Fridley, MN 55432
(612) 574-4237

Mr. Didier Kane
RADC/RBRE
Griffiss AFB, NY 13441-5700
(315) 330-4055

Mr. James W. Kersey
Sandia National Laboratories Livermore
P.O. Box 969
Livermore, CA 94550
(415) 422-2740

Dr. J. A. Koprio
Balzers AG
ABT ELA
FL9496 Blazers
Principality of Liechtenstein

Mr. Michael Leck
VG Gas Analysis
Aston Way, Middlewick
Cheshire, England CWO OMT

Mr. Jim C. Lawson
Teledyne Microelectronics
12964 Panama Street
Los Angeles, CA 90266
(213) 822-8229

Mr. Louis Liang
Fairchild Semiconductor Corporation
313 Fairchild Drive; M/S 4-390
Mtn. View, CA 94039
(415) 962-4164 or 4166

Ms. Patricia A. Long
Hughes Aircraft Company
P.O. Box 11337
Tucson, AZ 85734
(602) 295-5230

Mr. Robert K. Lowry
Harris Semiconductor
Box 883, MS 62-07
Melbourne, FL 32901
(305) 724-7566

Mr. Aaron Der Marderosian
Raytheon Co.
528 Boston Post Rd.
Sudbury, MA 01776
(617) 440-2791

Ms. Margie Marlow
Watkins-Johnson Co.
700 Quince Orchard Road
Gaithersburg, MD 20878
(301) 948-7550, x535

Mr. Craig B. Mauldin
General Electric Co. - NDD
7887 Bryan Dairy Road
Largo, FL 34294-2908
(813) 541-8811

Mr. Ralph McCullough
Texas Instruments
P.O. Box 655012, M/S 17
Dallas, TX 75265
(214) 995-3931

Mr. Benjamin A. Moore
RADC/RBRE
Griffiss AFB, NY 13440-5770
(315) 330-4055

Mr. Jay Mucha
AT&T Bell Labs
600 Mountain Avenue
Murray Hill, NJ 07974
(201) 582-3659

Mr. Robert Nearhoof
RCA/Solid State Division
Route 202
Somerville, NJ 08876
(201) 685-6465

Dr. C. A. Neugebauer
Corporate Research and Development
General Electric Company
P.O. Box 8, KWC-1603
Schenectady, NY 12301
(518) 387-5399

Mr. John A. Olenick
Westinghouse Electric Corporation
P.O. Box 746, MS 496
Baltimore, MD 21203
(301) 765-2259

Mr. Ronald Pacheco
Digital Equipment Corporation
100 Minuteman Road APO2/F2
Andover, MA 01810
(617) 689-1482

Mr. Carl T. Pallister
Martin Marietta Denver Aerospace
P.O. Box 179
Denver, CO 80201
(303) 977-4127

Mr. W. C. Peila
Sandia National Laboratories
Division 8153
P.O. Box 969
Livermore, CA 94550
(415) 422-2077

Ms. Maxine B. Pennington
Allied Bendix Aerospace
Bendix Kansas City Division
2000 E. 95th St., P.O. Box 419159
Kansas City, MO 64141-6159
(816) 997-4187

Mr. Wolf Penzel
Honeywell, Inc.
MN11-1812
600 2nd Street NE
Hopkins, MN 55343
(612) 931-6983

Mr. John C. Pernicka
Pernicka Corporation
112 Racquette Drive
Fort Collins, CO 80524
(303) 224-0220

Mr. Daniel J. Peters
Allied/Bendix Corporation
Kansas City Division
P.O. Box 419159
Kansas City, MO 64141-6159
(816) 997-5507

Mr. David A. Pinsky
Raytheon Co.
Hartwell Road
Bedford, MA 01730
(617) 274-4252

Mr. Greg Pitts
M.C.C.
12100 Technology Blvd.
Austin, TX 78727
(512) 331-6200

Ms. Bernedette Preston
Department of Defense
Y253
Ft. Meade, MD 20755
(301) 688-7739

Mr. Brian E., Reilly
Allied-Bendix Aerospace
P.O. Box 419159
Kansas City, MO 64141-6159
(816) 997-3564

Mr. Stephen P. Rogers
Motorola
5005 E. McDowell Road, M/S P166
Phoenix, AZ 85005
(602) 244-3711

Mr. Jack Ronning
Medtronic, Inc.
7000 Central Avenue, NE
Fridley, MN 55432
(612) 574-4761

Mr. Thomas J. Rossiter
Oneida Research Services, Inc.
One Halsey Road
Whitesboro, NY 13492
(315) 736-3050

Mr. David Ruben
Motorola
Maildrop H1023
8201 E. McDowell Road
Scottsdale, AZ 85252
(602) 481-8166

Mr. Philipp Schuessler
IBM/FSD
M/S 0570
Owego, NY 13827
(607) 751-4219

Mr. Stephen D. Senturia
Massachusetts Institute of Technology
77 Massachusetts Avenue, Room 39-567
Cambridge, MA 02139
(617) 253-6869

Mr. Glenn Shirley
Intel Corporation
145 S. 79th Street
Chandler, AZ 85226
(602) 961-5357

Mr. Ed Smith
Olin-MRL
91 Shelton Avenue
New Haven, CT 06511
(203) 789-5293

Mr. Robert J. Straub
Delco Electronics Corporation
1800 E. Lincoln
Kokomo, IN 46902
(317) 451-7027

Mr. Charles T. Taverner
Bell Aerospace Textron
P.O. Box 1, MS C-65
Buffalo, NY 14240
(716) 297-1000, x7474

Mr. Philip R. Troyk
IIT
10 W. 32nd Street
Chicago, IL 60616
(312) 567-5324

Mr. O. Manuel Uy
Applied Physics Laboratory
John Hopkins University
Johns Hopkins Road
Laurel, MD 20708
(301) 953-5334

Mr. Tom Walker
Mail Code 6051
Naval Weapons Support Center
Crane, IN 47522
(812) 854-3828

Mr. David Wall
Spectra-Physics, Inc.,
Laser Analytics Div.
25 Wiggins Avenue
Bedford, MA 01730
(617) 275-2650

Ms. Debra Waller
Digital Equipment Corp.
100 Minuteman Road
Andover, MA 01870
(617) 689-1552

Mr. Joel Weiner
Johns Hopkins Applied
Physics Laboratory
16-209
John Hopkins Road
Laurel, MD 20707
(301) 953-5000

Mr. Steve Weisskoff
Phys-Chemical Research Corporation
36 West 20th Street
New York, NY 10011
(212) 924-2070

Mr. David Wilson
Martin Marietta
P.O. Box 179
Denver, CO 80201
(303) 977-3838

Mr. Mark Wilson
Blazers
8 Sagamore Pk. Rd.
Hudson, NH 03051
(603) 889-6888

Mr. John Yim
National Semiconductor
2900 Semiconductor Dr.
Santa Clara, CA 95057
(408) 721-3870

* U.S. GOVERNMENT PRINTING OFFICE 1987; 181-100/62515

NBS-114A (REV. 2-80)

U.S. DEPT. OF COMM. BIBLIOGRAPHIC DATA SHEET (See instructions)	1. PUBLICATION OR REPORT NO. NBSIR 87-3588	2. Performing Organ. Report No.	3. Publication Date July 1987

4. TITLE AND SUBTITLE

RADC/NBS International Workshop on Moisture Measurement and Control for Microelectronics (IV)

5. AUTHOR(S)

D. Kane, B.A. Moore, and E.J. Walters, Editors

6. PERFORMING ORGANIZATION (If joint or other than NBS, see instructions)

NATIONAL BUREAU OF STANDARDS
U.S. DEPARTMENT OF COMMERCE
GAITHERSBURG, MD 20899

7. Contract/Grant No.

8. Type of Report & Period Covered

9. SPONSORING ORGANIZATION NAME AND COMPLETE ADDRESS (Street, City, State, ZIP)

10. SUPPLEMENTARY NOTES

[ ] Document describes a computer program; SF-185, FIPS Software Summary, is attached.

11. ABSTRACT (A 200-word or less factual summary of most significant information. If document includes a significant bibliography or literature survey, mention it here)

This fourth Workshop on Moisture Measurement and Control for Microelectronics served as a forum on moisture and/or materials reliability problems and on ways to control them or measure their extent. Twenty-two presentations are included which contain detailed information on hermeticity measurement and definition; development of standard packages for mass spectrometric calibrations; moisture interaction with various materials; and techniques that can be used to measure moisture micro-electronics. It was clear from several presentations in this workshop that a very systematic approach is needed when organic materials are involved; all the variables must be identified and studied one at a time. This is the key to lot-to-lot reproducibility, materials selection, and control; hence a better reliability at the design phase will decrease the need for testing, hence the cost, thus resulting in a greater satisfaction to the customer.

12. KEY WORDS (Six to twelve entries; alphabetical order; capitalize only proper names; and separate key words by semicolons)

Analysis of moisture content; hermetically packaged semiconductor devices; hybrid packages; mass spectrometer measurements; moisture; organic package materials; moisture generators; moisture sensors; quality control; reliability of semiconductor devices; semiconductor devices.

13. AVAILABILITY

[XX] Unlimited

[ ] For Official Distribution. Do Not Release to NTIS

[ ] Order From Superintendent of Documents, U.S. Government Printing Office, Washington, D.C. 20402.

[XX] Order From National Technical Information Service (NTIS), Springfield, VA. 22161

14. NO. OF PRINTED PAGES

342

15. Price

$30.95

USCOMM-DC 6043-P80